IMPULSE BREAKDOWN CHARACTERISTICS OF SF_6 AND ITS MIXTURES IN HIGHLY NON-UNIFORM FIELD GAPS

Thesis presented for the degree of Doctor
of Philosophy in Electrical Engineering
of the University of Strathclyde

Xiang Qun Qiu

August, 1998

Department of Electronic and Electrical Engineering
University of Strathclyde
Glasgow

Declaration of Author's Rights

ABSTRACT

The work reported in this thesis was undertaken in the Centre for Electrical Power Engineering, Department of Electronic and Electrical Engineering, University of Strathclyde to study the impulse breakdown characteristics of SF_6 and its mixtures in highly non-uniform field gaps. Of particular interest were the effects of space charge, artificial irradiation, different gas mixtures, different additive gases and different wavefronts on the impulse breakdown characteristics.

High divergent fields can exist in GIS under certain conditions as, for example, when a needle-like free metallic particle is attracted to the inner conductor or is deposited on the surface of an insulator. Such defects can result in very low breakdown levels and, with large defects(e.g. particles several mm long), failure can occur even at the working stress of the equipment. The breakdown characteristics of gases in nonuniform fields, however, are much more complicated than in uniform fields and are not fully understood. This is probably due to the complex effect of space charge on breakdown process[89] and the space charge effect on positive impulse breakdown characteristics of SF_6 and its mixtures in highly nonuniform field gaps has become an increasingly important subject on the gaseous dielectrics with high electric strength in high voltage apparatus. The main purpose of the present work is to acquire a better understanding of the corona stabilised breakdown mechanism in SF_6 gas under impulse voltages and to supply a physical base to choose an efficient additive for improving the insulating strength of SF_6 gas.

A general introduction is first given, based on a review of experimental and theoretical work on the subject to date. Descriptions of apparatus and experimental techniques are then given. Two newly developed space charge injection methods, namely corona pin arrangement and direct injection method were used throughout the work. In the case of positive lightning impulse voltage, injected positive space charge has little effect on minimum impulse breakdown, whereas a decrease in breakdown voltage is observed when negative space charges are injected into the gap. Artificial irradiation also decreases the minimum impulse breakdown voltage, though the reduction rate is lower. From these and other observations, it is generally concluded that the major source of initiatory electrons for positive impulse breakdown in an enclosed gap is from the electron detachment from unstable negative ions and initiatory electrons make an important contribution to the breakdown process. The conclusion is confirmed to a large extent by using a photomultiplier to observe the light emission during the discharge process.

The study of the effect of space charges and artificial irradiation shows that although initiatory electrons make an important contribution to the breakdown process, it appears that there is a limit beyond which the breakdown strength cannot be further decreased by increasing the electron or negative-ion population. The study of the addition to SF_6 of 5% R20 or R12 has shown that although space charges have a great effect on impulse breakdown strength in SF_6, there is little, if any, effect on breakdown strength in SF_6/R12 and SF_6/R20 mixtures. The result implies those additives containing chlorine preferentially produce very stable negative ions which do not readily detach. The impulse strength is increased in mixtures containing these

additives because there is then a reduced likelihood of successful development of the discharge channel through a scarcity of initiating electrons in the gap.

The initiating electrons will be produced mainly by the detachment from negative ions so that the rate of production in the critical volume will itself depend upon the applied waveform [143]. It has been found that the wavetail has little influence on impulse breakdown process [141,158] and only the effect of wavefront is studied. It had been found that the longer the wavefront, the higher the minimum impulse breakdown voltage. the reason is believed to be the sweeping off action which negative ions in the gap are swept out the effectively.

Suggestions for further research work are offered in Chapter 9.

Table of contents

Chapter 2 Apparatus and experimental techniques

Chapter 3 The effect of space charge

Chapter 4 The effect of artificial irradiation

Chapter 5 The combined effect of space charge and artificial irradiation

Chapter 6 The effect of different wavefront

Chapter 1 General Introduction

1.1 SF_6 basic properties

Sulphur hexafluoride(SF_6) is the most commonly used insulating gas in electrical systems to date[1]. It is used as an insulant in a wide range of power-system application, including switchgear, gas-insulated substation components, transformers and gas-insulated cables. When SF_6 was first discovered , its potential application was considered solely to be for insulation, because of its good dielectric properties(breakdown strength nearly three times higher than that of air at atmospheric pressure). Additionally, a major expansion in the use of SF_6 occurred when its excellent arc-quenching properties were appreciated. SF_6 circuit breakers were developed that are clearly superior in performance and cost to the competing oil and air-blast circuit breakers, and these took over the market for HV electric power systems. Compressed SF_6 is now extensively used in gas-insulated substations(GIS) and also used for insulation in metal-clad HV gas-insulated transmission lines including associated bushings, capacitors, and transformers. The SF_6-insulated transmission lines provide a cost-effective, compact alternative to overhead lines in situations where there are limitations and/or restriction on transmission rights-of-way such as congested or highly populated areas. Gas-insulated systems are now a major component of power transmission and distribution systems all over the world. They offer significant saving in land use, and aesthetically acceptable, have relatively low radio and audible noise emissions and enable substations to be installed in cities very close to the loads. Virtually every substation now being built uses SF_6 for circuit

breakers, and every GIS and gas-insulated transmission lines relies on SF_6 for insulation. SF_6 offers the following advantages as a dielectric medium:

SF_6 is:
- chemically stable
- non toxic
- non flammable

SF_6 has:
- good heat transfer characteristics
- high vapour pressure
- high dielectric strength
- excellent arc-quenching properties

1.1.1 Physical and chemical properties

The SF_6 molecule is octahedral, with the six fluorine atoms arranged around a central sulphur atom(Fig 1.1[2]). Because of the strong S-F bonds and the highly symmetrical configuration, SF_6 molecules do not readily form clusters and this is the reason for the very low condensation temperature (-68°C at 1 bar) for a gas with such a high molecular weight(MW=146).

Although the thermal conductivity of SF_6 is not very different from that of air, heat transfer by convection is much more efficient in SF_6 because of its greater density

and lower viscosity. The overall heat transfer coefficient in SF_6 at atmospheric pressure, allowing for both conduction and convection, is about twice that for air.

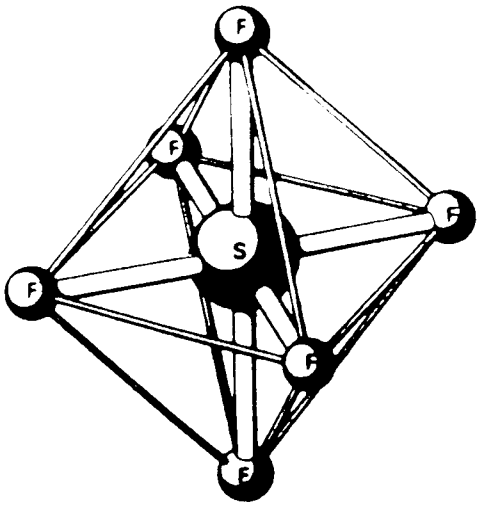

Figure 1.1 The SF_6 molecule [2]

The fact that SF_6 is highly stable and chemically inert is related to the presence of strongly bound fluorine atoms in the SF_6 molecule, as fluorine is a very strong oxidising agent and no other element will readily displace fluorine in SF_6. The high degree of chemical stability persists up to at least 500°C although above this temperature some decomposition is observed in the presence of certain metals(including silicon steel and copper) with formation of the lower fluorides(SF_4, SF_2).

The chemical inertness of SF_6 is also responsible for its complete lack of toxicity. It has been shown, for example, that mice and other laboratory animals are unaffected by exposure for several hours to an "atmosphere" of 80% SF_6 and 20% oxygen. The main hazard is the danger of suffocation if SF_6 in large quantities is released in a

confined space, where its high density may result in displacement of air at lower levels(for example in the basement of a building).

1.1.2 Decomposition products

Although SF_6 itself is stable and inert, chemically reactive and toxic products may be formed as a result of thermal decomposition in an arc or spark in the presence of impurities such as water or vapour, oxygen etc.

One of the most important reactions involves the formation of SF_4 which then reacts with water vapour to form SOF_2 and HF.

$$SF_6 \text{ (spark)} \rightarrow SF_4+2F$$

$$SF_4 + H_20 \rightarrow SOF_2+2HF$$

The formation of other oxyfluorides is also possible by reaction with oxygen or with oxygen radicals:

$$SF_4 + O_2 \rightarrow SO_2F_2+2F$$

$$SF_6 + O \rightarrow SO_2F_4+2F$$

These products may in turn react with water vapour:

$$SOF_2 + H_2O \rightarrow SO_2 + 2HF$$

$$SOF_4 + H_2O \rightarrow SO_2F_2 + 2HF$$

The decomposition products of sparked SF_6 can attack both metallic and solid insulation components of GIS. The free fluorine, for example, reacts with the arcing electrode to form metallic fluoride such as WF_6, ALF_3 etc. Degradation of solid-filled epoxy, glass or porcelain insulation can occur by reactions such as:

$$SF_4 + SiO_2 \rightarrow SiF_4 + SO_2$$

$$2SOF_2 + SiO_2 \rightarrow SiF_4 + 2SO_2$$

$$4HF + SiO_2 \rightarrow SiF_4 + 2H_2O$$

In equipment in which decomposition products are formed during normal operation(for example high voltage circuit breakers and disconnect switches) chemical absorbents such as soda lime and activated alumina are used to keep the gas dry and to remove the corrosive by products of arcing. Provided the system is filled with relatively dry SF_6(H_2O content $\leq$ 50ppm) such precaution are not necessary in other GIS components, although some manufacturers do install an activated alumina

absorber in each gas zone of the GIS bus. Table 1.1 reviews the SF_6 decomposition products detected[92].

Table 1.1 Decomposition products detected from sparked SF_6 at various laboratories

decomposition products	discharge	methods
SF_2,SF_4,HF,CO_2,H_2S	AC arc	IR
SF_2,SOF_2	high current AC arc	IR
S_2F_2	RF electrodeless	IR
SO_2F_2	500 W AC arc	IR
SOF_2,SO_2F_2	1-3 kA AC arc	MS
SOF_2,SO_2F_2,SOF_4	corona	GC,IR,MS
SOF_2,S_2F_2,SiF_4	0.75 A AC arc	MS
SOF_2,SO_2F_2,SOF_4,SF_4	5-10 A AC arc	GC,IR
SOF_2,SO_2F_2,SOF_4,SF_4,S_2F_{10},$S_2F_{10}O$	CD	GC,IR
SOF_2,SO_2F_2,SOF_4,HF,WF_6	400-500 A AC arc	GC,IR
SOF_2,SO_2F_2,CF_4,SiF_4,HF(cell not dried)	30kA AC arc	NMR
SF_4,S_2F_2,SOF_2,WF_6,SiF_4,COF_2,CF_4(cell dried)	30kA AC arc	NMR
SF_4,SOF_2,SOF_4,S_2F_2,S_2F_{10}	various	GC
SOF_2,SO_2F_2,SOF_4,SiF_4,F_2	RF electrodeless	GC,IR,MS
S	RF electrodeless	EPR
SF_4,SOF_2,SO_2F_2,SOF_4	0.2A AC arc	GC,MS
SF_4,SO_2F_2,CF_4,CO_2	1.8kA AC arc	GC
AlF_3	arc	PD
N_2O,SOF_2,SO_2F_2,SOF_4	DC corona	GC,MS

SF_4,SOF_2,SO_2,SO_2F_2,SOF_4,SiF_4,HF,WF_6	spark	MS

* IR, infrared spectroscopy: MS mass spectrometry: GC, gas chromatography: CD, capacitance discharge: NMR, nuclear magnetic resonance: EPR, electron paramagnetic resonance, PD, particle detector

1.1.3 Dielectric strength

SF_6 has a uniform-field dielectric strength which, at atmospheric pressure, is three times that of air and which, at ~8 bar, is comparable to that of transformer oil. Its high dielectric strength is due to its property of electron attachment. In this process a free electron moving in the applied field, which collides with a neutral molecule, may be attached to form a negative ion:

$$SF_6 + e \rightarrow (SF_6)^-$$

This process competes with that of collisional ionisation, by which an electron with sufficient energy can remove an electron from a neutral molecule to create an additional free electron:

$$SF_6 + e \rightarrow (SF_6)^+ + 2e$$

Ionisation is a cumulative process and, provided that the field is high enough, successive collisions can produce ever increasing numbers of free electrons which

can result in electrical breakdown of the gas. On the other hand, the heavy, slowly moving negative ions that are formed by attachment are unable to accumulate the energy required to cause ionisation and the attachment process therefore effective removes electrons and inhibits the formation of "avalanches" of electrons which might lead to breakdown.

Some gases, such as nitrogen, hydrogen and argon, do not form negative ions; others, such as oxygen and CO_2, are weakly attaching. SF_6, in common with a number of other gases containing fluorine or chlorine, is highly "electronegative"(i.e. exhibits strong electron attachment). Some gases have a dielectric strength significantly greater than that of SF_6 as shown in table 1.2. However, most present problems of one kind or another, including toxicity, limited operating pressure range, production of solid carbon during arcing etc. SF_6 is therefore the only dielectric which is accepted as suitable for GIS application although some high-strength gases have been considered for use in mixtures with SF_6.

Table 1.2 Relative dielectric strength of certain gases[2],[92]

Gas	***Relative Strength***	
H_2	0.18	non-attaching
Air	0.3	weakly attaching
CO_2	0.3	weakly attaching
CO	0.4	weakly attaching
C_2F_8	0.9	strongly attaching
CCl_2F_2	0.9	strongly attaching

SF_6	1.0	strongly attaching
c-C_4F_8	1.3	strongly attaching
c-C_4F_6	~1.7	strongly attaching
C_4F_6	~2.3	strongly attaching
2-C_4F_8	1.7	strongly attaching
1,3-C_4F_6	1.5	strongly attaching
2-C_4F_6	2.2-2.4	strongly attaching
c-C_5F_5	2.1-2.2	strongly attaching

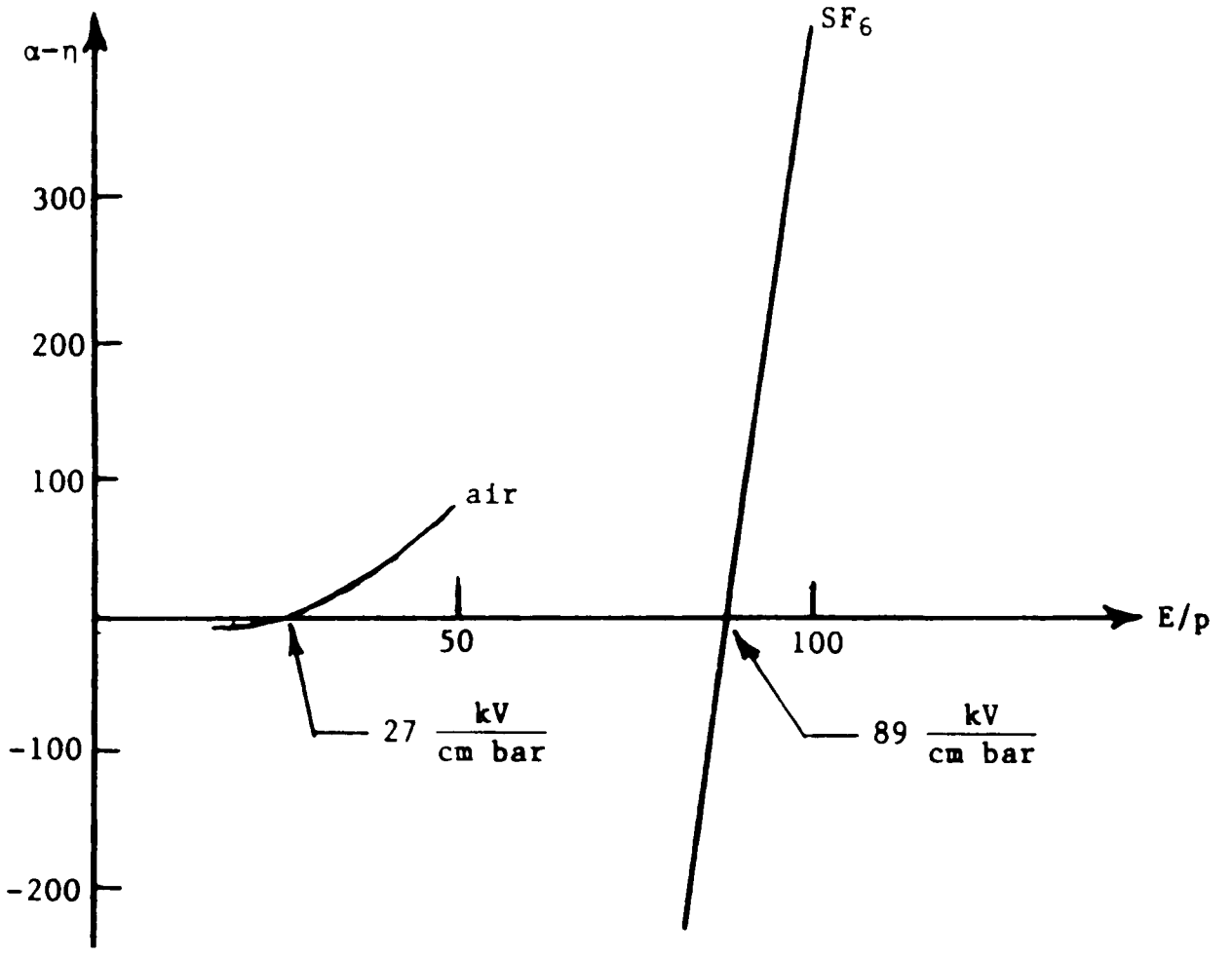

Figure 1.2 Effective ionisation coefficient in air and SF_6 [2]

Figure 1.2[2] shows the net (pressure-reduced) ionisation coefficient $(\alpha-\eta)/p$ as a function of E/p for air and SF_6. It can be seen that the critical field strength at which

$(\alpha-\eta) > 0$ is about 89kV/cm·bar in SF_6, compared to only about 27 kV/cm·bar in air. This explains the high dielectric strength of SF_6 relative to air as no build up of ionisation can occur until the field exceeds the critical value.

It is worth noting the steep slope of the curve of $(\alpha-\eta)/p$ versus E/p in SF_6. It means that SF_6 is a relatively "brittle" gas in that, once E_{crit} is exceed, the growth of ionisation is very strong. i.e. in a uniform electric field it will never break down when the field is below the critical value of 89kV/cm·bar, but should this value be exceeded by even a small amount breakdown is inevitable. This is significant in situations where stress-raising defects are present in gas-insulated equipment as intense ionisation activity will occur in the regions where $E>E_{crit}$ and this may initiate complete breakdown of the insulation.

1.1.4 Arc interruption properties

The choice of SF_6 for high power circuit breakers does not rely only upon its dielectric strength, but depends also upon its excellent arc quenching and control properties. At elevated temperature SF_6 dissociates into a large number of fragments which include highly reactive radicals. As a result, careful choice of materials for the arcing chamber is required, as is the need of high SF_6 purity.

The net radiated power from an SF_6 arc is less than from an air arc and a greater proportion of the emitted radiation is absorbed by the surrounding gas. Consequently

less radiation damage occurs to the circuit breaker enclosure with SF_6 than with air and a more controlled heating of the surrounding gas can be achieved.

When the current is at its peak. the core temperature of the arc plasma in SF_6 is in the region of 15-20,000K, which is similar to the arc temperature in air. However cooling is much more effective in SF_6, which for gas-blast condition has a convective cooling efficiency about four times that of air. As a result the arc diameter in SF_6 is less than half that in air at the same current.

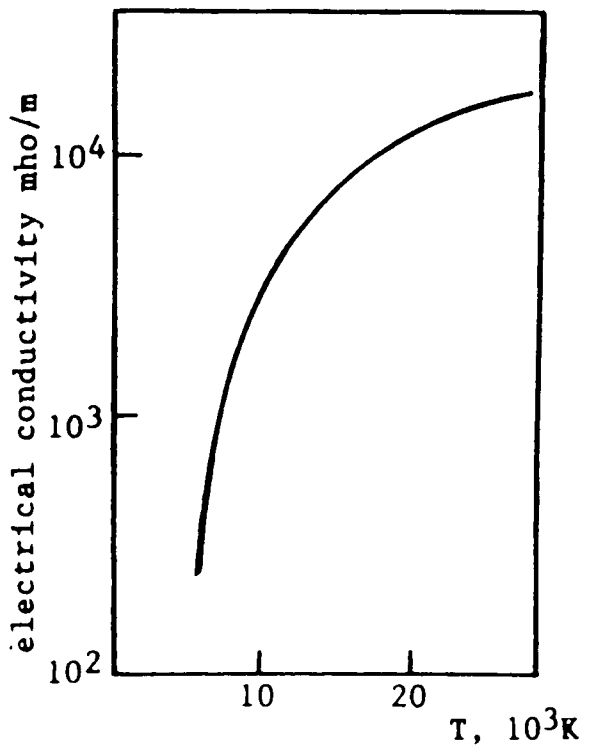

Figure 1.3 Electrical conductivity versus temperature in SF_6 [2]

As the current falls towards current zero the temperature of the residual arc column falls, there is a rapid drop in the electrical conductivity of the plasma (Figure 1.3[2]) as electrons are attached to form low-mobility negative ions. Because of the

electronegative nature of the dissociation fragments of SF_6 this rapid fall occurs at temperatures of ~8000k at which the gas is still fully dissociated.

During the thermal recovery period immediately after current zero, it is the thermal radial conduction which is the controlling mechanism, because of the small arc cross section and steep temperature gradient. As the temperature of the arc column falls below ~3000°C there are strong peaks in the thermal conductivity, because of the enhanced thermal diffusion associated with recombination processes and dissociation of the cold gas surrounding the arc column(Figure 1.4[2]). It is the combination of the rapid fall in electrical conductivity(reducing the power input to the column), followed as the arc cools further by a rise in the thermal conductivity, which is responsible for the very rapid thermal recovery of SF_6. The decay of arc conductance near current zero is approximately four times faster in SF_6 than in air.

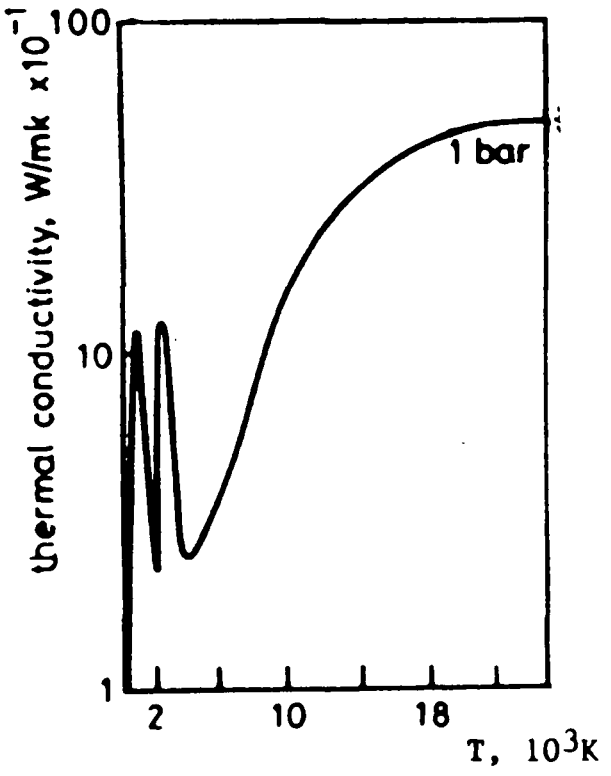

Figure 1.4 Thermal conductivity versus temperature in SF_6[2]

1.2 Basic breakdown mechanism

1.2.1 The Townsend breakdown mechanism

In the early 1900's, J.J.Thomsom[4] and J.S.Townsend [5]. working in the Cavendish laboratory, Cambridge, investigated the spatial development of ionisation in gases at low pressures and with potentials of less than 1000V. Resulting from this work was the now well known "Townsend Theory" of breakdown.

The Townsend theory of current growth describes the development of ionisation in uniform field. Consider the effect of increasing voltage applied to a pair of uniform field electrodes, one of which is emitting photo-electrons due to external irradiation(e.g., cosmic rays — which can produce approximately 40 ion pairs/$cm^3 \cdot MPa$[6], UV irradiation and background radiation etc). At moderately low voltages, ejected electrons return to the cathode due to back diffusion as a result of collisions with neutral gas molecules. If the voltage is increased sufficiently all of the liberated electrons are swept from the cathode and collected at the anode. This condition is indicated by saturation in electron current and the value of the anode current is directly related to the intensity of the external source of radiation. With further increase in applied voltage, liberated electrons can gain sufficient kinetic energy from the applied field to ionise, by collisionally created electrons may also be accelerated by the field, forming new electron avalanches and amplifying the number of free electrons.

At normal temperature and pressure. gases are excellent insulators. but due to factors such as cosmic radiation and radioactive substance present in the earth and the atmosphere, some free electrons and ions are always present. Under the influence of an electric field. these free electrons may gain sufficient energy to ionise a neutral molecule on collision. The number of new electrons produced by an electron per unit length of path is called the Townsend first ionisation coefficient. The electron-ion pair formed gives rise to accumulative processes which will eventually lead to an avalanche.

In developing the generalised Townsend theory of breakdown, all the relevant processes which change the state of ionisation in the gas must be considered. besides the fundamental processes mentioned above. These include the secondary ionisation processes, the processes of electron attachment , the process of detachment and also the ion conversion processes. However, the effects of some of these processes may be neglected without significantly affecting the final result. as their influences are weak. An example of this is that the positive ion ionisation in uniform field can be neglected as its probability of occurrence is small. Another example is that breakdown by the secondary photo ionisation process, can only occur under a very restricted condition.

In the detachment process, electrons are removed from the negative ions. In the case of an avalanche development where the effect of secondary ionisation is negligible. detachment will not only modify the electron current during the electron transit time.

but it will also result in an electron current which persists for much longer than that in its absence. In ion conversion processes, positive and negative ions are converted from one species to another in collisions with gas molecules, to yield light mobile electrons.

The secondary ionisation processes are those processes which follow as a consequence of the transfer of energy gained by the electrons in the avalanche to atoms. These processes become more influential at higher voltages. The electron attachment processes are those which occur in electronegative gases like SF_6, where free electrons, when they come into the vicinity of an atom, are captured to form stable and immobile negative ions by one of several possible processes. These processes deter the growth of ionisation and also breakdown.

- Ionisation and attachment coefficients

The ionisation and attachment coefficients have been measured by many workers including Behalf et al [27]. However these were confined to low gas pressure(up to 200mm Hg only). Thus an extrapolation is necessary for most practical applications. Kuffel et al [29] had shown that the variation of the effective ionisation coefficient over a wide range of pressure follows the empirical equation,

$$\frac{\alpha - \eta}{p} = A\frac{E}{p} - B \qquad (1.1)$$

in which A and B are constants whose values are 27.7/(kV) and 2460/cm· bar, respectively, and p is the gas pressure measured in bar. The critical field strength is therefore,

$$E_{crit} = \frac{B \cdot p}{A} = 89 kV / cm \cdot bar$$

This simple relationship is useful in estimating onset voltages in SF_6 insulation.

The number of free electrons in an avalanche will increase in any region where (E/p) exceeds $(E/p)_{lim}$ and will decrease otherwise . Therefore, an avalanche will either grow or decay during its transit across the gap.

Townsend defined the primary ionisation coefficient α as the average number of ionising collisions made by one electron travelling a unit distance. It was then predicted that the number of electrons and positive ions grows exponentially with the distance x from the original position of the seed ionising electron:

$$N_e(x)=N_e(0)\, e^{\alpha x} \qquad (1.2)$$

It should be noted that the above is only true for non-attaching gases(i.e., gases in which all the regenerated electrons are free to gain energy from the applied field.). The widely used insulant SF_6 is, however, a highly electron attaching gas due to the high electron affinity of the fluorine atoms in the SF_6 molecules. Electrons tend to attach to the molecules and form negative ions. The high mass to charge ratio of the

negative ions means that it is difficult for negative ions to accelerate under the applied field and to cause new ionisation. A parameter called the electron attachment coefficient η can be defined in the same way: η is the average number of attaching collisions made by one electron travelling over a unit distance. The exponential growth function of the number of electrons $N_e(x)$ is then modified to the following.

$$N_e(x)=N_e(0)\, e^{(\alpha-\eta)x} \qquad (1.3)$$

In order for this ionisation avalanche to continue, a regenerative or secondary process must be present to ensure that each avalanche can cause the production of at least one electron which can successfully initiate a further new avalanche. In uniform field gaps and non-attaching gases, the secondary processes are thought to be predominantly the release of electrons from the cathode surface: processes like photoelectric effect, positive ion bombardment and the incidence of metastable molecules.

The generalised Townsend type breakdown criterion can be written as:

$$\frac{\omega}{\alpha}\exp[\int_0^x \alpha(E/P)dx] = 1 \qquad (1.4)$$

$$\frac{\omega}{\alpha} = \frac{\beta}{\alpha} + \frac{\eta}{\alpha} + \gamma + \frac{\delta}{\alpha} + \frac{\varepsilon}{\alpha} \qquad (1.5)$$

where:

ω/α is the generalised secondary process in the gas. β is the coefficient of ionisation of gas molecules in collision with positive ions. η is the photo-ionisation coefficient, γ, δ and ε are the cathode secondary emission rate due to respectively the positive ions, photons and excited atoms.

• Paschen's law

The Townsend criterion, enables the breakdown voltage of the gap to be determined by the use of appropriate values $\overline{\alpha} / p$ and γ corresponding to the value E/p without ever taking the gap currents to high values, that is keeping them below 10^{-7} A, so that the space charge distortions are kept to minimum, and more importantly so that no damage to electrodes occurs. For short or long gaps and relatively low pressures, for which this criterion is applicable, good agreement has been found[7] between calculated and experimentally determined breakdown voltages.

An analytical expression for the breakdown voltage for uniform field gaps as function of gap length and gas pressure can be derived from the above equation (1.4) by expressing the ionisation coefficient $\overline{\alpha} / p$ as a function of field strength and gas pressure. If we put $\overline{\alpha} / p = f(E / p)$ in the criterion equation, the following can be obtained

$$e^{f(E/p)pd} = 1/\gamma + 1 \qquad (1.6)$$

or

$$f(E/p)pd=\ln(1+1/\gamma)=K \quad (1.7)$$

For uniform field $V_b=Ed$, where V_b is the breakdown voltage,

$$e^{f(Vb\,pd)}=K \quad (1.8)$$

or

$$V_b=F(pd) \quad (1.9)$$

which means that the breakdown voltage of a uniform field gap is a unique function of the product of pressure and the electrode separation for a particular gas and electrode material. Equation 1.8 is known as Paschen's Law which was established experimentally in 1889. The Law does not, however, imply that the sparking voltage increases linearly with the product *pd*, although it is found in practice to be nearly linear over certain regions. The relation between the sparking voltage and the product *pd* takes the form shown in Figure 1.5[110]. The breakdown voltage goes through a minimum value(Vb_{min}) at a particular value of the product(pd_{min}).

It is often more convenient to use the gas density δ instead of the gas pressure p in equation 1.8, since in the former case account is taken for the effect of temperature at constant pressure on the mean free path in the gas. The number of collisions by an electron in crossing the gap is proportional to the product δd and γ.

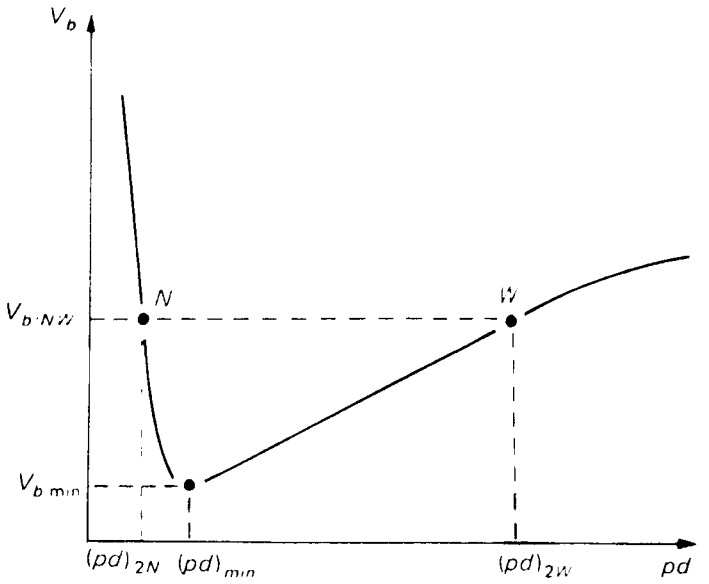

Figure 1.5 The sparking voltage-*pd* relationship (Paschen's curve) [110]

Atmospheric air provides the basic insulation for many practical high voltage installations(transmission lines, switchyards, etc). Since the atmospheric conditions(temperature and pressure) vary considerably in time and locations, the breakdown characteristics of various apparatus will be affected accordingly. For practical purpose, therefore, the breakdown characteristics can be converted to standard atmospheric conditions(p=760 Torr = 1.01 bar and t=20°C =293°K). Correction for the variation in the ambient conditions is made by introducing the relative density as

$$\delta = \frac{p}{760}\frac{293}{273+t} = 0.386\frac{p}{273+t} \qquad (1.10)$$

the breakdown voltage at standard conditions multiplied by this factor gives the breakdown voltage corresponding to the given ambient conditions approximately

$$V_b(\delta)=\delta V_b(\delta=1) \qquad (1.11)$$

Paschen's Law is found to apply over a wide range of the parameter values up to 1000-2000 Torr·cm. At higher products, however, the breakdown voltage(in non-attaching gases) is found to be somewhat higher than at smaller spacing for the same values of pd. This departure is probably associated with the transition from Townsend breakdown mechanism to the streamer mechanism, as the product pd increases above a certain value. We have seen that the streamer breakdown criterion is satisfied at higher values of $\overline{\alpha}d$ from about 8-10 to 18-20. At very low pressure deviations from Paschen's Law are observed when the breakdown mechanism ceases to be influenced by the gas particles and becomes electrode dominated(i.e., vacuum breakdown).

1.2.2 The streamer breakdown criterion

The Townsend theory of breakdown has been found to agree with experimental results obtained at low values of *pd*(<1000 Torr cm). For higher values of *pd*, however, the Townsend theory has severe limitations, especially under fast impulse voltage conditions where breakdown can occur in times faster than that predicted using electron avalanche velocities which are around 10^7 cm/s. Since the Townsend theory of breakdown involves regenerative processes it predicts the time to breakdown to be greater than at least one electron transit time. It has been shown[9,10] that when impulse voltages, of peak value greater than the dc breakdown level, are applied to a uniform field then the time lag can be considerably

less than the transit time. The time to breakdown is of the order of 10^{-7} second, reducing to 10^{-8} second with increasing voltage. Although the Townsend breakdown criterion applies for certain experimental conditions, an alternative process must be considered for impulse voltages and for larger values of *pd*. Also in nonuniform fields, for example in a point-plane gap geometry, the cathode has been found to play no role in the discharge because the breakdown voltage is independent of the cathode electrode material. Therefore, there must be a regenerative process occurring in the gas.

Reather[11] and Meek[12] simultaneously, although independently proposed similar theories taking into consideration the influence of the space charge field on the development of the discharge. Both of these theories predict that the filamentary ionisation phenomena called the streamer, will occur if the space charge field reached the magnitude of the applied field.

Reather proposed that breakdown could occur by a streamer mechanism when the number of electrons in an avalanche reaches a critical value at about 10^8, while Meek suggested that breakdown could occur when the radial space charge field at the tip of the streamer becomes comparable to that of the applied field. Both processes assume that photoelectrons in the gas produce secondary avalanches which augment the main avalanche. Due to the incidence of secondary avalanches, high space charge concentrations are created which propagate towards both the anode and cathode. The velocities of propagation can attain value which are significantly greater than electron avalanche velocities in undistorted fields. In both the Reather and Meek

criteria the field at the avalanche head is important. Approximate value of the space charge field can be calculated by assuming that all electrons are contained in a spherical volume of radius *r*. The field at the avalanche head for Raether's Criterion is given by.

$$E_r = \frac{qe^{\alpha x}}{4\pi\varepsilon_0 r^2} \qquad (1.12)$$

Meek gave the expression for the field at the head of the avalanche as

$$E_r = \frac{q\alpha e^{\alpha x}}{3\pi\varepsilon_0 r} \qquad (1.13)$$

where q is the electronic charge in both cases. In Raether's field equation, all the electrons are contained within the spherical avalanche head whereas Meek considered only those electrons which are just generated. The value of *r* in Raether's analysis is obtained from the diffusion equation where $r = \sqrt{2DT}$ and D is the electron diffusion coefficient. The transit time T is the time taken for the electrons to move from x=0 to x and can be expressed by relationship $T = \frac{x}{\mu E}$, where μ is the electron mobility. Meek's analysis takes slightly different approach by considering the avalanche radius as being a function of the energy lost per collision.

With further substitution and replacement with known values and constants, Raether and Meek expressed the streamer criterion for air as, respectively,

(1.14)

$$\left(\frac{E}{p}\right) - \frac{1}{2}\ln(pd) + \ln(d) \qquad (1.15)$$

ng.

criterion is often regarded as being satisfied when an electron itical number of 10^8 electrons(i.e., αd=18). Therefore if an electrons, breakdown will be preceded by a streamer.

eamer discharge has been verified both numerically and sidering the influence of space charge on avalanche growth, able to show, by a computer simulation technique, that rapid could be adequately explained by considering only the vicinity of the avalanche head [13]. This analysis was ly by Chalmers et al, who, using high speed photographic with increasing overvoltage, there was a transition from a of discharge(i.e. Townsend) to an accelerated form of which could cause breakdown in less than one electron

few mathematical expressions of the above model[15]. Pedersen[16] pointed out that due to the dominating influence of the exponential

growth which is associated with the electron avalanche development. all such expressions can be reduced to the following expression.

$$\int_0^{z_0} \overline{\alpha}(z)dz = k \qquad (1.16)$$

where $\overline{\alpha}$ is the effective coefficient of ionisation. z_0 is the critical avalanche length and k is a dimensionless parameter and is usually assumed to have a value of 18 for SF_6[16].

1.2.3 The leader breakdown process

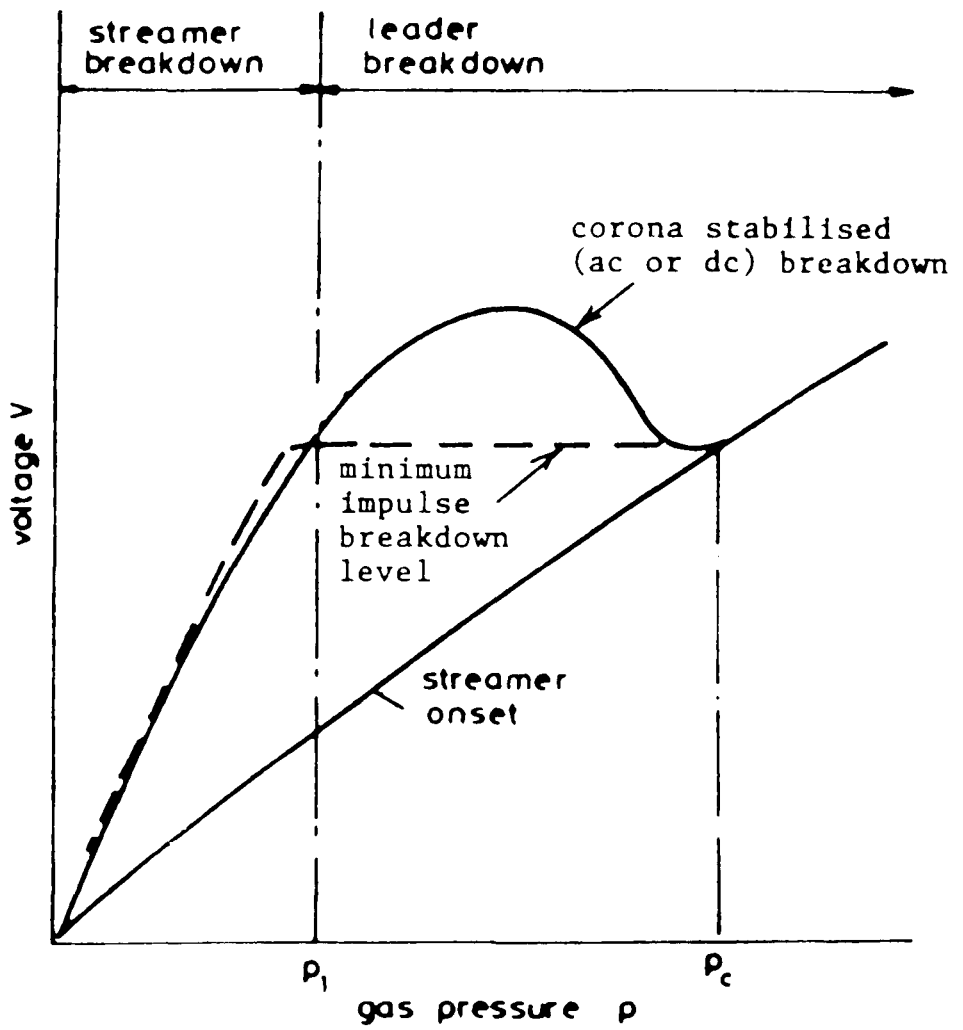

Figure 1.6 Idealised V-p characteristics for minimum-impulse(leader) breakdown and corona-stabilised(ac or dc) breakdown in a point-plane gap in SF_6[17]

Figure 1.6[17] is the idealised V-p characteristics for leader breakdown and ac or dc breakdown in a point-plane gap in SF_6. When the gap pressure is above P_1(the typical value is 0.5 bar) in Figure 1.6, there is a progressive loss of the effectiveness of the space charge shielding at the point and the breakdown mechanism change to one involving the development of leader discharges. Unlike streamer discharges, leaders are "hot" discharges which have an estimated temperature at about 2000K[18] and dissociation of the gas molecules can occur. The higher temperature means that the neutral density inside the filamentary leader channel is reduced when the thermodynamic expansion process occurs. The neutral density N is related to the optical quantity the refractive index n by Giadston's equation,

$$n-1=KN \qquad (1.17)$$

K being the Giadston's constant. The change of neutral density and hence the refractive index means that the leader channel can be revealed by the Schlieren method[19,20,21,22] and the interferometers[23,24].

For SF_6, the leader breakdown in short gaps at high pressure bears a similarity to the long gap air breakdown. When the voltage is below the leader inception level, the impulse corona is the only phenomenon observable. With the voltage above the leader inception level, streamer to leader transition takes place in the following way. There is a break or "dark period" when the light emission of the corona has ceased. Very little knowledge exists of what happens in this period, except some speculation

that there is probably a progressive increase in the conductivity of the discharge channel due to the increased ion density[17]. The duration of the dark period seems subject to statistical fluctuation. This dark period is followed by the sudden appearance of a new ionisation phenomenon close to the boundary of the corona, which is denoted by the term "leader precursor"[18]. The precursor is asymmetrical in its propagation. The cathode directed end does not propagate into the gap much beyond the corona boundary, while the other end quickly approaches the anode.

When the precursor touches the anode, a new corona is launched from the other end. the channel has become the first leader section serving as a virtual electrode for the second corona. The next leader section is formed in exactly the same manner except for one detail. The old leader section produces re-illuminations which are associated with measurable current pulse whereas the precursor re-illuminations are not(Figure 1.7[18]).

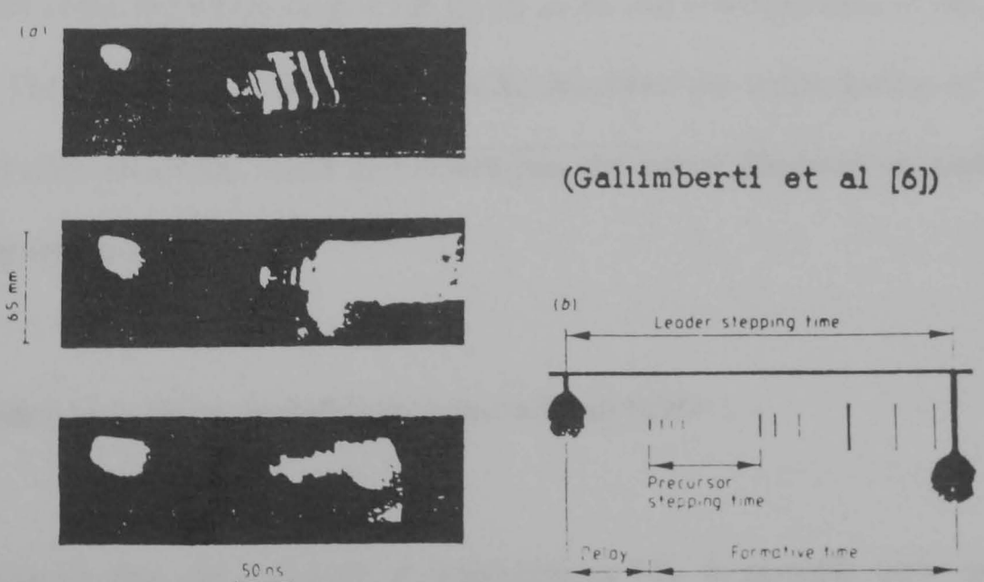

(a) Three examples of details of precursor structure in the rod plane gap at p=0.5 bar. The light gain increases from top to bottom. (b) A sketch of the streamer to leader transition with a definition of characteristics times.

Figure 1.7 [18]

The impulse voltage at which breakdown takes place by a leader mechanism is lower than that required for static breakdown. The relatively flat voltage to pressure characteristic for lightning impulse indicates that the minimum voltage for leader propagation is independent of gas pressure[25]. This characteristic of leader breakdown is also predicted by Pinnekamp and Niemeyer in a theoretical model[26], which concludes that leaders are able to propagate, provided their head potential U exceeds a critical voltage, U_{cr},

$$U_{cr} = \text{constant} \cdot \left(\frac{dC}{dXc} \right)^{-\frac{1}{2}} \qquad (1.18)$$

The constant includes the thermodynamic properties of the gas and some integral characteristics of the ionisation zone at the leader head, and is independent of the gas pressure P. The differential capacitance dC/dXc describes the redistribution of the electric field with advancing leader and determines the related displacement current input into the leader head.

1.3 Breakdown in uniform and slightly non-uniform fields

It is well known that the build-up of ionisation in SF_6 is possible only under conditions where the pressure-reduced field exceeds a critical value E_{crit} of about 89kV/cm·bar. For highly divergent fields(as, for example, for the case of a sharp protrusion on a high-voltage conductor) ionisation will be confined to a critically-

stressed volume around the tip of the protrusion. In this situation localised partial discharges, or corona, will be the first phenomena observed as the applied voltage is increased. Breakdown under these conditions is a complex process, because of the effect of the space charge injected by the prebreakdown corona.

As any stress-raising defect in gas-insulated equipment will result in partial discharge activity, it is important to understand nonuniform field discharge mechanisms. However, GIS and many other high voltage apparatus are designed for relative low field divergence and it will be useful firstly to consider the simple case of breakdown in SF_6 under uniform-field conditions before reviewing the phenomena associated with particulate contamination or other defects.

1.3.1 Breakdown in uniform field

As mentioned before for a perfectly uniform field(e.g. plane-plane electrode geometry) no ionisation activity can occur for field less than about 89kV/cm·bar. Above the level, ionisation builds up very rapidly and leads to complete breakdown of the insulation(formation of an arc channel). The first stage of the breakdown involves the development of an "avalanche" of electrons. The growth of this avalanche from a single "starter" can readily be found by computing the net electron multiplication. Considering a "swarm" that has grown to contain n(x) electrons at position x in the gap (Figure 1.8[71]), then in travelling a further increased discharge dx, these will generate a net new charge:

$$dn(x)=(\alpha-\eta)n(x)dx=\overline{\alpha}\, n(x)dx \qquad (1.19)$$

as a result of ionising and attaching collision with neutral molecules. where $\overline{\alpha}$ is the effective ionisation coefficient. Integration over the interval 0 to x gives the electronic charge in the avalanche tip at that stage in its growth:

$$\int_0^x \frac{dn(x)}{n(x)} = \int_0^x \overline{\alpha} dx \qquad (1.20)$$

therefore

$$n(x) = e^{\int_0^x \overline{\alpha} dx} = e^{\overline{\alpha} x} \qquad (1.21)$$

In crossing the whole gap, an avalanche of $e^{\overline{\alpha} d}$ electrons is created.

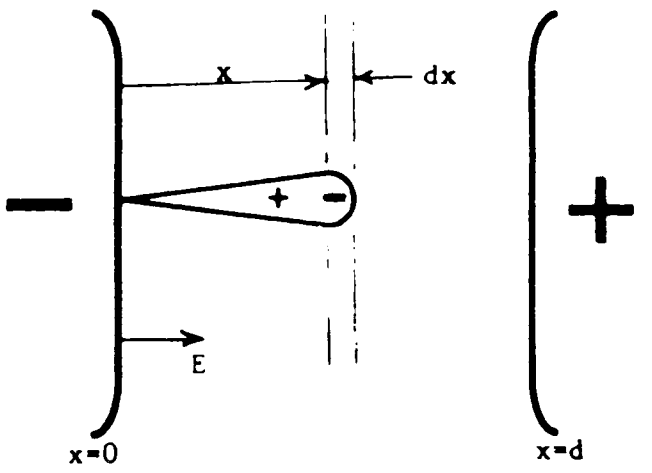

Figure 1.8 Development of an electron avalanche in a uniform-field gap[71]

In itself, the occurrence of avalanches does not constitute breakdown. For example, if the field was such that $\overline{\alpha}=5$ then, in a 1cm gap at 1 bar, the current gain would be $e^5(\cong 148.41)$. The very low "background" conduction current density(due to collection of free charges present in the gap) would be increased from about 10^{-13} A/cm^2 to about 10^{-11} A/cm^2, but the gap would still be a very good insulator.

However, $\overline{\alpha}$ increases very quickly when the field exceeds E_{cirt} and the multiplication can rapidly reach values of 10^6 or greater, with most of the charge confined to a very small region at the head of the avalanche, typically a sphere of about 10μm radius.

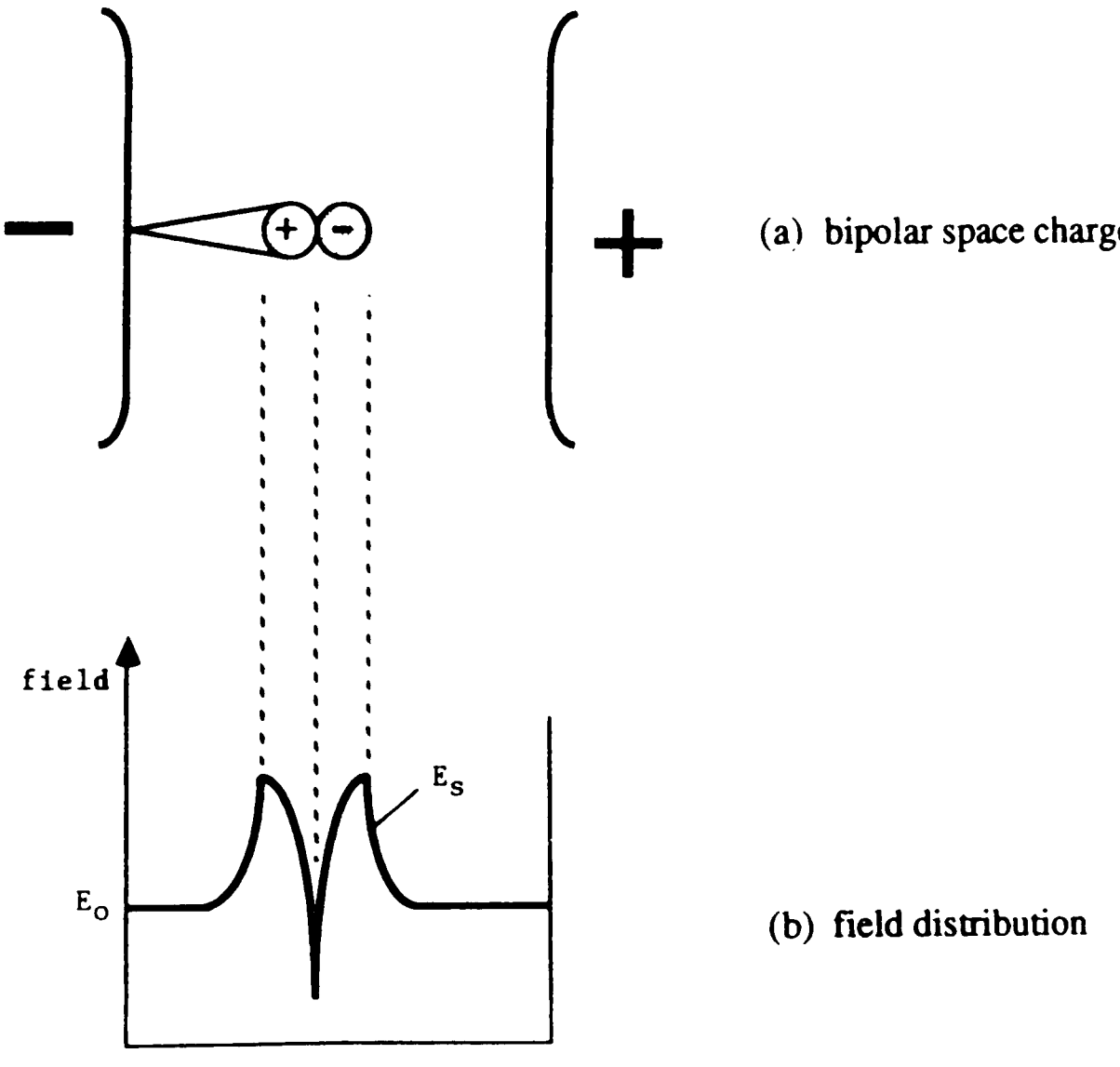

Figure 1.9 Field distortion caused by a large electron avalanche [71]

The bipolar space charge resulting from the ionisation process is shown in Figure 1.9(a)[71]. This results in distortion of the applied field E_0(Figure 1.9(b))such that ionisation activity ahead of and behind the avalanche tip is greatly enchanted. At a critical avalanche size ($e^{\overline{\alpha}x} = N_c$) the space-charge field E_s is high enough to generate rapidly moving ionisation fronts(streamers) which propagate at about 10^8 cm/s towards the electrodes. When these bridge the gap, a highly conducting channel is formed within a few nanoseconds

For pressures used in technical applications (p>1bar), the streamer process is the accepted breakdown mechanism in SF_6 under relatively uniform field conditions.

The values of ionisation and attachment coefficients have been measured in SF_6 in previous work[27,30]. Over a wide range of E/p, the effective ionisation coefficient, $\overline{\alpha}$, is described by the relationship,

$$\frac{\overline{\alpha}}{p} = A\left(\frac{E}{p}\right) - B \qquad (1.22)$$

in which A=27.7(kV)$^{-1}$ and B=2460(bar·cm)$^{-1}$. Studying the above equation, the low limit of E/p, below which $\overline{\alpha}$ is negative, the following can be concluded,

$$\left(\frac{E}{p}\right)_{lim} = \frac{B}{A} = 89\text{kV/cm}\cdot\text{bar} \qquad (1.23)$$

With field levels below the limiting field it should not be possible for breakdown to occur.

The rapid rate of change of $\overline{\alpha}/p$ with E/p accounts for the strong influence of local field distortions upon the breakdown strength observed in SF_6. In uniform and nonuniform fields the streamer criterion may be used to calculate the breakdown or inception voltage. When E is known then the streamer criterion is satisfied when.

$$\int (AE - Bp)dx = K \qquad (1.24)$$

where K is the mean electron amplification. The value of K for SF_6 has been determined by Pedersen[31] and reported as being 10.5 although other researchers[32] have used the value of 18 or even a value dependent on pd[33].

The breakdown of gases under uniform field conditions generally satisfies Paschen's law, which states that breakdown voltage is a function of the product pd. In SF_6 with pressures up to 1 bar and with pd values below 20 bar·mm, Pashen's law is obeyed, with the breakdown values tending towards the limiting field of 89 kV/cm·bar. But with higher gas pressures, a compressibility factor has to be introduced to account for the non-ideal behaviour of the gas[34].

With higher values of pd departures from Paschen's law are observed as mentioned in 1.2.1. The threshold for these departures varies depending on experimental

conditions. These conditions include electrode surface roughness, contamination of the gas by conducting particles, electrode material and the electrode area effect which will be discussed in 1.3.4.

1.3.2 Breakdown in slightly nonuniform field

If the field is varying with position across the gap, the initial avalanche formation will occur within a critical volume for which $(\alpha-\eta)>0$(i.e. E>89kV/cm·bar). Under these conditions, the streamer-inception criterion is:

$$e^{\int_0^{x_c}\overline{\alpha}(x)dx=N} \qquad (1.25)$$

where x_c is the position of the boundary of the ionisation region.

For coaxial-electrode geometry with inner radius of r_0 and outer radius of r_1, the field distribution is:

$$E(r)=\frac{V}{r}\cdot\ln\left(\frac{r_1}{r_0}\right) \qquad (1.26)$$

Also, at onset, $\alpha=0$ at position r_c, so that,

$$E(r_0)=E_{cirt}=\frac{Bp}{A} \qquad (1.27)$$

Using these relationships together with the streamer criterion, it can easily be shown that the surface field at onset is,

$$E(r_0) = \frac{Bp}{A}\left[1 + \left(\frac{k}{Bpr_0}\right)^{\frac{1}{2}}\right] \qquad (1.28)$$

and that,

$$x_c = \left(\frac{kr_0}{Bp}\right)^{\frac{1}{2}} \qquad (1.29)$$

With the above values of A and B mentioned in 1.3.1, this yields,

$$\frac{E(r_0)}{p} = 89\left(1 + 0.07\sqrt{pr_0}\right) \qquad (1.30)$$

$$x_c = 0.07\sqrt{\frac{r_0}{p}} \qquad (1.31)$$

where pr_0 is in bar·cm and x_c in cm.

Note that the streamer forms when primary avalanche has developed a relatively short distance. For r_0=8cm, p=4bar, for example, x_c will be about 1mm, the streamer

will then propagate until the combination of the space-charge field and the geometric field is unable to sustain further ionisation. In order for breakdown to occur, it will then be necessary to increase the surface field above the onset level. In the relatively low divergence field in a "clean" GIS system only very small increase above the onset voltage is necessary to initiate breakdown.

1.3.3 Surface roughness effect and particle initiated breakdown

- Surface roughness effect

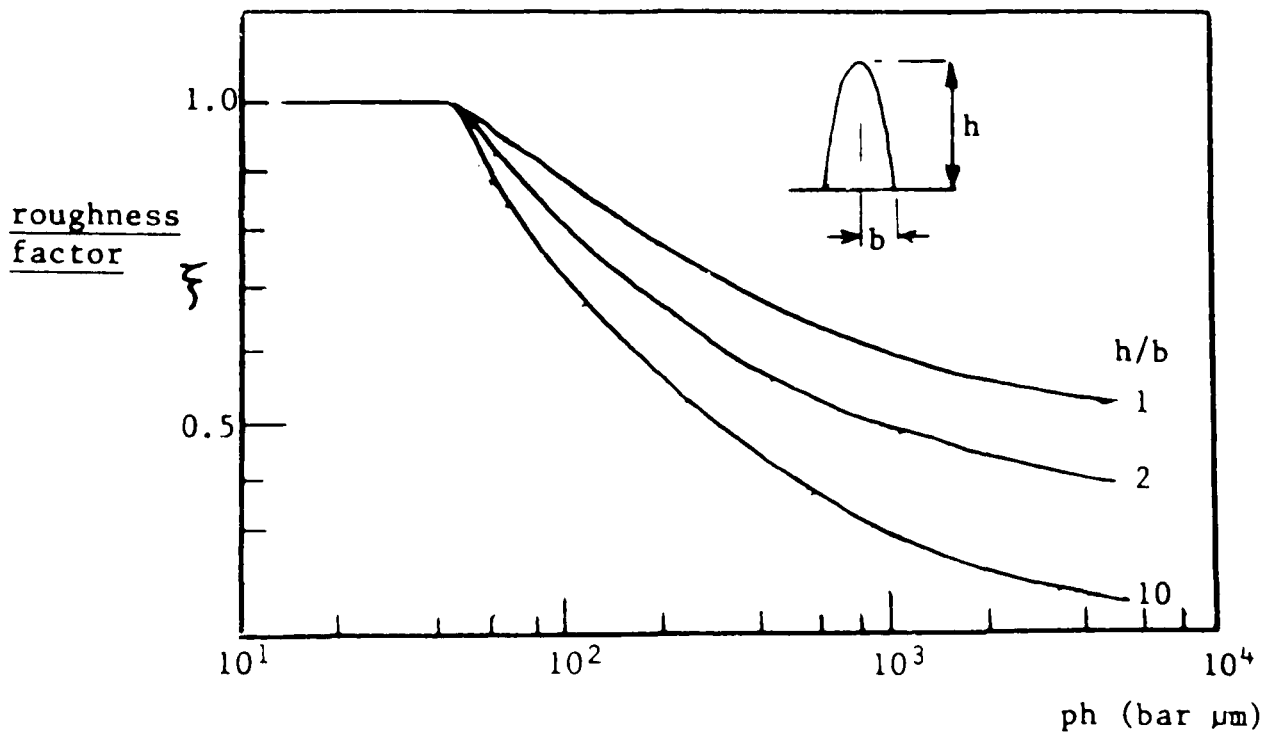

Figure 1.10[35]

Electrode surface roughness can lead to the existence of localised microscopic regions of field intensity with levels far greater than the average field at the gas

electrode boundary. Such regions of enhance field intensity can attain values which are above the limiting field and may therefore result in a reduction in the breakdown strength of the gap. For example, although laboratory measurements using polished coaxial electrodes are in agreement with the theoretical criterion that the inner surface field at breakdown should be close to the critical field of about 89kV/cm·bar, this value can not be sustained in large scale equipment with practical(machined) surface finish.

One reason for this is the fact increased ionisation occurs in the vicinity of microscopic surface protrusions (surface roughness). This results in the reduction of the breakdown field strength by a factor ξ. Figure 1.10[35] shows calculated values of the factor ξ as a function of the product ph (the product of pressure and protrusion height) for a range of spheroridal protrusions. It can be seen that the breakdown voltage can be reduced to a low level and that there is a critical protrusion size for the onset of roughness effects.

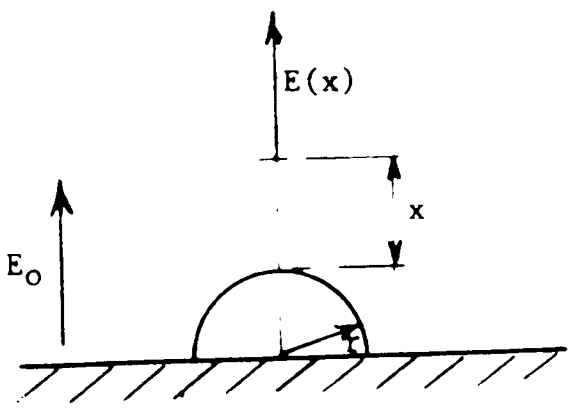

Figure 1.11 Hemispherical protrusion on a uniform-field electrode [154]

The existence of a threshold value of ph can readily be demonstrated for the hemispherical protrusion shown in Figure 1.11[154]. For this case, the field at a distance x above the protrusion is given as,

$$E(x) = E_0\left[1 + \frac{2r^3}{(x+r)^3}\right] \qquad (1.32)$$

For the protrusion to have no effect, E_0 (the macroscopic field) at onset must be equal to E_{crit} (=89kV/cm·bar),

Also,

$$\begin{aligned}\overline{\alpha}(x) &= AE(x) - Bp \\ &= Bp\left[1 + \frac{2r^3}{(x+r)^3}\right] - Bp \\ &= 2\frac{Bpr^3}{(x+r)^3} \qquad (1.33)\end{aligned}$$

Breakdown occurs when:

$$\int_0^{x_c} \overline{\alpha}(x)dx = k \qquad (1.34)$$

that is

$$2Bpr^3\left[-\frac{1}{2}(x+r)^{-2}\right]_0^{x_c} = k$$

$$1-\frac{r^2}{(x_c+r)^2} = \frac{k}{Bpr}$$

$$\frac{x_c}{r} = 1-\left(\frac{1}{1-\frac{k}{Bpr}}\right)^{\frac{1}{2}}$$

where k=12 and B=0.246/bar·μm,

$$x_c = r\left[1-(1-\frac{49}{pr})^{-\frac{1}{2}}\right] \qquad (1.35)$$

For x_c to be real, pr must be >50 bar·μm. At a working pressure of 5 bar, surface roughness would therefore begin to affect the onset level for protrusion heights greater than about 10μm. Because of surface roughness effects (and some other electrode phenomena such as microdischarges in charged oxide layers, etc), practical SF_6 insulated equipment is designed such that the maximum field is everywhere less than about 40% of the critical value.

A quantitative relationship has been determined by Pedersen[36], based on the streamer theory, for evaluating the effect of surface roughness in SF_6 insulated coaxial geometry with protrusion perturbed electrons. Form these investigations, it was suggested that if $pR_{max}<43$ bar·μm, where p is the gas pressure and R_{max} is the maximum protrusion height, then the breakdown voltage would remain unaffected by surface roughness. It was later reported by Somerville et al that the shape of the electrode protrusion was unimportant and only the protrusion height affected the breakdown strength[35].

• Particle initiated breakdown

Another type of nonuniform field breakdown in a gaseous medium is that from free conducting particles. Particles-initiated breakdown is one of the most severe problem in gas-insulated apparatus. These unwelcome contaminating particles can cause pre-discharge or even breakdown or flashover between the high voltage conductor and the enclosure. The use of compressed gas allows a much higher field strength than that at atmospheric to be applied, but at the same time increases the sensitivity to any disturbance of the field. Even pre-discharges of low current, emanating from the tip of the particle, are undesirable if they occur continuously.

Because particles are known to seriously reduce the breakdown strength of SF_6 significantly, provision is made in the design of most GIS equipment to remove particles by various filtering and trapping techniques. In a number of work[92,93,94,95], various aspects of this problem have been addressed.

Measurements of particle-initiated breakdown have been performed under a variety of conditions corresponding to different gas pressures and compositions, different forms and polarities of the applied voltage, and for different types, sizes, and configurations of metallic particles, these studies clearly show the dramatic decrease in the voltage withstand capabilities of SF_6 in the presence of particles. They also show that the breakdown voltage of SF_6 gas becomes virtually independent of gas pressure as the particle length increase.

For dc stress, particles will cross the gap at the onset voltage. For ac conditions, the particles initially make small "hopping" excursions at the outer electrode in a coaxial system. As the stress is increased, the excursions become longer and, because of inertial effects and the "bouncing" action at the electrode, the time of flight becomes longer. As the voltage is increased particles may cross the gap to the upper electrode where they will receive a new charge which depends on the polarity and magnitude of the applied voltage at the instant of contact, and will then move back towards the lower electrode. The crossing does not necessarily lead to breakdown, and a voltage increase will usually be necessary for the conditions for the leader breakdown to be achieved.

Although most studies have shown that conducting particles can drastically reduce the electric strength of SF_6 to as low as 10% of its uncontaminated value, it is very difficult to predict the magnitude of the reduction in the breakdown and the corona inception voltage, because these magnitudes depend on many factors, involving the particle and the insulation system.

1.3.4 Electrode area and material effect

In SF_6 the uniform field breakdown strength can be recovered by conditioning the electrodes[37]. This involves vapouring electrode weak points by repeated sparking until the breakdown strength has sufficiently increased. As the number of weak points is related to the area of the electrodes comparatively more conditioning is required for large-electrodes than for smaller ones[38]. If the electrodes have been conditioned at one pressure they are normally required to be re-conditioned if the gas pressure is changed[38]. Many quoted breakdown values represent the conditioned values whereas, unfortunately, from a practical approach, the pre-conditioned breakdown values, as well as because of the electrode surface finish, would be of greater interest.

The choice of electrode material has been found to have no influence on the breakdown characteristics of SF_6 for low values of pd. However, for high values of pd, where deviations from Paschen's law occur, the choice of electrode material is significant[37]. The breakdown voltage is primarily dependent on the cathode material, and this influence increases with the increasing gas pressure.

1.4 Breakdown in nonuniform field

The breakdown characteristics in nonuniform fields are more complicated than in uniform fields. In SF_6 insulated equipment, however, nonuniform fields are

inevitable. Highly divergent field conditions can exist locally due to the presence of free conducting particles, or electrode surface protrusions, and therefore there is considerable interest in the electrical breakdown characteristics of nonuniform field gaps in SF_6 and its mixtures. In Figure 1.12[39] is illustrated schematically the dependence of the breakdown voltage for a nonuniform field gap typical of point-plane geometry[39,40]. The breakdown voltage for such a system can be calculated using the streamer criterion when the pressure P exceeds a critical value P_c, which is itself a function of the type of applied voltage (e.g., dc or impulse voltage), for $P<P_c$, the estimated breakdown voltage coincides with the corona inception voltage, but the actual breakdown occurs at a higher voltage. Corona discharges occur only for $P<P_c$ and in the pressure region below P_c, they prevent breakdown from occurring at the predicted value. The enhancement in the breakdown voltage for pressures below P_c has been referred to as "corona stabilisation". It should be noted, however, corona stabilisation is largely absent or minimal for non-electronegative gaseous dielectrics such as N_2 gas. The increase in breakdown voltage when corona occurs is attributed primarily to the effect of space charge produced by the corona in reducing the local field. It was pointed out recently[41] that under some conditions, corona discharges produce electronically excited molecules in sufficient number to contribute to an enhancement in breakdown voltage. This can happen because electrons are known[42,43] to attach to molecules in electronically excited states with higher probability, i.e., with larger cross sections, than to molecules in the ground electronic state.

The breakdown voltage-pressure characteristics of such gaps show an almost linear increase up to a pressure P_1, with the breakdown voltage V_b being considerably greater than the corona-inception voltage V_i. As the pressure is increased, the breakdown curve exhibits a maximum, after which V_b fails rapidly until the pressure reaches a value P_c'. At a critical pressure P_c (which may coincide with P_c' or be considerably greater, depending on the field divergence) breakdown occurs directly at the inception voltage, without any preceding corona. The pressure range in which V_b exceeds V_i is known as the corona-stabilisation region, in which the field near the high stress electrode is stabilised near its onset value as a result of the homopolar space charges generated by corona.

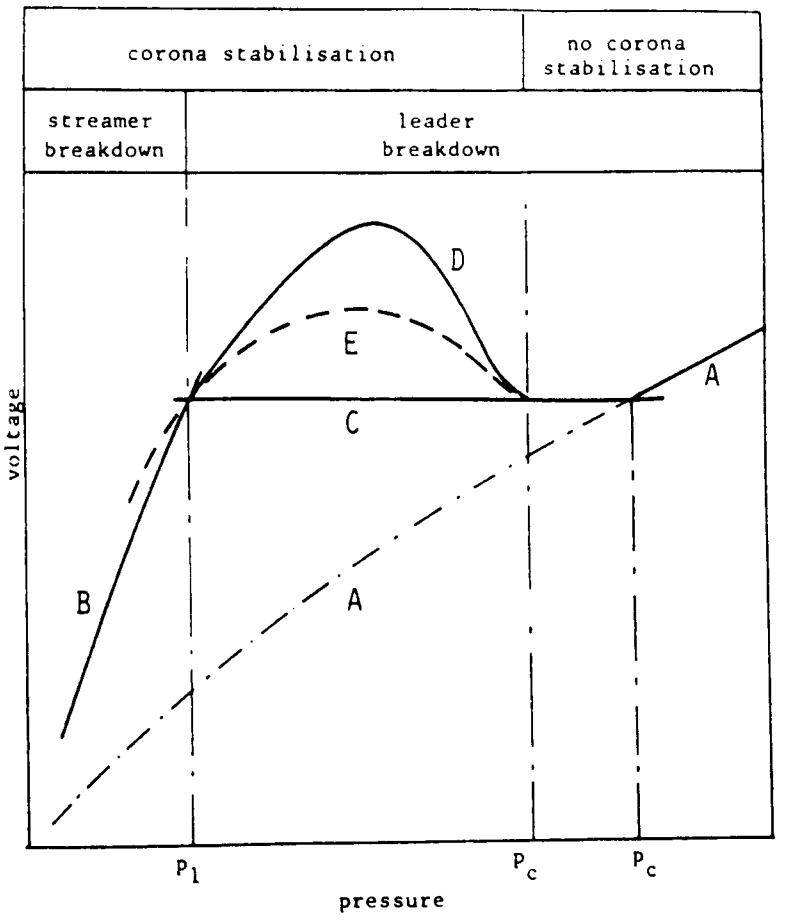

A: onset, B: streamer breakdown, C:minimum leader breakdown voltage, D: dc breakdown E: impulse breakdown

Figure 1.12 Breakdown regimes in nonuniform fields in SF_6[39]

1.4.1 Breakdown under steady-state voltages

For dc voltages, at gas pressures up to P_1, breakdown is preceded by a corona discharge at the point electrode. The space charges produced as a result of the corona limit the field around the point to the corona inception level. At the same time, the field in the remainder of the gap is enhanced. Breakdown takes place at a voltage considerably higher than the value for inception. For gas pressures above P_1, the effectiveness of corona stabilisation decreases, and the breakdown curve exhibits a maximum breakdown voltage. With further increases in pressure a negative voltage-pressure gradient is found to occur. The reduction in breakdown voltage with increasing pressure ceases when the "critical pressure" is reached. At the critical pressure P_c, and above, the breakdown voltage is found to coincide with the corona inception level, both of which increase with pressure.

1.4.2 Corona and its effect on breakdown

In uniform and quasi-uniform field gaps, the onset of measurable ionisation usually leads to complete breakdown of the gap. In non-uniform fields various manifestations of luminous and audible discharges are observed long before the complete breakdown occurs. These discharges may be transient or steady states are known as coronas. A review can be found on the subject [96] and the phenomenon is of particular importance in high voltage engineering where non-uniform fields are unavoidable. It is responsible for considerable power losses from high voltage

transmission lines and often leads to deterioration of insulation by the combined action of the discharge ions bombarding the surface and the action of chemical compounds that are formed by the discharge. It may give rise to interference in communications systems. On the other hand, there are various industrial applications such as ozone production, high-speed printing devices, electrostatic precipitation, paints sprayers, Geiger counters, etc. and more recently the use in the fabrication process of semi-conductor devices.

A great deal of interest has been directed towards understanding the mechanisms of electrical coronas in air. It is therefore useful to review corona discharges in air and use the knowledge in an attempt to understand corona discharge in SF_6, which are not fully understood. A qualitative analysis of electrical corona usually involves a cataloguing of the various types by voltage and polarity of the stressed electrode, as well as the pressure and nature of the gas.

The most convenient electrode configurations for the study of the physical mechanism of corona are hemisherically capped rod-plane or point-plane gaps. In the former arrangement, by varying the radius of the electrode tip, different degrees of field non-uniformity can be readily achieved. The point-plane arrangement is particularly suitable for obtaining a high localised stress and for localisation of dense space charge.

A number of recent studies[44-47] of the influence of factors such as field divergence, electrode geometry, polarity and spacing on corona-stabilised breakdown

have been conducted. Among the most important features are those illustrated for point-plane geometry in Figure 1.13[44], namely that the breakdown in the rising part of the characteristic is independent of the radius r_0 of the high stress electrode, and that the width of the stabilisation region, and hence the critical pressure P_c, increases as r_0 is reduced. Under impulse conditions, the behaviour at pressures greater than P_1 depends on impulse risetime[48,49] and on the availability of initiatory electrons[50,51]. The stabilisation peak is more pronounced with a switching-impulse risetime at about 100μs than for a front of less than 10μs[48]. For risetime of about 1μs the characteristic can be relatively flat in the pressure range from P_1 to P_c[51,52].

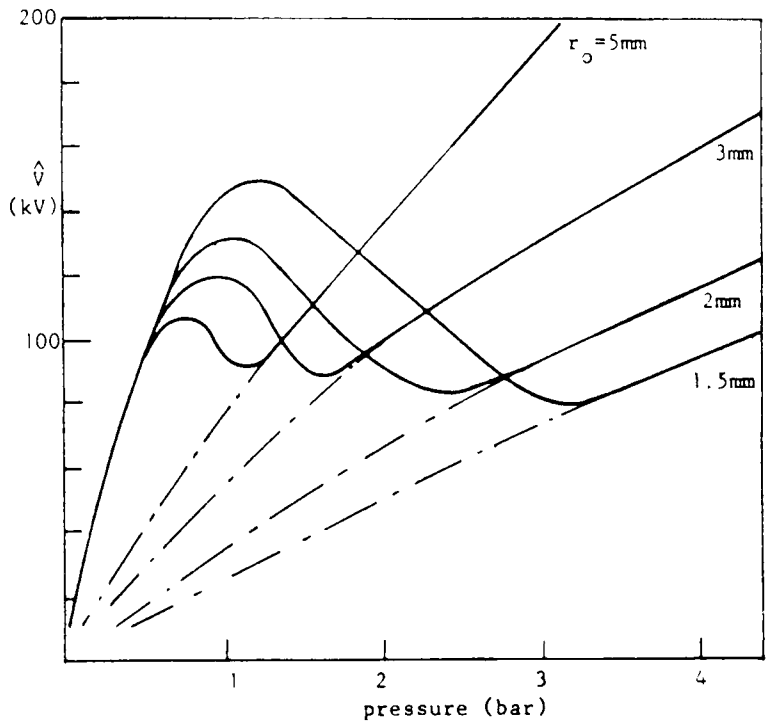

Figure 1.13 AC corona-onset and breakdown-voltage characteristics for a 40mm rod-plane gap in SF_6[44]

An understanding of the nature of prebreakdown corona activity in SF_6 is important in order to explain the above observation, and to provide a basis for modelling of breakdown under corona stabilisation conditions.

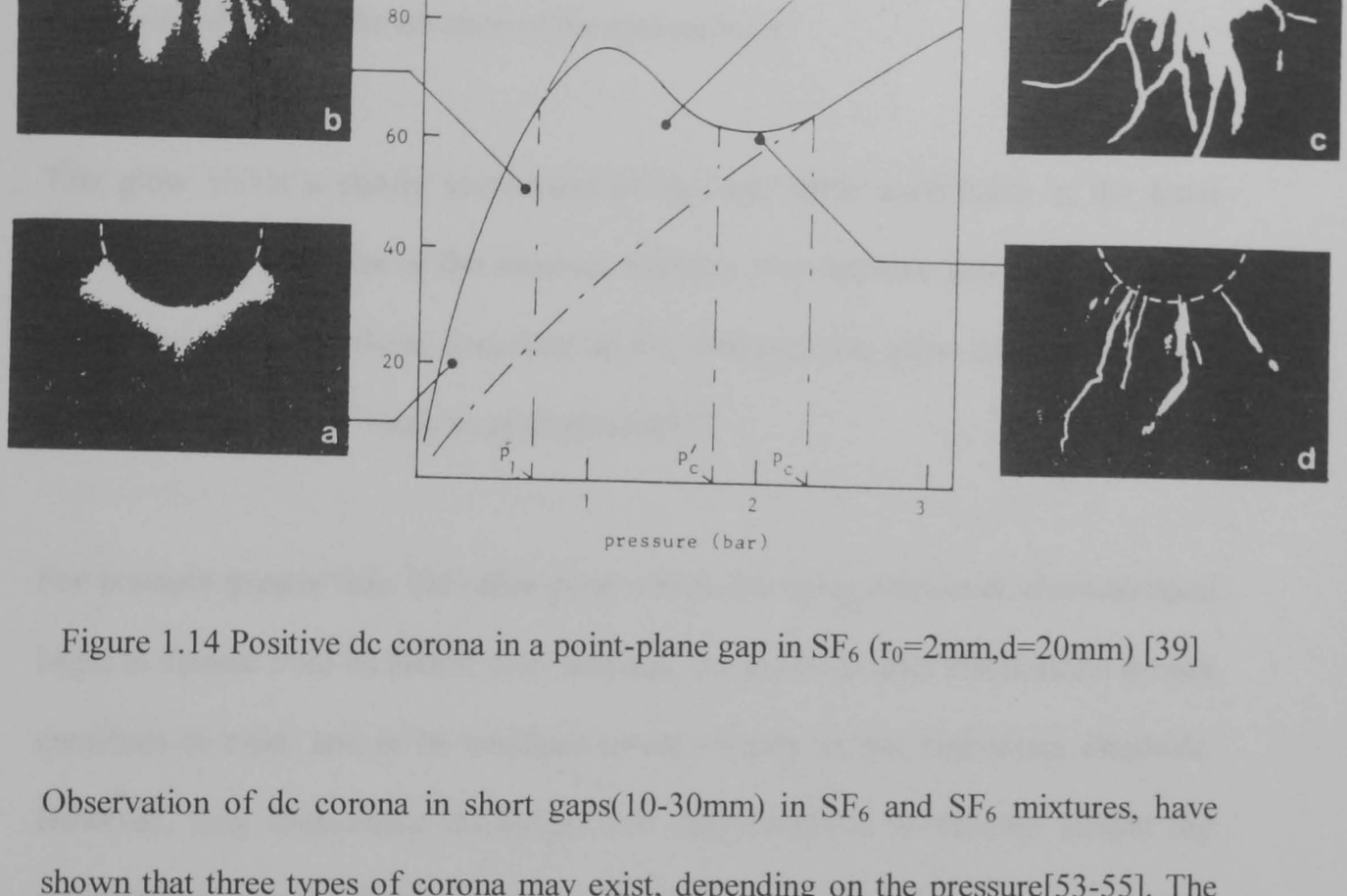

Figure 1.14 Positive dc corona in a point-plane gap in SF_6 (r_0=2mm,d=20mm) [39]

Observation of dc corona in short gaps(10-30mm) in SF_6 and SF_6 mixtures, have shown that three types of corona may exist, depending on the pressure[53-55]. The image-intensifier records (Figure 1.14[39]) show the visual appearance of the corona in a 20mm positive point-plane gap in SF_6[54]. At low pressure ($p<0.2$ bar) a diffuse glow type discharge occurs (Figure 1.14(a)). With increasing pressure, this gives way to short filamentary discharges which are restricted to a region within about 3 mm from the point (Figure 1.14(b)). These short filaments have been referred to as spatially-limited streamer discharges [54]. It should be noted that figure 1.14(b) represents an integration over 100ms, and in fact only a single filament is normally present at a given instant. Each filament is associated with a "burst" of about 100μs-

amplitude current pulses which continues for a few ms and when time-resolved using an image-intensifier camera [54] each filament is found to restrike at intervals of few μs. In SF_6/N_2 mixtures, the streak records are bright enough to show that the streamer filaments are accompanied by an even shorter-range filamentary glow, which burns steadily for the complete duration of the current burst.

This glow yields a steady component of current, while each pulse in the burst corresponds to a restrike of the streamer filament. For negative polarity, the corona modes are similar to those described above, although the glow component in the glow/streamer "bursts" tends to predominate[55].

For pressure greater than the value p_1 at which the voltage-pressure characteristics begin to deviate from its almost liner increase, the glow/streamer stabilisation corona continues to exist, and to be confined to the vicinity of the high-stress electrode. However, long filamentary discharges are now observed to develop around the stabilisation corona (Figure 1.14(c)). The current associated with this discharge consists of a single pulse of amplitude several orders of magnitude greater than those in the current burst of restriking streamer. On the basis of time-resolved studies of short-gap breakdown in SF_6/N_2 mixtures[50], and more recently by Schelieren observations in SF_6[40], these long filaments have been identified as leader discharges. The glow/streamer corona and the leader corona continue to coexist for pressure in the negative-slope region of the voltage-pressure characteristic. For pressures greater than P_c, the glow/streamer corona no longer occurs, and only leader discharges are observed (Figure 1.14(d)).

The transition from a streamer type corona at low pressure to a filamentary leader corona at high pressures has also been reported for impulse breakdown in long gaps about 300mm by Kurimoto and others[56,57] and by Bortnik and Vertikov[58]. Impulse discharge characteristics and leader development have also been studied by Takuma et al [59-60] and Pigini et al [61]. Voss[62], Rodrigo and Chatterton[63] and Kurimoto[64] studied the cases in SF_6/N_2 and SF_6/Air mixtures. The general behaviour is very similar to the dc case. At low pressure, only diffuse streamer corona occurs at the electrode prior to breakdown of the gap[57,58], at intermediate pressure, one or more diffuse corona is followed by the development of a stepped leader filament[57], at higher pressure, only the leader corona is observed. As with the long gap in air, the leader develops in a series of steps, with each channel extension being preceded by a burst of streamers from the tip of the leader. However, while faintly visible in SF_6 in still records using an intensifier[50], these leader tip streamers can be observed intimate resolved records only in SF_6/N_2 mixtures[50,62].

1.4.3 Streamer and leader discharges

In the pressure range up to P_1 in figure 1.14, the glow/streamer corona is confined to the area close to the point electrode. The ionisation region may then be regarded as small compared with the ion-drift region, and the behaviour of the system near breakdown can be analysed using the theory of unipolar-space-charge-dominated coronas[65,66]. The effect of the corona space charge is to limit the field at the high stress electrode to a level near its value at onset, while increasing the field in the

remainder of the gap. It has been shown that under these conditions breakdown occurs when the axial field distribution is such that the pressure-reduced field E/p everywhere exceeds a critical value of about 45kV/cm·bar[53]. It has been suggested [53,67] that this represents a minimum criterion for streamer propagation in SF_6. Sigmod[67] has proposed that the corresponding value of E/N along the axis may be increased because of the existence of a narrow jet of hot gas[68], and in recent work Sigmond et al [69] have shown that breakdown streamer/spark formation is preceded by a precursor discharge form the cathode. However, the important feature is that breakdown occurs under almost uniform field conditions and is determined by the space charge field in the gap, and not by conditions near the point electrode, this explains the observations that corona stabilised breakdown is insensitive to the value of r_0 in the rising part of the voltage pressure characteristic.

Static voltage breakdown for pressures greater than P_1 occurs when the leader corona is able to develop around the stabilisation corona and across the gap [54]. This results in the curved spark channels reported in this pressure range in SF_6[44,46,47]. With increasing pressure, there is a progressive loss of corona stabilisation until, at pressure P_c', the glow/streamer corona no longer occurs, under these conditions leaders propagate in a space-charge-free gap, their preferred path is axial, and the spark channels are again straight. When the pressure is increased to P_c the condition for leader propagation is satisfied at onset and direct breakdown occurs.

Under impulse voltage conditions, the measured breakdown characteristic depends on the pulse risetime [48,49,58]. For wavefronts of the order of 100μs, there is time

for corona shielding to develop. and the breakdown curve is similar in shape to the dc characteristic. For short risetime. the leader can develop axially in a space charge free field and the breakdown voltage is then a minimum. However. the behaviour is strongly dependent on the statistics of discharge initiation[50.51]. In wire-cylinder geometry, for example, where statistical time lag problems are minimised by the fact that the ionisation volume is relatively large[52], the impulse breakdown voltage is much lower than the dc value, and the breakdown characteristic is almost flat for pressures between P_I and P_c as shown in figure 1.15[52]. In point-plane geometry, the 50% breakdown probability can be relatively high[50] but as pointed out by Farish et al. [51]and Bortnik et al[58], the minimum impulse breakdown voltage is again independent of pressure. The conclusion is that the minimum impulse breakdown voltage for leader propagation is almost independent of pressure in the range of P_I to P_c, and this is a feature of models for leader propagation which have been proposed by Bortnik [58] and Niemeyer and Pinnekamp[70].

The main feature of corona stabilised breakdown in SF_6 can therefore be summarised, with reference to figure 1.12, as follows: the onset voltage (curve A) can be calculated using the formula for corona inception given by Nitta and Shibuya[71] and gives the breakdown curve above P_c. For pressure up to P_I, breakdown occurs when the space charge field in the gap reaches a critical value required for streamer propagation (curve B in figure 1.12). For pressures greater than P_I, the minimum breakdown voltage is determined by the condition for leader propagation in a space charge free gap (curve C in figure 1.12). Leader breakdown under dc conditions involves a progressive loss of corona stabilisation (curve D in

figure 1.12) and for pressures greater than P_c'. where there is no glow/streamer stabilisation corona, the characteristic follows curve C. The impulse breakdown voltage (curve E in figure 1.12) is subject to statistical variation, depending on field divergence and pulse wavefront, but the minimum impulse breakdown voltage again corresponds to the leader propagation criterion (curve C in figure 1.12).

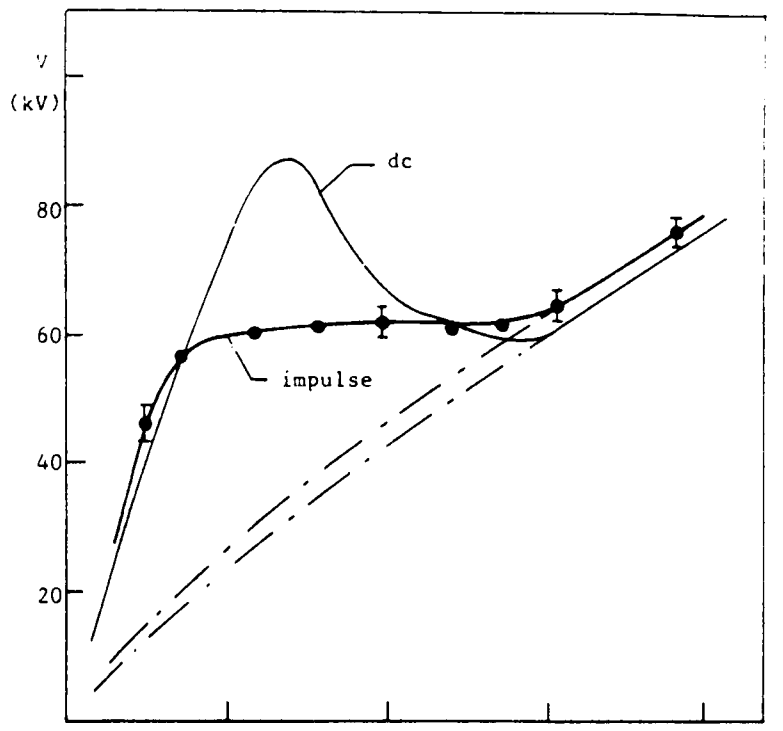

Figure 1.15 Comparison of positive impulse and dc breakdown characteristics in coaxial cylinders [52] (40%SF_6, 60% N_2 mixture, r_0=0.5mm, r_2=25mm)

- Streamer propagation

In principle, the minimum background field in which streamers can propagate in SF_6 can be derived on the basis of the energy-balance relationship used for air[72,73]. While the full computer model has not yet been applied to SF_6, a greatly simplified method[58,74] gave an estimate of 34-35 kV/cm·bar for the pressure reduced streamer stability field.

Similar values in calculations of the minimum space charge field in the gap just prior to breakdown in SF_6 in point-plane [54] and coaxial electrode geometries [52]. In the latter case, Poisson's equation may be solved directly to give the expression,

$$E(r) = \left\{ \left(\frac{r_1}{r} \right)^2 E_0^2 + \left[1 - \left(\frac{r_1}{r} \right)^2 \right] \frac{E_0 \cdot \rho_e \cdot r_1}{\varepsilon_0} \right\}^2 \qquad (1.36)$$

where E_0 is the onset field and ρ_e the space charge density at the inner electrode of radius r_0. For a given voltage, ρ_e is found by iteration such that integration of equation(1.36) satisfies the boundary conditions for potential, and the field distribution is then calculated. Figure 1.16[52] shows the calculated field distribution in a 0.5/25mm coaxial system in SF_6 at 0.6 bar for various voltages. It can be seen that, at breakdown, the minimum E/p on the gap is about 43 kV/cm·bar, while at voltage below V_b, this is exceeded only within a few millimetre of the inner conductor surface. Calculations for various coaxial and point-plane systems gave value for E/p of 45±5 kV/cm·bar, with slight dependence on geometry and pressure. In SF_6/N_2 mixtures, the values obtained were 20-25 kV/cm·bar with 10% SF_6 and 30-35 kV/cm·bar with 40% SF_6[52]. These values have been confirmed by measurement of the field at the plane using the biased field probe [75] which shows excellent agreement with the calculation [52,54].

- Leader propagation

As the leader discharge develops across the gap, its advance involves the transformation of the cold, high-field streamer filaments at its tip to form a new section of hot and relatively low-gradient leader channel. Even for the case of long-gap breakdown in air, which has been the subject of intensive study in recent years, notably those by the Renardieres Group[76], the physical processes governing the transformation are not yet fully identified[77].

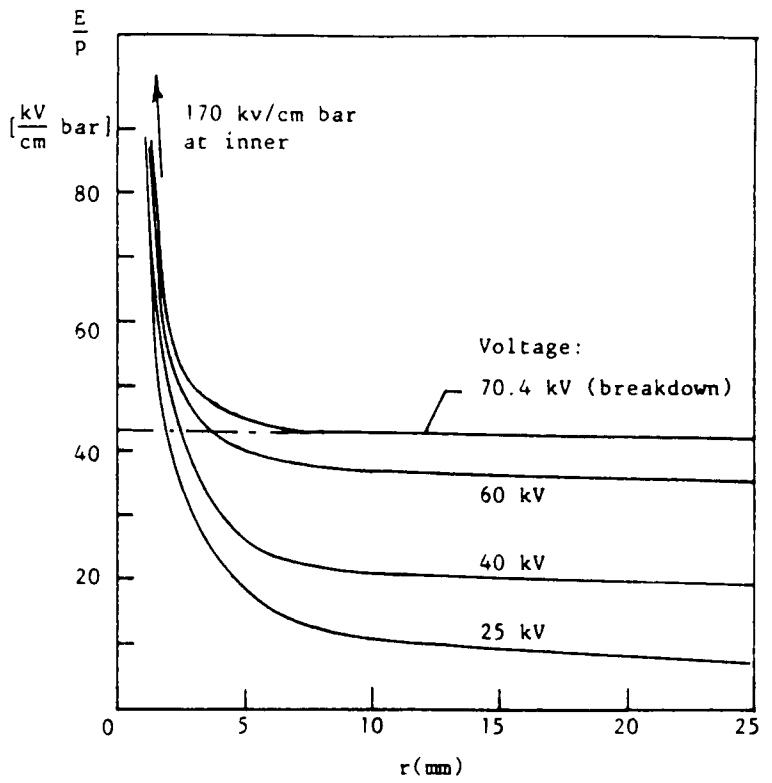

Figure 1.16 Calculated space-charge-modified field distribution in coaxial electrodes in SF_6 (p=0.6bar, r_0=0.5mm, r_1=25mm, V_i=20kV) [52]

In the absence of a complete physical model, quite a few authors have developed empirical and semi-empirical criteria for leader breakdown in SF_6. The simplest of these involves the model used by Lemke [78] to represent the situation just before the final jump stage of long gap breakdown, in which the breakdown voltage is given by,

$$U_b = E_l \cdot l_{crit} + E_s(d - l_{crit}) \qquad (1.37)$$

in which E_l and E_s are the average gradients in the leader and streamer channels respectively and l_{crit} the maximum leader extension just prior to breakdown, such that the leader-tip corona streamers just reach the plane. However, information on the parameters in equation (1.37) is still incomplete. Ibrahim [74] found that, if the data for E_l and l_{crit}/d obtained at 1 bar by Voss [74] is used, together with the streamer stability field [54], the calculated minimum breakdown voltage shows a stronger pressure dependence than it is suggested by the impulse characteristics. The model was simplified [58] assuming a constant streamer potential drop of about 60 kV and a constant leader gradient of about 6 kV/cm. The average leader channel gradient for the leader to cross the gap was computed [57] assuming that the leader tip field has to maintained at its value at leader inception, and obtained a value of about 5 kV/cm at 1 bar for a 30 cm gap. Further experimental work is necessary to determine the pressure dependence of the leader gradient and of the length of the final "jump" in SF_6.

A recently developed leader propagation model [70] has been used in the discussion of corona stabilised breakdown[79,80], particle triggered breakdown [81] and volt-time characteristics in SF_6 [82]. In this model, the enthalpy input required to fully dissociate the gas in the channel and raise its temperature to about 2100°C is estimated as Δh_{cr} at $\sim 10^7$ J/Kg, an energy balance calculation is then performed between the energy $\Delta w = \rho_0 \cdot \pi \cdot r_c^2 \cdot l \cdot (\Delta h_{cr})$, required to transform a section *l* of a

channel of radius r_c, and the energy input to the ionisation zone at the leader tip. This is given as $\Delta w=\Delta Q\cdot\Delta U$, where ΔQ is the charge pulse associated with the streamer and $\Delta U=\varepsilon U$ (where ε is scaling factor as in equation 1.39) is the potential drop in the streamer zone of a channel whose tip potential is U. ΔQ is expressed in terms of the rate of change of capacitance C between the advancing leader channel at position *x* and the plane electrode, as

$$\Delta Q = U\Delta C = \frac{UdC}{dx}\cdot 1 \qquad (1.38)$$

If the channel cross sectional area is assumed to vary inversely with pressure, the energy balance gives the minimum tip potential for leader propagation as [70]

$$U_{cr} = \left[\left(\frac{\rho_0}{P_0}\right)\Delta h_{cr}\frac{\delta}{\varepsilon}\right]^{\frac{1}{2}}\cdot\left(\frac{dC}{dx}\right)^{-\frac{1}{2}} \qquad (1.39)$$

in which δ and ε are scaling factors. An approximate treatment of the leader channel behaviour [70] indicated that the leader gradient is independent of pressure and , since C_{ur} does not explicitly depend on pressure, the minimum breakdown voltage according to the model corresponds to the form assumed in [58] as

$$U_b=E_l\cdot d+U_{cr} \qquad (1.40)$$

At this stage, the Niemeyer and Pinnekamp model must be regarded as largely empirical, since the properties of the ionisation zone enter equation (1.39) only through scaling parameters, and since the claimed pressure-independence of U_{cr} depends directly on the assumption that r_c varies as $P^{-1.2}$. Also, the capacitance C is calculated on the basis of an electrostatic leader radius $R(>>r_0)$ whose physical interpretation (and pressure dependence) is unclear. Although an attempt has been made [70] to compare the model with measurement on surface discharges in SF_6[83], its validation for gas gap breakdown will require further experimental evidence. In particular, the model would be strengthened if the prediction that the leader channel gradient is independent of pressure were to be confirmed experimentally.

• The critical pressure

Pressure P_c should be obtained by equating the minimum leader propagation voltage given by [46] with the corona inception voltage V_i. This is obtained using the simple inception criterion

$$\int_0^{x_c} \overline{\alpha}(x)dx = k \qquad (1.41)$$

where x_c is the critical distance at which the net ionisation coefficient $\overline{\alpha}$ is zero. For SF_6, $\overline{\alpha}$ is given by the liner relation $\overline{\alpha}$=(AE-Bp) and, for point-plane gaps with point radius r_0, the inception voltage is then obtained as [71],

$$V_i = \frac{Bpd\left[1+(kBpr_0)^{\frac{1}{2}}\right]^2}{Af} \qquad (1.42)$$

where f is the field nonuniformity factor.

In some instance, it may be useful to estimate P'_c, the pressure at which the localised stabilisation corona disappears, as for some geometry this may give the minimum value in the breakdown voltage curve. A criterion for P'_c was derived [84-86] which depends on the fact that, at low pressure, secondary electrons are produced relatively far from the point where they attach, to give a steady flux of negative ions which maintain the stabilisation corona. With the increase in pressure, the range of ionising photons shrinks faster than the ionisation distance x_c so that a pressure is reached at which the photosecondaries are produced only in the high field region where they can contribute to filamentary discharge development. The critical pressure for ions of stabilisation was given in [84],

$$P_c = \frac{BC^2}{kr_0} \qquad (1.43)$$

where B, k, r_o are as in equation (1.42) and C is a constant estimated from breakdown measurements as about 0.05 bar·cm. A similar criterion can be found in [57] and in [85] for impulse breakdown in long gaps.

1.4.4 Impulse breakdown characteristics

For the initiation of breakdown an electron must be available to start the avalanche. With slowly rising voltages (d.c. and a.c.), there are usually sufficient initiatory electrons created by cosmic rays and naturally occurring radioactive sources. Under surge voltages and pulses of short duration, however, the gap may not break down as the peak voltage reaches the lowest breakdown value (V_s) unless the presence of initiatory electrons is ensured by using artificial irradiation. V_s is a voltage which leads to breakdown of the gap after a long time of application. With weak irradiation the peak value may have to be greatly increased so that the voltage remains above the d.c. value for long intervals of time.

The time which elapses between the application of voltage to a gap sufficient to cause breakdown and the breakdown is called the time lag(t). It consists of two components: one is the time which elapses during the voltage application until a primary electron appears to initiate the discharge and is known as the statistical time lag (t_s); and the other is the time required for breakdown to develop once initiated and is known as the formative time lag (t_f).

The statistical time lag depends on the amount of preionisation in the gap. This in turn depends on the size of the gap and the radiation predicting the primary electrons. The appearance of such electrons is usually statistically distributed. The techniques generally used for irradiating gaps artificially, and thereby reducing the statistical time lag, include the use of ultra violet light, radioactive materials and illumination by auxiliary sparks. The statistical time will also be greatly reduced by the application of an overvoltage (i.e. V_p-V_s) to the gap.

The formative time lag (t_f) depends essentially on the mechanism of spark growth in question. In case when the secondary electrons arise entirely from electron emission at the cathode by positive ions, the transit time from anode to cathode will be the dominant factor determining the formative time. The formative time lag increases with the gap length and the field non-uniformity, but it decreases with the applied overvoltage.

• Impulse breakdown probability

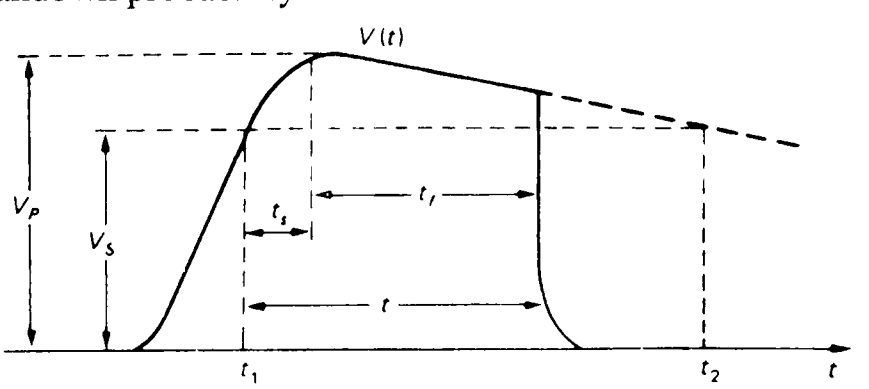

Figure 1.17 Breakdown under impulse voltage[29]

An impulse voltage is a unidirectional voltage which rises rapidly to a maximum value and then decays slowly to zero. When an impulse voltage of a peak value higher than V_s is applied to a gap, as shown in figure 1.17[29], there is a certain probability but not a certainty that breakdown will follow. For breakdown it is essential that the spark develops during the interval of overvoltage ($V(t)-V_s$) duration, i.e. the overvoltage duration must exceed the time lag ($t<(t_2-t_1)$). For a given impulse voltage waveshape the overvoltage duration will increase with the voltage amplitude(V_p).

Because of the statistical nature of the time lag, when a given number of impulse of an amplitude V_p, exceeding the static value V_s, is applied to a gap only a certain percentage will lead to breakdown. We therefore obtain a breakdown probability P for each given applied maximum impulse voltage V_p. The breakdown probability for a given impulse voltage is obtained by applying a large number of identical impulses and taking the ratio of the number of impulses that lead to breakdown to the total number applied. Figure 1.18[29] illustrates an example of the breakdown probability distribution function for impulse voltages of amplitude V_p. $V_{b\text{-}100}$ represents the 100% breakdown voltage, i.e. each voltage application of this magnitude leads to breakdown. This voltage is of particular importance in determining protective levels.

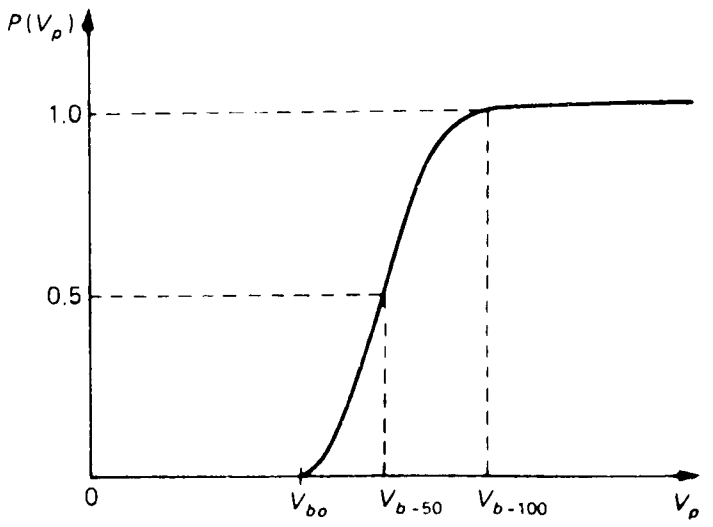

V_{bc}:impulse withstand level; $V_{b\text{-}50}$:50% impulse breakdown; $V_{b\text{-}100}$:100% breakdown-protective level

Figure 1.18 Breakdown probability under impulse voltage[29]

$V_{b\text{-}50}$ is the 50% breakdown voltage, i.e. half of the applied voltages at this level lead to breakdown. $V_{b\text{-}0}$ represents the highest impulse voltage that does not lead to breakdown. It is known as the "impulse withstand level" and is important in the design of insulation. In practice it is convenient to present the $P(V_p)$-V_p data on a logarithmic scale known as Gaussian probability scale which gives linear

relationship. The distribution can also be presented by the normal (Gaussian) distribution shown in figure 1.19[29]. Because of the asymptotic approach of the curve to the value $V_{b\text{-}0}$ and $V_{b\text{-}100}$ the exact values($V_{b\text{-}0}$ and $V_{b\text{-}100}$) can only be obtained from a very large number of experimental observations. These values, however, can be approximately obtained from the distribution of breakdown values about the middle value enclosed between the limits of standard deviation S. For example, if we count all breakdown enclosed between ± 3S, i.e.

$$V_{b\text{-}0} = V_{b\text{-}50} - 3S$$

$$V_{b\text{-}100} = V_{b\text{-}50} + 3S$$

the range includes the breakdown probability from 0.15% to 99.85%.

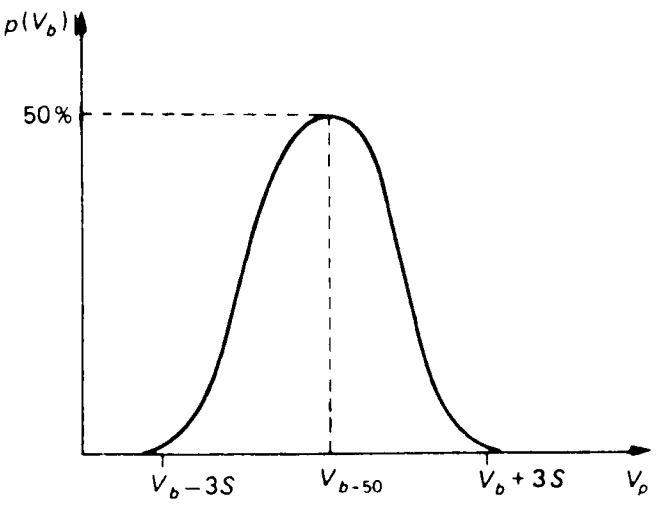

Figure 1.19 Gaussian probability distribution curve[29]

It should be noted that though 50% probability breakdown voltage is widely used, it can be argued that the low probability level is a much more interesting and meaningful value. The minimum level is obviously that to which practical equipment must be designed if insulation failure is to be avoided and also, in terms of physical

mechanisms, this is the stress level at which the gap will just breakdown if all necessary statistically varying conditions are simultaneously satisfied. The importance of minimum impulse breakdown will be discussed in detail in 2.2.3.1.

• Volt-time characteristics

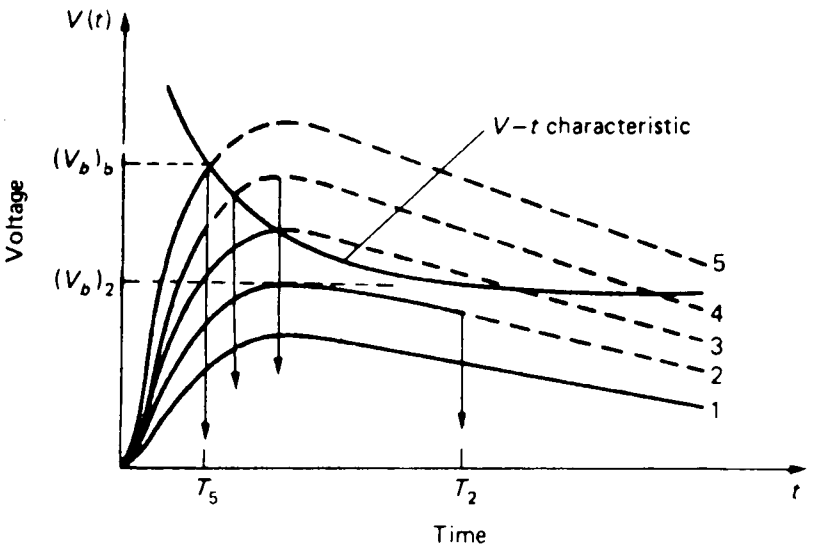

Figure 1.20 Impulse-time-volt characteristics[29]

When an impulse voltage of a value $V_{b\text{-}100}$ or higher is applied to a gap, breakdown will result on each voltage application. The time required for the spark development (time lag) will depend upon the rise rate of voltage and field geometry. Therefore, for each gap geometry it is possible to construct a volt-time characteristic by applying a number of impulses of increasing amplitude and noting oscillographically the time lag. A schematic plot of such a characteristic is shown in figure 1.20[29]. In uniform and quasi-uniform field gaps, the characteristic is usually sharply defined and it rises steeply with increasing the rate of rise of the applied voltage. In nonuniform field gaps, however, due to larger scatter in the results, the data fall into a dispersion band as shown in figure 1.21[29]. The time to breakdown is less sensitive to the rate of

voltage rise. Hence. quasi-uniform field gaps(sphere-sphere) have often been used as protective devices against overvoltages in electric power systems. The volt-time characteristic is an important practical property of any insulating device or structure. It provides the basis for establishing the impulse strength of the insulation as well as for the design of the protection level against overvoltages.

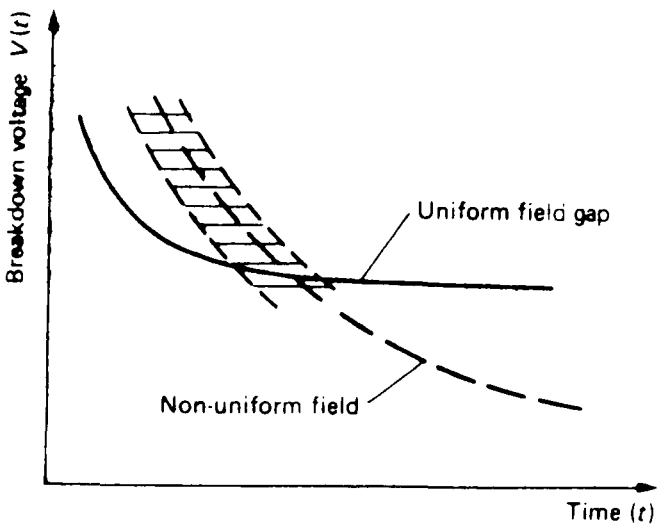

Figure 1.21 Schematic diagram of volt-time characteristics for uniform and non-uniform field gaps[29]

• Time lags

Time lags have been studied in the past. In the techniques generally used either a constant voltage is applied to an irradiated gap and a spark is initiated by a sudden illumination of the gap from a nearby spark, or an overvoltage is suddenly applied to a gap already illuminated.

In the former case the time lag is measured from the flash until breakdown occurs, while in the latter, the time lag is measured between the voltage application and the gap breakdown. The overvoltaged conditions may be obtained either by

superimposing a step voltage pulse upon a direct voltage already applied to the gap or by using an impulse voltage of a suitably short front duration. The measured time lags for given experimental conditions are usually presented graphically by plotting the average time lags against the overvoltage. The latter is defined as the percentage ratio of the voltage in question to the minimum direct voltage which will cause breakdown. In the case when an impulse voltage is used on its own, the time lags are plotted against the impulse ratio defined as the ration of the applied impulse voltage to the minimum direct breakdown voltage.

The measured values are affected by factors such as the intensity of the background irradiation, the nature and the condition of the electrode surface, the gap length, the electron affinity of the gas, etc.

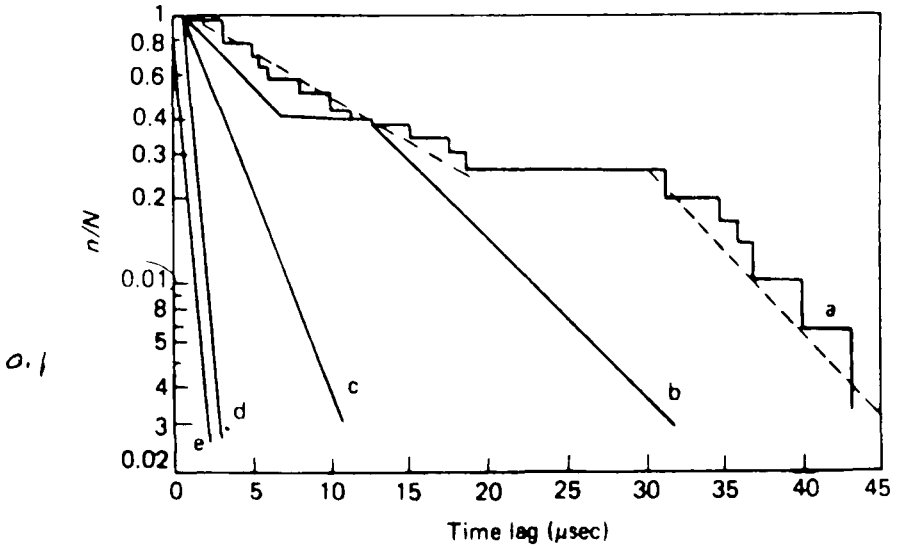

overvoltages: (a)10%; (b)15%; (c)20%; (d)25% for SF_6; (e)5.3% for air

Figure 1.22 Time lag distribution in SF_6 and air [29]

Long and highly scattered time lags have been observed in strongly electronegative gases under irradiated conditions. Figure 1.22[29] compares time lags observed in SF_6 with those obtained in air under similar experimental conditions. It was impossible to attribute these long time lags to the shortage of initiatory electrons. It

was suggested that the long time lags are associated with the complex nature of the growth of spark in the highly electron attaching gases.

An alternative method for presenting time lags has been developed by Laue[99] and Zuber[100]. These authors showed that the time lag in spark gaps may be represented in the form,

$$\frac{n}{N} = e^{-\int_0^t \rho_1 \rho_2 \beta dt} \qquad (1.44)$$

where N represents the total number of time lags observed, n is the number of time lags of length greater than t, β is the rate at which electrons are produced in the gap by irradiation, ρ_1 is the probability of an electron appearing in a region of the gap where it can initiate a spark, and ρ_2 is the probability that an electron at a given field strength will lead to the development of the spark. The factor ρ_1 is a function of the gap length and the gas density, while ρ_2 is a function of the applied field. The factor β is dependent on the source of irradiation providing that the primary current in the gap is constant and the applied field remains constant with respect to time, equation 1.44 can be written as:

$$\frac{n}{N} = e^{-kt} \qquad (1.45)$$

Equation 1.45 gives a linear relation between $\ln\frac{n}{N}$ and time t. The method gives a truer representation of the results in the case of highly scattered results.

1.5 SF_6 gas mixtures

There have been many investigations on the nonuniform field breakdown characteristics of mixtures of SF_6 with other gases which have included H_2 [87], air [64,88], He and CO_2[89] and a lot of work has been done on N_2 [50,60,90].

In some cases, remarkably strong stabilisation peaks have been observed with the addition of small amounts of SF_6 to a buffer gas. In air with 1% SF_6[64,88], for example, the corona stabilised breakdown voltage at 0.1 MPa was found to be twice that for pure SF_6 at the same pressure.

Although such "weak" SF_6 mixtures have possible uses in testing of metalclad equipment [88], they have the disadvantage that their limiting field strength is close to that of their main constituent, so that they have a low corona-onset voltage and a much reduced uniform field strength compared to SF_6. However, recent work [51,91] has shown that a marked improvement in corona stabilisation can be achieved in SF_6 by means of the addition of small quantities (about 0.1%) of an easily ionisable compound such as triethylamine(TEA), without any significant loss of similarity-law performance. From a comparison of static-voltage characteristics and corona activity in an SF_6/TEA mixture[51], it can be seen that the effect of TEA is to give a very intense stabilisation corona and to inhibit leader formation. Thus, at a pressure of 0.2

MPa, the corona is still rather diffuse even at a voltage 50% higher than the breakdown voltage in pure SF_6. It has been suggested [51] that enhanced photoionisation in the mixture allows the discharge to spread around the point and prevents the interruptions of the stabilisation corona current observed in pure SF_6 [54]. The additive also appeared to give a substantial increase in the minimum impulse breakdown voltage [51]. This would indicate that it influences leader propagation as well as improves the stabilisation effect, but further work will be necessary to identify the mechanisms involved.

1.5.1 Synergism and Penning effect

It has been found that the addition of a certain percentage of some common gas to SF_6 can result in a significant increase in the impulse breakdown strength. For example, the SF_6/air mixture with a mixing ratio of 90/10 has a higher impulse breakdown strength than pure SF_6 in nonuniform fields at a total gas pressure of 0.1 MPa[108]. This is the so called synergism effect.

Paschen's Law is not applicable in many gaseous mixtures. The outstanding example is the neon/argon mixture. A small admixture of argon in neon reduces the breakdown strength below that of pure argon or neon. The reason for this lowering in the breakdown voltage is that the lowest excited state of neon is metastable and its excitation potential (16eV) is about 0.9eV greater than the ionisation potential of argon. The metastable atoms have a long life in neon gas, and on colliding with

argon atoms there is a very high probability of ionising them. This phenomenon is known as the Penning effect.

1.5.2 High dielectric strength gas mixtures

It should be noted that there are many aspects of a gas/gas mixture which must be considered in determining whether or not it has any clear superiority or advantages over commonly used SF_6 and these include: (1) cost of gas/gas mixture, (2) performance(e.g. electrical strength, carbonisation, vapour pressure, toxicity, immunity to adverse effects of moisture, contamination and particles etc), (3) system requirements(e.g. stability and overall compatibility with other likely components of the system) and (4) environmental acceptability.

Alternative high-strength gases, notably those containing C and F(e.g. C_4F_6, c-C_5F_8) may have higher dielectric strength. Some thirty pure gases as well as mixtures with SF_6 were considered[4,5,6,7] but all have problems such as toxicity, low vapour pressure, release of solid carbon during arc.

Gases that were fluorine containing were studied, examples of which included: CF_3SF_5, $C_2F_5OC_2F_5$,CF_3OSF_5,$(CF_3)_2S$,$(CF_3)_3N$,CF_3CF_2CN,CF_3SO_2F. As an example, CF_3SF_5 is a known good dielectric. It has a boiling point of -21°C and a high dielectric strength. Unfortunately, it is relatively unstable, and rapidly decomposes in a low current(about 1mA, 30 seconds) arc into CF_4 and SF_4 with an associated increase in pressure. Carbonisation was pointed out as an important

problem from a practical point of view. Some gases such as CF_3-C≡C-CF_3 that initially have dielectric strengths greater than SF_6 show marked decline in breakdown strength after a breakdown has occurred . In the case of CF_3-C≡C-CF_3, large carbon deposits are left on the electrodes after several breakdowns, and these may eventually build up to the extent that they bridge the electrode gap. Work[4] has been done on mixtures of fluorocarbons with other gases like air, N_2 and N_2O, but found no dramatic improvement over using SF_6. Thus clearly fluorocarbons are not very arc stable although arc stability can be improved by adding SF_6. Effects to find "better" gaseous dielectrics than SF_6 trace back a few decades. An extensive search, especially in the seventies[3,9,10,11], showed that alternatives to SF_6 do exist with superior dielectric properties. For example, the breakdown strengths of some perfluorocarbons and their mixtures are 2.5 times the breakdown strength of pure SF_6. Unfortunately, these are greenhouse gases and often have other undesirable properties.

In summary, it was noted, (1)No single, pure gas has been found that is "superior" to SF_6 in all respects. (2) The commercially available fluorocarbons are unstable and not considered suitable as a way of achieving gas cost reduction. (3) If fluorocarbons are to be used, then they must be mixed with an arc stabiliser, e.g., SF_6. (4) Particle effects on mixtures are unknown and more work on this problem is required. There is no significant improvement in dielectric strength over SF_6/N_2 or SF_6/air mixtures could be achieved using SF_6 mixed with available fluorocarbon mixtures, and since there is uncertainty over their effects on solid insulation they are not considered as possible alternatives.

1.5.3 SF_6 gas mixtures with buffer gases

Because of its outstanding electrical and physical properties, SF_6 has gained wide acceptance as the dielectric of choice for GIS applications. Nevertheless, despite its many advantages, it is recognised that SF_6 has some drawbacks as an insulating medium, these include,

(1)Cost. The relative high cost of SF_6 especially in GITL(gas-insulated transmission lines) and other kind of apparatus where large amount of gas is needed.

(2)Sensitive to particle effects. In practice the electrical breakdown strength of compressed SF_6 is very often determined by local field enhancement due to protrusion, surface roughness and conducting particles left in the system.

(3)Restricted working-temperature range. SF_6's liquidized temperature limits the outdoor application in severe climatic condition if the temperature is less than -30°C.

(4) SF_6 is a potent greenhouse gas as it was pointed out very recently[8].

There has been a growing interest in using gas mixtures consisting of SF_6 and other common gases(i.e. buffer gases, such as N_2, Air, CO_2 etc) to reduce the insulation cost and minimise the possible hazard of particle-initiated breakdown since there are at least four ways in which SF_6 gas mixtures with buffer gases may be superior to SF_6 used alone in industrial practical high-voltage system. First of all, higher total gas pressures may be used without raising the minimum operating temperature. Secondly, the cost of mixtures for a given pressure can be reduced considerably depending on the cost of the second component. Thirdly, gas mixtures offer the

possibility of some degree of immunity from the breakdown initiated by local(microscopic) field non-uniformities associated with electrode irregularities(e.g. roughness) or free conducting particles[12]. Last but not the least, the use of SF_6 mixtures with buffer gases could be a short-term solution to the problem of eliminating the potential contribution of SF_6 to global warming.

Mixtures of this type rely on the fact that SF_6 can be diluted up to 50% by volume with non-attaching or weakly attaching gases such as N_2, CO_2 and air without a correspondingly large reduction in dielectric strength.

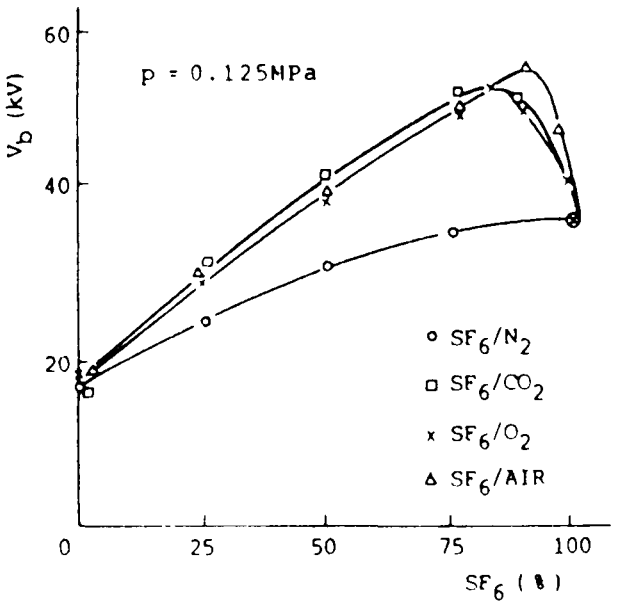

Figure 1.23 Breakdown voltages of SF_6/N_2, SF_6/CO_2, SF_6/O_2 and SF_6/air in the 10mm point-plane gap under positive lightning impulse voltage [153]

The dielectric strength of SF_6/N_2, SF_6/CO_2, SF_6/O_2 and SF_6/air has been studied[13,14,15,151,152,153 and 155]. Figures 1.23[153] and 1.24[153] show the breakdown voltage of SF_6/N_2, SF_6/CO_2, SF_6/O_2 and SF_6/air mixtures in the point-plane gap under the positive polarity standard lightning impulse and dc voltages, respectively. It is quite apparent that the breakdown voltage of these four SF_6 gas

mixtures do not differ very much from one another under dc voltages. but that is not the case under lightning impulse voltages. It can be seen in Figure 1.23 that while SF_6/air. SF_6/CO_2 and SF_6/O_2 have about the same positive impulse breakdown voltages exhibiting a maximum value at the mixing ratio of 90/10 or 85/15. the SF_6/N_2 mixture is obviously different from the other three gas mixtures with its breakdown voltage versus SF_6 concentration being a monotonic rising curve.

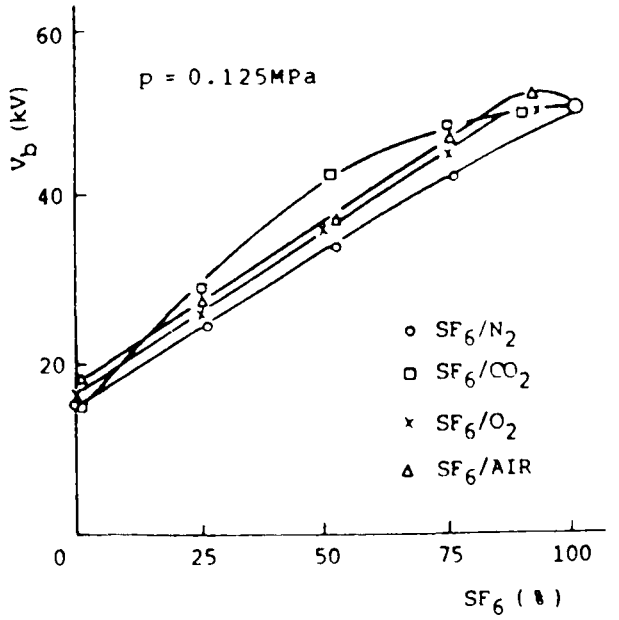

Figure 1.24 Positive dc breakdown voltages of SF_6/N_2, SF_6/CO_2, SF_6/O_2 and SF_6/air in the 10mm point-plane gap [153]

SF_6/air

Although earlier study has shown that the addition of 1% of SF_6 to air can result in a significant increase in the positive switching impulse breakdown voltage over that for air or SF_6 along[18], such an SF_6/air mixture is obviously of no practical importance to engineering applications because its breakdown strength will be reduced to that of air in the case of slightly non-uniform fields. On the other hand, it is quite interesting to note in Figure 1.23 that the impulse breakdown voltage of the

SF_6/air with a mixing ratio of 90/10 is 45% higher than that of pure SF_6. As the air in cubicle type GIS(C-GIS)is removed by SF_6 using a displacement method[17], residual air inside C-GIS is not only inevitable but also beneficial to dielectric strength under the lightning impulse. The more non-uniform the field, the higher the impulse breakdown strength of SF_6/air than that of SF_6. The good corona stabilisation effect shown in the SF_6/air mixture is probably on account of the faster space charge movement in SF_6/air than in SF_6 gas.

SF_6/CO_2

SF_6/CO_2 is also quite promising, especially in highly non-uniform fields and in a gas-impregnated film insulation encountered in the case of gas-insulated transformer(GIT). Figure 1.24 shows that the impulse breakdown strength of SF_6/CO_2 is 40% higher than that of SF_6 in highly non-uniform fields[13], which looks very promising because it is the impulse withstand level that determines the insulation dimensions. While SF_6/N_2 might be the best gas mixture to be used in GIS and GITL, it can be used in GIT to improve the impulse breakdown characteristics. But in the latter case SF_6/CO_2 might have some advantages over SF_6/N_2 because gas/film insulation and highly non-uniform field problems are encountered[13]. The main problem with SF_6/CO_2 is that CO_2 is a green house gas and may have some undesirable properties.

SF_6/N_2

Nitrogen(N_2) is the main component of air, and widely used in many technical and industrial applications. Its physical and chemical properties have been thoroughly studied and are well understood. Unlike SF_6, N_2 is not an electronegative gas, but it is effective in slowing down electrons i.e., it is a good electron "thermalizer". It has been the subject of extensive studies partly because of its dominant presence in the atmosphere and its use in gas-discharge and gas-dielectric applications. Neither the N_2 molecules nor the N atoms have an affinity for electrons in their ground electron states. In many respects, N_2 is an ideal buffer gas to use in dielectric applications. It is abundant, cheap, inert, non-toxic, nonflammable, and unquestionably environmentally acceptable. Existing studies indicate that,

1. N_2 is less susceptible than SF_6 (and other electronegative gases) to low non-uniform field breakdown. This advantage is understood on the basis of the energy dependence of the electron attachment and ionisation cross sections[11,19] and can be quantified in terms of the so-called figure of merit *M* value[20].

2. The breakdown strength of N_2 is less sensitive than that of SF_6 to conductor surface roughness[21,22].

3. The electric strength of N_2 is about one third that of SF_6 under uniform-field conditions at low pressures(less than 3bar), and as SF_6, it increases with pressure[11,23].

4. The dc or ac breakdown voltage of N_2 increases with pressure as does that of SF_6[11,23,24,25], but tends toward saturation at high pressures approaching 10bar.

5. When particles are present in the gas[10,26], the breakdown strength of pure N_2 compares favourably with that of pure SF_6 at pressures of about 10bar.

These and other findings suggest that pure N_2 used at about two or three times the pressure of pure SF_6 may be a viable alternative to pure SF_6 as an insulating gas in some applications. From the practical point of view, SF_6/N_2 gas mixture shows promise for industrial applications and is often considered to be the best substitute for SF_6 in GIS and GITL[14]. This is mainly because 1) N_2 is a cheap inert gas; 2) the mixture of SF_6 with N_2 exhibits an ideal saturation of breakdown voltage as the percentage concentration of SF_6 is increased and; 3) its dielectric strength in a uniform field is higher than that of gas mixtures of SF_6 with most common gases[27]. Studies on SF_6/N_2 mixture have shown that,

1. A mixture of SF_6 and N_2 has a higher breakdown strength than that calculated on a ratio basis. The reason for this synergistic behaviour is that collisions between free electrons and N_2 molecules slow the electrons down to low-energy region where they are captured more efficiently by SF_6.

2. Small amounts of SF_6 in N_2 rapidly increase the breakdown strength, but above 50% SF_6(the mixture containing 50% SF_6 has a dielectric strength that is about 88% of that for pure SF_6 in uniform fields) the increase is gradual. This pronounced saturation effect seen for the SF_6/N_2 mixture that makes the mixture particularly attractive as a practical gaseous dielectric.

3.An SF_6/N_2 mixture containing 30% SF_6 by volume ratio has about 75% of the dielectric strength of pure SF_6 in a uniform field at the same pressure[28].

4.An SF_6/N_2 mixture containing 25% SF_6 by volume ratio has the same breakdown strength as pure SF_6 if the mixture pressure is about 50% higher than that of pure SF_6 in a uniform field[3.29].

5.An SF_6/N_2 mixture containing about 10% SF_6 by volume ratio has nearly the same breakdown voltage as pure SF_6 if the total pressure for the mixture is twice that for SF_6 under quasi-uniform field conditions(e.g. for cylindrically concentric electrodes) and for total pressure in the range 1.01 to 10.1 bar[3,29].

6. In non-uniform fields at high pressures(i.e., as may apply in service) mixtures containing only a few percent of N_2 can have breakdown strengths almost as high as pure SF_6. Experiment[155] show that the mixture containing 75% SF_6 can increase the maximum breakdown voltage by 12%(Figure 1.25) in highly non-uniform field, which is inevitable in high voltage insulation.

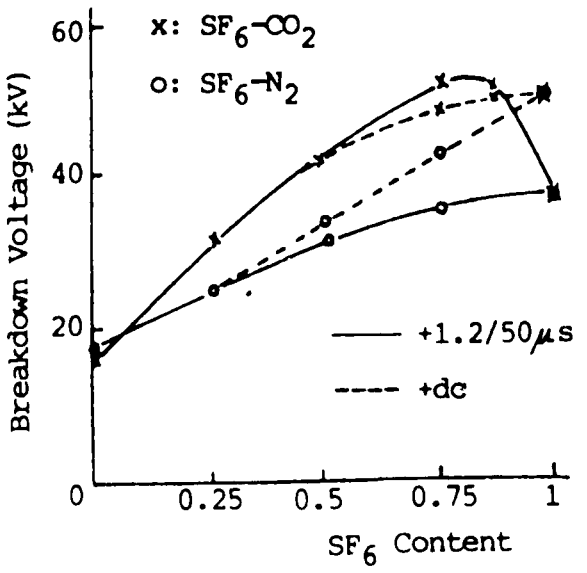

Figure 1.25 Impulse and dc breakdown voltages SF_6/N_2 and SF_6/CO_2, in a point-plane gap(P=1.25bar) [155]

7. The SF_6/N_2 mixtures are expected to exhibit less sensitivity than SF_6 to electric field nonuniformities associated with surface roughness and particles based on the electrical breakdown strength of N_2 is less sensitive than that of SF_6 to nonuniform

electric fields. Indeed a number of studies[22,30,31,32,33,34,35,36]have shown that SF_6/N_2 mixtures are less sensitive to electrode surface roughness and particle contamination than pure SF_6.

7.1. For a given electrode surface roughness and gas pressure there is little gain in electric breakdown strength by increasing the percentage of SF_6 beyond a certain amount. At 4 bar the limit for a 30μm finish is 30% SF_6, and for a 100μm finish it is 10% SF_6.

7.2. In the presence of particles, SF_6/N_2 mixtures can perform at least as well as pure SF_6, and may be comparable to pure SF_6 in terms of voltage withstand capability(pure N_2 at pressure about 10 bar may also be as good as pure SF_6)[9,10,37,38]. This is of practical importance and warrants further investigation, especially for SF_6/N_2 mixtures containing small percentage of SF_6. Breakdown-voltage-measurement on SF_6/N_2 mixtures in the presence of particles using cylindrical geometries[9,10] indicated that the effect of particles on the breakdown strengths of these mixtures depends not only on the total gas pressure of the mixture, but also on the partial pressures of the constituent gases.

8. In a concentric-cylinder and other geometries, breakdown strength measurement on SF_6/N_2 mixtures at total gas pressures of 5 to 15 bar using lightning and switching impulses, compared to pure SF_6 at 10 bar, a 50/50 mixture retains about 85% of the breakdown strength. An increase of N_2 content to a total pressure of 15 bar gives a breakdown strength equal to that of pure SF_6 at 10 bar. The condensation temperature is thereby lowered from -15°C to -40°C, and with a saving in gas cost by up to 50%[39].

9.A study[24] on SF_6/N_2 mixtures in a coaxial cable using lightning and switching impulses, in the pressure range 1 to 6.2 bar has shown that the mixtures with N_2 look promising for CGIT applications, with, for example, a 50/50 mixture at typical pressure of 5.4 bar being able to replace pure SF_6 at 4.5 bar without loss of breakdown strength and with a typical 40% saving in gas cost.

10. Studies[40,41,42,43,44] have shown that there is very little chemical interaction between SF_6 and N_2 in discharge, and the predominant oxidation by-products are those seen in SF_6 such as SO_2,SOF_2,SO_2F_2, and SOF_4(i.e., no additional toxic decomposition products were found in sparked SF_6/N_2 as compared with sparked SF_6). Because the products of SF_6 decomposition in mixtures are essentially the same as those found for electrical-grade SF_6, there is no reason to believe that removing discharge by-products from SF_6/N_2 mixtures should be any more difficult than removing them from SF_6 itself.

In general, there are abundant data on the basic properties of the individual constituents SF_6 and N_2 to enable reliable predictions and interpretations of many properties of SF_6/N_2 mixtures. Extensive calculations and measurements have been made on the dielectric strengths and the related breakdown voltages for the SF_6/N_2 mixtures. In these respects, SF_6/N_2 mixtures appear to be among the most thoroughly studied and understood dielectric gas mixtures. Nevertheless, it appears that the "self-healing" property of SF_6 in discharge is compromised when it is used in gas mixtures, thus rendering the latter less suitable as an arc quenching and interrupting medium required in circuit-breaker applications. From the technical point of view, the use of SF_6/N_2 mixtures as possible replacements for SF_6 appears to be most

promising and feasible for conditions where the mixture gas is used primarily as an insulating medium such as in bus lines, bushings, and transformers. It should be noted that SF_6/N_2 mixtures are already used by power industry as an insulating gas in extremely cold climates where pure SF_6 deviates from ideal gas behaviour[45]. The mixtures have also been recommended for use in gas-insulated transmission line systems[14]. However, there is a reluctance by industry to use gas mixtures in power systems, primarily because SF_6 adequately serves the present needs. The industry already has extensive experience and familiarity with SF_6 insulated equipment and little, if any, experience with gas mixtures. Despite possible advantages of SF_6/N_2 mixtures in some applications, there are likely disadvantages from added cost associated with redesigning or retrofitting equipment that could utilise gas mixtures and possible added complexities in handling, recycling and purifying the mixtures. Also, storing and handling the mixture presents practical difficulties, for example SF_6 is stored in its liquid state at about 20 bar but N_2 as a gas at some thousands of bar.

1.5.4 SF_6 gas mixtures with trace additives

As mentioned earlier, the performance of SF_6 is limited, not by its uniform field strength, but by the effects of local field enhancement, i.e., localised high-field sites associated with electrode protrusions or with filamentary conducting particles present in the insulating system. This is its most undesirable characteristic. Breakdown in such fields involves the stepped-leader mechanism, however, there is no direct correlation between the uniform field strength(or limiting field strength) of a gas or

gas mixture and the leader-breakdown threshold under the nonuniform field(or local field enhancement), because the two breakdown mechanisms are different.

In a typical industrial application the nonuniform field breakdown predominates, it is clear that the requirement is not necessarily for a gas with superior uniform field strength, but rather for a gas or gas mixtures which offers a significant improvement over SF_6 under the nonuniform field conditions associated with particles or other stress raisers. The key factor is that there should be an increase in the voltage required for leader propagation, without a significant loss of uniform field strength. The propagation of the leader which cause breakdown in a non-uniform field can be inhibited by adding traces of compounds such as triethylamine($(C_2H_5)_3N$, hereafter referred as TEA) and some original refrigerants freon(e.g. R113, R12 etc), which, when added to SF_6 in small quantities(<1%), result in improved corona stabilisation and an increase in the leader propagation field. Because of the small concentrations used, there is little change in the effective ionisation coefficient and hence in the uniform field strength relative to pure SF_6, but the particle triggered breakdown voltage may be increased by 50%.

Previous work on additives, including TEA[46], MEK(methylethylketone)[47] and R113($C_2Cl_3F_3$, trichlorotrifluoroethane)[46,48,49,50], R12(CCl_2F_2, difluorodichloro-methane[51] has been done. Initial trials of such mixtures were made using point-plane gaps under both impulse and ac or dc voltage. General speaking, the effect is to extend the corona stabilisation region to higher pressures, and to increase both stabilisation peak and the minimum-impulse(leader) breakdown voltage.

Figure 1.26[52] shows the results obtained with 1% R113 in SF_6 for a 10mm point plane gap. The important feature is the approximately 50% increase in the minimum impulse breakdown voltage, as this will correspond to the worst case in a real GIS(i.e., the ac breakdown threshold with free particles). Investigation of the leader mechanism in SF_6 with traces of additives such as Freon have shown that the effect of the additive is to inhibit both inception and the development of the leader channel.

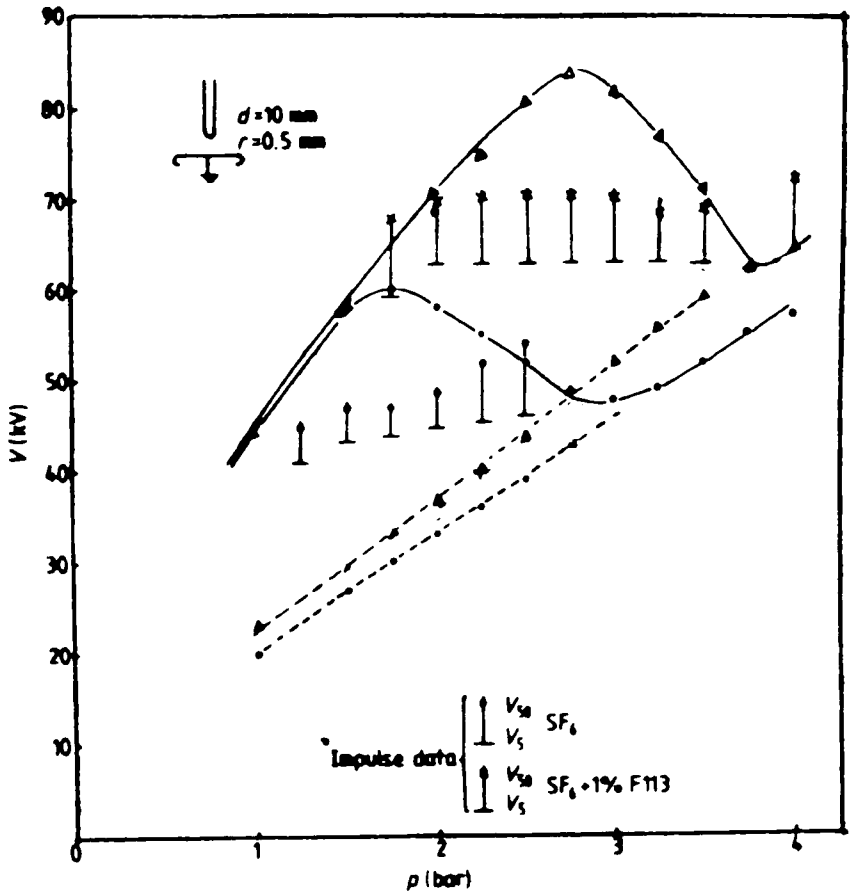

Full curves: dc breakdown, Vertical bar: 1/50μs impulse data for 50% and 5% probability levels

Figure 1.26 V-p characteristics for a 10mm point-plane gap in SF_6 and SF_6+1%R113[52]

Following the point-plane gap studies, measurements were made in a large-coaxial electrode assembly[53] in order to determine whether a similar degree of improvement would be obtained under alternating-voltage conditions with FCPs

present in the system. These tests were made with particles of length 2-10mm and additive concentrations(TEA or R113) of 0.1-1%. The effect of the additives was to increase the particle-triggered breakdown voltage by 40-60%. It has been shown for 10mm particles injected into a 125/375mm coaxial system with 1% R113 in SF_6, the breakdown voltage with particles is increased from about 350kV to above 500kV at a pressure of 4 bar. Monitoring of the point-on-wave at breakdown showed that the flashover always occurred with the inner conduction positive and when the voltage wave was just past the peak value. As is typical of a leader-type breakdown , the breakdown voltage was relatively insensitive to pressure in the range of 2-6 bar.

The coaxial arrangement used in these tests was contained within a 1m long, 620mm diameter test chamber which was mounted at the end of a 5m section of GIS bus with a standard conical epoxy barrier between the two gas zones. Following large number of breakdown trails with the additives present in the SF_6, there was no evidence of any reduction in the "clean" (i.e., particle-free) withstand level, and no breakdowns occurred along the barrier surface. There is therefore no evidence of any effect of the additives or their breakdown products on the material of the spacer, although further study of long-term compatibility will be required before such additives could be accepted for use in commercial GIS equipment.

The above-mentioned additives, however, are unlikely to be used in electric power apparatus because TEA and MEK are highly toxic. Some SF_6/freon mixtures were once considered to be very attractive, but R113 and R12 are among the five

chlorofluorocarbons whose production should be restricted in order to protect the ozone layer in stratosphere.

1.6 The aim of the present study

For a non-uniform field , the impulse breakdown mechanism is much more complicated than for a uniform field. This is probably due to the complex effect of space charge on the breakdown process[3]. In some earlier work, it has been pointed out that space charges greatly affect the breakdown strength of SF_6 in non-uniform-fields[101]. Recent work[102-104] has also shown that the positive impulse breakdown voltage in a point-plane gap is affected by the presence of space charge and it has been realised that non-uniform field breakdown in SF_6 involves the development of a series of streamer/leader steps[105] which propagate from the point electrode towards the plane. Farish et al. [106] suggested that the successful development of impulse breakdown relies on there being a supply of electrons in the gap volume such that each streamer step can be initiated. Boggs et al [107] concluded that the probability of failure of SF_6 insulated switchgear(GIS) under positive surge waveforms depends on the presence of free electrons. In a typical industrial application the nonuniform field breakdown predominates, therefore it is of considerable importance to study space charge effects on breakdown strength in non-uniform-field geometries.

The aim of the present study was to investigate the positive impulse breakdown characteristics of SF_6 and its mixtures in highly non-uniform field gaps. The study

was emphasised on the effect of space charge. artificial irradiation. different additive gases and different wavefronts on the breakdown strength by using two different injection methods — namely, corona pin method and direct injection method. In the hope that some mechanism of breakdown process in nonuniform field could be clarified. In particular, to acquire a better understanding of the corona stabilised breakdown mechanism in SF_6 gas under impulse voltage and to supply a physical base to choose an efficient additive for improving insulating strength of SF_6 gas.

Chapter 2 Apparatus and experimental techniques

2.1 Apparatus

2.1.1 Pressurised chamber and test gap assembly

The pressurised test vessel was constructed from mild steel fitted with four orthogonally arranged windows, each of 100 mm diameter. The 100mm diameter clamps, which contained the quartz windows when the vessel was pressurised, were used for observation and photomultiplier recording and they are all UV-transmitting quartz. Most measurements were made for a point-plane gap which the gap length is adjustable (the gap length could be varied up to 32.5mm with an accuracy of 0.02mm), both electrodes are stainless steel. The point electrode was formed from a 4mm diameter rod with a 40° conical end; the tip radius was 0.5mm and the plane electrode was 40mm in overall diameter. The electrodes were mounted in the above mentioned vessel designed for a maximum pressure of 1.2 MPa. The high voltage connection to the vessel was through a PVC bushing.

2.1.2 The vacuum and gas handling system

The gases used in these experiments were sulphur hexafluoride(SF_6), nitrogen(N_2), atmosphere air, R12(CCl_2F_2) and R20($CHCl_3$). The SF_6 gas used through out the tests was supplied in bottled form by BOC Ltd, which has a purity of 99.9%. The main impurities are air(200ppm), CF_4(10ppm) and H_2O(5ppm). Before filling with

gas or gas mixture, the test vessel was evacuated by an "Edwards" high vacuum rotary pump(model E2M2) to about 10^{-2} torr and flushed with appropriate gas(in the case of gas mixture, the relative cheaper component was used) then re-evacuated. After that, the test vessel was filled to the required gas pressure and the pressure was monitored using a "Budenberg" vacuum/pressure gauge. For binary gas mixtures used in these experiments, the gas with a lower mix ratio was always filled first until the certain percentage of the total pressure for the gas mixtures in question was reached, thereafter filled with the gas with higher concentration to the predetermined total pressure. After filling, the vessel was left for at least 24 hours before testing in order to achieve a uniform gas distribution.

2.1.3 High voltage supplies and Marx impulse voltage generator

- High voltage dc supply

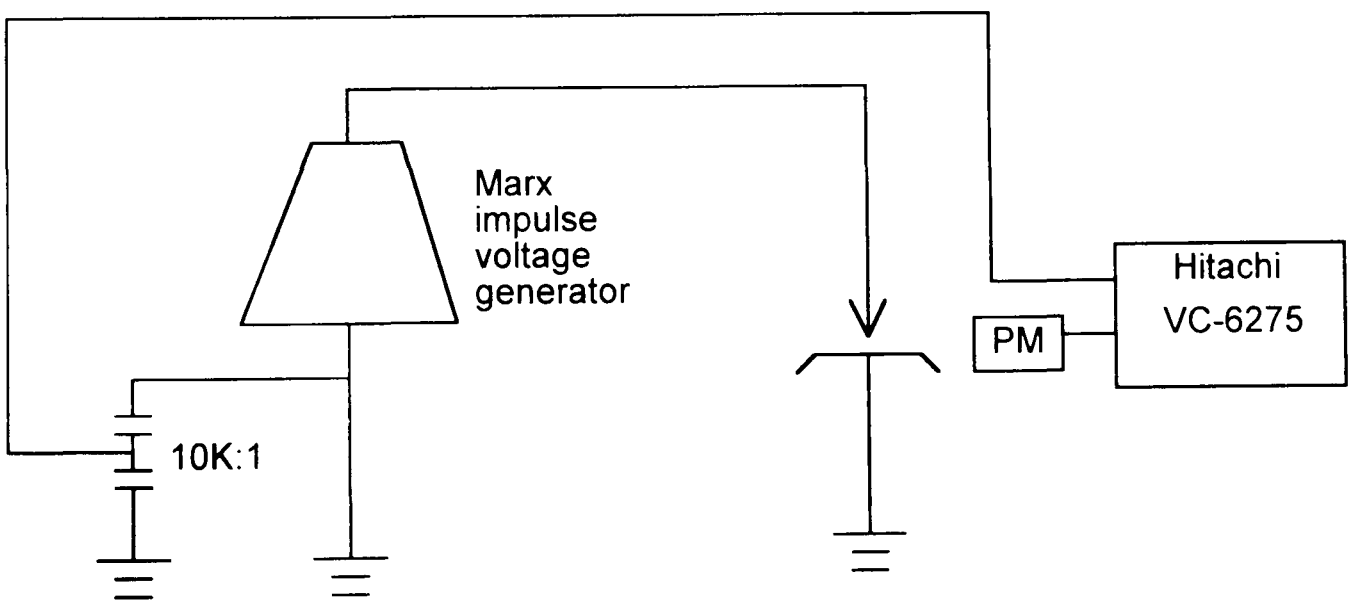

Figure 2.1 Simplified testing circuit

Figure 2.1 is the simplified testing circuit used for the tests. Two high voltage dc generators were used. One is a Glassman type WR100R2 which was capable of providing either positive or negative dc voltage up to 100kV and the other is a Branderburg type MR50 which has an output voltage up to 50kV of either positive or negative polarity. The output voltage of both dc high voltage generators is continuously variable with a ripple of 0.05% and 0.1%, respectively.

• Marx impulse voltage generator

A multistage Marx impulse voltage generator(300kV, 50J maximum) was used throughout the test and the equivalent circuit is illustrated in figure 2.2. The impulse voltage generator was charged to the required voltage using the above mentioned Glassman dc generator. The output impulse voltage value and waveform were measured and observed using a Hitachi VC-6275 digital storage oscilloscopes.

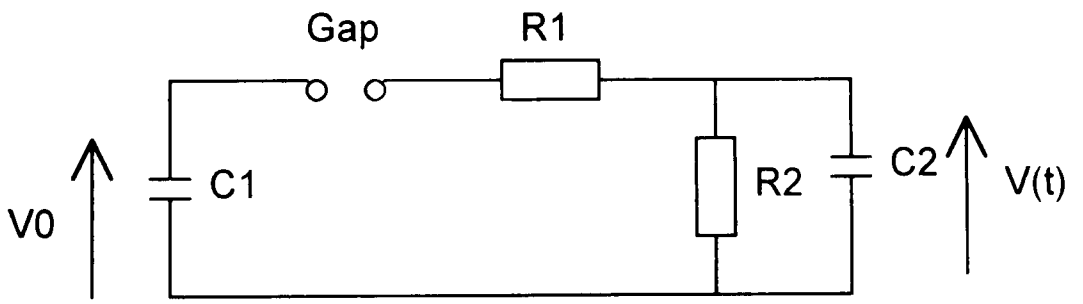

Figure 2.2 Equivalent circuit of the impulse voltage generator

where,

C_1: discharge capacitance

C_2: load capacitance

R_1: front or damping resistance

R_2: discharge resistance

A brief analysis of the circuit will be given here. As the C_2 is initially uncharged and $R_2 >> R_1$. we have,

$$V(t) = V_2(1 - e^{-\frac{t}{T_1}})$$

where:

$$T_1 = R_1 C_1 \frac{C_2}{C_1 + C_2}$$

$$V_2 = V_0 \frac{C_1}{C_1 + C_2}$$

At $t=3T_1$, $V(t) \cong 0.95V_2$. If this time is approximated to be the wavefront time, T_f. then,

$$T_f = 3R_1 C_1 \frac{C_2}{C_1 + C_2}$$

After C_2 is charged, both C_2 and C_1 discharge through R_2, so that,

$$V(t) = V_2 e^{-\frac{t}{T_d}}$$

where

$T_d=R_2(C_1+C_2)$

Since at the time of wavetail, i.e., $t=T_t$, $V(t)=50\%V_2$, then,

$0.5 = e^{-\frac{T_t}{T_d}}$, we have,

$T_t=0.693R_2(C_1+C_2)$

2.1.4 Electrical and optical recording facilities

2.1.4.1 Digital storage oscilloscope

A Hitachi VC-6275 digital storage oscilloscope(thereafter referred as the oscilloscope) is used to record and observe the impulse voltage and the output signal of the photomultiplier. The oscilloscope can record signals up to 100MHZ and it has a four kilo-words per channel memory capacity. The measuring accuracy is ±3% and the rise time is approximately 3.5ns. It has a maximum sampling rate of 200 Mega-sampling per second at one channel sampling.

2.1.4.2 Basic physics and statistics of photomultipliers

If we consider a photomultiplier as part of a system we can describe it as a transducer which converts an optical signal into an electrical one and then amplifies it. The required parameters will then be the photocathode conversion efficiency and the current gain of the multiplier system. It would be helpful to consider the two basic processes involved, photo-emission and secondary emission which are essentially quantum ones. It should be noted, however, the theory refers to ideal performance whilst a real photomultiplier will necessarily behave in a more complicated and possibly less satisfactory manner.

- **Photo-emission**

Einstein's law states that the kinetic energy E of the electron emitted when a photon of frequency v is incident on a surface with work function Ψ is given by[70]:

$$E=hv-\Psi$$

where h is Planck's constant. Write this in unit of eV and measuring the wavelength of the photon in nm gives:

$$E=\frac{1240}{\lambda}-\Psi$$

The electrons are emitted in all directions and have a distribution of energy with a cut-off at ($h\nu$-Ψ). Note that this average energy will be greater for incident light of shorter wavelength. The emission from available cathode materials always occurs very rapidly, less than 10^{-11}s.

The photons arriving at the cathode behave independently of each other and all have the same probability of releasing an electron. (This is not true for very intense beams from pulsed lasers but since the cathode would be destroyed by the beam this case needs not to be considered.) The response is therefore linear, provided that the current which flows does not alter the potential distribution. It also follows that, if N/η photons are incident, it is only the mean number of electrons produced which is equal to N. The problem is similar to the basic one in probability theory which applies to tossing dice or drawing cards from a pack — the statistics of the number of photo-electrons must be given by the binomial distribution. This will apply exactly, except possibly in the ultra violet region of the spectrum where it is energetically possible for an individual photon to produce more than one electron.

- **Secondary emission**

The variation of the mean number of secondary electrons $\bar{\delta}$ with the energy of the incident electron has the same general shape for all surfaces. The secondary electrons emerge in all directions and have a wide distribution of energies. About 1% of the incident electrons may be elasticity scattered at the dynode and appear as very high energy secondaries while a rather large proportion loses some of their energy by

inelastic scattering. The true secondaries have a most probable energy in the region of 2eV.

If each primary electron arrives with the same energy, it contributes, on average, the same number of secondary electrons. Each electron acts independently, so it follows that the secondary current is exactly proportional to the primary current.

Although the average number of secondary electrons can readily be measured, the statistical distribution is a much more intractable problem because it can only be determined indirectly. Theoretical discussion is not very helpful; if each secondary electron required a particular energy to be emitted then $\bar{\delta}$ might be very board. It is customary to assume that the distribution is a Poisson one but it must be stressed that this assumption has no theoretical basis.

- **Photomultiplier response**

For an idealised photomutiplier we can assume that η and $\bar{\delta}$ are constant on the surface of each electrode and also that all the electrons emitted are collected by the following stage. If the voltage between each pair of dynodes is the same the output charge for each electron leaving the cathode is just $\bar{\delta}^n e$ for an n-stage-tube. Writing $G=\bar{\delta}^n$ the output charge for N photo-electron is then q=GNe (problems due to space charge which, particularly if N is large, may arise in the latter stages of the tube, are ignored in this treatment, as are effects due to the finite transit times of the electrons).

If the quantum efficiency of the cathode as a function of wavelength, $\eta(\lambda)$, is known then the response to any number of incident photons is completely established.

For use in measuring a light flux the quantum efficiency of the cathode, $\eta(\lambda)$, needs to be transformed into the radiant power efficiency, $\eta'(\lambda)$.

As photon energy is $\frac{1.987 \times 10^{-25}}{\lambda}$ joules (λ in m), a flux of one photon/second is $\frac{1.987 \times 10^{-16}}{\lambda}$ watts (λ in nm) and one electron/second is 1.602×10^{-19} A, we get $\eta'(\lambda)$ equals $0.806\lambda\eta(\lambda)\text{mAW}^{-1}$ (λ in nm).

Although it is natural for physicists to measure radiant energy in watts, the appropriate unit for optics is the lumen. This essentially a physiological unit because it provides a measure of the optical sensation produced; its relationship to the watt depends on the spectral properties of the radiation considered. Hence the lumen is defined in terms of the relative sensitivity of the eye $V(\lambda)$ and the luminous efficiency of a cathode is only meaningful for a given source (usually black-body radiation at 2856K).

Some important parameters are briefly discussed here.

- **Luminous (or cathode) sensitivity**

This is the most commonly used photocathode parameter. PM tube is operated as a diode. with among 100 and 500 volts applied from cathode to collector electrodes. The specified effective area of the photocathode is illuminated by a tungsten filament lamp (operated at 2856K) at a flux of a millilumen or less. The measured photocurrent is normally expressed in terms of microamps per lumen (μA/L), having subtracted any leakage current. Typical values depend upon the photocathode type, and vary from 20 to over 300μA/L.

- **Spectral Sensitivity**

This is expressed in terms of quantum efficiency per incident photon or absolute radiant sensitivity (in milliamps per watt), at a specified wavelength. It is measured under the diode conditions specified earlier, but using a monochromatic source of radiation. Absolute calibration may be achieved by comparison with measurements taken on a standard photocathode, previously calibrated by the national standard laboratory. The accuracy of the measurements is obviously much higher than for a luminous sensitivity test, and manufactures will carry out a single wavelength measurement or complete spectral response calibration on request. In general it is possible to achieve better than ±5% accuracy (of measured value) over the range 350 to 650 nm, with less accuracy towards the U.V. and I.R. regions. However quite substantial differences in absolute calibration have been recorded between national standards laboratories in a recent survey, and therefore even radiant sensitivity figures are subject to some calibration uncertainty.

The quantum efficiency (Q.E.) can be calculated from the absolute radiant sensitivity, S (in mAW^{-1}) at any wavelength λ (in nm) by the simple relationship:

$$Q.E. = \frac{S \times 1.2395}{\lambda}$$

2.1.4.3 Corona activity measurement

An optical photomultiplier (thereafter refereed as PM) was used to monitor the low level light emission from the gap of prebreakdown corona activity. The high-gain Thorn EMI^{TM} PM type 9125QB was used to detect the low level light emission from the gap when prebreakdown ionisation occurs and it was mounted on the outside of the observation window so as to record the transmitted light from the corona. The photomultiplier arrangement consisted of 13 venetian blind dynodes with CsSb secondary-emitting surfaces. The recommended maximum anode cathode potential difference was 1500V. The voltage was supplied by a stabilised 3.0kV Thorn EMI PM28B photomultiplier power supply unit. The output signals were recorded using the Hitachi VC-6275 digital storage oscilloscope.

2.2 Experimental techniques

2.2.1 Space charge injection method

Two different space charge injection methods were used in the present work. One is the corona pin method and another is the direct injection method.

2.2.1.1 Corona pin method

The positive and negative charges were injected into a point-plane gap by means of four auxiliary needle electrodes surrounding the gap with the needles being approximately in line with the point electrode tip. The length of each needle is 1mm. The four needle electrodes were mounted on an insulation ring (with a diameter of 80 mm) and connected with the Brandenburg high voltage dc power generator. Figure 2.3 shows the arrangement of the corona pins.

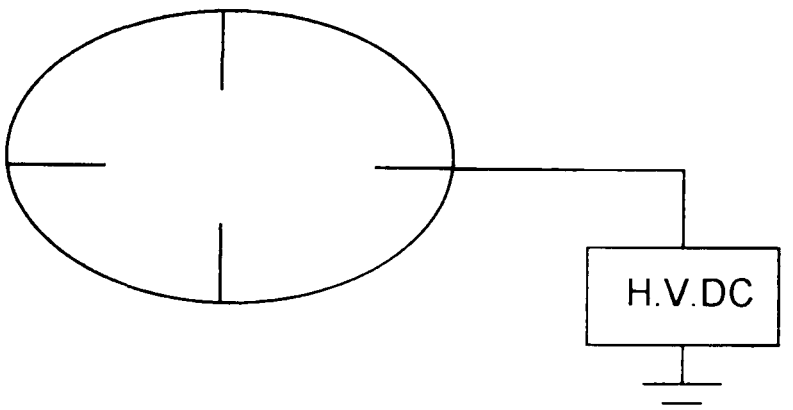

Figure 2.3 Corona pins arrangement

It should be stressed that the electrostatic capacitance between the point electrode and the needles has to be small enough so that the corona pins do not affect the electric field of the point-plane gap. This has been experimentally verified by the fact that the static breakdown voltage of the point-plane gap was not influenced by the dc bias voltage on the corona pin electrodes which is shown in figure 2.4. Clearly the dc breakdown voltage is almost the same under different dc bias voltages in a 15mm point-plane gap filled with SF_6.

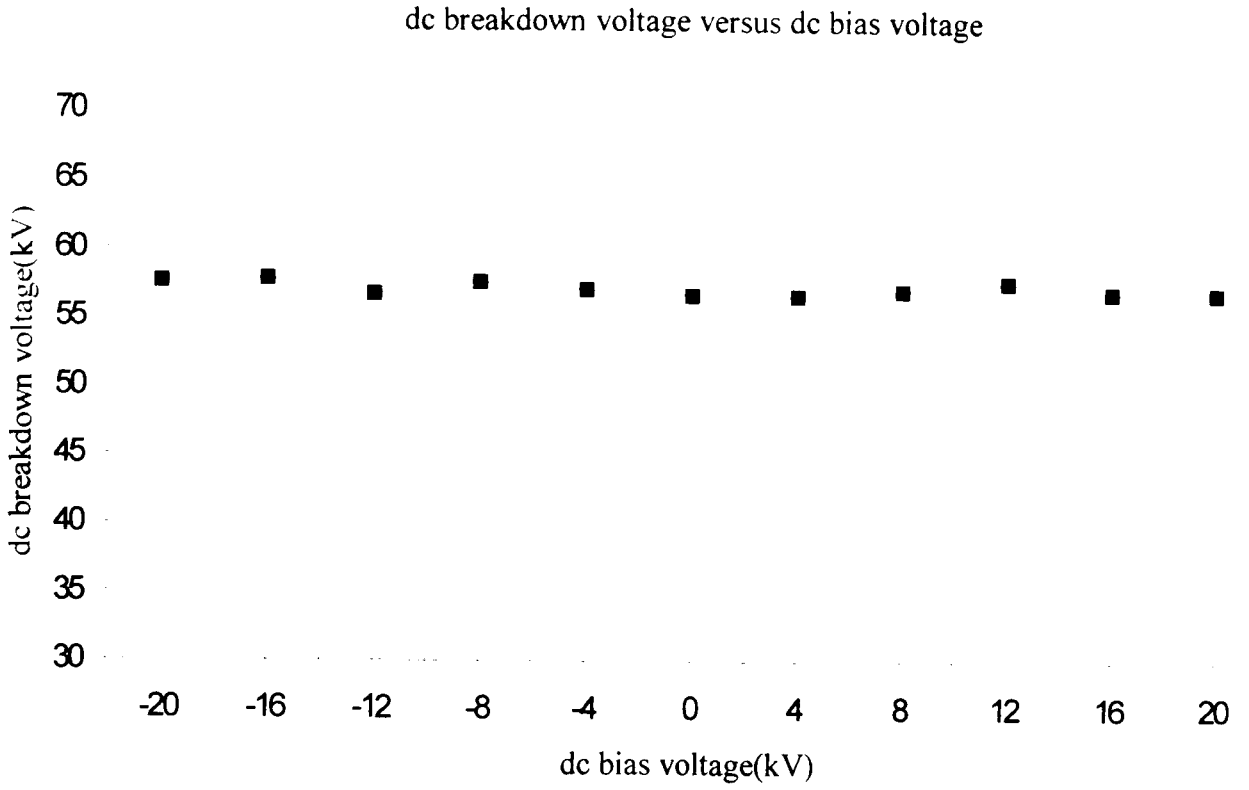

Figure 2.4 SF_6, P=0.1MPa, gap=15mm

2.2.1.2 Direct injection method

Another space charge injection method used throughout the test is the direct injection method in which dc voltage was applied to the point electrode before impulse voltage was applied. The circuit is shown in Figure 2.5. R_1 and R_2 are two wire wound resistors($2\times500k\Omega$) in series with the Brandenburg dc voltage generator. The two resistors and a high voltage switch K are used here as a protection system in case of any damage on dc generator due to the impulse voltage. A capacity $C_1(0.25\mu F)$ was used to prevent any influence on impulse voltage generator from the dc generator.

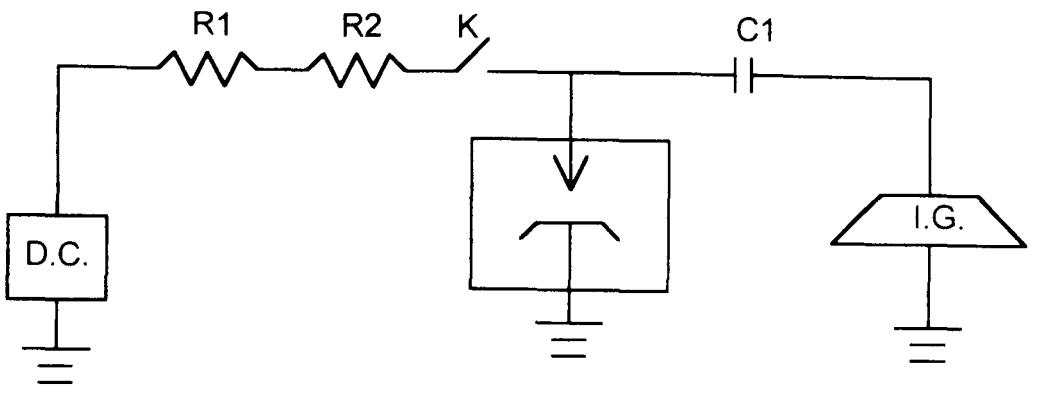

Fig.2.5 Test circuit for direct injection method

2.2.2 Artificial Irradiation

In experiments involving space charge injection, it is necessary to provide free electrons and compare the difference between various space charge injection methods. It is well known that the artificial irradiation increases the availability of the initiating electrons and in the present work two irradiation techniques were employed.

2.2.2.1 Ultra-violet irradiation

When the experiments were carried out in air, the point-plane gap was irradiated by a 125W quartz-mercury arc lamp. The lamp was placed approximately 120mm from the gap. In the case of a diverging beam of ultra-violet light photoelectrons are released from the whole illuminated area of the gaps, but only a small proportion of the electrons will accelerate across the gap from the cathode to provide breakdown. The quartz-mercury arc lamp used in this work proved itself as a satisfactory irradiation source possible on account of its shorter wave length spectrum[109].

2.2.2.2 Irradiation using radioactive isotope

In experiments involving N_2, SF_6, SF_6/N_2, SF_6/Air, SF_6/R12 and SF_6/R20 gases/gas mixtures, UV irradiation is often considered to be insufficient for gaps due to photon absorption in these gases and gas mixtures. So a 5mCi capsule ^{137}Cs was placed close to the point electrode (approximately 100mm from the point electrode) to provide γ ray. The production rate (electrons/s· cm^3) of the radiation source is not available, but considering the current experimants are to compare the effect of with or without irradiation, this value would be relatively insiginicant.

2.2.3 Minimum impulse breakdown voltage measurement

2.2.3.1 The importance of minimum impulse breakdown voltage

It should be noted that though 50% probability (V_{50}) is widely used, it has been shown[50] that care should be exercised when considering V_{50} data in nonuniform field gaps in which corona stabilisation peaks are exhibited. Depending on a number of factors including the impulse waveshape and the gap geometry and irradiation, although the V_{50} level can sometimes be increased, the low probability level, which is naturally of greater importance in terms of design, often remains practically unchanged or can sometimes even decrease. Also, most, if not all of these mixtures suffer from the fact that due to the relative low strength of the carrier gas, the uniform field performance is poor and therefore, the corona onset level at any given pressure in the nonuniform field gap is low compared to that of SF_6. Thus it is clear

that the low probability level is a much more interesting and meaningful value. The minimum level is obviously that to which practical equipment must be designed if insulation failure is to be avoided and also, in terms of physical mechanisms, this is the stress level at which the gap will just break down if all necessary statistically varying conditions are simultaneously satisfied.

2.2.3.2 The measurement and the procedure

Before any test was carried out, the electrodes were first cleaned in normal manner, set to the desired spacing and the system was pumped, flushed, repumped and then filled to the desired pressure with appropriate gas/gas mixture. The minimum impulse breakdown voltage values and waveforms were measured using a Hitachi VC-6275 storage oscilloscope in conjunction with a 10K:1 ratio capacitor divider.

In each test sequence, the 50% breakdown level was first determined by the normal up-and-down method, and then the charging voltage of impulse voltage generator was reduced in steps of 0.5kV to give the level at which only 1 flashover in 40 was recorded, this gave the minimum (2.5% level) breakdown voltage. The impulse voltage had a waveform of 1.2/50μs and the impulse breakdown voltages were measured with one minute time interval after each breakdown to ensure complete deionisation of the gap and cooling of the electrodes surface.

Chapter 3 The effect of space charge

3.1 Introduction

In non-uniform field gaps, the appearance of first streamer may lead to breakdown or it may lead to the establishment of a steady-state corona discharge which stabilises the gap against breakdown. Accordingly, there may be a corona stabilised or direct breakdown. Whether direct or corona stabilised breakdown occurs will depend on factors such as the degree of field non-uniformity, gas pressure, voltage polarity and the nature of the gas. For example, in air the corona stabilised breakdown will extend to higher pressures than in SF_6 due to the relative immobile SF^- ions. The breakdown mechanism is much more complicated than for a uniform field and it has been realised that this is probably due to the complex effect of space charge on breakdown process[3].

The positive and negative point-plane gap breakdown characteristics measured in air as a function of gas pressure are compared in figure 3.1[29]. The breakdown characteristics for the two polarities at very small spacing are almost the same and no corona stabilised region is observed. As the spacing is increased, the positive characteristics display distinct high corona breakdown up to a pressure of about 0.7 MPa, followed by a sudden drop in breakdown strengths. Under negative polarity the corona stabilised region extends to much higher pressures.

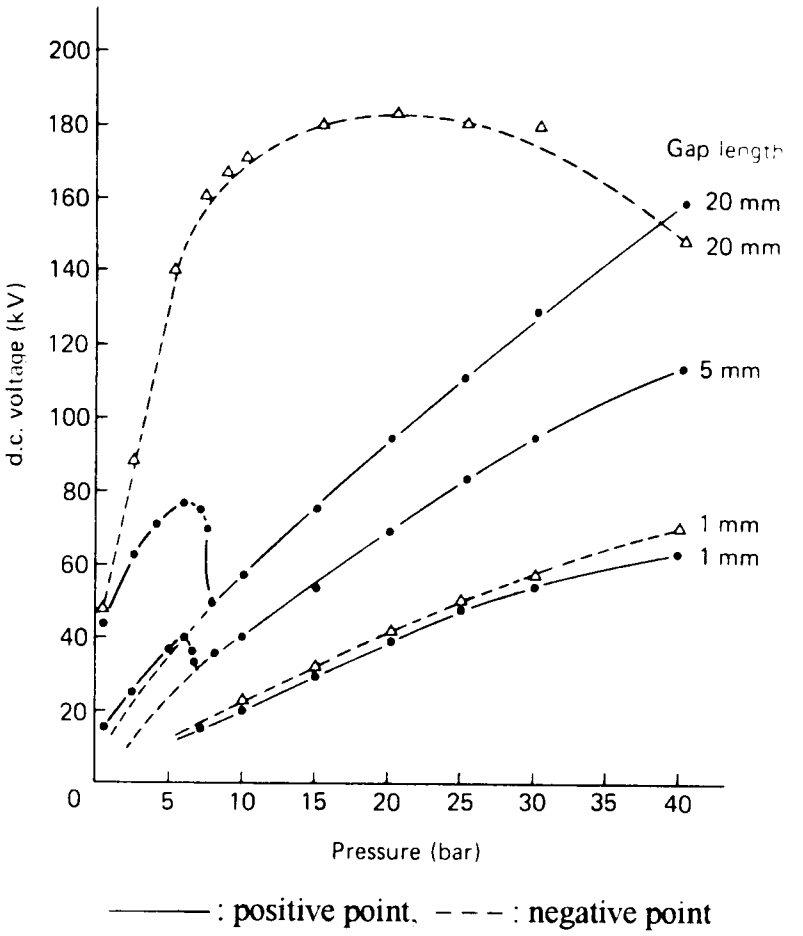

Figure 3.1 Point-plane breakdown and corona inception characteristics in air (radius of curvature of point r=1mm) [29]

In SF_6, experiments show that the region of corona stabilised breakdown under positive voltage is limited to pressure below approximately 0.15MPa. Extensive studies[95,96] of breakdown and corona inception in highly divergent fields in SF_6 have shown that whilst the corona stabilised voltage increased rapidly as the field becomes more divergent, the critical pressure beyond which the breakdown strength fall abruptly is not much affected by the field non-uniformity and for all geometries studies it is limited to pressure below 0.2MPa.

A practical non-uniform field geometry that is frequently used in the construction of high voltage apparatus is the coaxial cylindrical arrangement. By properly choosing

the radial dimensions of the cylinders it is possible to optimise such a system for the maximum corona free breakdown.

Take a system of two coaxial cylinders with inner and outer radii of r_i and r_0 for example. It can be readily shown that in the interelectrode space at radial distance r the field strength is given by,

$$E_r = \frac{V}{r \ln \frac{r_0}{r}} \qquad (3.1)$$

in which V is the applied voltage. As the breakdown or corona onset will follow when the voltage stress as the smaller wire reached the breakdown stress(E_b) the above equation can be written as,

$$V_b = E_b r_i \ln \frac{r_0}{r_i} \qquad (3.2)$$

where E_b is the breakdown (or corona inception) field strength of the system. The maximum breakdown voltage of the system is obtained by differentiating the above equation with respect to r_i. The field strength E_b depends on the gas density as well as the inner conductor radius r_i. Neglecting this dependency, which would hold approximately for not too small radii r_i and/or strongly attaching gases (with a steep increase of $\bar{\alpha}/p=f(E/p)$, we may assume that E_b is a constant value. Then, keeping r_0 constant this condition gives the optimal design of the system,

$$\frac{dV_b}{dr_i} = E_b\left(\ln \frac{r_0}{r_i} - 1\right) = 0 \qquad (3.3)$$

or

$$\frac{r_0}{r_i} = e \qquad (3.4)$$

and

$$(V_b)_{max} = E_b r_i \qquad (3.5)$$

The relationship between the breakdown voltage and the radius of the inner cylinder for a fixed radius r_0 of the outer cylinder is shown in figure 3.2[29]. The maximum breakdown voltage is also indicated. The dotted curve indicates quantitatively the corona onset voltage and the solid curve the breakdown voltage.

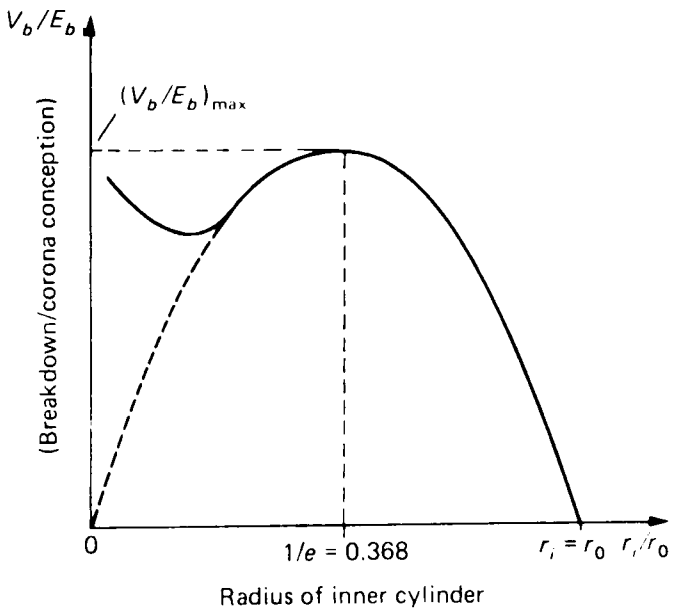

Figure 3.2 Relationship between breakdown voltage and inner radius in a coaxial cylinder system [29]

In the case of a positive point-plane gap shown in figure 3.3(a)[29] then an ionisation by electron collision takes place in the high field region close to the point. Because of their higher mobility, electrons will be readily drawn into the anode, leaving the positive space charges behind. The space charges will cause a reduction in the field

further away from it. The field distortion caused by positive space charges is shown in figure 3.3(b)[29]. The dotted curve represents the original undistorted field distribution across the gap while the solid curve represents the distorted field. The high field region is in time moving further into the gap extending the region for ionisation. The field strength at the tip of the space charge may be high enough for the initiation of a cathode-directed streamer that subsequently may lead to complete breakdown. With the negative point (as shown in figure 3.4[29]), the electrons are repelled into the low field region and in the case of attaching gases become attached to the gas molecules and tend to hold back the positive space charges which remain in the space between the negative charges and the point. In the vicinity of the point, the field is grossly enhanced, but the ionisation region is drastically reduced. The effect is to terminate ionisation. Once ionisation ceases, the applied field sweeps away the negative and positive ion space charges from the vicinity of the point and the cycle starts again after the cleaning time for the space charges. To overcome this retarding action of the ions, a higher voltage is required, and hence negative breakdown voltage is higher than the positive breakdown voltage in gaps with marked asymmetrical fields.

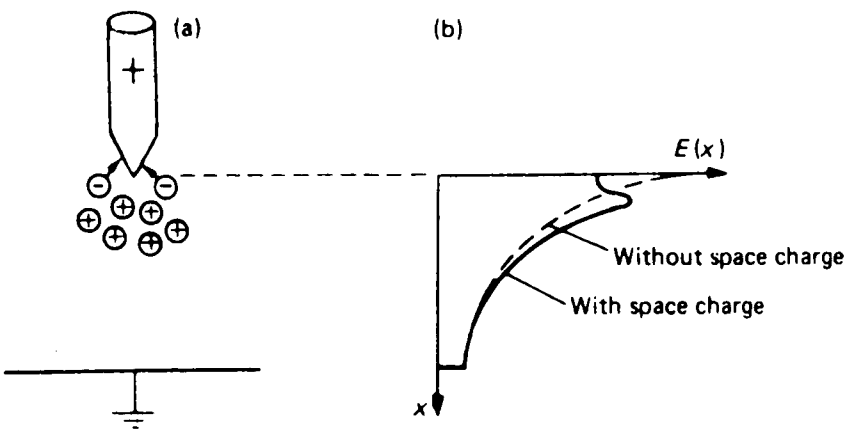

Figure 3.3 (a) Space charge build-up in positive point-plane gap (b)Field distortion by space [29]

Mathematically at any given time the voltage across the gap is given by the field integral $\int E(x)dx = V$. Integration of the space charge distorted field in figure 3.3 and figure 3.4 respectively shows that, $V_b(+point)<V_b(-point)$.

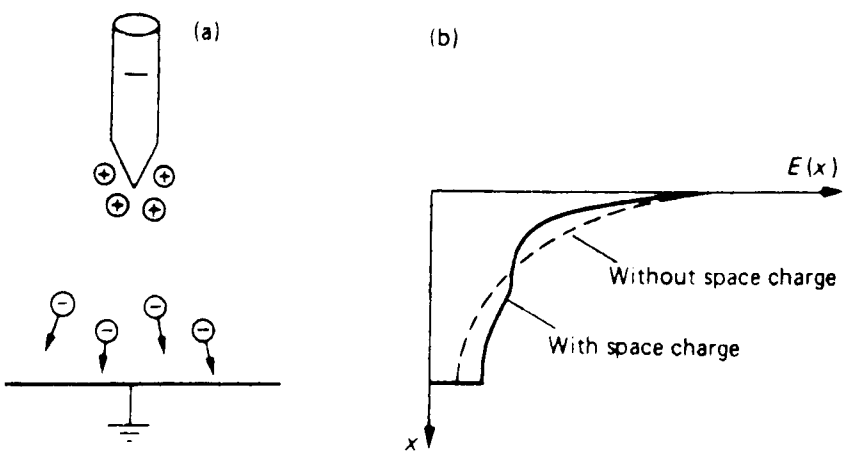

Figure 3.4 (a) Space charge build-up in negative point-plane gap (b)Field distortion by space [29]

As mentioned in Chapter 1, although SF_6 is the most commonly used insulating gas in electrical system to date [1], because of its high cost, sensitive to particle effects, restricted working-temperature range and the green house effect, there has been an increasing interest in the study of alternative gas mixtures. It seems fair to conclude from previous studies [63,64,89,90,117,141,144,151,152,153 and 155]that only some SF_6 mixtures with buffer gases are possible for industrial applications. Of those studied, SF_6/N_2 and SF_6/air are quite promising and are of research interest. It has been proved that there are at least four ways in which SF_6 gas mixtures with buffer gases may be superior to SF_6 commonly used alone in industrial practical high-voltage systems. Firstly, higher total gas pressure may be used without raising the minimum operating temperature. Secondly, the cost of mixtures for a given pressure

can be reduced considerably depending on the cost of the second component. Thirdly, gas mixtures offer the possibility of some degree of immunity from the breakdown initiated by local (microscope) field non-uniformities associated. Last but not the least, the use of SF_6 mixtures with buffer gases could be a short-term solution to the problem of eliminating the potential contribution of SF_6 to global warming.

The study of trace additives [106,137,138 and 139], especially some original refrigerants freon (e.g. R113, R12 etc) had shown that though these SF_6/freon mixtures have high dielectric strength and they were once considered to be very promising, they have no industrial prospects because they are environmentally unfriendly. Chalmers et al. [119] suggested that the marked improvement in the insulating performance of SF_6 and hence to the tolerance of the gas to metallic particle in GIS when a chlorinated freon is present is related to ion chemistry. A better physical understanding of the factors that contribute to "good" insulating gases will assist in making informed choices for the next generation of GIS.

3.2 Experimental setup and procedure

The pressurised chamber and the test gap assembly are well documented in chapter 2 and therefore would only be briefly commented upon here. The point-plane electrodes were first cleaned in normal manner before test, and set to the required spacing. The test chamber was vacuumed, flushed, re-vacuumed and then filled to the pressure of 0.1MPa. The minimum impulse breakdown voltage, corona activity and time lag to breakdown were measured and recorded by the oscilloscope.

The tests reported in this chapter were carried out in SF_6, SF_6/air(50/50), SF_6/N_2(50/50), SF_6/R12(95/5) and SF_6/R20(95/5). For the gases used, SF_6, N_2, R12 (CCl_2F_2) and R20 ($CHCl_3$) were supplied in bottles but air was of atmosphere air. Before filling gas mixtures, the test vessel was evacuated to about 10^{-2} torr and flushed with the relative cheaper component of the mixture. The gas with the lower mix ratio was always filled first until the certain percentage of the total pressure for the gas mixtures in question was reached and thereafter filled with the gas with higher concentration to the predetermined total pressure. The vessel was left for at least 24 hours before testing in order to achieve a uniform gas distribution. Throughout the tests, the gap length was 15mm and the gas pressure was 0.1MPa. Two different kinds of space charge injection methods were investigated and compared before tests were carried out, which will be discussed in sections 3.3.

For corona pin methods, both positive and negative polarities dc voltages (up to ±20kV) were applied to the four needle electrodes for injection of positive and negative space charges. Positive lightning impulse voltage with a waveform of 1.2/50μs was applied to the point-plane gap while the dc bias voltage was applied on the needle electrodes. The test circuit of direct injection method (figure 2.5) is shown in 2.2.1.2. The dc voltage (V_c) was applied to the point electrode for one minute then the high voltage switch was switched off, shortly after the impulse voltage was applied to the point electrode. The time of dc voltage application is an important factor on breakdown characteristics[111]. Therefore, the relationship between dc applied time (Δt) and minimum impulse breakdown voltage (V_b) was tested prior to

any experiment. Figure 3.5 shows the $\Delta t \sim V_b$ curve for SF_6. It can be noticed that for either positive or negative applied dc voltage, the minimum impulse breakdown voltage becomes constant when the dc voltage applied time is longer than one minute. The same is true for the results obtained in gas mixtures. Figure 3.6 shows the $\Delta t \sim V_b$ curve for SF_6/air(50/50).

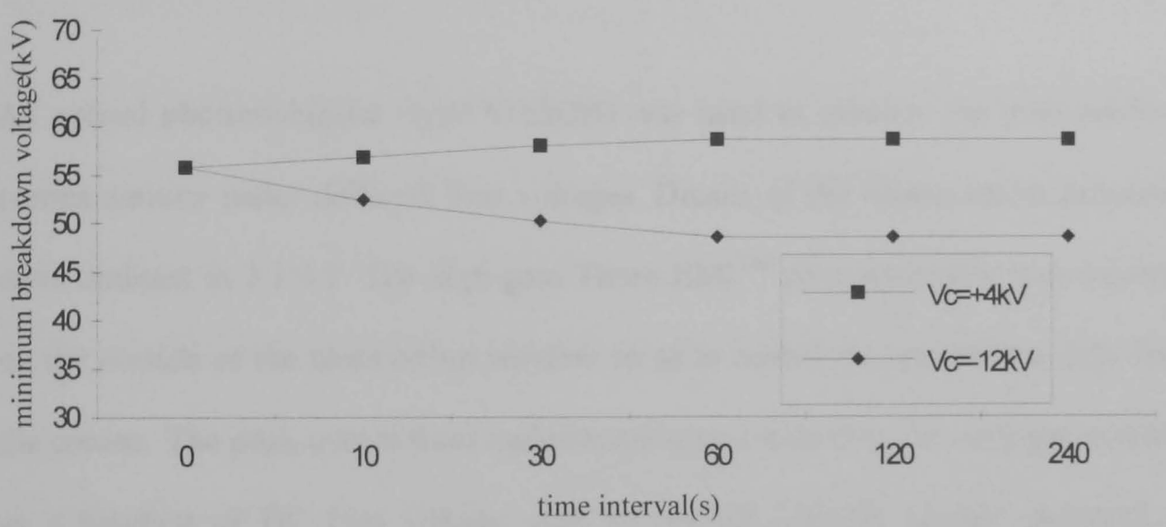

Figure 3.5 DC applied time versus minimum impulse breakdown voltage in a 15mm SF_6 point-plane gap

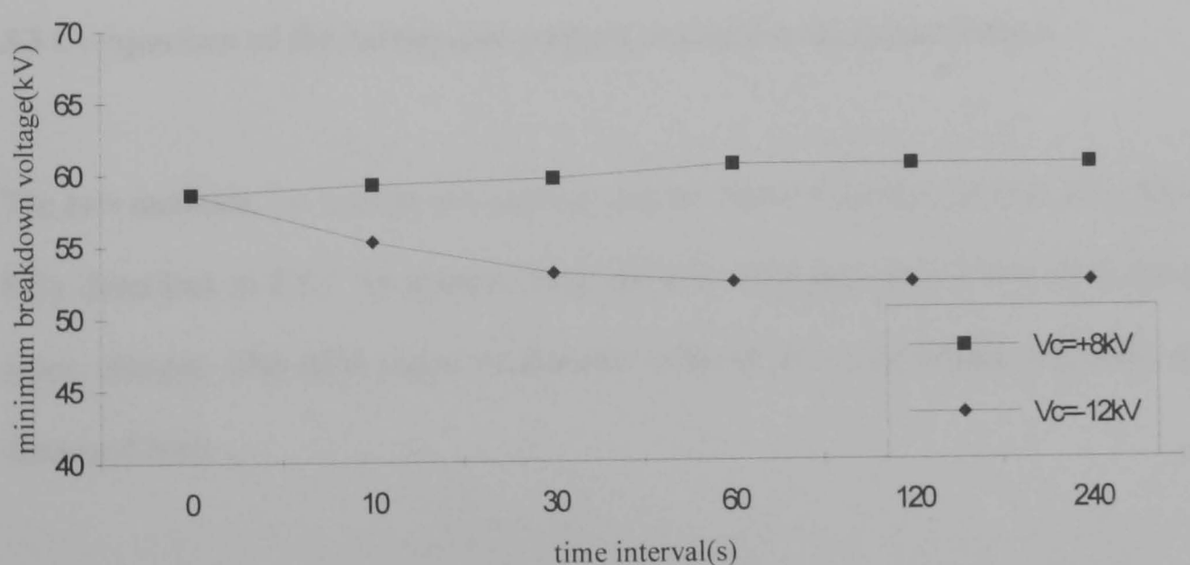

Figure 3.6 DC applied time versus minimum impulse breakdown voltage in a 15mm SF_6/air(50/50) point-plane gap

• Time lag measurement

A sequence of 100, positive impulse voltages were applied to the gap with a voltage corresponding to the 90% breakdown level. The time lag to breakdown was recorded on the oscilloscope and results were given in column charts.

- Prebreakdown corona activity measurement

An optical photomultiplier (type 9125QB) was used to monitor the prebreakdown corona activity under different bias voltages. Details of the measurement procedure were outlined in 2.1.4.3. The high-gain Thorn EMI^{TM} photomultiplier was mounted on the outside of the observation window so as to record the transmitted light from the corona. The peak output from a photomultiplier (observing the total gap activity) as a function of DC bias voltage with an applied impulse voltage provided no breakdown occurs was recorded.

3.3 Comparison of the corona-pin method and direct injection method

The two methods, i.e. corona pin method and the direct injection method have been fully described in 2.2.1. In general, both methods have the same effect of injecting space charges. The differences of the two methods in space charge injection are discussed here.

- Direct injection method

The amount of space charges injected (Q_i) into the gap from the point electrode can be expressed as[112].

$$Q_i \propto r^2 E_i (\frac{V_{dc}}{V_i} - 1)^2 \qquad (3.6)$$

where r is the radius of the point electrode, E_i the maximum field strength at the tip of point electrode when dc corona onset occurs, V_{dc} the dc voltage applied on the point electrode and V_i the corona onset voltage. It should be noted that (3.6) is only correct when $V_{dc}>V_i$, that is no space charges are injected if $V_{dc}\leq V_i$. According to the relationship between corona current I_c and dc applied voltage V_{dc}[113],

$$I_c \propto V_{dc}(V_{dc} - V_i) \qquad (3.7)$$

it can be seen that the Q_i and I_c increase as the V_{dc} increases.

• Corona pin method

Four auxiliary needle electrodes surrounding the gap with the needles being approximately in line with the point electrode tip so that both positive and negative charges could be injected into the gap by means of alternating the polarity of the dc voltage source which is connected to the needle electrodes. Considering the electric circuit effect, the auxiliary needle electrodes act as a capacitor in parallel with the test gap. The capacitance between the point electrode and the needles should be

small enough compared with the capacitance of the test gap to avoid electric field distortion near the high stress electrode caused by the bias voltage. Measurement [53] showed that the electrostatic capacitance of the 10-20mm test gap is approximately 10-20pF while the electrostatic capacitance between the point electrode and the needles is only 0.2pF. Also experiments (figure 2.4 in section 2.2.1.1) showed that the positive dc breakdown voltage is independent of the dc bias voltage which indicates that auxiliary needle electrodes have no effect on the electric field of the test gap. When dc applied voltage on needle electrodes is higher than corona inception voltage($V_{dc}>V_i$), space charges are injected into the gap according to equation 3.6.

3.4 Low-probability impulse breakdown voltages

- SF_6 and its mixtures with N_2 and air

Figure 3.7 shows the minimum impulse breakdown voltages(V_b) measured in the 15mm SF_6, SF_6/N_2(50/50) and SF_6/air(50/50) gaps as functions of the bias voltages(V_c) on the corona pin arrangement, from which the following common observations were made, (The V_{50} values are also given in table 3.1 for comparison)

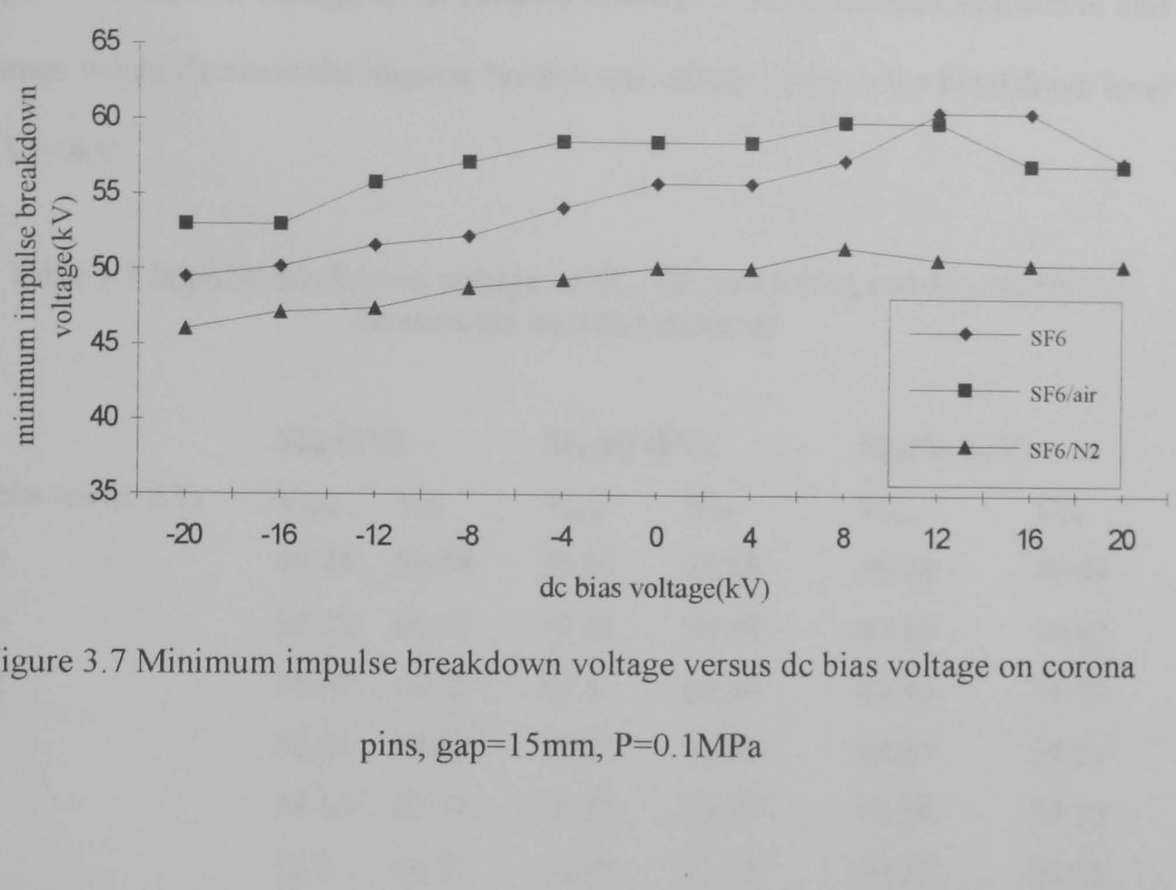

Figure 3.7 Minimum impulse breakdown voltage versus dc bias voltage on corona pins, gap=15mm, P=0.1MPa

(1)Without dc bias voltage, SF_6/air has the highest minimum impulse breakdown voltage (105% of sure SF_6), and SF_6/N_2 also has about 90% of the minimum impulse breakdown strength of pure SF_6. The impulse breakdown properties of SF_6/air and SF_6/N_2 are extremely attractive under the current unfavourable environmental issues concerning SF_6 and the attendant quest for alternative gases.

(2)With the increase in negative dc bias voltage, the minimum impulse breakdown voltages for all three gases considered decreases. SF_6 decreases to 88.7% (compared with the breakdown voltage at V_c=0kV) when V_c=-20kV while the decreasing rate for SF_6/air is 90.5% and for SF_6/N_2, 91.7%. However, it can be seen that there is a saturation effect. As V_c exceeds -16kV, the minimum impulse breakdown voltage decreases very little (SF_6 and SF_6/N_2) or remains constant (SF_6/air).

(3)With the increase in positive dc bias voltage, there is little increase in minimum impulse breakdown voltage for SF_6 and its mixtures. Further increase in positive bias voltage would decrease the impulse breakdown voltage close to the breakdown level as V_c=0kV.

Table 3.1 Impulse breakdown voltage of SF_6, SF_6/air(50/50) and SF_6/N_2(50/50) (corona pin injection method)

	SF_6 (kV)		SF_6/air (kV)		SF_6/N_2 (kV)	
dc bias voltage (kV)	V_{min}	V_{50}	V_{min}	V_{50}	V_{min}	V_{50}
-20	49.48	58.08	53.01	56.58	46.04	49.94
-16	50.22	60.11	53.01	56.58	47.15	50.92
-12	51.62	60.75	55.8	60.30	47.43	51.73
-8	52.24	60.83	57.2	60.68	48.83	52.51
-4	54.14	61.71	58.59	62.27	49.38	54.19
0	55.8	61.71	58.59	62.27	50.22	54.35
4	55.8	62.82	58.59	63.45	50.22	54.68
8	57.45	63.77	59.99	64.32	51.62	55.86
12	60.73	65.65	59.99	65.56	50.86	56.13
16	60.73	64.69	57.2	63.22	50.56	56.58
20	57.45	63.24	57.2	63.22	50.56	56.69

As the result of using the direct injection method, figure 3.8 shows the minimum impulse breakdown voltages(V_b) measured in the 15mm SF_6, SF_6/N_2(50/50) and SF_6/air(50/50) gaps as functions of the dc applied voltages on the point electrode (V_c), it can be noticed that, (The V_{50} values are also given in table 3.2 for comparison)

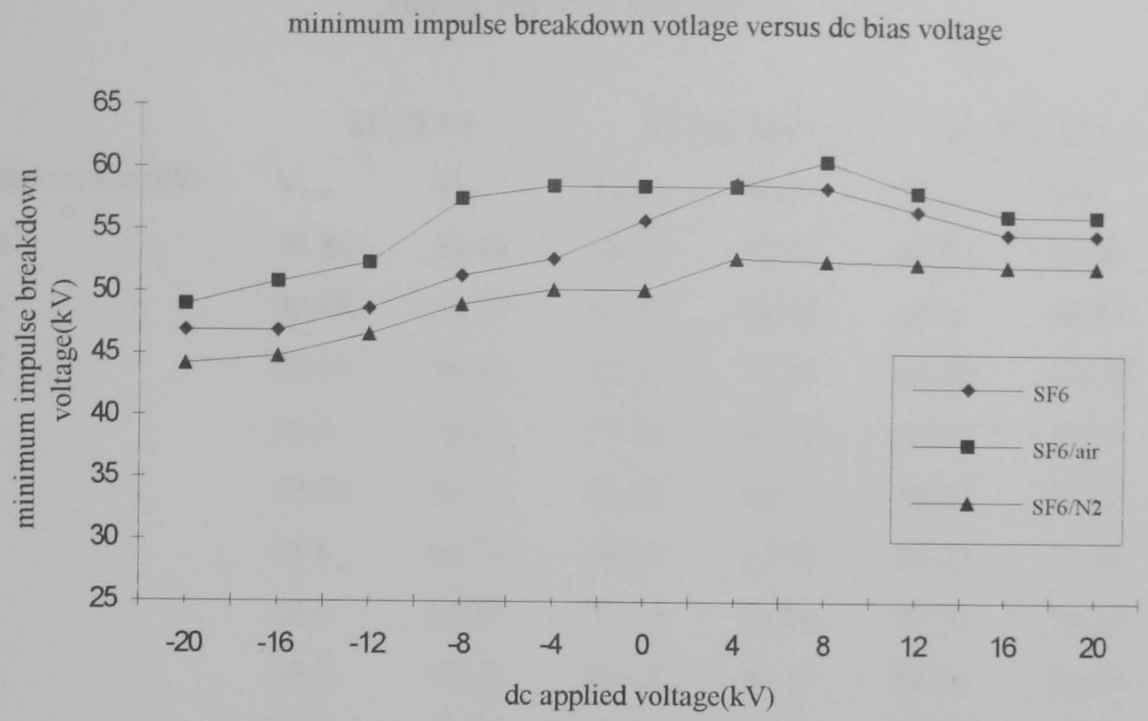

Figure 3.8 Minimum impulse breakdown voltage versus dc applied voltage on point electrode, gap=15mm, P=0.1MPa

(1)With the increase in negative dc applied voltage, the minimum impulse breakdown voltages for all three gases concerned decrease, which is consistent with the results obtained by using corona pin arrangement (figure 3.7). For SF_6 gap, the minimum impulse breakdown voltage decreases to 84% when V_c=-20kV. For SF_6/air it is 83.6% and SF_6/N_2, 87.9%. The saturation effect is again noticed here as the negative applied voltage is over -16kV.

(2)With the increase in positive dc applied voltage, there is an increase in minimum impulse breakdown voltage then there is a decrease in impulse breakdown voltage as the positive dc applied voltage increases, which is the same tendency as observed in figure 3.7.

Table 3.2 Impulse breakdown voltage of SF_6, SF_6/air(50/50) and SF_6/N_2(50/50) (direct injection method)

	SF_6 (kV)		SF_6/air (kV)		SF_6/N_2 (kV)	
dc bias voltage (kV)	V_{min}	V_{50}	V_{min}	V_{50}	V_{min}	V_{50}
-20	46.88	53.48	48.96	52.67	44.17	48.26
-16	46.88	54.77	50.77	54.45	44.8	48.67
-12	48.68	56.81	52.35	56.75	46.59	50.69
-8	51.3	58.89	57.56	61.42	49.01	52.46
-4	52.73	59.72	58.59	62.72	50.22	55.23
0	55.8	61.71	58.59	62.72	50.22	54.35
4	58.8	65.82	58.59	63.24	50.22	54.35
8	58.5	65.35	60.67	64.19	52.64	56.68
12	56.7	61.02	58.2	63.27	52.46	57.73
16	54.9	60.86	56 36	62.58	52.27	58.29
20	54.9	58.92	56.36	62.58	52.27	58.29

- SF_6/freon mixtures

The results obtained in R12 and R20 additives are shown in figure 3.9. Minimum impulse breakdown voltage versus dc bias voltage (V_c) on corona pins was measured in SF_6/R12(95/5) or SF_6/R20(95/5). The V_{50} values are also given in table 3.3 for comparison.

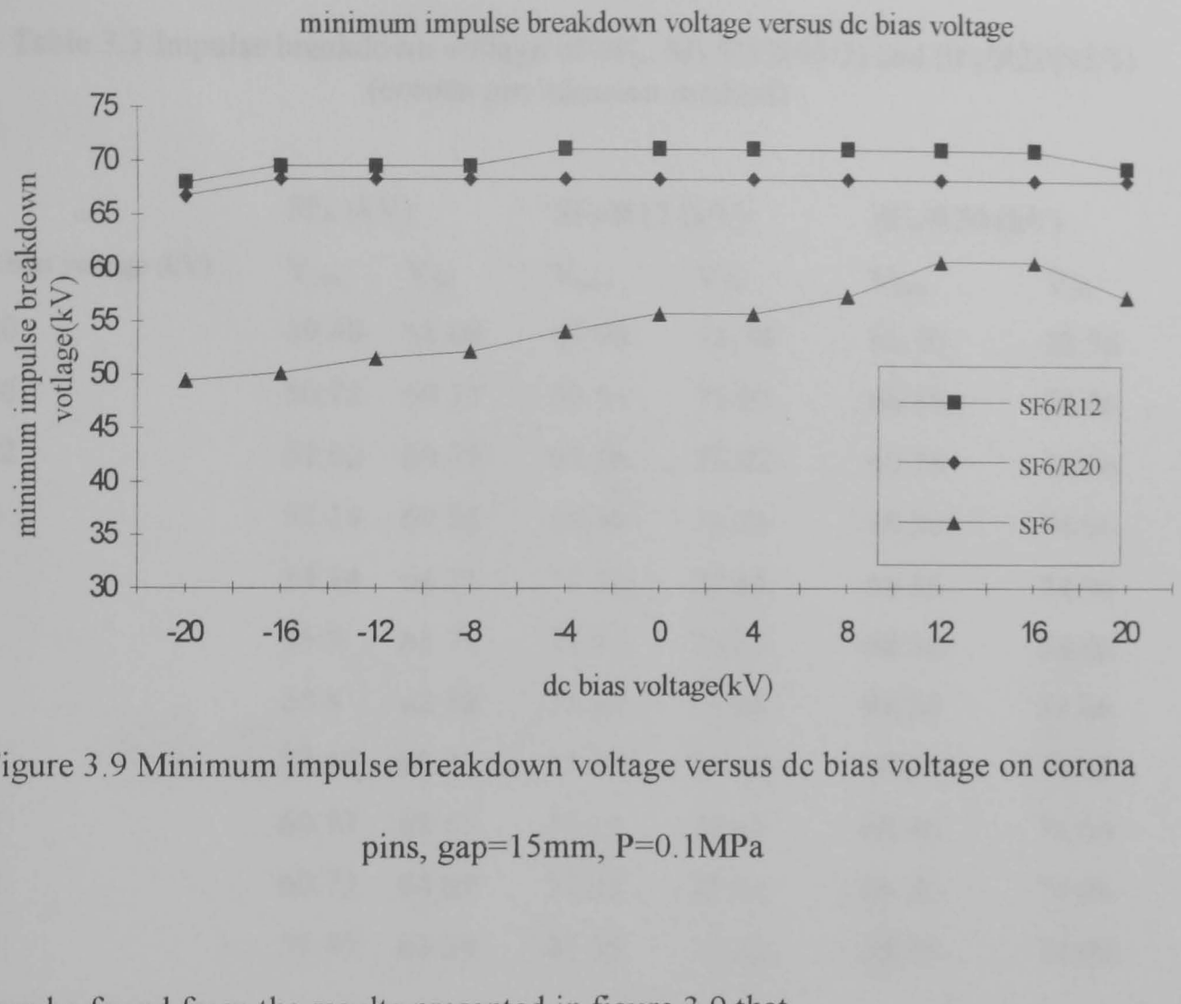

Figure 3.9 Minimum impulse breakdown voltage versus dc bias voltage on corona pins, gap=15mm, P=0.1MPa

It can be found from the results presented in figure 3.9 that,

(1)The presence of the two freon additives (R12 and R20) increases the minimum impulse breakdown voltage by 27.5% and 22.5% respectively compared with that of SF_6 under the condition no space charge is injected (i.e. V_c=0kV).

(2)With the injection of negative ions, the minimum impulse breakdown voltage decreases very little compared with the results obtained in SF_6, SF_6/N_2 and SF_6/air (figure 3.7).

(3)With the injection of positive ions, there is almost no effect on minimum impulse breakdown voltage.

Table 3.3 Impulse breakdown voltage of SF_6, SF_6/R12(95/5) and SF_6/R20(95/5) (corona pin injection method)

	SF_6 (kV)		SF_6/R12 (kV)		SF_6/R20 (kV)	
dc bias voltage (kV)	V_{min}	V_{50}	V_{min}	V_{50}	V_{min}	V_{50}
-20	49.48	58.08	67.98	73.78	66.76	72.56
-16	50.22	60.11	69.56	75.02	68.36	74.06
-12	51.62	60.75	69.56	75.02	68.36	74.06
-8	52.24	60.83	69.56	76.24	68.36	74.06
-4	54.14	61.71	71.15	76.65	68.36	74.06
0	55.8	61.71	71.15	76.65	68.36	74.06
4	55.8	62.82	71.15	76.65	68.36	74.06
8	57.45	63.77	71.15	76.65	68.36	74.06
12	60.73	65.65	71.15	76.65	68.36	74.06
16	60.73	64.69	71.15	75.02	68.36	74.06
20	57.45	63.24	69.56	75.02	68.36	74.06

The results obtained in R12 and R20 additives by using the direct injection method are very similar to those obtained using corona pin arrangement method.

3.5 Time lag measurement

Time lag to breakdown was measured in 15mm SF_6, SF_6/air(50/50), SF_6/N_2(50/50), SF_6/R12(95/5) and SF_6/R20(95/5) gaps under both space charges injection methods when V_c=0, -16kV and 8kV. Figures 3.10 to 3.12 show the results obtained in the 15mm SF_6 gap as the space charges were injected using corona pin arrangement method. The positive impulse voltages were applied to the gap with a voltage

corresponding to the 90% breakdown level. For SF_6 gap, the values are 57.8kV when V_c=0kV (fig.3.10), 55.2kV when V_c=-16kV (fig. 3.11) and 59.8kV when V_c=8kV (fig. 3.12).

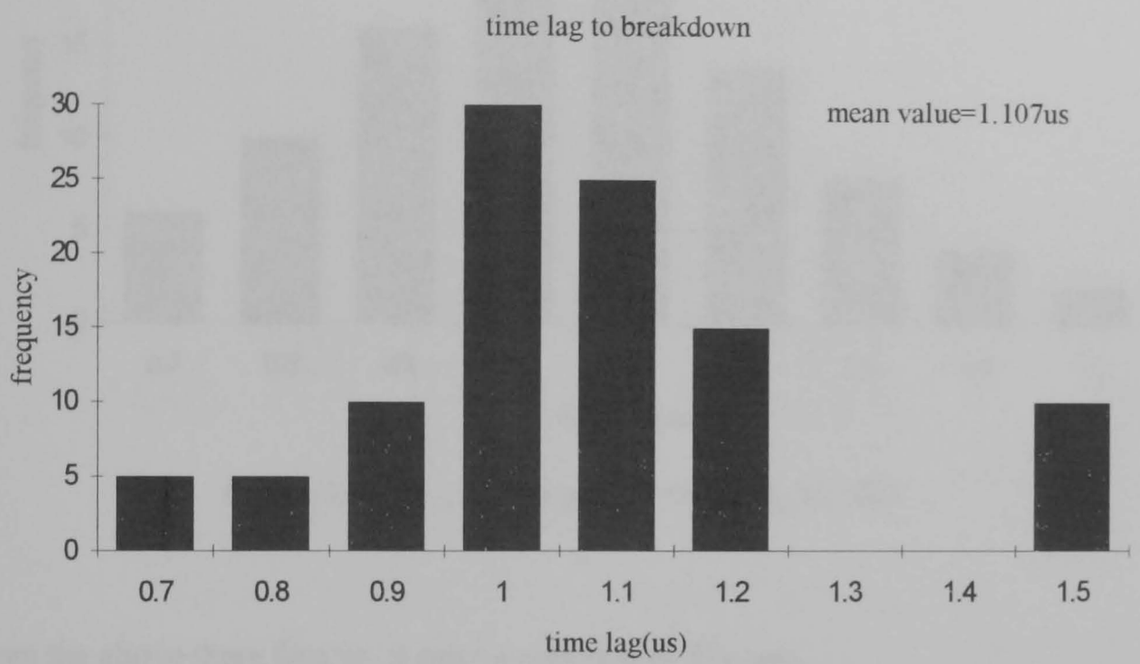

Figure 3.10 SF_6, 15mm gap, P=0.1MPa, V_c=0kV

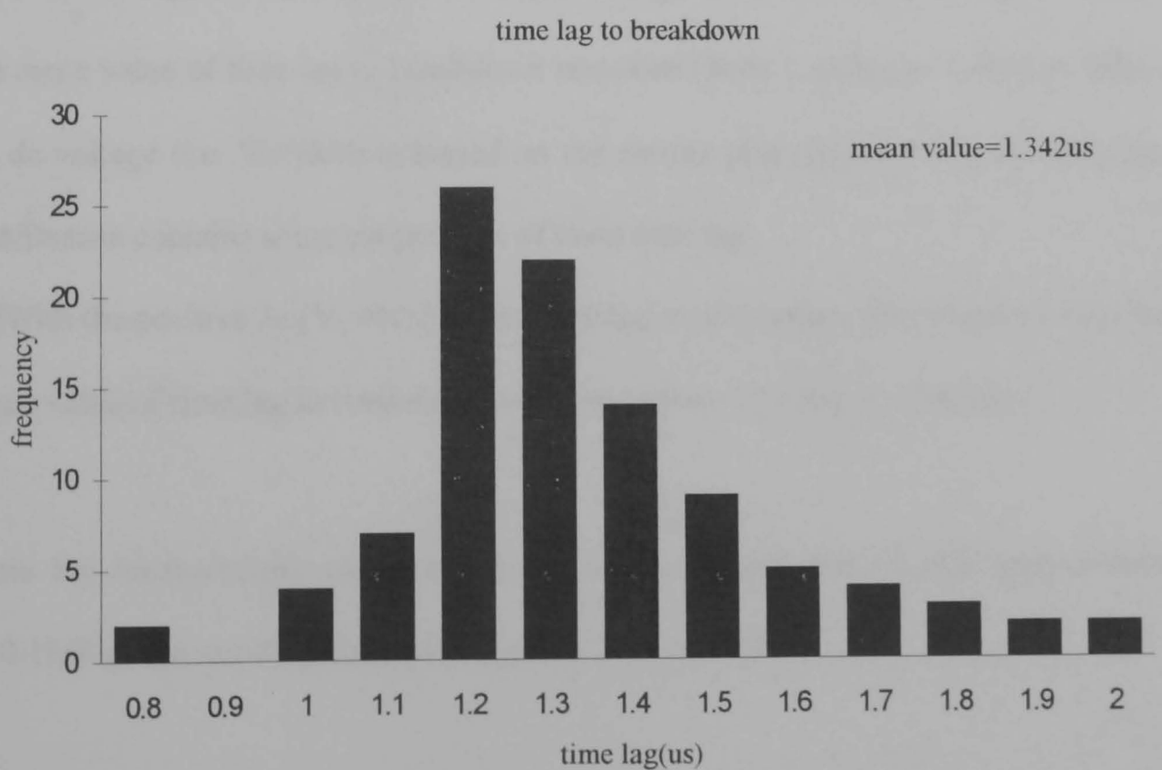

Figure 3.11 SF_6, 15mm gap, P=0.1MPa, V_c= -16kV

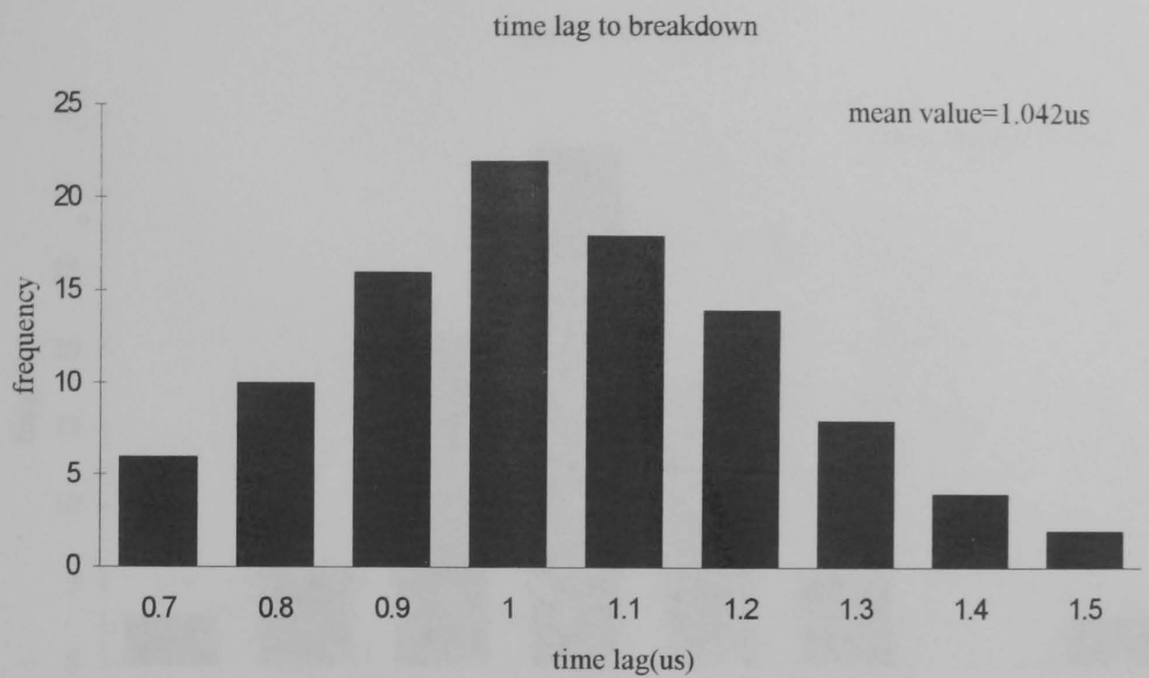

Figure 3.12 SF_6, 15mm gap, P=0.1MPa, V_c=8kV

From the above three figures, it can be seen that in SF_6 gap,

(1)With the negative dc (V_c=-16kV) biased voltage on the corona pins (figure 3.11) , the mean value of time lag to breakdown increases (from 1.107μs to 1.445μs). When no dc voltage (i.e. V_c=0kV) is biased on the corona pins (figure 3.10), the time lag distribution contains some proportions of short time lag.

(2)With the positive dc (V_c=8kV) biased voltage on the corona pins (figure 3.12), the mean value of time lag to breakdown decreases (from 1.107μs to 1.042μs).

Time lag measurement was also carried out in SF_6/air and SF_6/N_2 (gap=15mm, P=0.1MPa), the results are shown in figures 3.13 to 3.18.

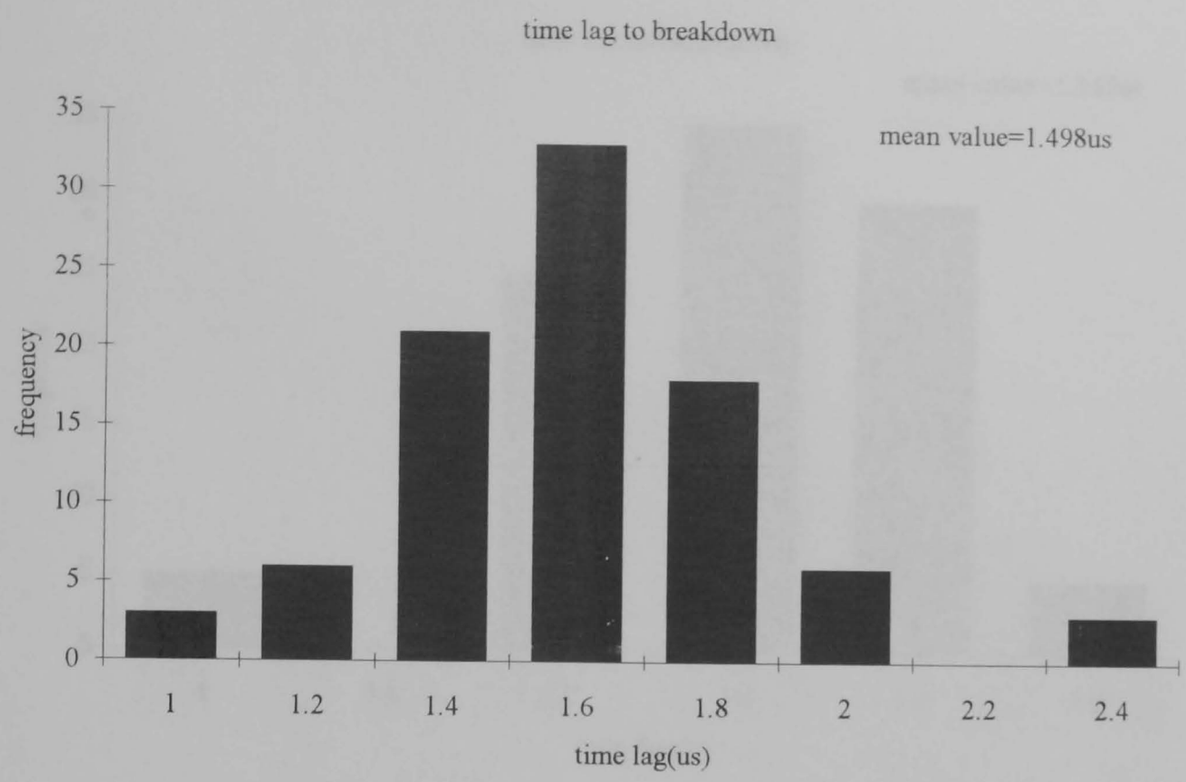

Figure 3.13 SF_6/air(50/50), 15mm gap, P=0.1MPa, V_c=0kV

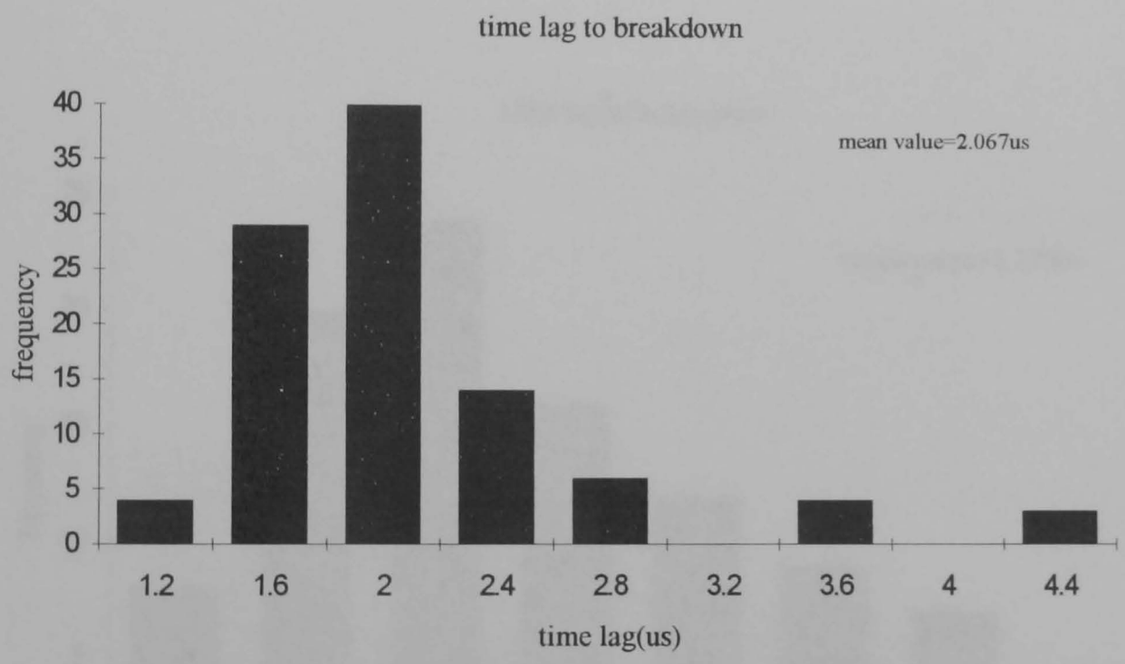

Figure 3.14 SF_6/air(50/50), 15mm gap, P=0.1MPa, V_c=-16kV

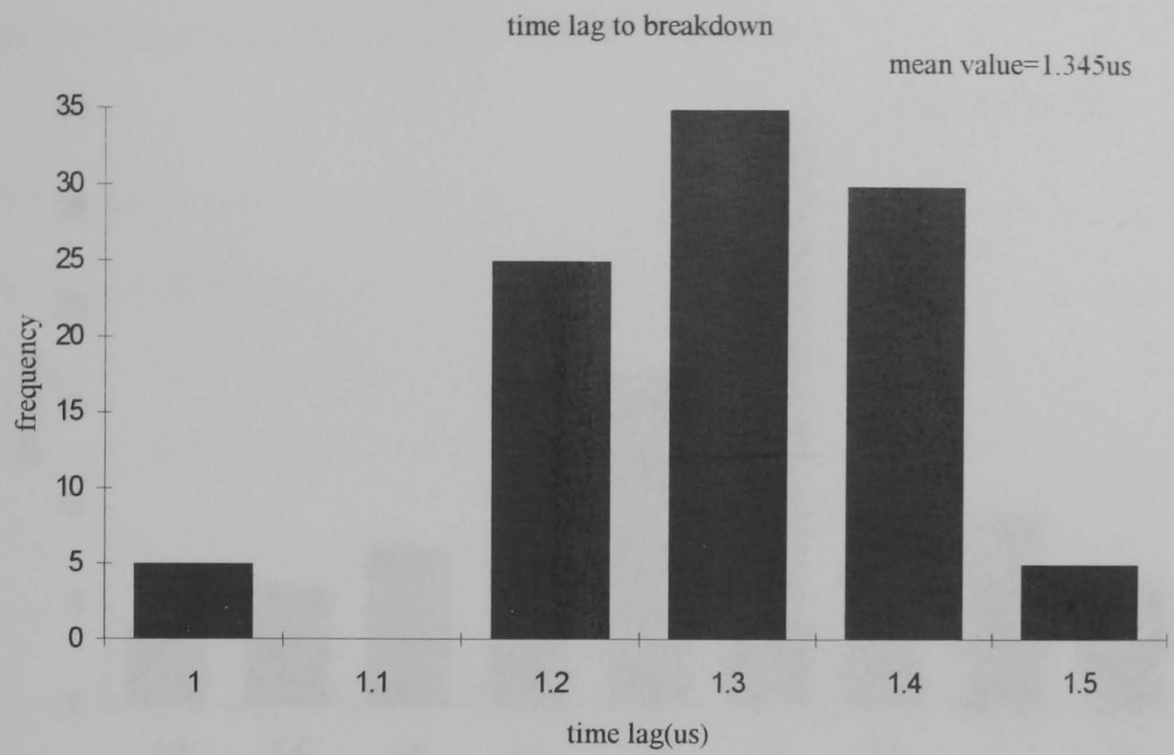

Figure 3.15 SF_6/air(50/50), 15mm gap, P=0.1MPa, V_c=8kV

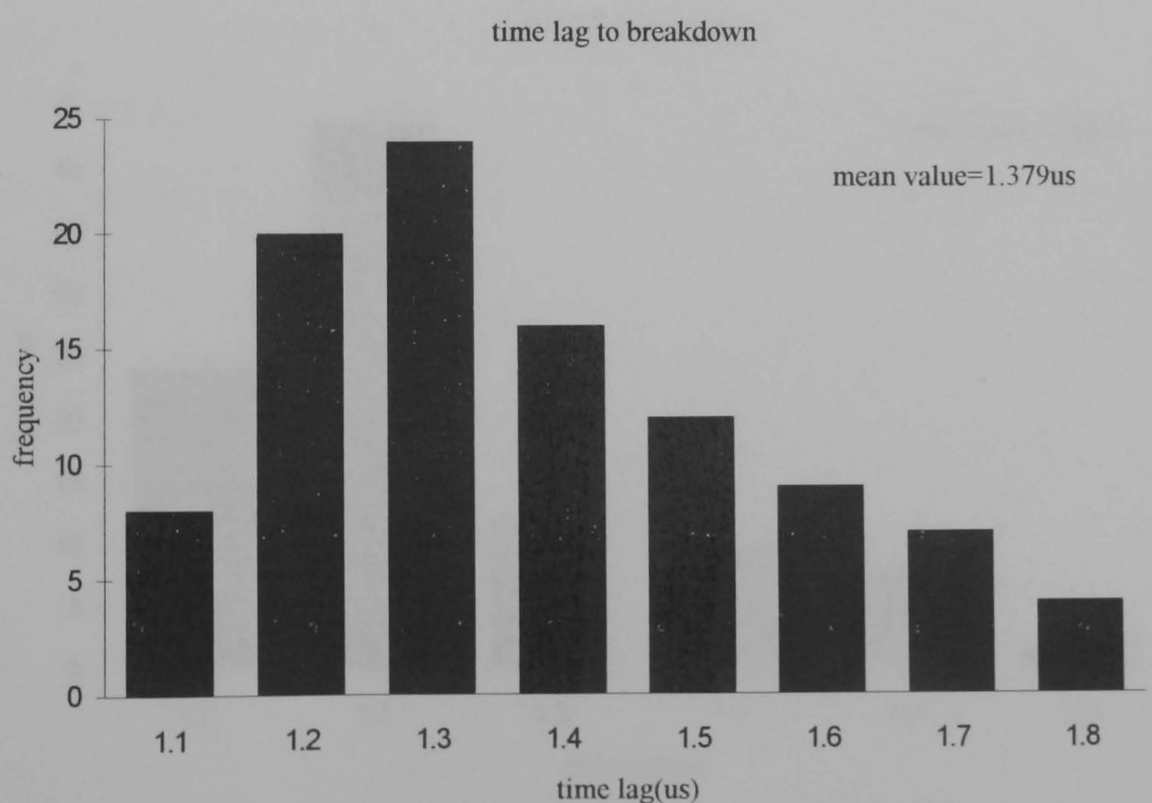

Figure 3.16 SF_6/N_2(50/50), 15mm gap, P=0.1MPa, V_c=0kV

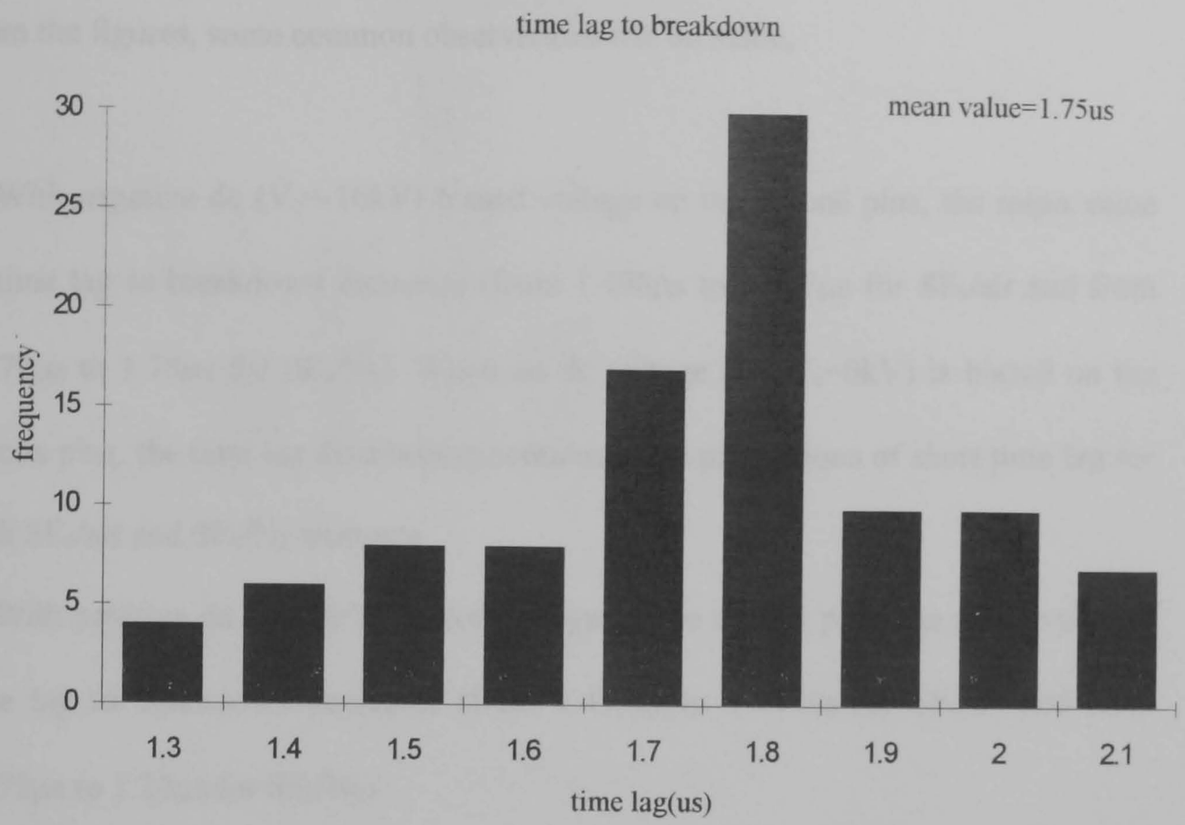

Figure 3.17 SF_6/N_2(50/50), 15mm gap, P=0.1MPa, V_c=-16kV

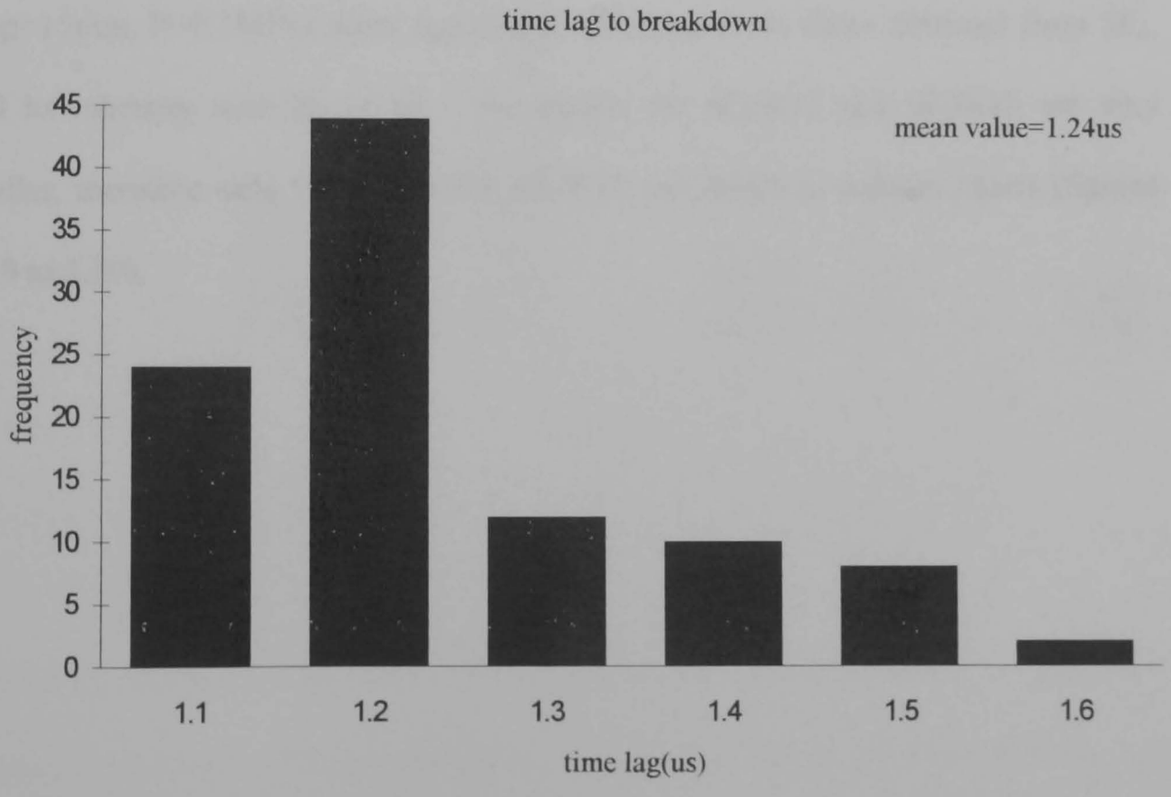

Figure 3.18 SF_6/N_2(50/50), 15mm gap, P=0.1MPa, V_c=8kV

From the figures, some common observations can be made.

(1)With negative dc (V_c=-16kV) biased voltage on the corona pins, the mean value of time lag to breakdown increases (from 1.498μs to 2.067μs for SF_6/air and from 1.379μs to 1.75μs for SF_6/N_2). When no dc voltage (i.e. V_c=0kV) is biased on the corona pins, the time lag distribution contains some proportions of short time lag for both SF_6/air and SF_6/N_2 mixtures.

(2)With positive dc (V_c=8kV) biased voltage on the corona pins, the mean value of time lag to breakdown decreases (from 1.498μs to 1.345μs for SF_6/air and from 1.379μs to 1.24μs for SF_6/N_2).

The results of time lag measurement obtained in SF_6/R12 and SF_6/R20 mixtures (gap=15mm, P=0.1MPa) show significant difference from those obtained from SF_6, and its mixtures with N_2 or air. The results for SF_6/R12 and SF_6/R20 are very similar, therefore only the results for SF_6/R12 are shown in column charts (figures 3.19 to 3.20).

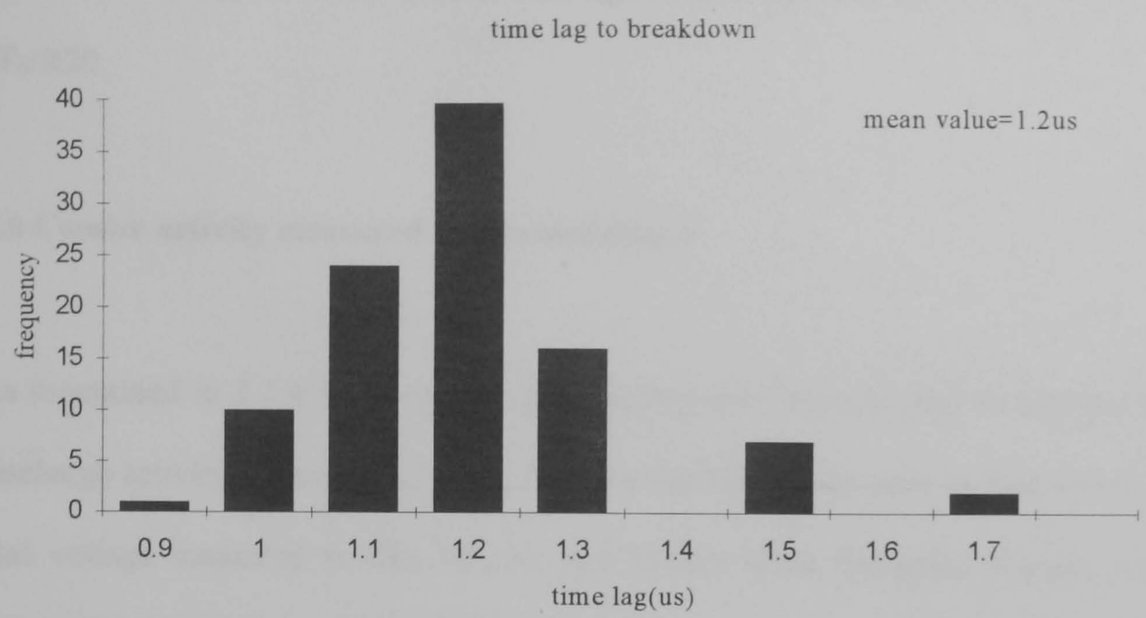

Figure 3.19 SF_6/R12(95/5), 15mm gap, P=0.1MPa, V_c=0kV

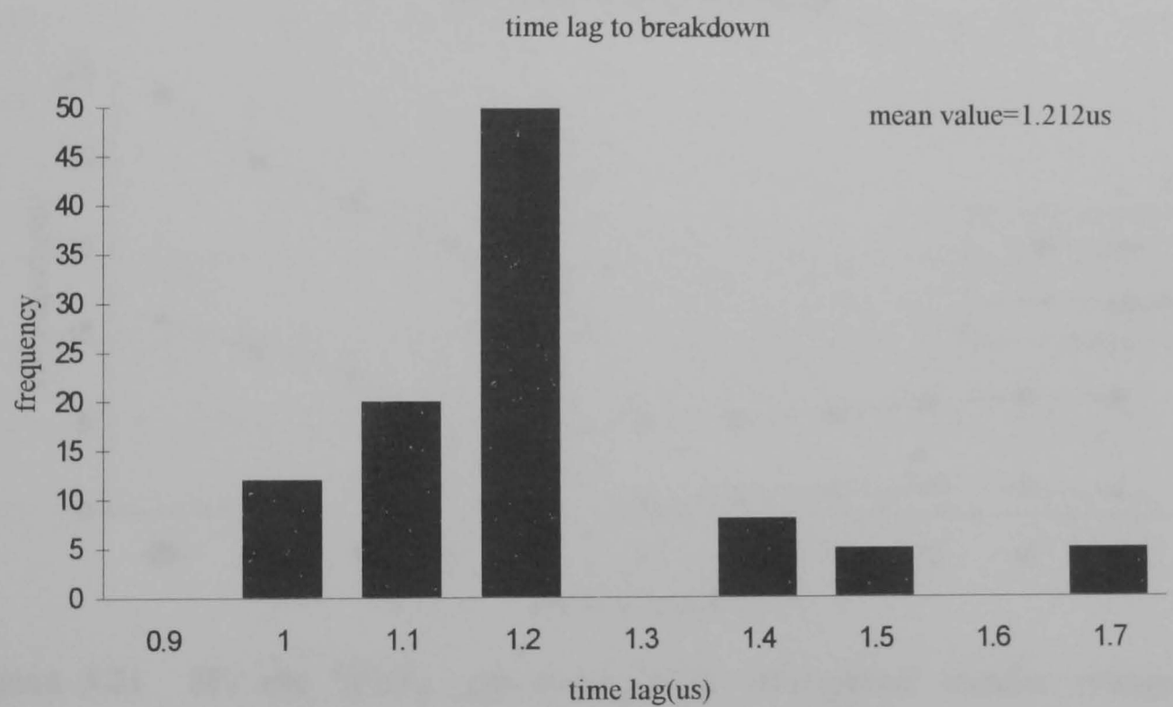

Figure 3.20 SF_6/R12(95/5), 15mm gap, P=0.1MPa, V_c=-16kV

With negative bias voltage (V_c=-16kV, figure 3.20) on the corona pins, the mean value of time lag to breakdown changes very little (from 1.2μs to 1.212μs, for SF_6/R20, from 1.114μs to 1.087μs). With positive bias voltage(V_c=8kV, column

charts not shown), the mean value of time lag remains the same for both SF_6/R12 and SF_6/R20.

3.6 Corona activity measured by photomultiper

As mentioned in 2.1.4.3, the optical photomultiplier(PM) was used to monitor the discharge activity. Figures 3.21 and 3.22 show the PM output value as function of dc bias voltage measured in SF_6, SF_6/N_2 and SF_6/air when the space charges were injected using the corona pin arrangement.

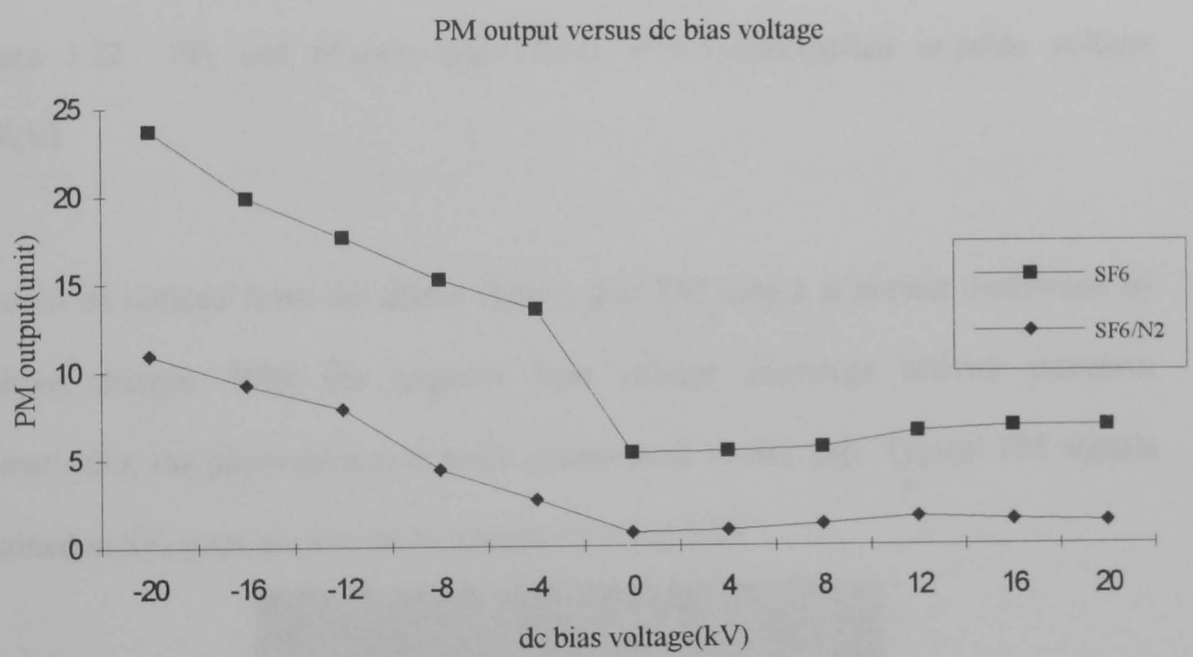

Figure 3.21 SF_6 and SF_6/N_2, gap=15mm, P=0.1MPa(applied impulse voltage =36kV)

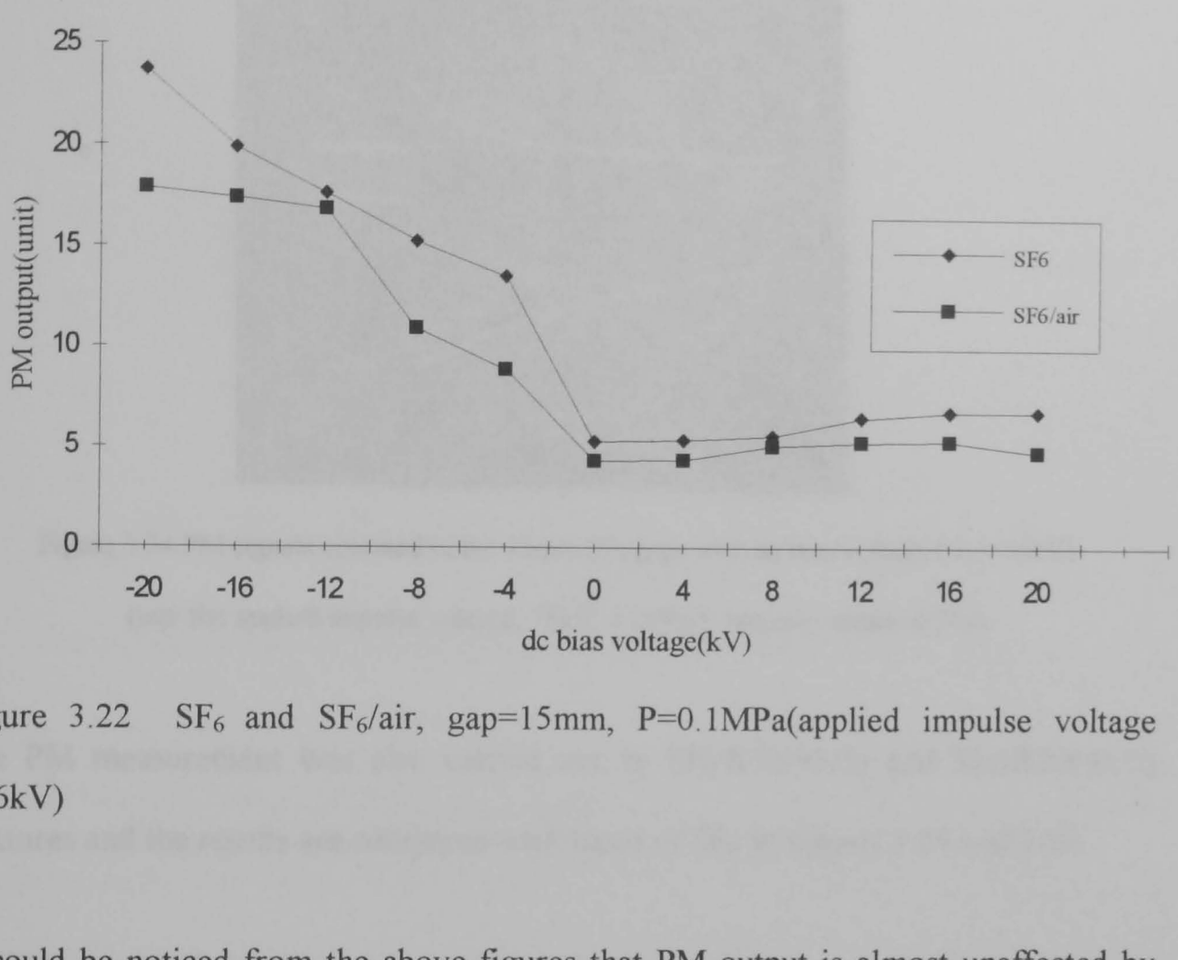

Figure 3.22 SF_6 and SF_6/air, gap=15mm, P=0.1MPa(applied impulse voltage =36kV)

It could be noticed from the above figures that PM output is almost unaffected by positive charges. With the negative bias voltage discharge activity increases dramatically, the phenomenon is more pronounced in SF_6 gap. Typical PM signals obtained in SF_6 gaps are shown in figures 3.23 and 3.24.

Figure 3.23.PM signals obtained in the 15mm SF_6 gaps without dc bias voltage (V_c=0kV)

(top: the applied impulse voltage, 36kV, 1.2/50μs, bottom: output of PM)

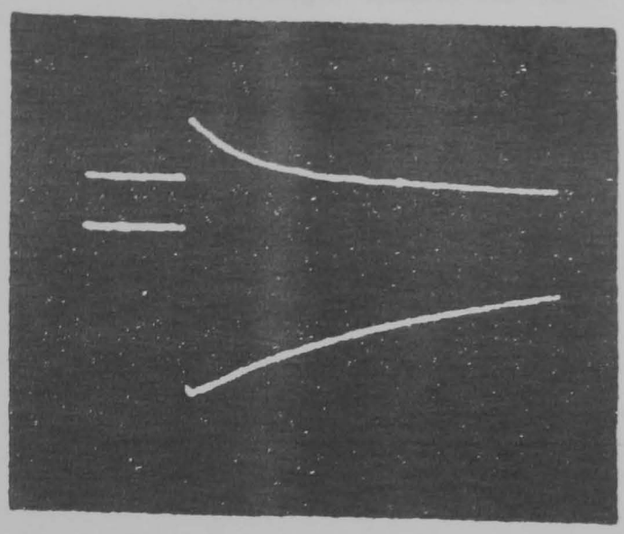

Figure 3.24.PM signals obtained in the 15mm SF_6 gaps with dc bias voltage (V_c=-16kV)

(top: the applied impulse voltage, 36kV, 1.2/50μs, bottom: output of PM)

The PM measurement was also carried out in SF_6/R12(95/5) and SF_6/R20(95/5) mixtures and the results are compared with those of SF_6 in figures 3.25 and 3.26.

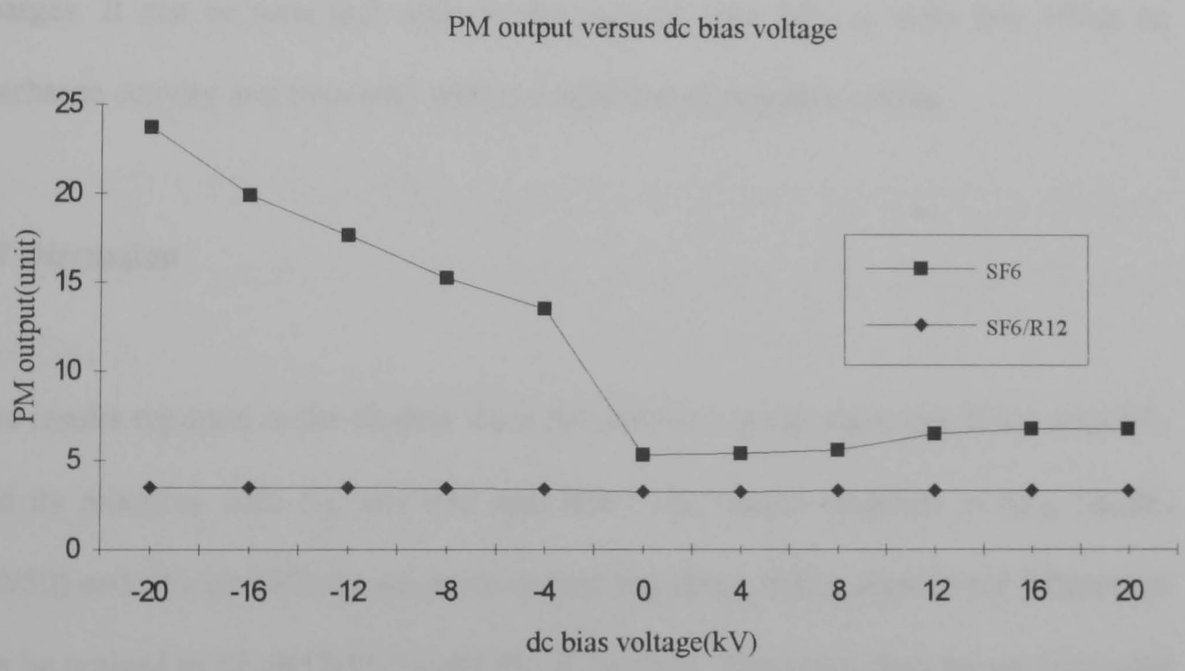

Figure 3.25 SF_6 and SF_6/R12, gap=15mm, P=0.1MPa(applied impulse voltage =36kV)

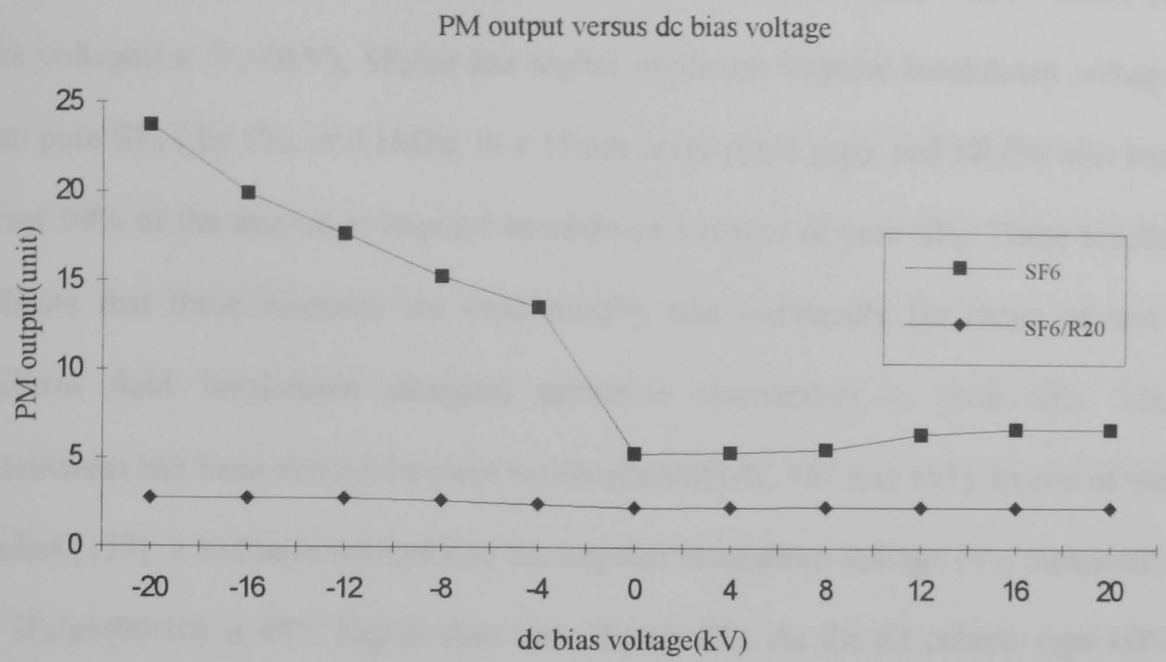

Figure 3.26 SF_6 and SF_6/R20, gap=15mm, P=0.1MPa(applied impulse voltage =36kV)

It could be noticed from the above two figures that in SF_6/R12 or SF_6/R20 gaps, PM output changes very little, if any, under the effect of either positive or negative space charges. It can be seen that only in the case of pure SF_6, is there any effect on discharge activity and then only with the injection of negative charge.

3.7 Discussion

The results reported in the chapter were obtained in a point plane gap filled with SF_6 and its mixtures with N_2, air, R12 and R20. The results obtained in SF_6, SF_6/N_2 (50/50) and SF_6/air (50/50) are more or less the same, whilst significant differences can be noticed in SF_6/R12(95/5) and SF_6/R20(95/5). The space charges were injected using two different methods — corona pin arrangement and direct injection method.

Results obtained in SF_6, SF_6/N_2(50/50) and SF_6/air(50/50) had shown that without dc bias voltage(i.e. V_c=0kV), SF_6/air has higher minimum impulse breakdown voltage than pure SF_6 (by 5%, at 0.1MPa, in a 15mm point-plane gap), and SF_6/N_2 also has about 90% of the minimum impulse breakdown strength of pure SF_6. These results indicate that these mixtures are economically and technically (in terms of non-uniform field breakdown strength) attractive alternatives to pure SF_6. The phenomena had been noticed in some earlier studies[141, 153 and 155]. In one of the studies [153], it had been noticed that the impulse breakdown voltage (V_{50} measured) of SF_6/air(90/10) is 45% higher than that of pure SF_6. As the air cubicle type GIS (i.e. C-GIS) is removed by SF_6 using a displacement method [154], residual air inside C-GIS is not only inevitable but also beneficial to dielectric strength under impulse. The mechanism is, however, not fully understood and should be further studied. The effect of the air additive on impulse breakdown of SF_6 was supposed to be due to its faster space charge movement [153]. Gallimberti and van Brunt [18,131] suggested this might due to the component in air — O_2, drastically influences the minimum precursor inception level of SF_6, which seems to be related to its ability of producing photo-electrons further away from an ionisation region than pure SF_6.

With the increase in negative dc bias or applied voltage (using either injection method), the minimum impulse breakdown voltages decrease for SF_6 and its mixtures with N_2 and air. The reason is believed due to the abundance of initiatory electrons resulting from detachment from plentiful negative ions. The results are in agreement with recent work[102,117] which has shown that the positive impulse

breakdown voltage in a point plane gap is affected by the presence of space charge. Chalmers and others[105] have pointed out that non-uniform-field breakdown in SF_6 involves the development of a series of streamer/leader steps which propagate from the point electrode towards the plane. It also has been realised[106] that the successful development of impulse breakdown relies on there being a supply of electrons in the gap volume such that each streamer step can be initiated. Availability of seed electrons within the point/plane gap volume has been discussed previously [119] in terms of its effect upon propagation of stepped discharge from the point. Whether or not a "stabilising corona" occurs for any given set of conditions, may be critically dependent upon the statistics associated with the production of initiating electrons in the critical volume of the gap[143]. As the availability of electrons increases then the probability of a corona discharge at the end of each leader step also increases and this leads to an associated increase in breakdown probability and consequent decrease in breakdown strength. These initiating electrons are generally believed to result from detachment from the negative ions [124 and 132]. The findings of the present work confirm to a large extent the suggestion that the breakdown strength of a non-uniform field gap in SF_6 is greatly affected by the availability of initaitory electrons throughout the gap volume to allow the streamer/leader step progression to take place.

When negative space charges are injected by direct injection method, with the increase in negative dc applied voltage, the minimum impulse breakdown voltages decrease more rapidly than those obtained under corona pin arrangement method.

This seems to imply that more space charges are injected using the direct injection method.

Also noticed is that when the negative dc bias/applied voltage (V_{dc}) is relatively low, the minimum impulse breakdown voltage decreases very little(for SF_6/air, the minimum impulse breakdown remains constant when the negative dc bias voltage is less than -4kV). This could be understood on the basis of V_{dc} is lower than the corona onset voltage (V_i) as previously discussed in 3.3. When V_{dc} is lower than V_i, no or very few space charges are injected. There is something of a saturation effect as the negative dc bias voltage is increased, the breakdown strength becomes progressively less sensitive to further increase. As can be seen in figures 3.7 and 3.8 that impulse breakdown voltages become constant or change very little when the negative dc bias voltage was more than -16kV. This seems to imply that there are already sufficient initiatory electrons resulting from detachment of plentiful negative ions injected. It would be reasonable to assume that there is a limit beyond which the breakdown strength cannot be further decreased by increasing negative-ion population. Further study presented in chapter 5 confirms the assumption.

When positive ions were injected, by either method, there is little increase in minimum impulse breakdown voltages and the breakdown voltages decrease slightly then remain almost constant as the V_c increased from 0 to +20kV. The increase in minimum impulse breakdown voltage is probably owing to the sweeping effect[118], i.e., the ionising particles produced may be swept out of the gap before the applied voltage level reaches the normal breakdown value. In [120], a so called "sweep

voltage" (+2kV DC) was applied, and it has been found that it is possible to obtain improved pulsed voltage recovery characteristics by depleting the ion population. The result obtained with positive bias/applied voltage would then correspond, at least in kind, to those previously measured in mixtures of SF_6 and additives[119] which are believed to bind the electrons to stable negative ions and thus remove them from active participation in breakdown process. It is of much interest to notice that further increase in positive bias or applied voltage results in a reduction in minimum impulse breakdown voltage and the breakdown levels are close or equal to the value as V_c=0kV. The sweeping effect is probably most effective at lower dc bias voltage, i.e. below the onset voltage level. Above the onset level, the positive ions, as they were studied and pointed out [124], do not play any role in the initiating process.

The minimum impulse breakdown voltages for SF_6/R12 (95/5) and SF_6/R20 (95/5) are much higher than that of pure SF_6 gas when no space charges were injected. The phenomena that the breakdown level can be significantly increased by the presence of freon additives had been noticed in non-uniform field previously [137, 138, 139, 141], the results cannot readily be explained by the concept of enhanced corona stabilisation. For example, previous measurement showed that although the minimum impulse breakdown strengths of SF_6 in a highly non uniform field gap can be dramatically improved by an R12 additive, yet corona measurement indicated that the R12 additive produces no measurable increase in corona activity in the gap[138, 139]. Recently Chalmers et al [119] suggested that the chlorine molecule is associated with the enhanced dielectric strength of the mixture and R12/R20, or indeed any other additive which is capable of producing negative ions of chlorine,

will be beneficial in that it will mitigate the reduction in performance associated with the almost inevitable presence of water vapour and metallic conducting particles in high voltage application. All the additives addressed in the work contain chlorine (i.e. R12 — CCl_2F_2, R20 — $CHCl_3$) , the assumption being that it is the stable Cl^- ion which is responsible for any ameliorating effects observed. When either of the two chlorine-bearing additives is present, injection of charges of either polarity has little effect on minimum impulse breakdown voltage (figure 3.9). Successful development of impulse breakdown relies upon there being a supply of electrons in the gap volume such that each streamer step can be initiated. These initiating electrons are generally believed to result from negative ions such as SF^- and OH^- as discussed previously. Certain additives, particularly those containing chlorine, preferentially produce very stable negative ions (such as Cl^-) which do not readily detach or may play a part in causing increased attachment and in slowing the charge separation process [106]. These stable Cl^- ions also make the direct ionisation process difficult[157] which will be discussed later. The impulse breakdown strength is increased in mixtures containing those froen additives because there is then a reduced likelihood of successful development of the discharge channel through a scarcity of initiating electrons in the gap. It is not surprising, in this sense that there is not much change in minimum impulse breakdown voltage when space charges are injected since the detachment process is much more difficult to be initiated and maintained.

For environmental reasons, there would be an understandable reluctance to use any of these freons. However, it is of great importance to have a better understanding of

how these Cl^- ions affect the breakdown process so that it might be possible to investigate other more benign additives or combination of additives which might perform the same function as the chlorine containing freons.

From the results of time lag measurement shown in figures 3.13 to 3.20, it is clear that for SF_6 and its mixtures with N_2 and air, the time lag to breakdown is affected by the injected space charges, especially by negative space charges. The mean value of time lag to breakdown increases as negative space charges are injected, and decreases as positive space charges are injected. With a high negative dc bias voltage (V_c=-16kV), there is an almost 100% probability that an initiating electron will appear in the critical volume when the voltage has reached the corona onset voltage. A filamentary corona will be established and it is necessary that the voltage be increased to a higher value and the field near the plane electrode be space-charge enhanced before breakdown can take place. Thus the time lag to breakdown is relatively longer. When no space charge is injected, there is a finite probability that no electron will appear until a much higher voltage is reached at which a streamer can develop which is sufficiently large. Breakdown will then take place shortly after the appearance of the initiating electrons.

When relatively low positive dc bias voltage (V_c=+8kV) was applied, there are less initiatory electrons compared with the situation when no space charges were injected (i.e. V_c=0kV) because of the sweeping effect. Therefore the time lag to breakdown is relatively shorter.

The results of time lag measurement obtained in SF_6/freon mixtures (both R12 and R20) are totally different from those obtained in SF_6 and its mixtures with N_2 or air. The time lag is not affected by the space charge, either negative or positive. This is consistent with the breakdown voltage data which point to the fact that in SF_6 and its mixtures with N_2 and air, the injection of negative ions enhances the discharge activity through the creation of unstable negative ions which can detach and provide electrons. When the chlorinated additive is present, stable chlorine ions are formed and no matter their number, they do not readily detach and therefore do not contribute to the discharge development.

Figures 3.21 to 3.26 show the results of the PM output as the function of the dc bias voltage. It can be seen from the results obtained in SF_6/air and SF_6/N_2 that as the negative dc voltage increases the output of the PM increases which in another way strongly suggests the negative ions have a great influence on discharge and breakdown processes. Clearly the positive ions have little effect as the PM output almost remains constant as the positive bias voltage increases. The results suggest that the prebreakdown corona activity and breakdown characteristics are greatly affected by the negative ions, but are not much affected by the positive ions.

The results obtained in SF_6/R12 and SF_6/R20 are different from those obtained in SF_6 and it mixtures with buffer gases. PM output changes very little whether positive or negative ions are injected. The observation is consistent with breakdown measurement and suggests that stable chlorine ions do not readily detach and therefore do not contribute to the discharge development.

3.8 Conclusions

From the above experimental results and discussion, the following conclusions were made.

The SF_6/N_2 (50/50) and SF_6/air (50/50) mixtures look promising in terms of their breakdown strength in non-uniform field is close to (SF_6/N_2) or no less (SF_6/air) than that of pure SF_6. Under the current unfavourable environmental issues on SF_6, there is a drive to explore alternative gases to pure SF_6. Improved gaseous dielectrics have been studied and so designed on the basis of knowledge of fundamental electron-molecule interaction. The most important electron control mechanism in gas under electrical stress is electron attachment to gas molecules [164]. Attachment becomes more difficult for all attaching gases at high electron energies (typically above 2 eV), so that gas components are included which can remove energy from electrons escaping the efficient low-energy attachment range, returning them the energy from electrons escaping the effective and away from the ionisation threshold. It is generally accepted that binary mixtures should team one gas that primarily de-energises free electrons and one gas that removes free electrons from the dielectric by electron attachment [165]. N_2,O_2,CO and CO_2 are some typical electron retarding gases in which fast electrons can be slowed and the electron energy can be reduced. Why the SF_6/air mixture (50/50) has a higher minimum impulse breakdown voltage than that of pure SF_6 is not fully understood and should be further studied. Although

there are suggestions that the faster space charge movement [153] and/or the production of photo-electrons [18 and 131] may be responsible.

The fact that SF_6 and its mixtures with N_2 and air are affected by the injection of negative ions is in good agreement with some recent studies [102,103,104]. This would suggest that, at least for those levels of mixtures, the breakdown process is similar to that obtained in pure SF_6 and can therefore be significantly affected by the presence or lack of negative ions in the gap volume so that initiatory electrons can be detached. It has been found that the positive ions do not affect the discharge development too much. Although the minimum impulse breakdown voltage can be slightly increased when relatively lower positive dc voltage is biased or applied. It is suggested that sweeping effect is responsible and it is only effective when the voltage is low.

The minimum impulse breakdown voltage of SF_6/R12 and SF_6/R20 is much higher than that of SF_6 and the minimum impulse breakdown voltages of the mixtures are not affected by the injection of either negative or positive ions. The results add further evidence to the suggestion [119] that the marked improvement in the insulating performance of SF_6 and hence to the tolerance of the gas to metallic particle in GIS when a chlorinated freon is present is related to ion chemistry. The presence of such chlorinated additives results in the preferential production of highly stable negative ions of chlorine which cannot detach within the time scale necessary and thus cannot significantly provide the seed electrons in the gap necessary for the propagation of steeping process.

The study of these mixtures and the different effects of space charge on them is informative and helpful to have a better physical understanding of the factors which contribute to "good" insulating gases. Further study may allow tailoring of specific gases to provide appropriate mixtures for particular applications especially where the use of pure SF_6 may be undesirable.

Chapter 4 The effect of artificial irradiation

4.1 Introduction

The study of space charge in Chapter 3 has shown that the initiatory electrons play an important role in non-uniform field breakdown process in SF_6 and its mixture with air and N_2. Some previous work [101,102,117,122] pointed out that the production of initiating electrons in the critical volume of the gap is quite important for the development of breakdown process. It has been well established that [121] there are mainly two possible sources of free electrons, one is the detached electrons from the negative ions such as SF_6^- and OH^-, which was studied in Chapter 3, the other is from the direct ionisation of neutral molecules by artificial irradiation or natural irradiation [122], such as cosmic radiation from the space (which can produce approximately 2×10^{-5} electrons/s.cm^3.Pa [127]), radiation from the radioactive components in the earth's crust and from the materials used for building, e.g., granite, etc. It has been found that in an enclosed highly non uniform field gap in air [122,123] and SF_6 [120] the impulse breakdown voltage decreases under the condition of strong irradiation. From the industrial viewpoint, it was concluded [107] that the probability of failure of SF_6 insulated switchgear (GIS) under positive surge waveforms depends on the presence of free electrons. The study of artificial irradiation in conjunction with space charge injection would be beneficial to a better understanding of the breakdown mechanism with particular reference to the role of initiatory electrons.

For the work described in this chapter, two artificial irradiation sources were used, i.e., an 125W quartz-mercury arc lamp and a piece of 5mCi capsule ^{137}Cs (6MeV gamma source). Although the main purpose of the thesis is to study the impulse breakdown characteristics of SF_6 and it mixtures, a series of experiments were carried out in air as the first step to study the effect of artificial irradiation and the quartz-mercury arc lamp was used to provide ultraviolet ray irradiation (hereafter referred as UV irradiation). Because UV irradiation is often considered insufficient for gaps in SF_6 and its mixtures due to photon absorption, so a piece of 5mCi capsule ^{137}Cs was used as the irradiation source.

4.2 Experimental setup and procedure

The pressurised chamber and the test gap assembly are well documented in chapter 2. The point-plane electrodes were first cleaned in normal manner and set to different gap length before each test. The minimum impulse breakdown voltage and time lag to breakdown were measured and recorded by the oscilloscope.

Positive lightning impulse voltage with a waveform of 1.2/50 μs was applied to a point-plane gap in a mild steel pressurised test vessel fitted with four orthogonally arranged windows as described in Chapter 2. The tests were carried out with and without artificial irradiation source for comparison. Air, SF_6 and its mixtures with N_2, air, R12 or R20 were studied in this chapter. With experiments carried out in air, the point-plane gaps were irradiated by the 125W quartz-mercury arc lamp which was placed approximately 120mm from the gap. For air gaps, the point-plane gaps

were placed in the vessel either with the four observation windows to enclose the gaps (hereafter refers as "enclosed air gaps"), or the gaps were placed in the open air in the vessel without the 4 observation windows fitted on(hereafter refers as "open air gaps"). For gaps filled with SF_6 and its mixtures, a piece of 5mCi capsule ^{137}Cs was placed close to the point electrode (approximately 100mm from the point electrode) to provide the γ ray.

- Time lag measurement

A sequence of 100, positive impulse voltages were applied to the gap with a voltage corresponding to the 90% breakdown level. The time lag to breakdown was recorded on the oscilloscope and results were given in column charts.

4.3 Low-probability impulse breakdown voltages

- **air gaps**

Figure 4.1 compares the minimum impulse breakdown voltage versus gap length in enclosed air gap with and without UV irradiation. The test was repeated using the same point-plane geometry in open air and the results are shown in figure 4.2. From the figures, it can be seen that,

(1)There is significant difference between the minimum impulse breakdown voltages obtained in open and enclosed air gaps. The minimum impulse breakdown voltage

decreases (by 15.9% for 15mm gap) when the experiments were carried out in open air gaps.

(2)There is very little decrease (by 2.8% for 15mm gap) in minimum impulse breakdown voltage with and without UV irradiation when the experiments were carried out in open air gaps. However, for enclosed air gaps, the minimum impulse breakdown voltages decrease significantly (by 17.6% for 15mm gap) under the effect of UV irradiation and the phenomenon is more pronounced as the gap spacing increases.

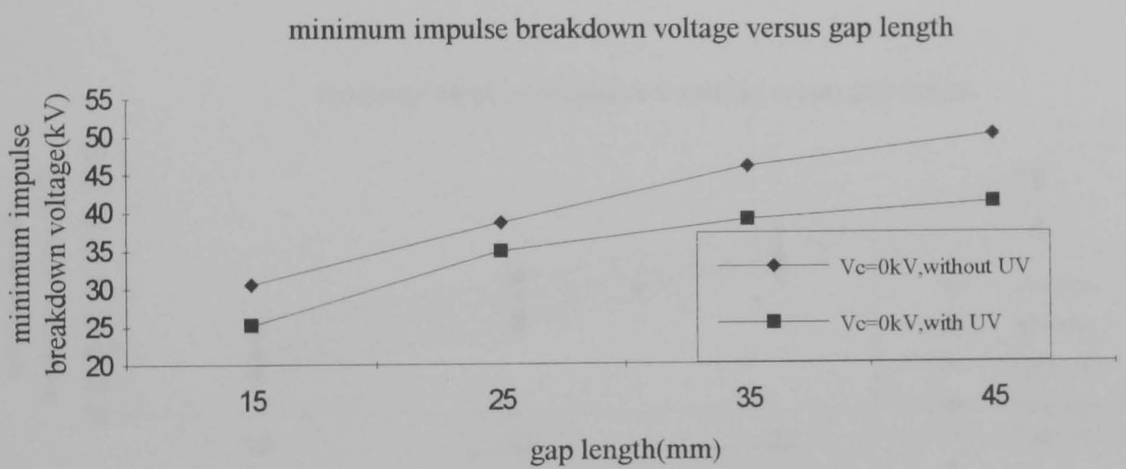

Figure 4.1 Enclosed air gap, P=0.1MPa

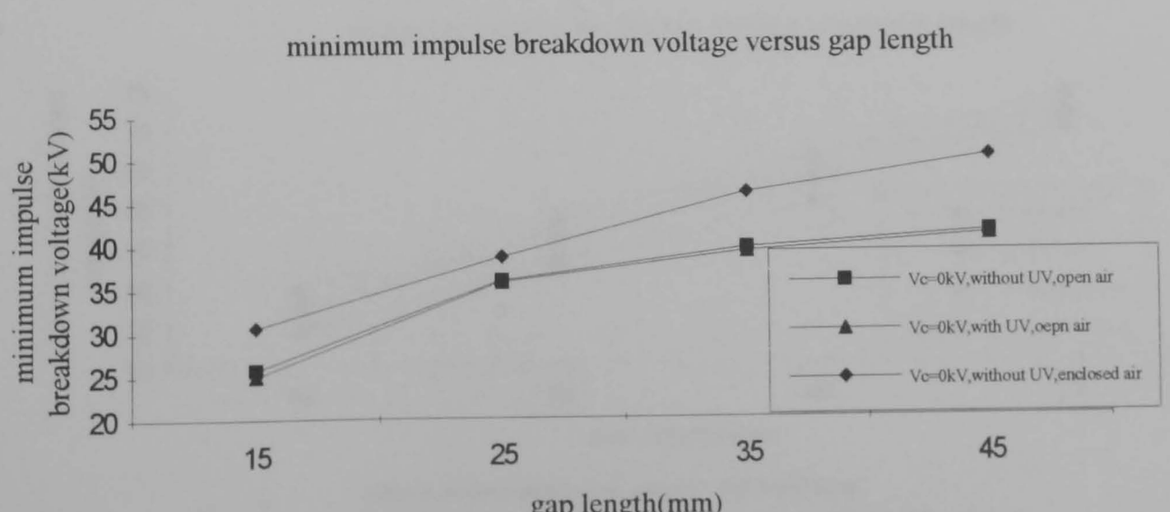

Figure 4.2 Open air and enclosed air gap, P=0.1MPa

•SF_6 and its mixtures with air, N_2

Figures 4.3 and 4.4 show the results obtained in SF_6, SF_6/air (50/50) and SF_6/N_2 (50/50) gaps with and without the irradiation of ^{137}CS. The minimum impulse breakdown voltage decreases (for SF_6 by 5.1% for the 15mm gap, by 3.4% for SF_6/N_2 and by 3.2% for SF_6/air) with the application of ^{137}CS irradiation which is similar to the results obtained in enclosed air gaps with UV irradiation. But the rates of decreasing in SF_6 and its mixtures with air and N_2 are much smaller than that of enclosed air gaps.

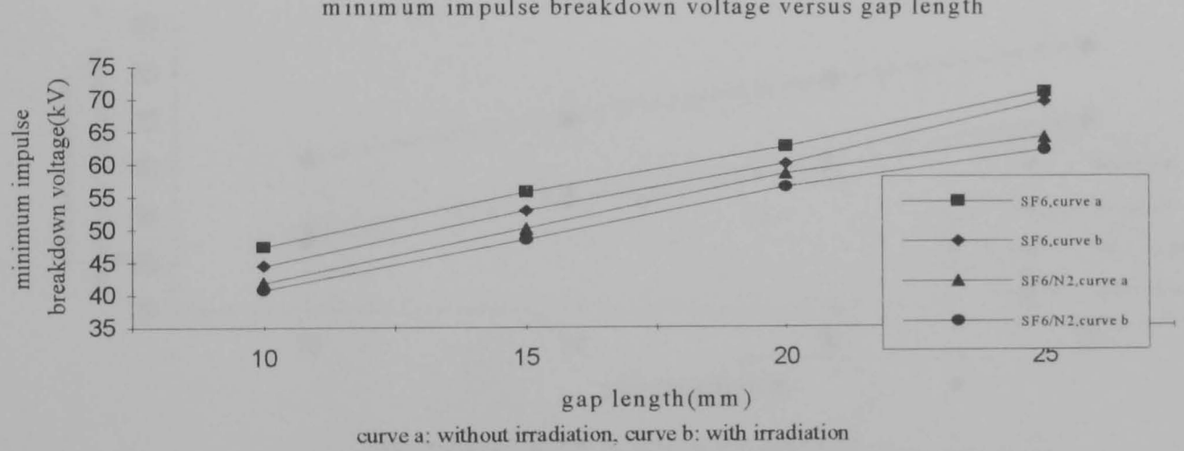

curve a: without irradiation, curve b: with irradiation

Figure 4.3 Minimum impulse breakdown voltage versus gap length, P=0.1MPa

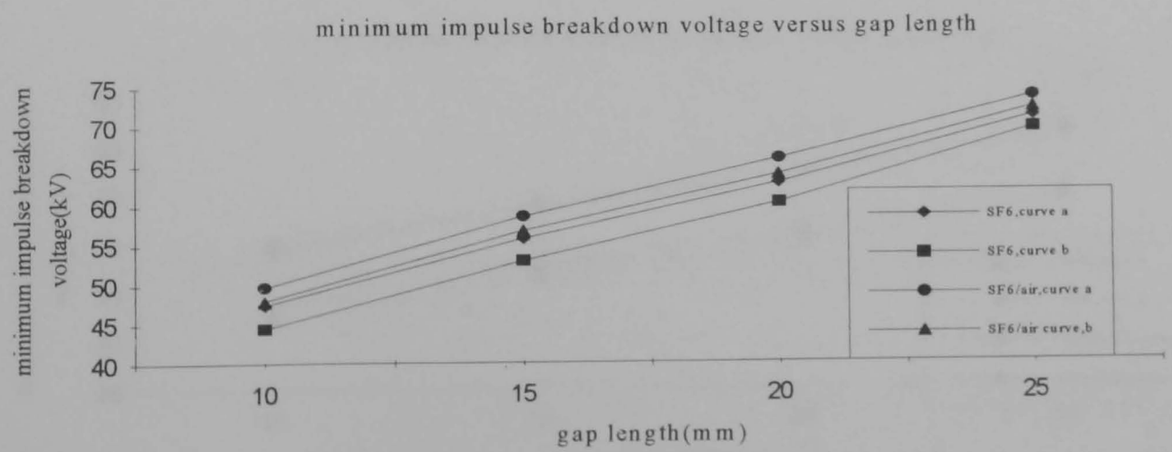

curve a: without irradiation, curve b: with irradiation

Figure 4.4 Minimum impulse breakdown voltage versus gap length, P=0.1MPa

Also noticed is that the minimum impulse breakdown levels of SF_6/air (50/50) are higher than pure SF_6, while the breakdown levels of SF_6/N_2 (50/50) are lower. The attractive non-uniform breakdown characteristics of SF_6 mixtures had been discussed in chapter 3.

•SF_6 mixtures with freon

Tests were carried out in SF_6/R12 (95/5) and SF_6/R20 (95/5) gaps with and without ^{137}CS irradiation.

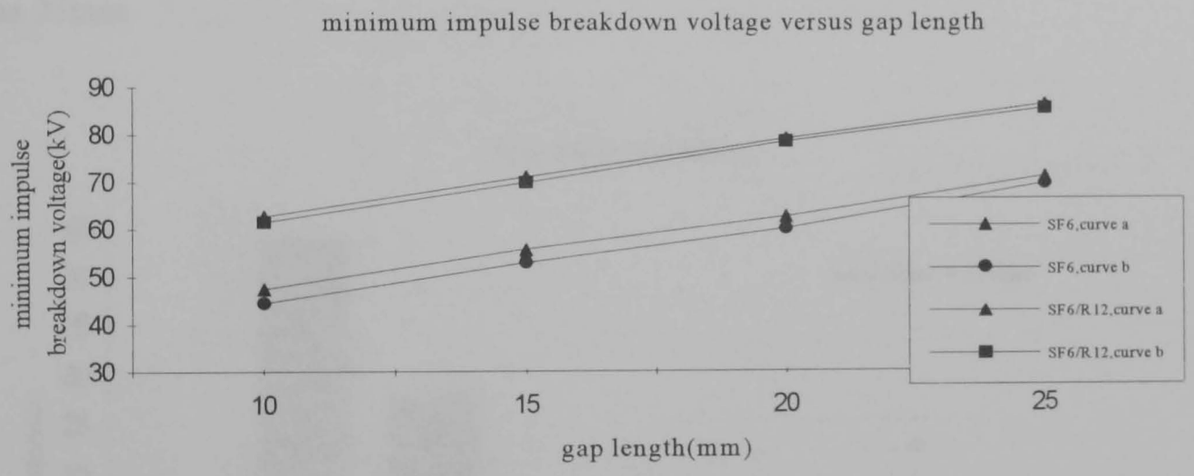

curve a: without irradiation, curve b: with irradiation

Figure 4.5 Minimum impulse breakdown voltage versus gap length, P=0.1MPa

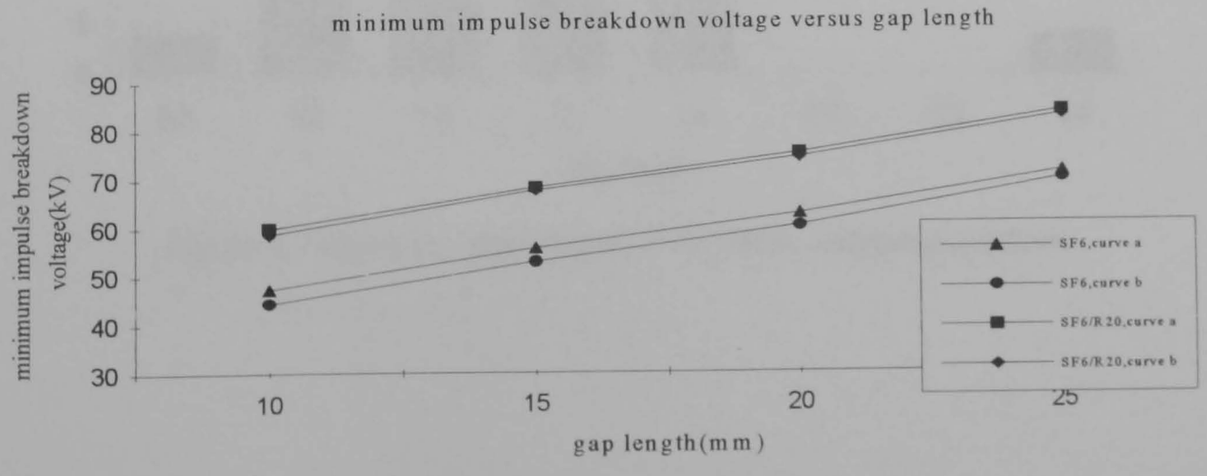

curve a: without irradiation, curve b: with irradiation

Figure 4.6 Minimum impulse breakdown voltage versus gap length, P=0.1MPa

The minimum impulse breakdown voltages decrease very little under the effect of irradiation for both SF_6/freon mixtures. While on the other hand, the presence of freon additives increases the minimum impulse breakdown voltage significantly as it was observed and discussed in chapter 3.

4.4 Time lag measurement

Time lag to breakdown was measured in open and enclosed air gaps with and without UV irradiation. The results are shown in figures 4.7 to 4.10. The gap length was 25mm.

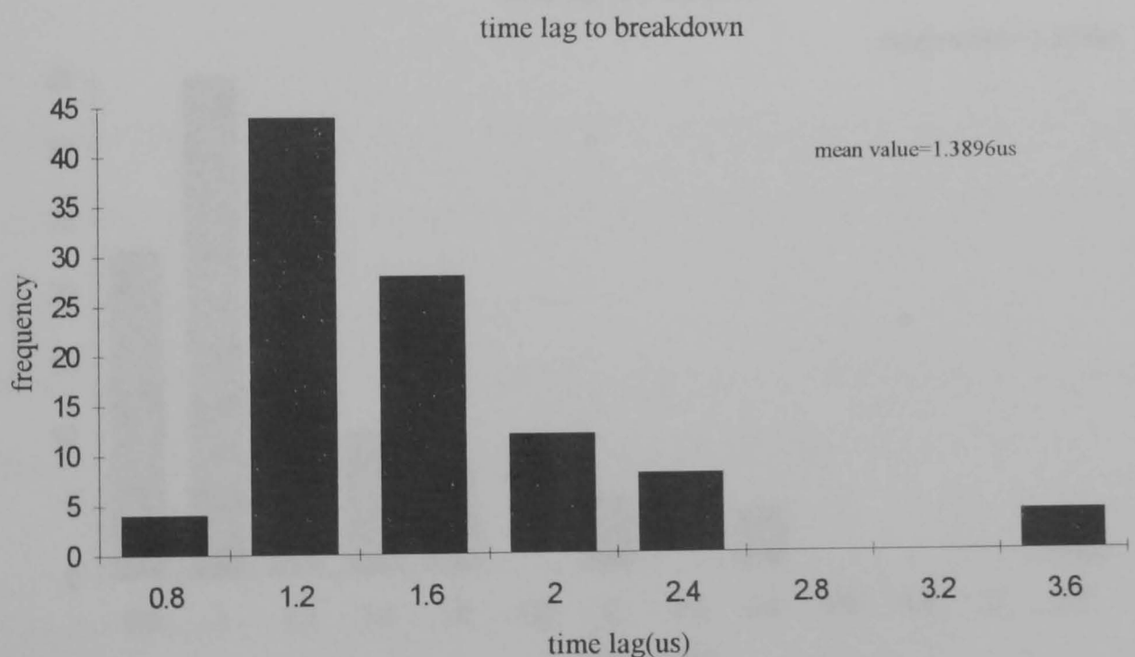

Figure 4.7 Open air, gap=25mm, P=0.1MPa, without irradiation

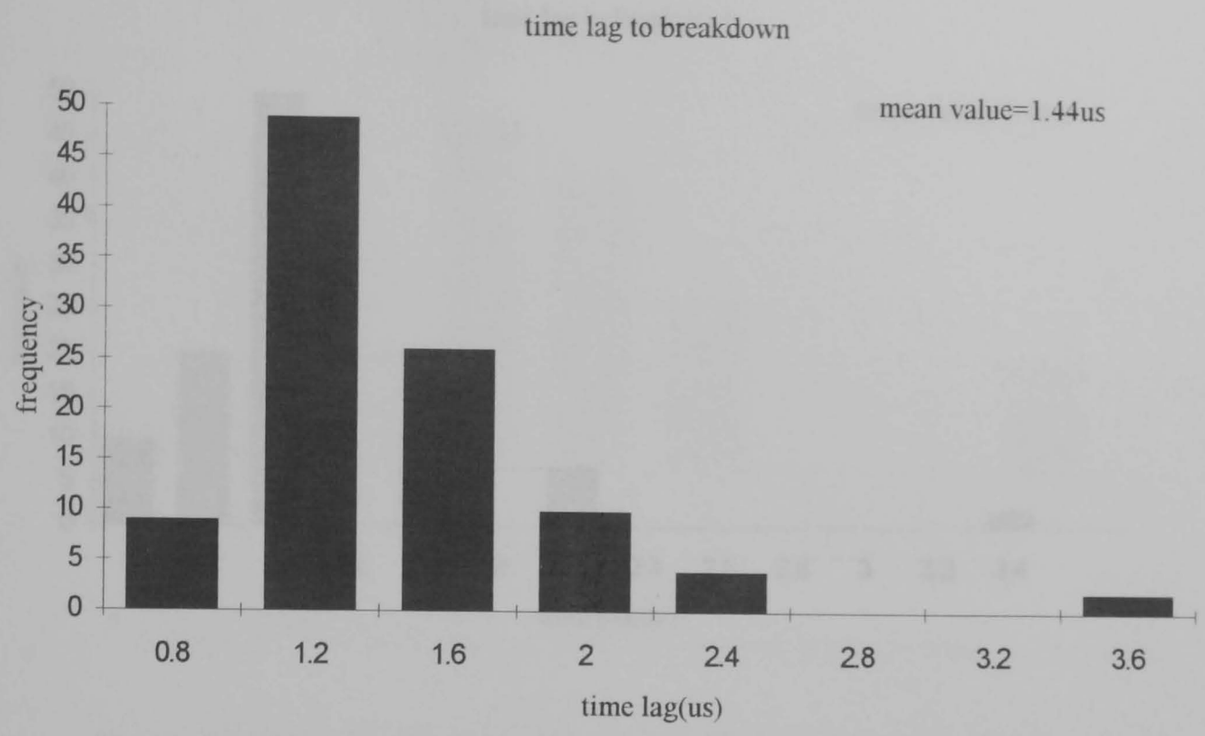

Figure 4.8 Open air, gap=25mm, P=0.1MPa, with irradiation

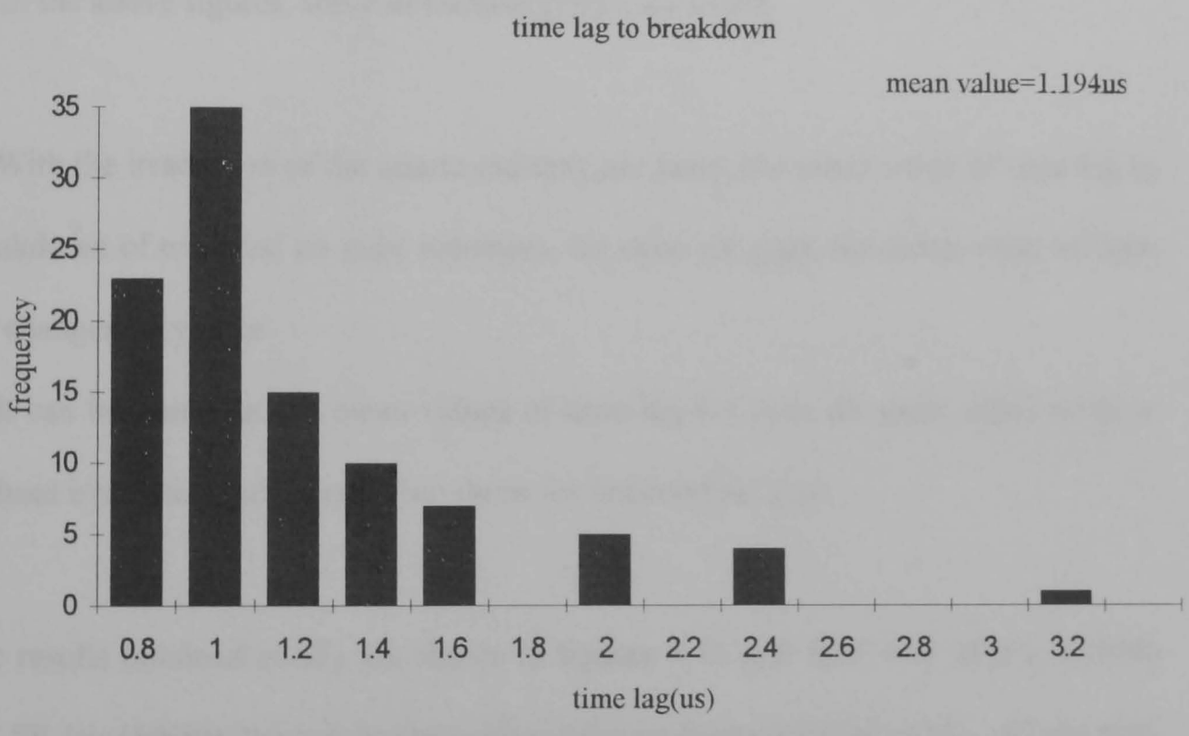

Figure 4.9 Enclosed air, gap=25mm, P=0.1MPa, without irradiation

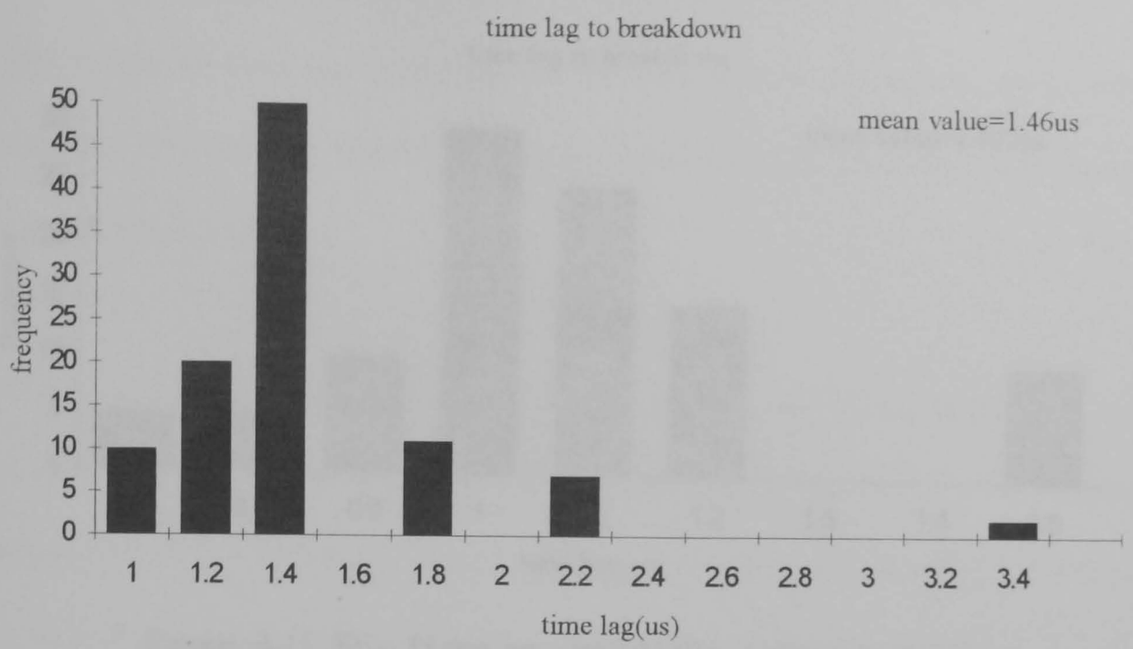

Figure 4.10 Enclosed air, gap=25mm, P=0.1MPa, with irradiation

From the above figures, some interesting points are noted,

(1)With the irradiation of the quartz-mercury arc lamp, the mean value of time lag to breakdown of enclosed air gaps increases; for open air gaps, the mean value of time lag changes very little.

(2)It can be seen that the mean values of time lag for open air gaps, either with or without irradiation, are longer than those for enclosed air gaps.

The results obtained in SF_6 are shown in figures 4.11 and 4.12. For SF_6/N_2 (50/50) and SF_6/air (50/50), the results are quite similar to those obtained in SF_6. All the tests were carried out at the gap length of 15mm. The column charts for the time lag measurements in the mixtures are not shown but the results will be commented.

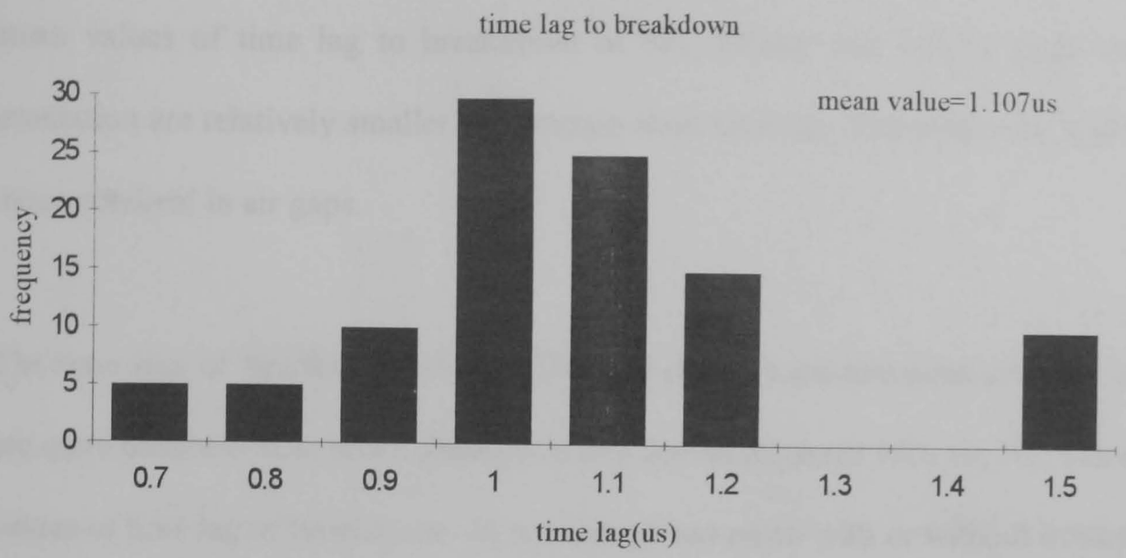

Figure 4.11 SF_6, 15mm gap, P=0.1MPa, without irradiation

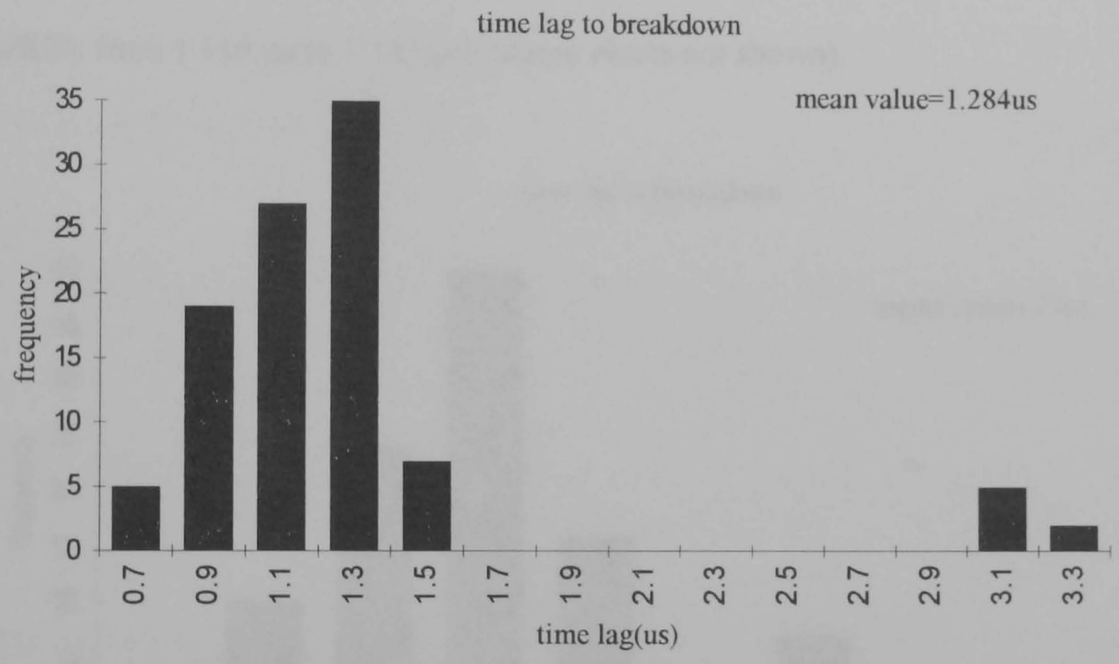

Figure 4.12 SF_6, 15mm gap, P=0.1MPa, with irradiation

From the above two figures, it can be seen that with the ^{137}Cs irradiation, the mean value of time lag to breakdown increases from 1.107 μs to 1.284 μs. The same phenomenon is observed in SF_6/air (50/50) and SF_6/N_2 (50/50) mixtures (column charts not shown). The mean value of time lag increases from 1.498μs to 1.922μs

with ^{137}Cs irradiation in SF_6/air gaps. For SF_6/N_2 gaps, from 1.379μs to 1.654μs. The mean values of time lag to breakdown of SF_6, SF_6/air and SF_6/N_2 gaps without irradiation are relatively smaller and contain short time lag. The results are similar to those obtained in air gaps.

The time lags of SF_6/R12 (95/5) and SF_6/R20 (95/5) were measured and the results are quite different from those obtained in SF_6 and its mixtures with air, N_2. The mean values of time lag to breakdown do not change too much with or without irradiation. For example, for SF_6/R12, the values change from 1.20 μs to 1.188 μs as the irradiation source was applied (column charts shown in figures 4.13 and 4.14). For SF_6/R20, from 1.114 μs to 1.111μs (column charts not shown).

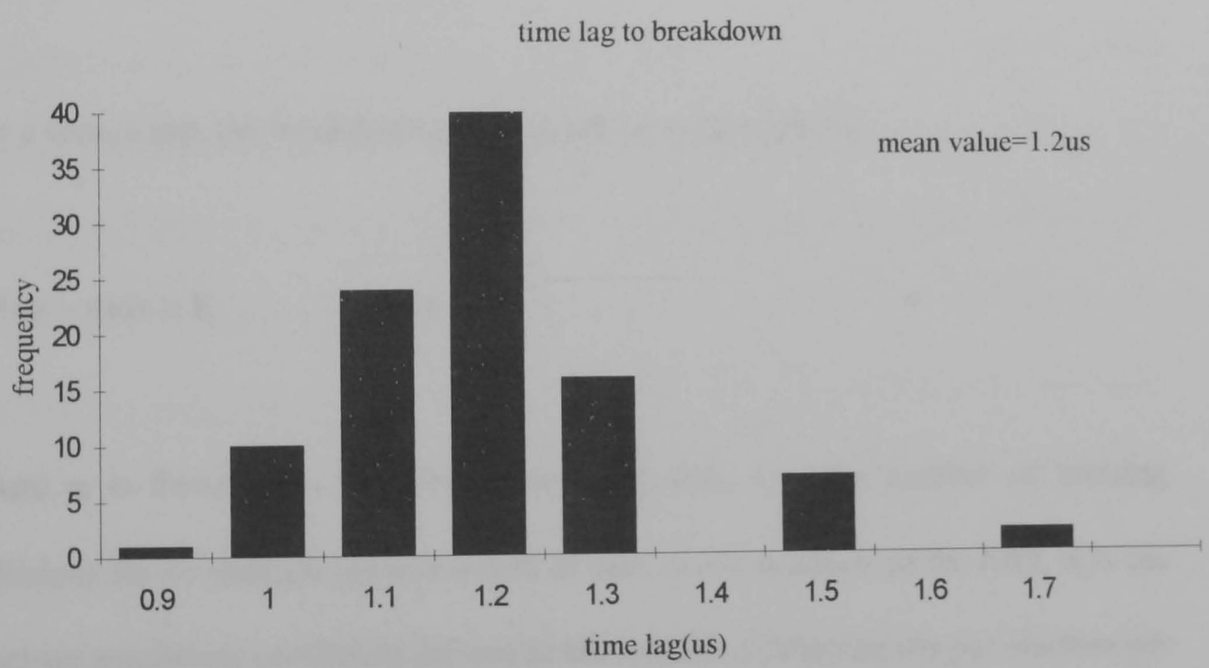

Figure 4.13 SF_6/R12 (95/5), 15mm gap P=0.1MPa, without irradiation

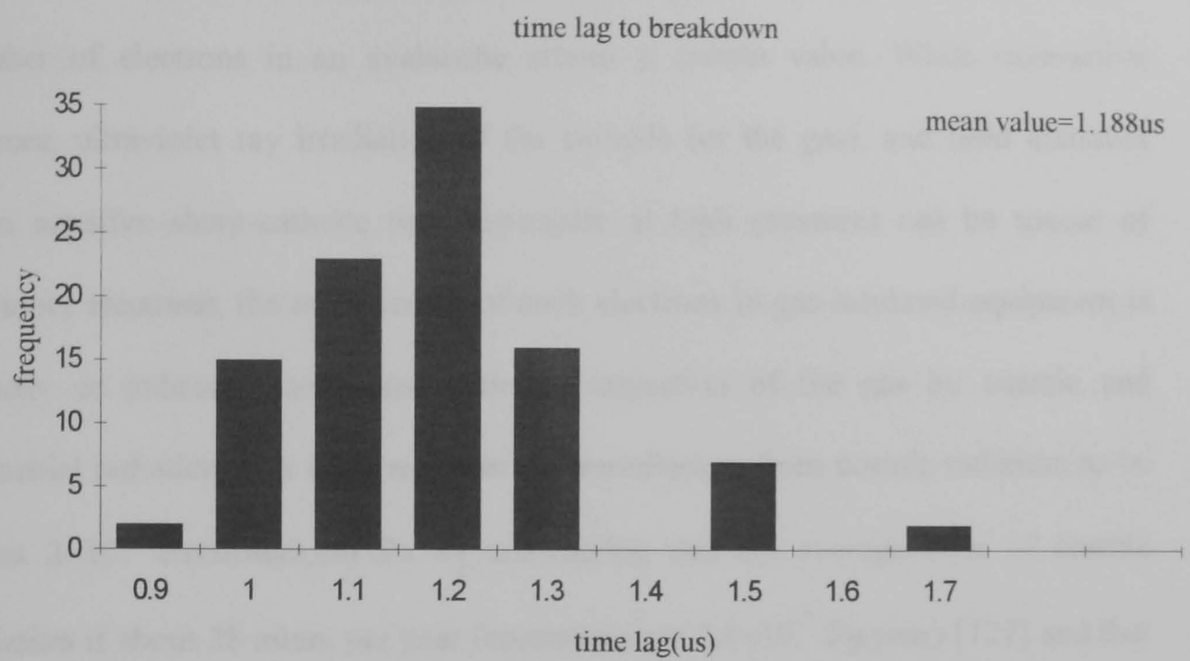

Figure 4.14 SF_6/R12 (95/5), 15mm gap, P=0.1MPa, with irradiation

4.5 Free electrons from irradiation

For a certain gap, the breakdown criterion can be written as[16],

$$\int_0^{x_c} (\alpha - \eta)dx \geq K \qquad (4\text{-}1)$$

where α is Townsend's first ionisation coefficient, i.e., the number of ionising collisions for an electron per unit length of path in the direction of the field, η is the electron attachment coefficient defined as the number of attachments per electron per unit length of path in the direction of the field, x_c is the co-ordinate where α-η=0, K is a constant (for SF_6, K=10.5 [125]).

Equation (4-1) can be readily explained as that breakdown occurs when the total number of electrons in an avalanche attains a certain value. While radioactive sources, ultraviolet ray irradiation of the cathode (or the gas), and field emission from negative sharp-cathode tips (especially at high pressure) can be source of initiatory electrons, the main source of such electrons in gas-insulated equipment is directly or indirectly connected with the ionisation of the gas by cosmic and terrestrial radiation. It is estimated that the contribution from cosmic radiation to be about 2×10^{-5} electrons/s.cm^3.Pa by considering that the average dose of cosmic radiation is about 28 mrem per year (approximately 2.8×10^{-7} J/g·year) [127] and that the average energy to produce an electron-ion pair (i.p) in most gases of interest is between 25 and 36 eV/i.p [128,129]. In addition to this, ionisation from natural terrestrial sources can produce about 10^{-4} electrons/s.cm^3.Pa[128]. However, since about 80% of these latter electrons are produced by α and β particles [126] which normally would not penetrate the metallic enclosures of practical systems, the relevant free electron production rate due to terrestrial radiation is also about 2×10^{-5} electrons/s.cm^3.Pa, bringing the total to about 4×10^{-5} electrons/s.cm^3.Pa[128]. In non electron attaching gases this is the rate at which the free electrons become available for breakdown initiation. In electron attaching gases, the electrons produced by cosmic and terrestrial radiation are captured by the gas molecules forming negative ions. It is estimated [107] that the equilibrium concentration of negative ions in SF_6 insulated systems is about 10^4/cm^3 by assuming an electron production rate of 4×10^{-5} electrons/s.cm^3.Pa. It, therefore, seems that the major source of breakdown-initiating free electrons is electron detachment from these negative ions[130,131,132] and

occurs with highest probability in the vicinity of positive-stressed electrode under nonuniform field condition.

In enclosed gaps, however, most electrons are shielded by the enclosure [126] but there are few electrons that enter the enclosure, and they can be attached to form negative ions and initiatory electrons can be detached from the negative ions, as for SF_6,

$$SF_6 + e \Leftrightarrow SF_6^- \qquad (4\text{-}2)$$

$$SF_6 + e \Leftrightarrow SF_5 + F^- \qquad (4\text{-}3)$$

Without the effect of electric field, the density of free electrons can be estimated considering the ion formation and recombination[126], as,

$$n_e = \sqrt{\frac{AS}{R(1+\frac{B}{D})}} \cdot n \qquad (4\text{-}4)$$

where A is the photo ionisation probability coefficient, B is the electrons attachment probability, D is the electrons detachment probability, S is the radiation intensity, R is the recombination probability of electrons and positive ions, and n is the density of the gas.

From (4-4), it can be seen that the number of free electrons increases as the radiation intensity increases. In enclosed gaps, about 80% of the electrons which are produced

by α and β rays in normal condition [126] would not penetrate the metallic enclosures of practical system, thus the free electrons are less. As the availability of electrons decreases and then the probability of a corona discharge at the end of each leader step also decreases and this leads to an associated decrease in breakdown probability and consequent increase in breakdown strength as the results shown in this chapter (figures 4.1 to 4.4).

4.6 The detachment of negative ions

As previously discussed, it has been well established that [121] there are mainly two possible sources of free electrons, one is the detached electrons from the negative ions such as SF_6^- and OH^-, which was studied in chapter 3. The other is from the direct ionisation of neutral molecules by artificial irradiation or natural irradiation as discussed in 4.5.

The electron detachment process from negative ions is very complicated, detailed discussion on the topic can be found in [126]. A brief discussion is given here in terms of SF_6^- negative ions detachment process, it is generally believed that there are four kinds of detachment forms in SF_6,

(1)Self-detachment:

$SF_6 + e$ ($\leftarrow$ detach) ($\rightarrow$ attach) $(SF_6^-)^*$

The unstable $(SF_6^-)^*$ can be formed by SF_6 molecule and electron through attachment process, and after a certain time the stable state SF_6^- can be formed. The unstable $(SF_6^-)^*$ is very easy to release electron through detachment process and SF_6 molecule is formed again[92]. In nonuniform field, the electrons can only initiate breakdown if they are released within the $\bar{\alpha}$ ($\bar{\alpha}=\alpha-\eta$)>0 critical area (this area is extremely small) near the point electrode and the volume(V_{cr}) of the critical area decreases as the gas pressure increases [126]. Thus the self-detachment has little effect on breakdown initiation until the $(SF_6^-)^*$ is moved into the V_{cr} area.

(2)Field-induced detachment:

$$SF_6^- \rightarrow SF_6 + e$$

It has been shown that the field-induced detachment can only occurred when the electric field strength is extremely high, and in many gas discharge experiments the breakdown initiation can not be attributed to electric field-induced detachment since the electric field strengths in these studies were too low for any significant electric field-induced detachment to occur [135]. Electric field-induced electron detachment is an unlikely source of initiatory electrons in gas-insulated systems unless negative ions with very small electron binding energies exist in the discharge process.

(3)Photo-detachment:

$$h\nu + SF_6^- \rightarrow SF_6 + e$$

Photo-detachment only occurs when there is irradiation of very short wave length. There is evidence that in GIS system photo-detachment is very unlikely to happen [131].

(4)Collision detachment:

$$SF_6^- + SF_6 \rightarrow \begin{cases} SF_6 + SF_6 + e^* \\ (SF_6)_2 + e^\bullet \end{cases}$$

*: unassociative detachment

•: associative detachment

It is generally believed that the detachment process is mostly collisional [126,132,136]. Even though the collisional velocities of SF_6^- and SF_6 under field-free conditions are so small for collisional detachment, the shift in the velocity distribution of the negative ions to higher velocities under an applied electric field may result in significant collisional detachment. The negative ions in SF_6 can be produced mainly through these processes,

$SF_6 + e \rightarrow (SF_6^-)^* \rightarrow SF_6^-$

$SF_6 + e \rightarrow (SF_6^-)^* \rightarrow SF_5^- + F$

$SF_6 + e \rightarrow (SF_6^-)^* \rightarrow SF_5^- + F^-$

Recent studies [133,134] on field-assisted collisional detachment involving F^-, SF_5^-, and SF_6^- in SF_6, have shown that of these three negative ions the one (F^-) with the highest electron affinity energy (EA) and the lowest cross section of formation has

the highest electron detachment rate [126]. The electron detachment coefficient δ is defined as the number of detachments per electron per unit length of path in the direction of the field,

$$dn_e = \delta n^- dx \qquad (4\text{-}5)$$

where n_e is the number of electrons in the unit volume, n^- is the number of negative ions in the unit volume. The production rate of electrons can be expressed as,

$$\frac{dn_e}{dt} = \delta \cdot v_d \cdot n^- \qquad (4\text{-}6)$$

where v_d is the velocity of negative ion in electric field.

Detachment coefficient δ can be expressed as,

$$\delta = \frac{n}{v_d} \int_0^\infty \sigma_d(v_r) v_r f(v_r) dv_r \qquad (4\text{-}7)$$

where n is the number of molecule in the unit volume, v_r is the relative velocity of collisional particles, σ_d is the cross section of collisional detachment, $f(v_r)$ is the distribution function of the relative velocity. There is no published literature on the measurement of the collisional detachment cross section of negative ions in SF_6. According to the collisional detachment cross section of O_2^-, the cross section of collisional detachment σ_d can be expressed as,

$$\sigma_d = \begin{cases} \sigma_0 \left(\dfrac{v}{v_{min}} - 1 \right) & v > v_{min} \\ 0 & v \le v_{min} \end{cases} \qquad (4\text{-}8)$$

where v_{min} is the minimum velocity that negative ions can be detached through collision process and it can be determined by the experiments. In electronegative gases, the v_{min} is much larger than that of air, because the negative ions have to

overcome the electron affinity energy, and the electrons detached from negative ions must have enough energy so that they are not to be attached.

The impulse breakdown probability in the certain time t according to the *Boeck* volume-time criteria[132] can be expressed as,

$$W(t) = 1 - \exp\left[-\int_0^t \int_{V_{cr}} \frac{\partial n_e}{\partial t}\left(1 - \frac{\eta}{\alpha}\right) dv \cdot dt\right] \quad (4\text{-}9)$$

It can be seen from (4-9) that in the critical volume V_{cr}, the breakdown probability depends on the initiatory electron production rate, i.e., the detachment of negative ions increases the breakdown probability.

4.7 Discussion

The results reported in this chapter were obtained in point plane gaps filled with air, SF_6 and its mixtures with air, N_2, R12 or R20 with and without irradiation. The air gaps were tested under enclosed and open air conditions.

From the test results obtained in enclosed air gaps, it can be seen that there is significant decrease in minimum impulse breakdown voltage with UV irradiation but there is almost no decrease in minimum impulse breakdown with UV irradiation under the same condition if the gaps are in open air. The differences between these sets of data can be explained by the fact that, in enclosed air gaps, due to the shielding from cosmic radiation and stray UV irradiation, there will be something of a scarcity of free electrons or negative ions capable of yielding initiatory electrons. In the open air gaps, on the other hand, UV irradiation from the impulse generator [6]

as well as cosmic radiation (which can produce approximately 2×10^{-5} electrons/s.cm^3.Pa [127]) will more or less guarantee a relative abundance of free electrons which cannot be significantly increased by artificial UV irradiation. This is also the reason why the minimum impulse breakdown voltages measured in open air gaps are much lower (by 15.9% for 15mm gap) than those obtained in enclosed air gaps. The fact that minimum impulse breakdown voltage does not decrease much under the effect of artificial irradiation in open air gaps may imply that, there is limit beyond which the breakdown strength cannot be further affected. This saturation effect will be studied in chapter 5.

From the results obtained in air, SF_6 and its mixtures with air or N_2, it has been shown that the minimum impulse breakdown voltages in the point-plane gaps decrease when the artificial irradiation is applied. These results are in good agreement with some earlier work as it [122] was pointed out that the production of initiating electrons in the critical volume of the gap is quite important for the development of breakdown and the fact that in an enclosed highly non uniform field gap in air [122,123] and SF_6 [120], the impulse breakdown voltage decreases under the condition of strong irradiation. The effect of external irradiation on the initial discharge activity was also studied by observing photomultiplier (PM) oscillograms. With irradiation, the inception pulse and the subsequent corona activity tended to be greater[120].

It is well known that when a gaseous dielectrics is stressed electrically a free electron must be present and suitably placed before any discharge can develop. This is

confirmed in the present work and one can only assume that the decrease in breakdown strength is associated with a relative abundance of electrons within the critical volume around the highly stressed electrode. However, as indicated previously [106], initiatory electrons are also required throughout the gap in order to promote the stepwise development and whilst it is easy to explain how electrons can be so generated using the corona pin arrangement and direct injection method, it is more difficult to explain the existence of electrons or negative ions capable of detachment within the gap volume when the caesium 137 is present. The radioisotope, emitting gamma radiation, would be expected to generate electrons only close to the metal surface and not in the mid gap. A high ion density may assist leader propagation presumably by providing seed electrons which favour continued leader development. Alternatively, the seed electrons may be required to assist in the initiation of leader channel restrikes which occur between leader steps. The role of artificial irradiation in highly non-uniform fields is not fully resolved and must be further studied.

In any case the rate of reduction in breakdown strength due to the radioisotope is clearly less than that produced by the ion injection methods. Take the SF_6 15mm gap for example, the minimum impulse breakdown voltage decreases by 5.1% due to the irradiation. While under the effect of ion injection (using corona pin arrangement, V_c=-20kV), the minimum impulse breakdown voltage decreases by more than 11%.

As previous results shown in chapter 3, the minimum impulse breakdown voltage is unaffected by the injection of ions in SF_6/freon mixtures, while the breakdown

voltages of SF_6 and its mixtures with air and N_2 are much affected by the injected ions. It can be concluded that the presence of negative ions in SF_6 and its mixtures with air or N_2 which almost inevitably contain traces of water vapour, affects the impulse breakdown voltage in highly nonuniform gaps by providing seed electrons, detached from negative ions (such as,OH^-,SF^-) to allow the streamer/leader stepping process to propagate. From the results obtained in this and last chapters, the fact that injected charges has little effect when a chlorine bearing additive is present, endorses the view that the presence of such additives results in the preferential production of highly stable negative ions of chlorine which cannot detach within the time scales necessary and thus cannot significantly provide the seed electrons in the gap necessary for the propagation of the stepping process.

From the results of time lag measurement shown in figures 4.7 to 4.10, it can be seen that:

(1)The mean values of time lag measured in open air gaps, are larger than those measured in enclosed air gaps.

(2)With irradiation, the mean values of time lag to breakdown measured in enclosed air gaps, SF_6 and its mixtures with air or N_2 gaps increase.

(3)The mean values of time lag do not change much in open air gaps whether with or without irradiation.

(4)In SF_6/freon mixtures, the mean values of time lag do not change too much.

The above phenomena can be explained by the fact that with the irradiation sources, there is an almost 100% probability that an initiating electron in the critical volume when the voltage has reached the corona onset voltage. A filamentary corona will be established and it is necessary that the voltage be increased to a higher value and the field near the plane electrode be space-charge enhanced before breakdown can take place, thus the time lag to breakdown is relatively longer. When no irradiation is presented, there is a finite probability that no electron will appear until a much higher voltage is reached at which a streamer can be developed which is sufficiently large that it can propagate across the gap by virtue of its own localised space charges. Then, breakdown will take place shortly after the appearance of the initiating electrons. The time lags to breakdown obtained in open air gaps which are almost not affected by the irradiation and the fact that the mean values of time lag in open air gaps are longer than those of enclosed gaps can also be explained by the above viewpoint. The observation of time lag measurements in SF_6 and its mixtures with air, N_2 or SF_6/freon is absolutely consistent with the breakdown voltage data and again points to the fact that in SF_6, the injection of negative ions enhances the discharge activity through the creation of unstable negative ions which can detach and provide electrons. When the chlorinated additive is present, stable chlorine ions are formed and, no matter their number, they do not detach and therefore do not contribute to the discharge development.

4.8 Conclusions

The initiatory electrons produced from the direct ionisation of neutral molecules by artificial irradiation (supplied by either an 125W quartz-mercury arc lamp or a piece of 5mCi capsule ^{137}Cs) and/or natural irradiation (refers to the background radiation from radioactive materials in the ground and from cosmic radiation from space, etc) affect the minimum impulse breakdown voltage in nonuniform field. The present work has confirmed that the breakdown strength of air, SF_6 and SF_6 mixtures with nitrogen and air, at least to the 50/50 level, is affected by the presence of artificial irradiation as has been found previously under the effect of injected ions. This would suggest that air, SF_6 and its mixtures with air and N_2 can be affected by the presence or lack of negative ions in the gap volume. Although the rate of decreasing under the effect of artificial irradiation is much less than that of injected ions, and the explanations of the existence of electrons or negative ions capable of detachment within the gap volume when irradiation is present or ions are injected would not be the same.

The present results add further evidence to the suggestion [119] that marked improvement in the insulating performance of SF_6 and hence to the tolerance of the gas to metallic particle in a GIS when a chlorinated freon is present is related to ion chemistry. It is unlikely, however, due to environmental pressures, that in GIS installations chlorinated freons would be considered as feasible. Indeed, at the present time, and again for environmental reasons, there is a drive to explore alternative gases to pure SF_6. A better physical understanding of the factors that contribute to "good" insulating gases will assist in making informed choices for the next generation of GIS.

Chapter 5 The combined effect of space charge and artificial irradiation

5.1 Introduction

In chapters 3 and 4, the effect of space charge and artificial irradiation had been studied respectively. It had been proved that the development of breakdown process production may be critically dependent upon the statistics associated with the production of initiating electrons in the critical volume of the gap[143]. It is well known that when a gaseous dielectric is stressed electrically a free electron must be released from a bound atomic or molecular state before any discharge can develop. There are many mechanisms whereby electrons can be released from their bound states. Generally the electron can be emitted either from the cathode of the electrode system or from within the gaseous volume. The effect of cathode processes can be eliminated by using a non-uniform field geometry in an electronegative gas where the electric field at the cathode is small. Under such circumstance the low electric field at the cathode ensures that any electron emission is reduced, and even if an electron is released it will attach to a neutral molecule very quickly as the attachment coefficient will also be very much greater than the ionisation coefficient (i.e $\eta >> \alpha$). For these particular conditions, there are really only two possible sources of free electrons, one is from the direct ionisation of neutral molecules by some of the known processes (e.g. by alpha, bata, gamma or cosmic radiation), the other is detached electrons from negative ions. The study in this chapter is emphasised on the combined effect of space charge and artificial irradiation.

5.2 Effect of space charge

In highly nonuniform electric field gaps within a certain pressure range of SF_6 or its mixtures, it is well established that corona stabilised breakdown exists. It is generally thought that the enhancement in corona stabilisation is affected by increasing the homopolar charge near the high-stress electrode [94]. For instance a low ionisation energy gas or vapour additive like cis-2-C_4H_8 [94] or TEA [137] may greatly increase the positive dc corona stabilised breakdown voltages of SF_6 in a point plane gap. However, corresponding results for impulse breakdown can not readily be explained by the above concept because there is insufficient time for space charge movement to modify the electric field in the gap. In addition, some additives which do not produce enhanced corona also have the similar effect. For example, the positive impulse breakdown voltage of SF_6 in a highly nonuniform field can be apparently increased by the R113($C_2Cl_3F_3$) vapour additive, yet corona measurements indicate that the R113 additive causes no increases in corona activity in the gap [138,139]. This is not surprising because the dielectric strength of R113 is higher than that of SF_6 [140]. A similar phenomenon has been observed in SF_6 with an R12(CCl_2F_2) additive [141] in which the dielectric strength of R12 is no less than that of SF_6 [142]. For a non-uniform-field gap, the breakdown mechanism is much more complicated than for a uniform field. This is probably due to the complex effect of space charges on the breakdown process [3]. In some earlier work, it has been pointed out that space charges greatly affect the breakdown strength of SF_6 in non-uniform-fields [101, 102,103,104,117]. The mechanism of breakdown under impulse

conditions is not fully understood, although it is now known to involve the development of a series of streamer/leader steps [105] which propagate from the point electrode towards the plane. It has recently been suggested [106] that the successful development of impulse breakdown relies upon there being a supply of electrons in the gap volume such that each streamer step can be initiated. These initiating electrons are generally believed to result from the detachment from the negative ions or result from direct ionisation of neutral molecules by irradiation. Certain additives, particularly those containing chlorine (as studied in previous chapters), preferentially produce very stable negative ions which do not readily detach and thus the suggestion [106] is that the impulse strength is increased in mixtures containing those additives because there is then a reduced likelihood of successful development of the discharge channel through a scarcity of initiating electrons in the gap.

5.3 Effect of artificial irradiation

It had been noticed in some earlier work that in an enclosed highly nonuniform field gap filled with air [122,123] and SF_6 [124], the impulse breakdown voltage decreases under the condition of strong irradiation. In chapter 4, the results obtained in enclosed air, SF_6 and its mixtures had shown that the minimum impulse breakdown voltages in the point-plane gaps decrease when the artificial irradiation(either a quartz-mercury arc lamp or a piece of 5mCi capsule ^{137}Cs) is applied. The reason was concluded to be the detachment of free electrons from the direct ionisation of neutral molecules by irradiation.

Although natural irradiation, such as cosmic radiation from the space (which can produce approximately 2×10^{-5} electrons/s·cm^3·Pa [127]), radiation from the radioactive components in the earth's crust and from the materials used for building, e.g., granite, etc. will more or less provide some kind of irradiation and guarantee a relative abundance of free electrons. It is known that in enclosed gaps, about 80% of the electrons which are produced by α and β rays in normal condition [126] would not penetrate the metallic enclosures of practical system, thus the effect by natural irradiation is presumably very much decreased. A series of experiments were carried out in enclosed air and open air gaps (figure 4.2). The minimum impulse breakdown voltages were measured as the functions of gap length, the distinguish differences (the minimum impulse breakdown voltage decreases by 15.9% for 15mm open air gap) between the two sets of data, at first sight, to be surprising to what one might expect. In open air gaps ultraviolet irradiation from the impulse generator [6] as well as natural radiation will more or less guarantee a relative abundance of free electrons. In enclosed air gaps, however, due to shielding from natural irradiation and stray UV irradiation, there will be something of a scarcity of free electrons or negative ions capable of yielding free electrons.

5.4 Experimental setup and procedure

Details of the pressurised chamber and the test gap assembly were well documented in chapter 2. The point-plane electrodes were first cleaned in normal manner and set to different gap length before each test. The minimum impulse breakdown voltage,

corona activity and time lag to breakdown were measured and recorded by the oscilloscope.

The tests were carried out with combined effects of space charge and artificial irradiation. Space charges were injected by means of four auxiliary needle electrodes (corona pin arrangement) surrounding the gap with the needles being approximately in line with the point electrode tip. The four needle electrodes were connected with a Brandenburg high voltage dc power generator and both positive and negative charges can be injected into the point-plane gap. The artificial irradiation was provided by either an 125W quartz-mercury arc lamp for tests carried out in air or a piece of 5mCi capsule ^{137}Cs (6MeV γ ray source) for tests carried out in SF_6 and its mixtures with air, N_2, R12 or R20. The quartz-mercury arc lamp or the ^{137}Cs radiation source was placed approximately 120mm or 100 mm from the point electrode, respectively.

- Minimum impulse breakdown voltage measurement

The minimum impulse breakdown voltage was determined by the following procedure: in each test sequence, the 50% breakdown level was first determined by the normal up-and-down method, and then the charging voltage of impulse voltage generator was reduced in steps of 0.5kV to give the level at which only 1 flashover in 40 was recorded and this voltage value is regarded as the minimum (2.5% breakdown probability) breakdown voltage.

- Time lag to breakdown measurement

A sequence of 100, positive impulse voltage were applied to the gap with a voltage corresponding to the 90% breakdown level. The time lag to breakdown was recorded on the oscilloscope and the results were given in column charts.

• Prebreakdown corona activity measurement

An optical photomultiplier (type 9125QB) was used to monitor the prebreakdown corona activity under different gap length with or without irradiation provided no breakdown occurs. More detailed information was outlined in 2.1.4.3. The high-gain THORN EMI^{TM} photomultiplier was mounted on the outside of the observation window so as to record the transmitted light from the corona. The peak outputs from the photomultiplier (observing the total gap activity) as functions of the gap length provided no breakdown occurs were measured.

5.5 Low-probability impulse breakdown measurement

Figures 5.1 to 5.3 show the minimum impulse breakdown voltages measured in enclosed air gaps SF_6 and its mixtures with N_2 or air gaps as functions of the gap length. The tests were carried out with negative dc high voltage applied to the four auxiliary needle electrodes to supply space charges. For tests carried out in enclosed air gaps, the dc bias voltage was -12kV. For SF_6, SF_6/N_2 (50/50) and SF_6/air (50/50) the dc bias voltage was -16kV. Tests were carried out either with or without artificial irradiation source.

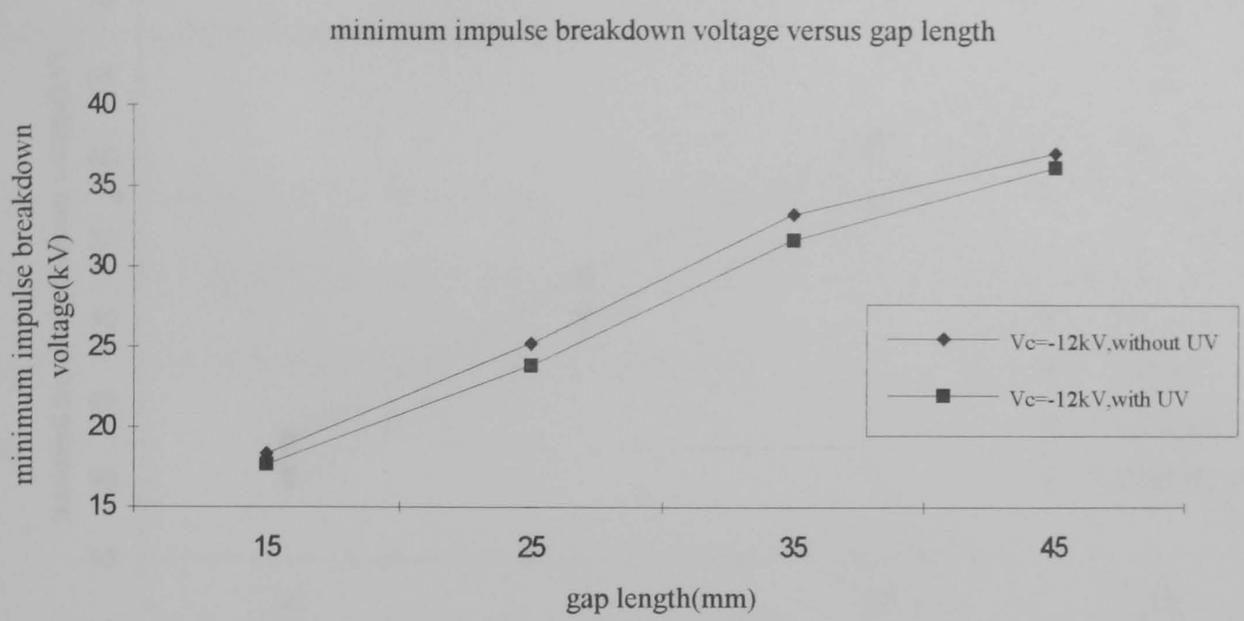

Figure 5.1 Minimum impulse breakdown voltage versus gap length, enclosed air gaps, P=0.1MPa, with dc bias voltage of -12kV

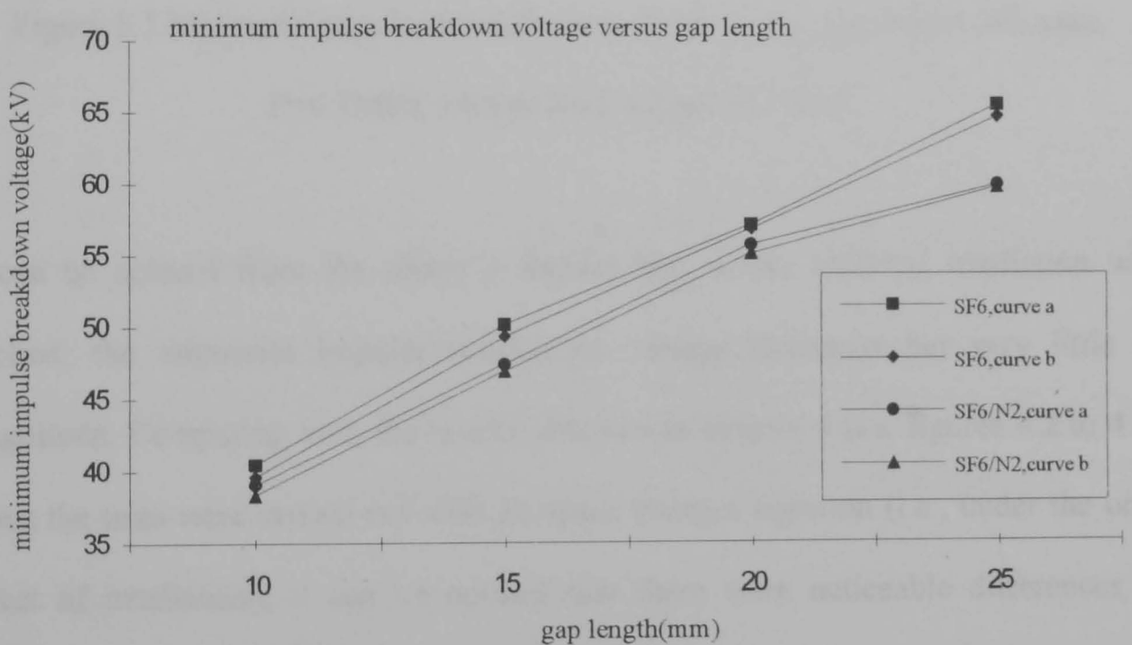

curve a :without irradiation, curve b: with irradiation

Figure 5.2 Minimum impulse breakdown voltage versus gap length, SF_6 gaps, P=0.1MPa, with dc bias voltage of -16kV

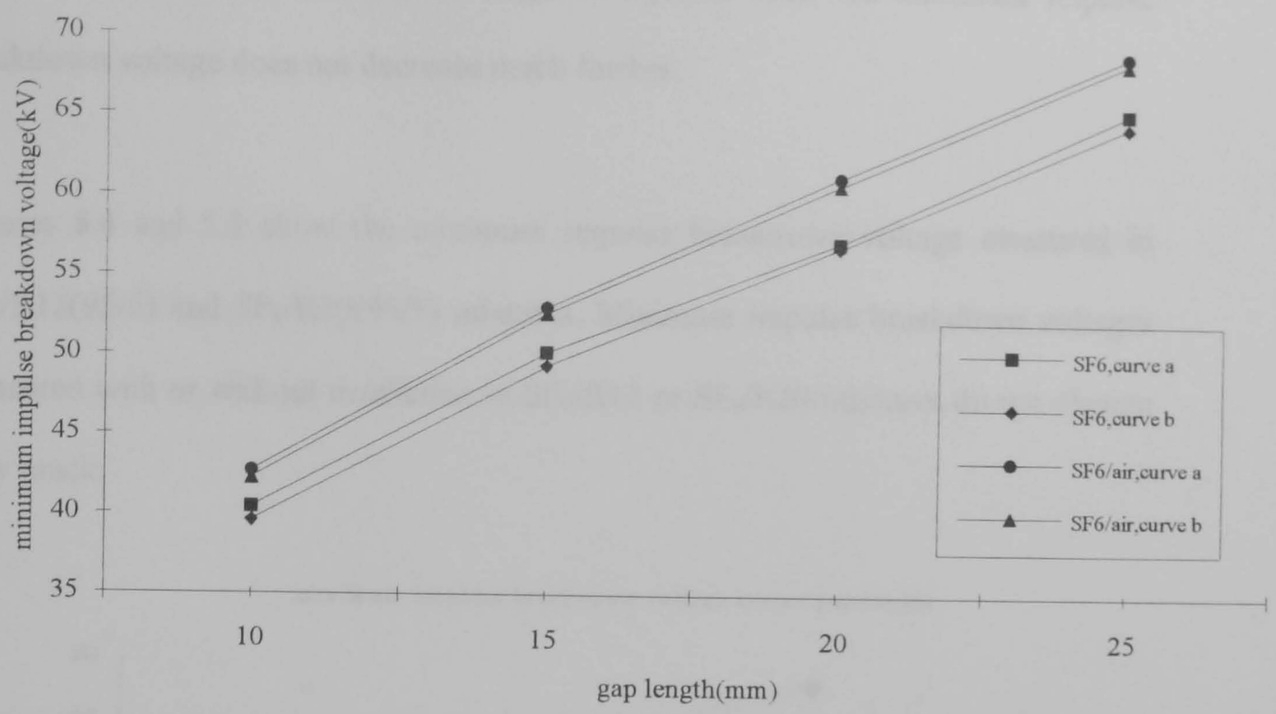

curve a :without irradiation, curve b: with irradiation

Figure 5.3 Minimum impulse breakdown voltage versus gap length, SF_6 gaps, P=0.1MPa, with dc bias voltage of -16kV

It can be noticed from the above 3 figures that as the artificial irradiation was applied, the minimum impulse breakdown voltage decreases but very little in magnitude. Comparing with the results obtained in chapter 4 (i.e. figures 4.2 to 4.4) when the tests were carried out with no space charges injection (i.e., under the only effect of irradiation), it can be noticed that there were noticeable differences in minimum impulse breakdown voltages when the tests were carried out with or without irradiation. Also comparing the results obtained in chapter 3 (i.e. figures 3.7 and 3.8), the minimum impulse breakdown voltage decreases significantly when negative ions were injected. So under the only effect of irradiation or negative injected ions, the minimum impulse breakdown voltage decreases. But under the

combined effect of irradiation and negative injected ions, the minimum impulse breakdown voltage does not decrease much further.

Figures 5.4 and 5.5 show the minimum impulse breakdown voltage measured in SF_6/R12(95/5) and SF_6/R20(95/5) mixtures. Minimum impulse breakdown voltages measured with or without irradiation in SF_6/R12 or SF_6/R20 mixtures do not change very much.

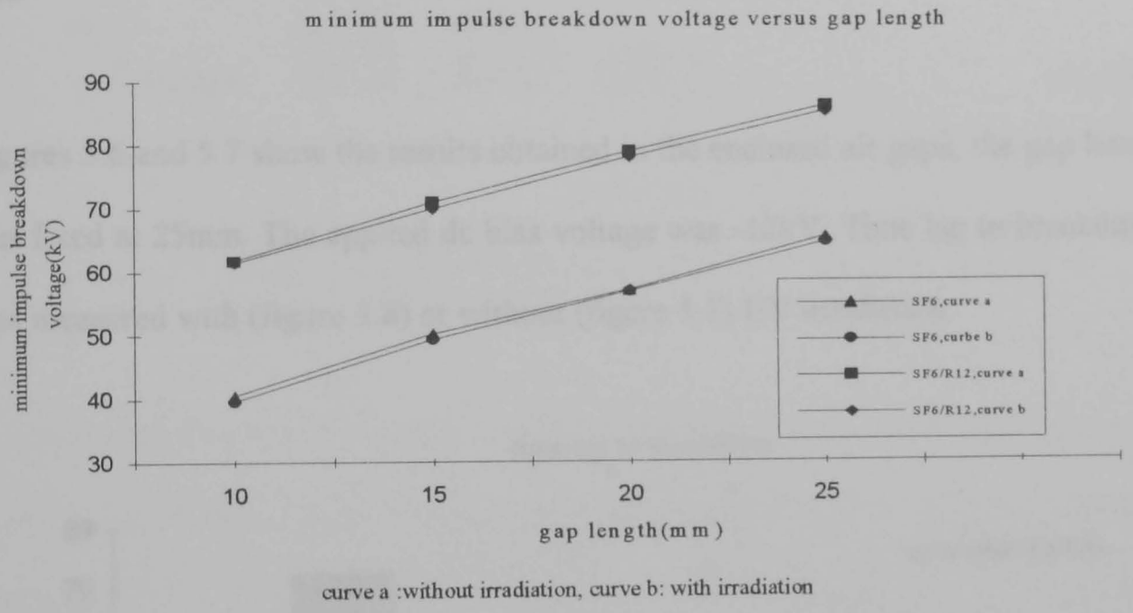

curve a :without irradiation, curve b: with irradiation

Figure 5.4 Minimum impulse breakdown voltage versus gap length, SF_6 gaps, P=0.1MPa, with dc bias voltage of -16kV

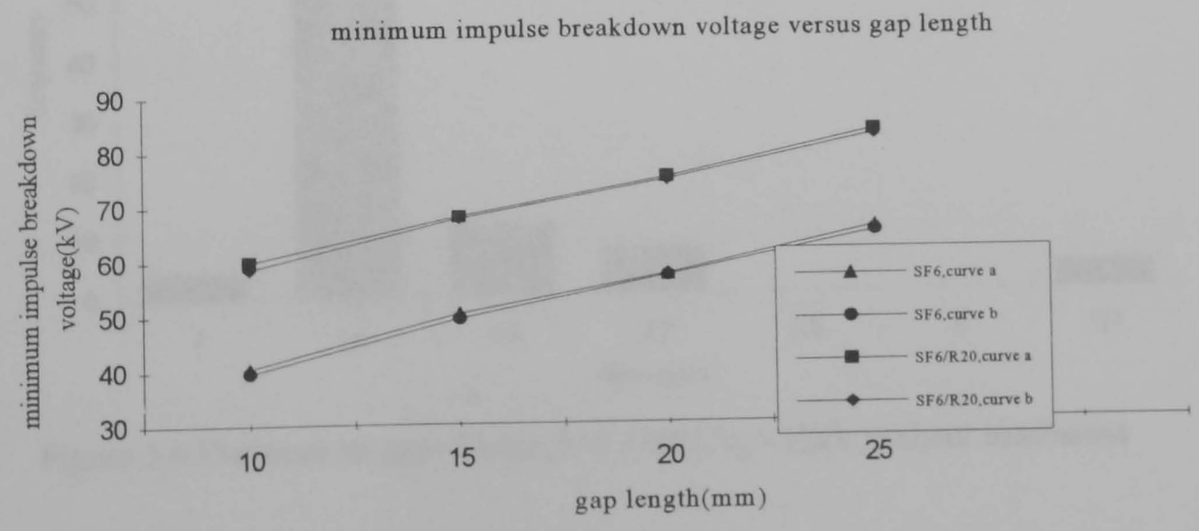

curve a :without irradiation, curve b: with irradiation

Figure 5.5 Minimum impulse breakdown voltage versus gap length, SF_6 gaps, P=0.1MPa, with dc bias voltage of -16kV

5.6 Time lag measurement

Time lag to breakdown was measured in enclosed air, SF_6 and its mixtures with N_2, air, R12 or R20 gaps with dc bias voltage (V_c) applied to the four needle electrodes. The tests were carried out either with or without artificial irradiation source.

- air

Figures 5.6 and 5.7 show the results obtained in the enclosed air gaps, the gap length was fixed at 25mm. The applied dc bias voltage was -12kV. Time lag to breakdown was measured with (figure 5.8) or without (figure 5.7) UV irradiation.

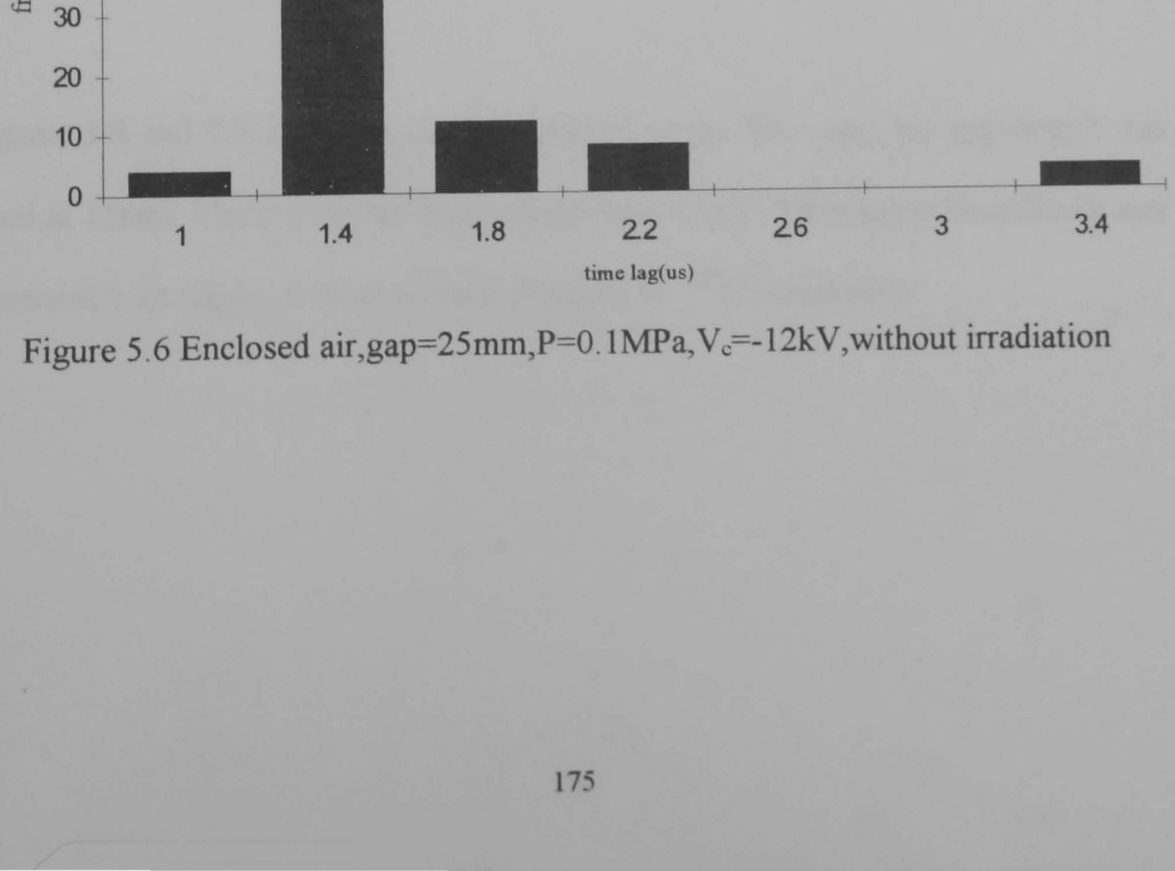

Figure 5.6 Enclosed air,gap=25mm,P=0.1MPa,V_c=-12kV,without irradiation

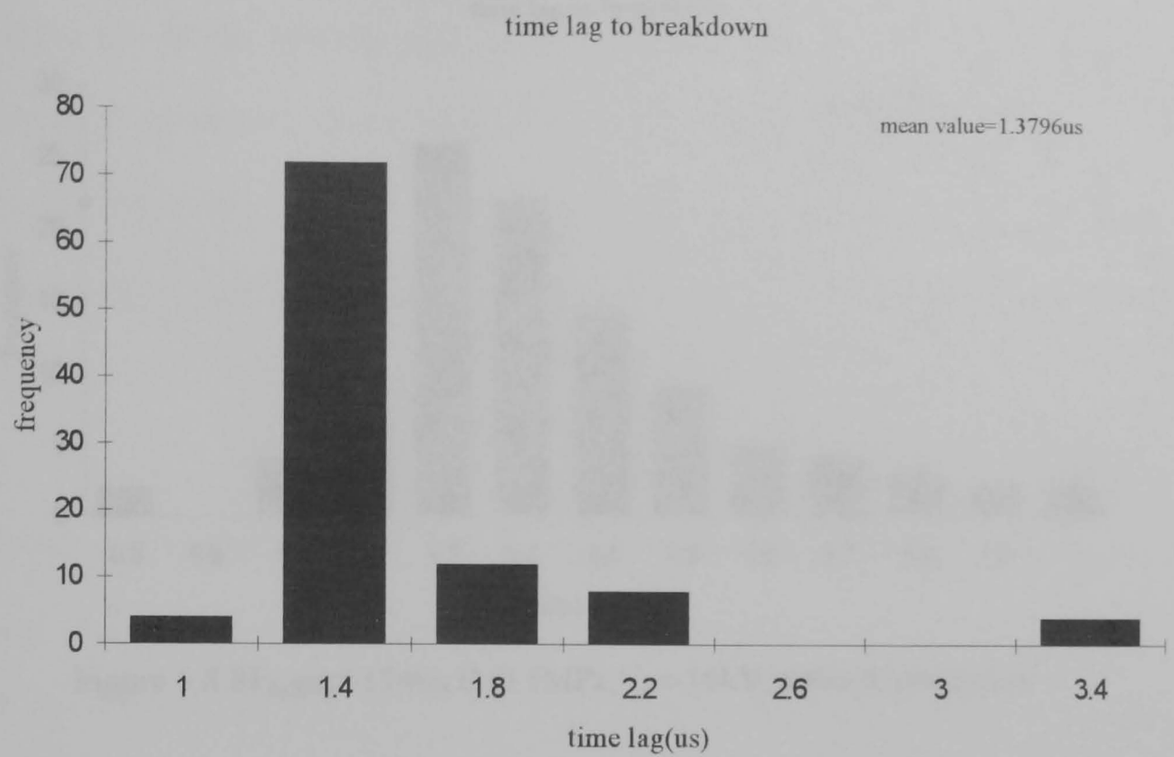

Figure 5.7 Enclosed air,gap=25mm,P=0.1MPa,V_c=-12kV,with irradiation

It can be seen from the above figures, when the UV irradiation source was added, the mean value of time lag to breakdown increases very little, i.e., from 1.3784μs to 1.3796μs.

- SF_6 and its mixtures with air or N_2

Figures 5.8 and 5.9 show the results obtained in the SF_6 gaps, the gap length was fixed at 15mm. The applied dc bias voltage was -16kV. Time lag to breakdown was measured with (figure 5.9) or without (figure 5.8) ^{137}Cs irradiation.

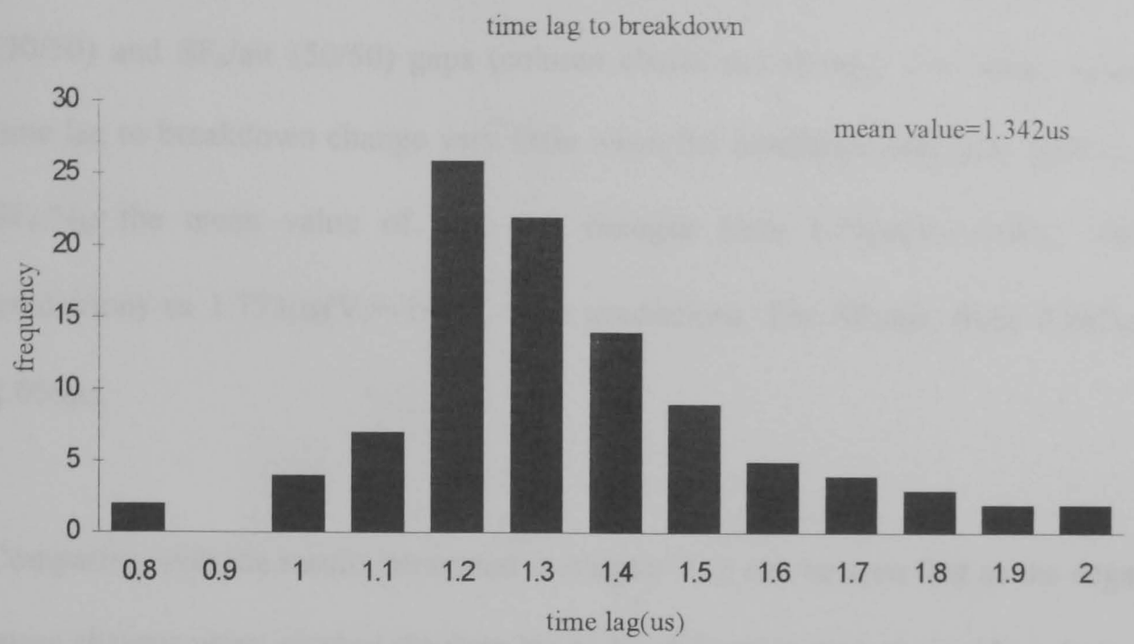

Figure 5.8 SF_6,gap=15mm,P=0.1MPa,V_c=-16kV,without irradiation

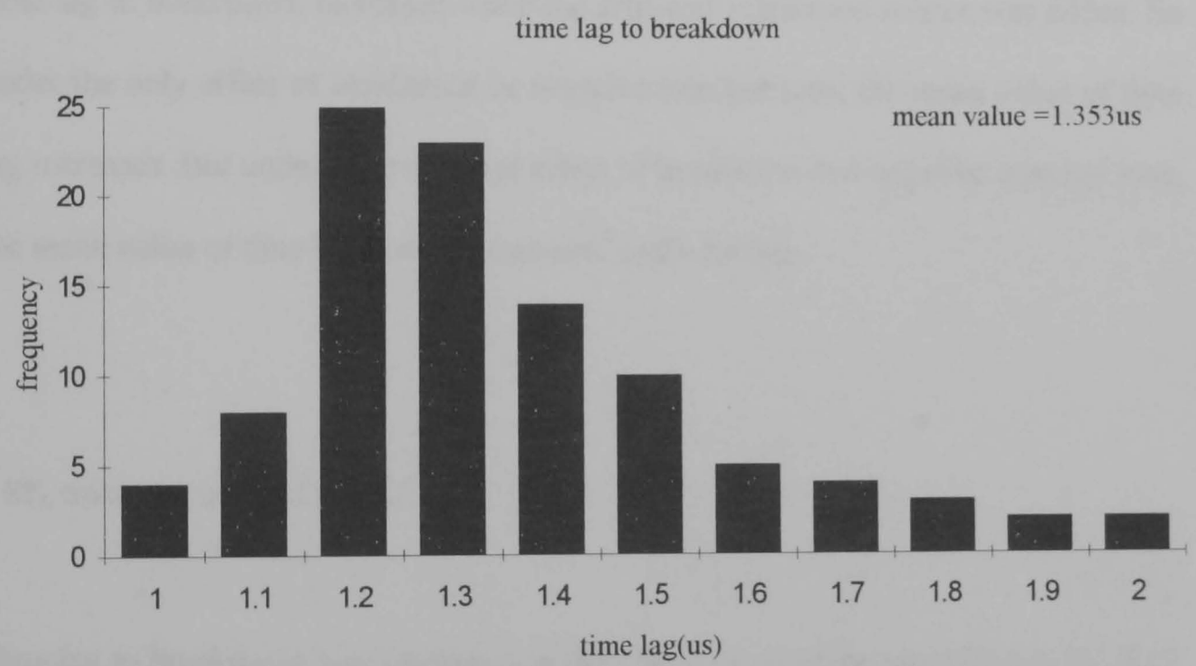

Figure 5.9 SF_6,gap=15mm,P=0.1MPa,V_c=-16kV,with irradiation

It can be seen from the above figures, when the ^{137}Cs irradiation source was added, the mean value of time lag to breakdown increases very little.

The same was observed as the time lag measurements were carried out in SF_6/N_2 (50/50) and SF_6/air (50/50) gaps (column charts not shown). The mean values of time lag to breakdown change very little when the irradiation source is applied. For SF_6/N_2, the mean value of time lag changes from 1.75μs(V_c=-16kV, without irradiation) to 1.753μs(V_c=-16kV, with irradiation). For SF_6/air, from 2.067μs to 2.056μs.

Comparing with the results presented in chapter 3, it can be seen that as the negative space charges were injected the time lag to breakdown increased significantly in SF_6 and its mixtures with air or N_2. Also can be seen from the results in chapter 4 that the time lag to breakdown increased when the artificial irradiation source was added. So under the only effect of irradiation or negative injected ions, the mean value of time lag increases. But under the combined effect of irradiation and negative injected ions, the mean value of time lag does not increase much further.

- SF_6 mixtures with R12 or R20

Time lag to breakdown was measured in the 15mm point-plane gap fill with SF_6/R12 (95/5) and SF_6/R20 (95/5) mixtures with or without ^{137}Cs irradiation whilst negative space charges were injected (V_c=-16kV). Figures 5.10 and 5.11 show the results obtained in SF_6/R12 mixtures.

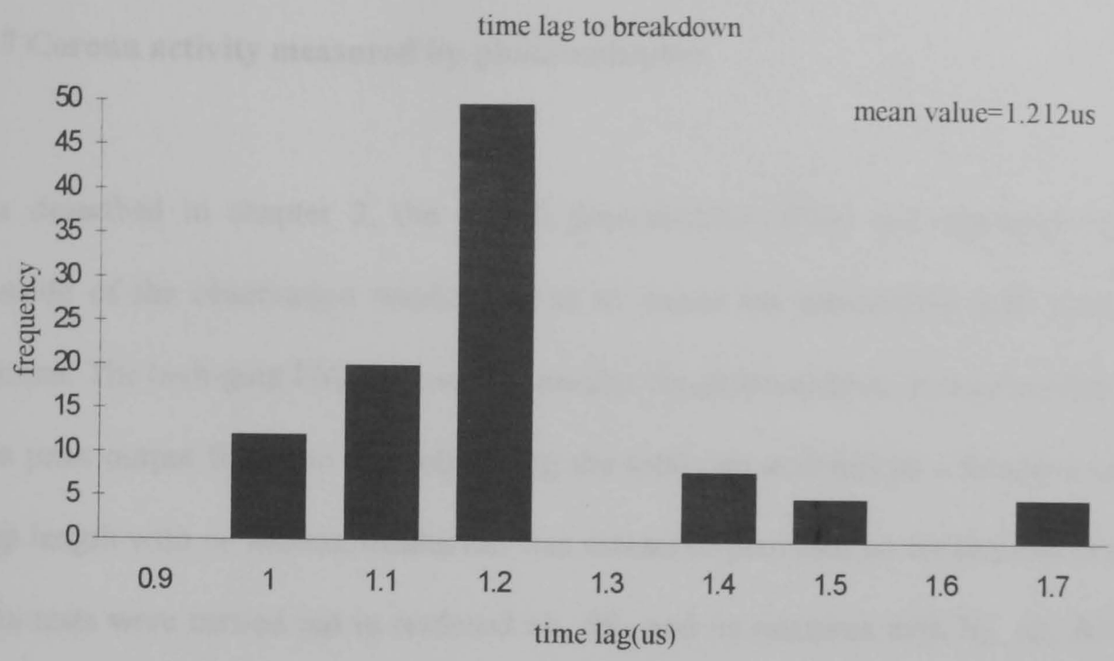

Figure 5.10 SF_6/R12, gap=15mm,P=0.1MPa,V_c=-16kV,without irradiation

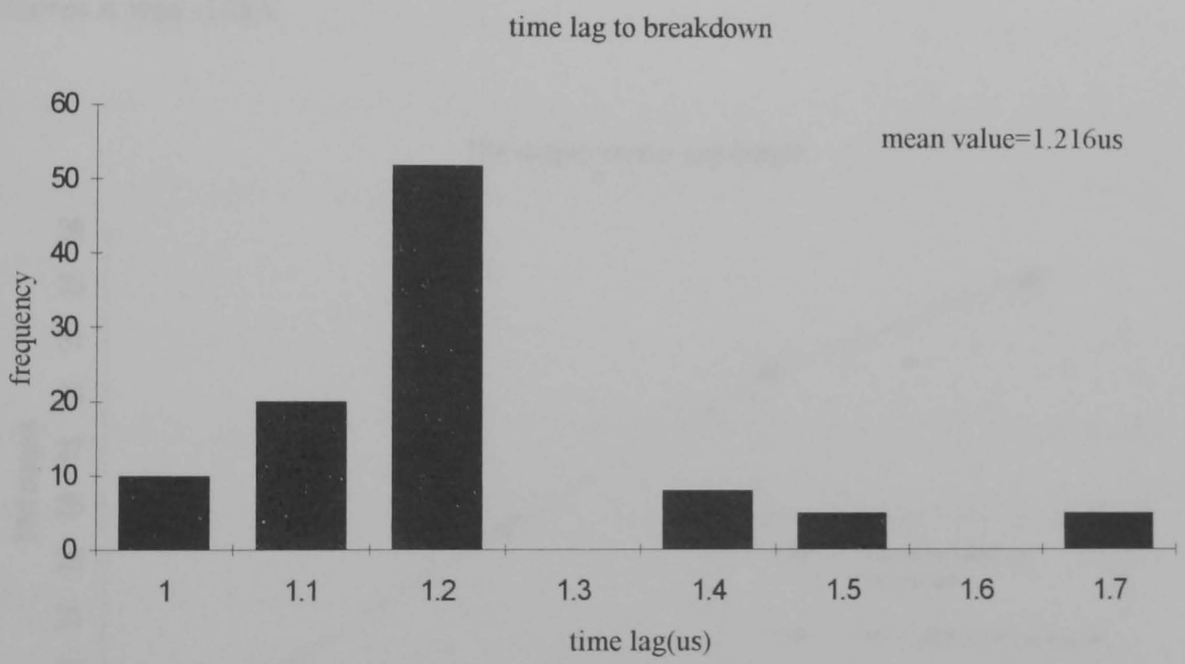

Figure 5.11 SF_6/R12gap=15mm,P=0.1MPa,V_c=-16kV,with irradiation

The mean value of time lag does not change much for SF_6/R12 whether with or without irradiation, i.e. from 1.212μs to 1.216μs. The same is true for SF_6/R20 mixtures, i.e. from 1.087μs to 1.091μs (column charts not shown).

5.7 Corona activity measured by photomultiplier

As described in chapter 2, the optical photomutilier (PM) was mounted on the outside of the observation window so as to record the transmitted light from the corona. The high-gain PM was used to monitor the prebreakdown corona activity and the peak output from the PM (observing the total gap activity) as a function of the gap length with or without irradiation was measured provided no breakdown occurs. The tests were carried out in enclosed air, SF_6, and its mixtures with N_2, air, R12 or R20 gaps. A dc bias voltage (V_c) was always applied to the four needle electrodes. For tests carried out in enclosed air gaps, the V_c was -12kV and for all other gases or mixtures it was -16kV.

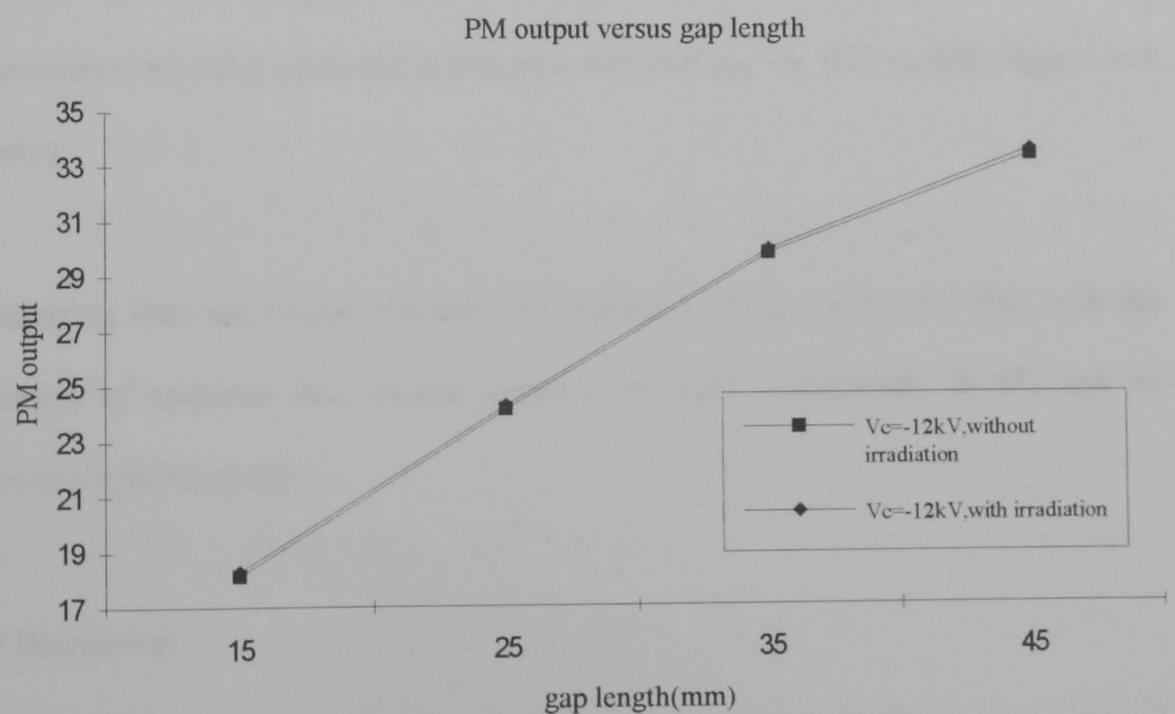

Figure 5.12 enclosed air gaps, P=0.1MPa, V_c=-12kV

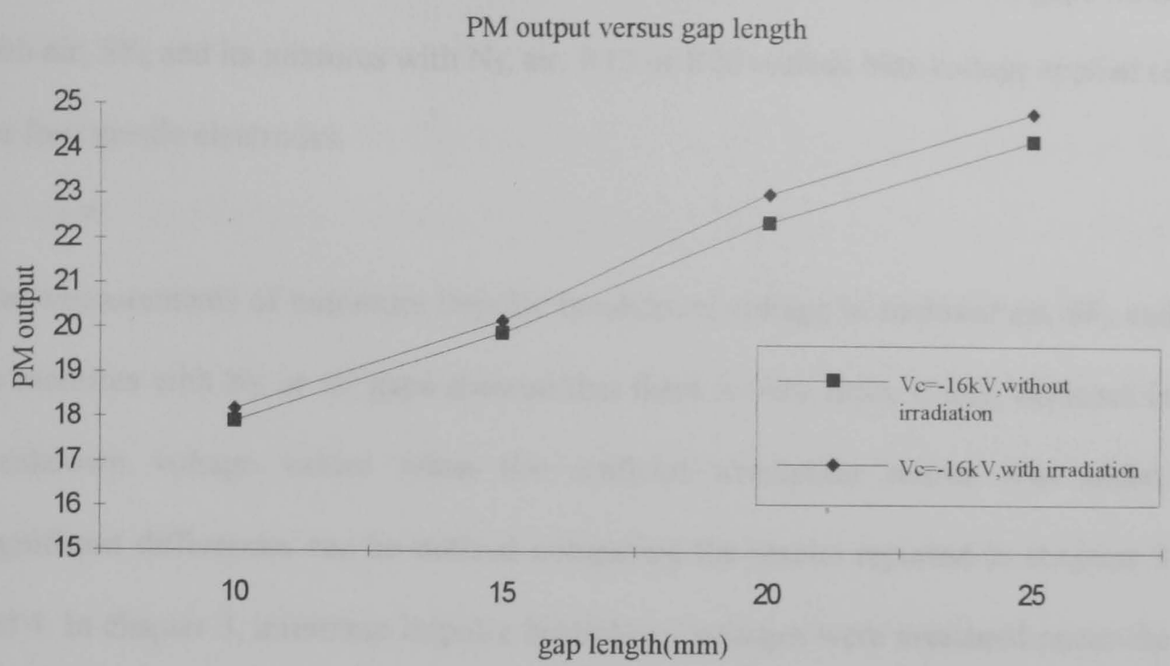

Figure 5.13 SF_6 gaps, P=0.1MPa, V_c=-16kV

It can be noticed from the above figures that PM outputs increase very little in enclosed air and SF_6 gaps when artificial irradiation was applied. The same phenomenon was also observed in SF_6 mixtures with air, N_2, R12 or R20 (figures not shown).

Comparing with the results presented in chapter 3, it can be noticed that with the injection of negative ions, corona activity increased dramatically in SF_6 and its mixtures with N_2 or air.

5.8 Discussion

All the test results reported in this chapter were carried out in point plane gaps filled with air, SF_6 and its mixtures with N_2, air, R12 or R20 with dc bias voltage applied to the four needle electrodes.

The measurements of minimum impulse breakdown voltage in enclosed air, SF_6 and its mixtures with N_2 or air gaps showed that there is very little, if any, decrease in breakdown voltage values when the artificial irradiation source was added. Significant differences can be noticed comparing the results reported in chapters 3 and 4. In chapter 3, minimum impulse breakdown voltages were measured under the only effect of space charge, and it can be seen that when negative space charges were injected, the minimum impulse breakdown voltage decreased significantly in SF_6 and its mixtures with N_2 or air. In chapter 4, minimum impulse breakdown voltages were measured under the only effect of irradiation. It can be seen that when artificial irradiation source was added or when natural irradiation was available, the minimum impulse breakdown voltage also decreased in SF_6 and its mixtures with N_2 or air. Under the combined effect of space charge and artificial irradiation, however, there was not much further decrease in minimum impulse breakdown voltage. It was concluded in previous chapters that the breakdown strength is affected by the initiatory electrons whether resulting from the detachment of negative ions or the direct ionisation of neutral molecules by artificial or natural irradiation. The results reported in this chapter, however, strongly suggest that there is a limit beyond which the breakdown strength cannot be further affected by increasing initiatory electron population. It is well established that [101, 102, 117, 122] the production of initiating electrons in the critical volume of the gap is quite important for the development of

breakdown process. It [105] has been pointed out that non-uniform-field breakdown involves the development of a series of streamer/leader steps which propagate from the point electrode towards the plane and it [106] has been realised that the successful development of impulse breakdown relies on there being a supply of electrons in the gap volume such that each streamer step can be initiated. The conclusion had been made based on the results reported in previous chapters that breakdown process of a non-uniform field gap in SF_6 and its mixtures with N_2 or air is greatly affected by the availability of initiatory electrons throughout the gap volume to allow the streamer/leader step progression to take place. From the results presented in this chapter, however, it seems fair to conclude that there is a threshold which the number of initiatory electrons has to be reached so breakdown process can be initiated and be further affected. Those initiatory electrons exceeding the threshold value make no or very little contribution to breakdown process. This conclusion is implied by some test results presented in chapters 3 and 4. From figure 3.7, the saturation effect was noticed that with the increase in negative dc applied voltage, the minimum impulse breakdown voltage decreases significantly at first, but then becomes constant or decreases very little when the dc applied voltage was over -16 kV. This could suggest that the number of initiatory electrons reach the threshold value when the dc applied voltage is over -16kV. Further increase in the dc applied voltage does not affect the minimum impulse breakdown voltage too much. From figure 4.2, it also can be noticed that there is almost no difference in minimum impulse breakdown voltage with or without UV irradiation when the tests were carried out in open air gaps although there is significant difference in minimum impulse breakdown voltage with or without UV irradiation when the tests were

carried out in enclosed air gaps. The phenomenon seems surprising at first sight, but considering the initiatory electrons threshold it is relatively easy to explain. In enclosed air gaps, due to the shielding from natural radiation and stray UV irradiation, there will be something of a scarcity of free electrons or negative ions capable of yielding initiatory electrons. In open air gaps, on the other hand, UV irradiation from the impulse generator [6] as well as natural radiation will more or less guarantee a relative abundance of free electrons. Thus further artificial irradiation does not affect the minimum impulse breakdown voltage too much.

As it was noticed previously, minimum impulse breakdown, time lag to breakdown or PM out measured in either SF_6/R12 or SF_6/R20 does not change too much with the injection of space charges or irradiation. The results obtained in this chapter, showed that in SF_6/R12 and SF_6/R20, these values do not change much even under the combined effect of space charge injection and irradiation. Previous work at Strathclyde [137,138] and elsewhere [139, 140] has shown by adding small amounts of R113($C_2Cl_3F_3$) or R12(CCl_2F_2) to SF_6, the dielectric strength of the gas can be greatly improved under certain condition. It is interesting that the additives do not produce enhanced corona. Recently it had been suggested that the chlorine molecule is associated with the enhanced dielectric strength of the mixture and R113, or indeed any other additive which is capable of producing negative ions of chlorine, will be beneficial in that it will mitigate the reduction in performance associated with the almost inevitable presence of water vapour and metallic conducting particles in GIS. It is believed that these chlorinated freons, preferentially produce very stable negative ions (Cl^-) which do not readily detach. The impulse strength is increased in

mixtures containing those additives because there is then a reduced likelihood of successful development of the discharge channel through a scarcity of initiating electrons in the gap.

The time lag measurements were carried out in enclosed air, SF_6 and its mixtures with air, N_2, R12 or R20 with or without artificial irradiation, a dc bias voltage was always applied to the four needle electrodes. It is quite apparent that under the combined effect of space charge and artificial irradiation, the time lag to breakdown changed very little, if any, compared with the time lag measurements presented in chapters 3 and 4, there was significant difference in time lag measurements under the only effect of space charge or artificial irradiation. With irradiation source or negative space charge injection, there is an almost 100% probability that an initiating electron will appear in the critical volume when the voltage has reached the corona onset voltage. A filamentary corona will be established and it is necessary that the voltage be increased to a higher value and the field near the plane electrode be space-charge enhanced before breakdown can take place, thus the time lag to breakdown is relative longer. Without the irradiation or negative space charge injection, there is a finite probability that no electron will appear until a much higher voltage is reached at which a streamer can be developed which is sufficiently large that it can propagate across the gap by virtue of its own localised space charges. Breakdown will then take place shortly after the appearance of the initiating electrons and the time lag to breakdown is relatively shorter. When artificial irradiation was applied, since negative space charge injection has already provided significant initiatory electrons, it is expected that those electrons resulting from direct ionisation by irradiation

which exceed the initiatory electron threshold in number have very little effect on time lag to breakdown.

The peak output from a photomultiplier (observing the total gap activity) as the function of gap length was also measured. The results are compared as the artificial irradiation was applied or not. It can be seen that in all gases or gas mixtures concerned, the output of PM (i.e., discharge activity) changed very little whether the artificial irradiation was applied or not. This observation is absolutely consistent with the minimum impulse breakdown voltage and time lag measurements and confirms that there is a limit beyond which the breakdown process cannot be further affected by increasing initiatory electron population. Considering the threshold of the initiatory electrons, more than enough electrons make very little or no contribution to the prebreakdown and breakdown processes.

5.9 Conclusions

The following conclusions were drawn based on the results and discussion presented here and in previous chapters. Whilst the initiatory electrons resulted from either the detachment of negative ions or the direct ionisation of neutral molecules by irradiation have considerable effect on prebreakdown and breakdown processes, the results shown in this chapter strongly suggest that there is a limit beyond which the prebreakdown/breakdown process cannot be further affected by increasing initiatory electron population. The term "threshold of initiatory electrons" was introduced in this chapter. The term means that there is a certain number of initiatory electrons that

has to be reached so that breakdown process can be initiated and further affected. It is also concluded from the results that any extra initiatory electrons exceeding the number of threshold make very little, if any, contribution to the prebreakdown/breakdown process.

Chapter 6 The effect of different wavefront

6.1 Introduction

The behaviour of point-plane gaps in SF_6 and its mixtures under impulse voltage application has been the subject of considerable research in recent years and the mechanism is not fully understood. It is believed, however, the complex effect of space charge on the breakdown process has great effect on breakdown process. There is evidence that the abundance of initiatory electrons plays an important role in breakdown process [102,117,143]. The initiating electrons will be produced mainly by the detachment from negative ions and so their rate of production in critical volume will itself depend upon the applied waveform [143]. Previous work [49] has shown that the V_{50} characteristic is strongly wavefront dependent, showing a more and more pronounced stabilisation peak as the wavefront is increased. The above experimental observations have been explained qualitatively [80] on the basis of a theoretical model for point-plane breakdown. It is assumed that the point corona takes the form of radial sheath similar to that previously suggested for dc voltage application [85]. The radius of the sheath is assumed to be time and voltage dependent and clearly, if the voltage is applied rapidly, then insufficient time is available for the radial development of the sheath, and breaks down when impulse voltage reaches the minimum voltage necessary for propagation of a leader from point to plane. If, on the other hand, a long-fronted wave is applied to the gap, then the corona sheath can develop to a greater or lesser extent depending upon the

duration of the front, and the impulse characteristics will show some form of "partial" stabilisation peak.

Little is known at present of the mechanism controlling the spatial and temporal development of corona in SF_6 and its mixtures. The available evidence from time-resolved under both static [54] and impulse voltage [50,56,57] suggests that corona consists of individual, mutually-exclusive, re-illuminating filaments, each of which can last for many hundreds of microseconds before extinguishing and giving way to another filament at some other site. However, it is somewhat difficult to reconcile the observation with the picture of a radial sheath as proposed [80, 85] and it is far from certain, therefore, if the model for corona formation as proposed by these authors or the concept of "partial stabilisation" is applicable, even for long-fronted impulses. However, such a conclusion is not consistent with time lag measurement [143] and V-p characteristic measured [52,143]. It [143]had been suggested that there is no such phenomenon as "partial stabilisation". A stabilising corona discharge capable of inhibiting breakdown either forms or does not form under impulse conditions, depending upon a number of factors. The most important of these is the statistics associated with the production of electrons in the gap.

Earlier studies have found that wave tail has little influence on impulse breakdown process of SF_6 and its mixtures [141, 158] and the effect of wave front on breakdown process is studied in this chapter.

6.2 Experimental setup and procedure

The pressurised chamber and the test gap assembly were well documented in chapter 2. The tests were carried out with the injection of space charge of both polarities under different types of wavefronts, i.e., 1.2, 9 and 19μs. The wave tail was kept constant at 50μs.

Space charges were injected by means of four auxiliary needle electrodes (i.e., corona pin arrangement), surrounding the gap with the needle electrodes connected with a Brandenburg high voltage dc power generator and both positive and negative charges can be injected into the point-plane gap.

The minimum impulse breakdown voltages under different wavefronts were measured by the oscilloscope. The procedure to determine the minimum impulse breakdown voltage was outlined in chapter 5.

6.3 Experiments under different impulse wavefronts

6.3.1 SF_6

Figure 6.1 shows the minimum impulse breakdown voltages measured under different wavefronts, i.e., 1.2, 9 and 19 μs. Either positive or negative space charges were injected.

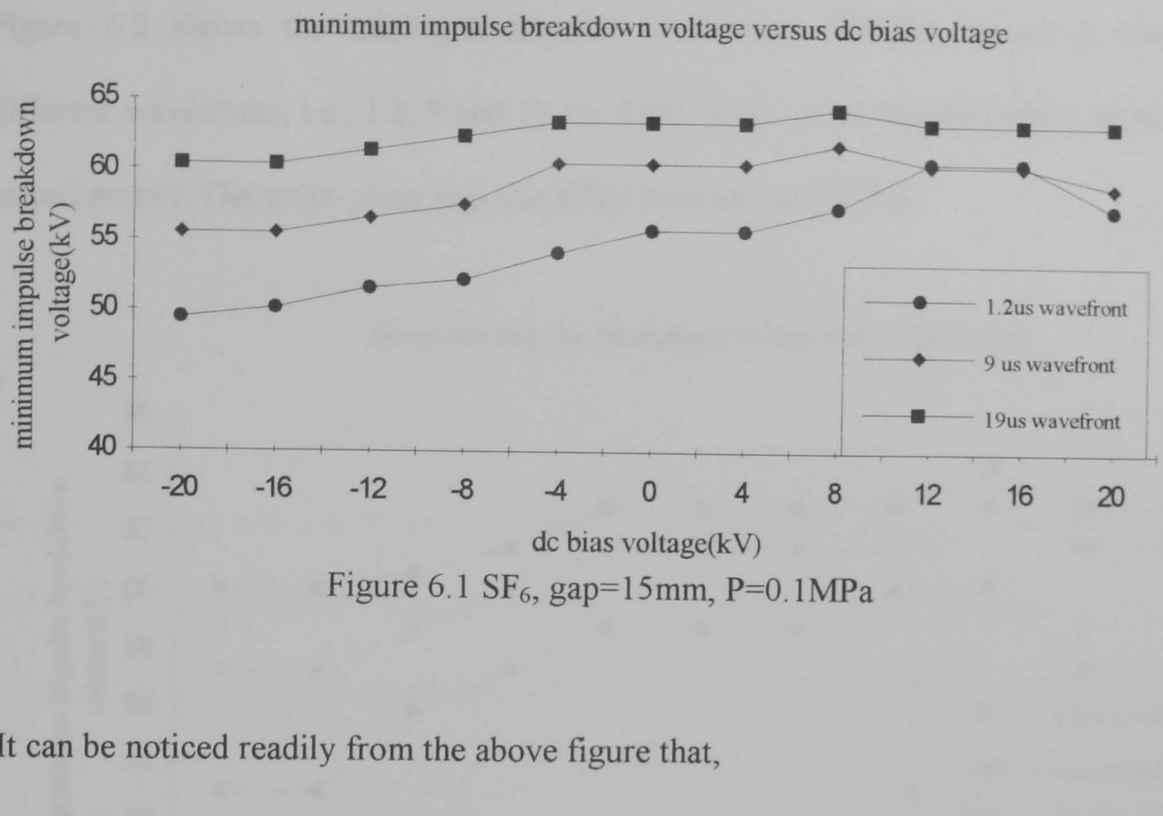

Figure 6.1 SF_6, gap=15mm, P=0.1MPa

It can be noticed readily from the above figure that,

(1)Without the injection of space charge (i.e. V_c=0kV), the minimum impulse breakdown voltage increases as the wavefront increases.

(2)When negative space charges were injected, the minimum impulse breakdown voltages decrease. The longer the wavefront, the smaller the decreasing rate. The minimum impulse breakdown voltage decreases by 11.3% when V_c=-20kV for 1.2μs wavefront, 8.2% for 9μs wavefront and 4.8% for 19μs wavefront.

(3)When positive space charges were injected, the minimum impulse breakdown voltages increase a little bit and then decrease to the levels as no space charge was injected. The minimum impulse breakdown voltage is not too much affected by the positive space charges.

6.3.2 SF_6/air

Figure 6.2 shows the minimum impulse breakdown voltages measured under different wavefronts, i.e., 1.2, 9 and 19 μs. Either positive or negative space charges were injected. The point-plane gap was filled with SF_6/air(50/50).

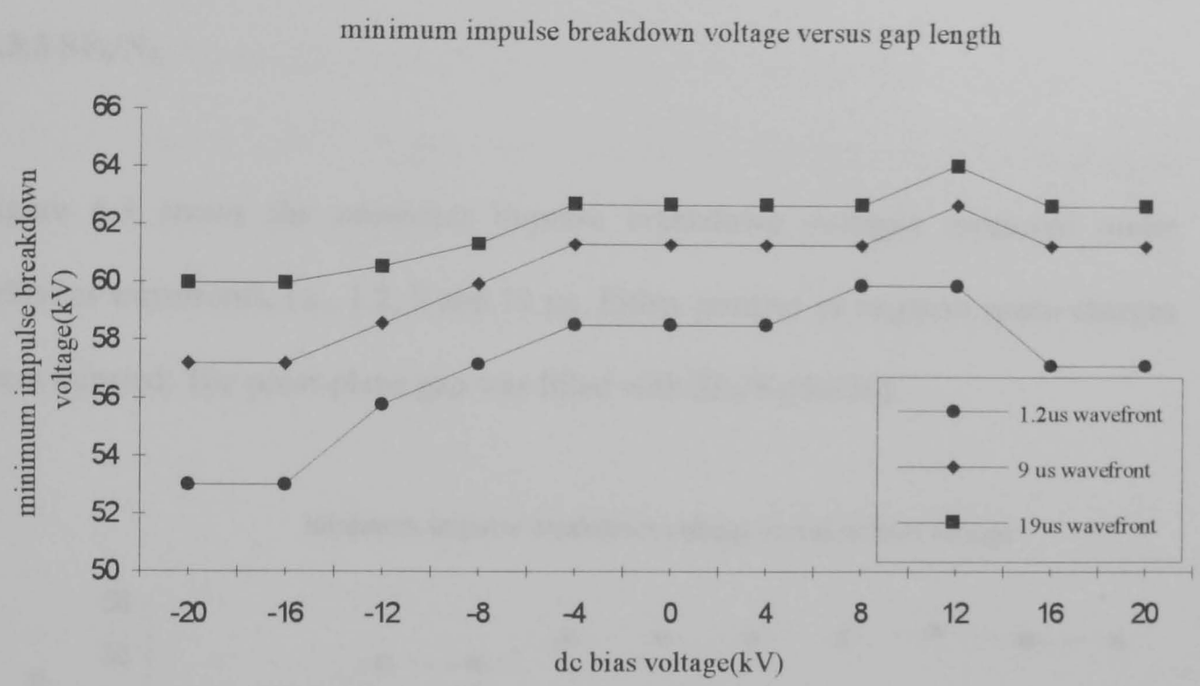

Figure 6.2 SF_6/air(50/50), gap=15mm, P=0.1MPa

It can be noticed readily from the above figure that,

(1)Without the injection of space charge (i.e. V_c=0kV), the minimum impulse breakdown voltage increases as the wavefront increases.

(2)When negative space charges were injected, the minimum impulse breakdown voltages decrease. The longer the wavefront, the smaller the decreasing rate. The minimum impulse breakdown voltage decreases by 9.5% when V_c=-20kV for 1.2μs wavefront, 6.8% for 9μs wavefront and 4.4% for 19μs wavefront.

(3)When positive space charges were injected, the minimum impulse breakdown voltages increase a little bit and then decrease to the levels as no space charge was injected. The minimum impulse breakdown voltage is not too much affected by the positive space charges.

6.3.3 SF_6/N_2

Figure 6.3 shows the minimum impulse breakdown voltages measured under different wavefronts, i.e., 1.2, 9 and 19 μs. Either positive or negative space charges were injected. The point-plane gap was filled with SF_6/N_2(50/50).

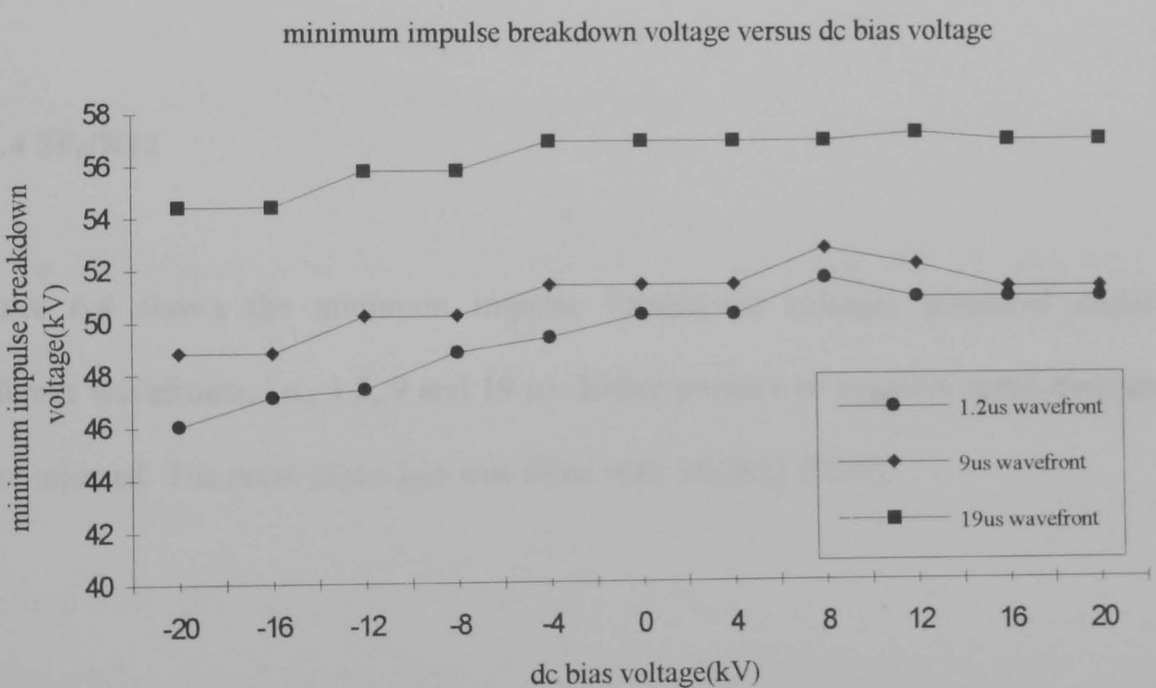

Figure 6.3 SF_6/N_2 (50/50), gap=15mm, P=0.1MPa

It can be noticed readily from the above figure that,

(1)Without the injection of space charge (i.e. V_c=0kV), the minimum impulse breakdown voltage increases as the wavefront increases.

(2)When negative space charges were injected, the minimum impulse breakdown voltages decrease. The longer the wavefront, the smaller the decreasing rate. The minimum impulse breakdown voltage decreases by 8.4% when V_c=-20kV for 1.2μs wavefront, 4.9% for 9μs wavefront and 4.4% for 19μs wavefront.

(3)When positive space charges were injected, the minimum impulse breakdown voltages increase a little bit and then decrease to the levels as no space charge was injected. The minimum impulse breakdown voltage is not too much affected by the positive space charges.

6.3.4 SF_6/R12

Figure 6.4 shows the minimum impulse breakdown voltages measured under different wavefronts, i.e., 1.2, 9 and 19 μs. Either positive or negative space charges were injected. The point-plane gap was filled with SF_6/R12 (95/5).

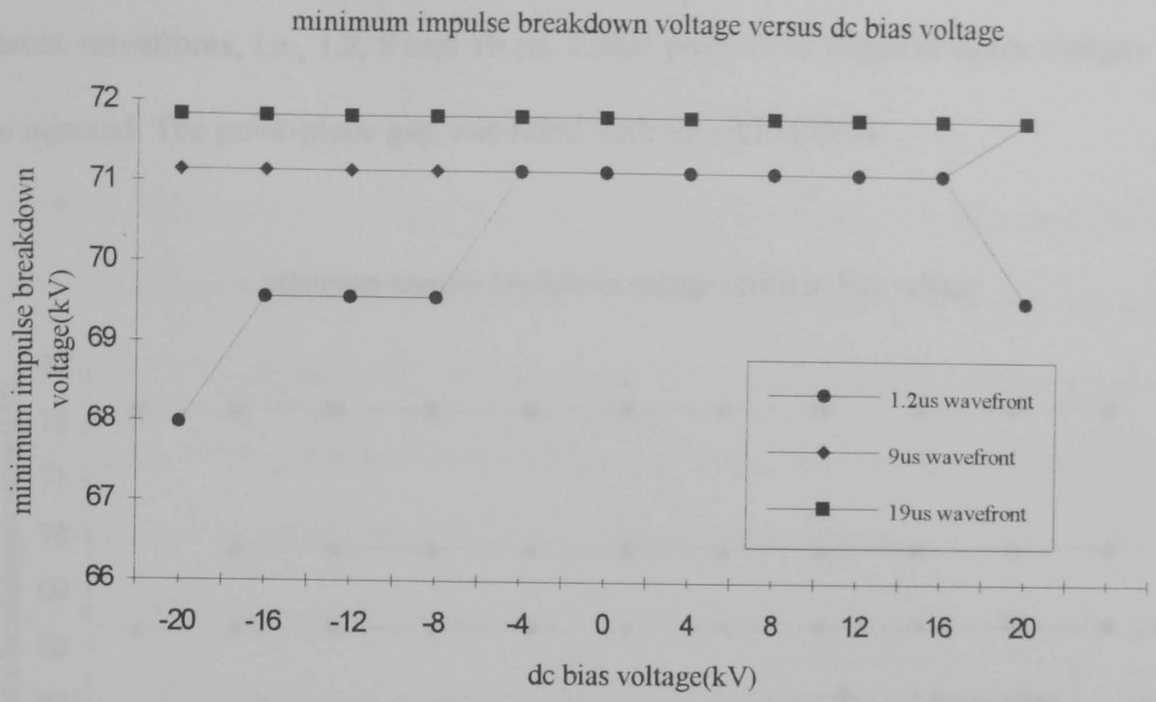

Figure 6.4 SF_6/R12(95/5), gap=10mm, P=0.1MPa

It can be noticed readily from the above figure that,

(1)The minimum impulse breakdown voltages increase slightly as the wavefront increases.

(2)The minimum impulse breakdown voltages decrease as the negative ions were injected when the wavefront is 1.2μs. For longer wavefronts (i.e. 9μs and 19μs), the minimum impulse breakdown voltages remain constant.

(3)The minimum impulse breakdown voltage is not much affected by the positive ion injection.

6.3.5 SF_6/R20

Figure 6.5 shows the minimum impulse breakdown voltages measured under different wavefronts, i.e., 1.2, 9 and 19 μs. Either positive or negative space charges were injected. The point-plane gap was filled with SF_6/R20 (95/5).

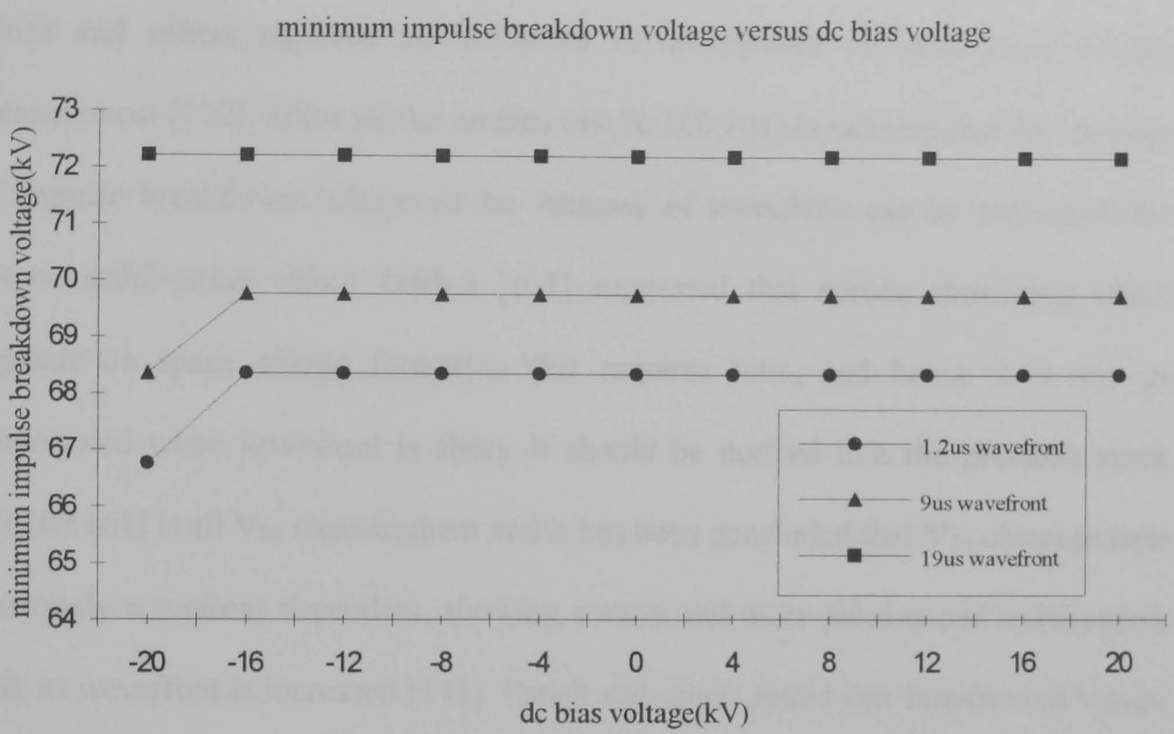

Figure 6.5 SF_6/R20(95/5), gap=10mm, P=0.1MPa

It can be noticed readily from the above figure that,

(1)The minimum impulse breakdown voltages increase very little as the wavefront increases.

(2)The minimum impulse breakdown voltages decrease as the negative ions were injected when the wavefront is 1.2μs. For longer wavefronts (i.e. 9μs and 19μs), the minimum impulse breakdown voltages remain constant.

(3)The minimum impulse breakdown voltage is not affected by positive ion injection.

6.4 Discussion

It has long been noticed that the wavefronts can affect breakdown characteristics. Binns and others reported the influence of wavefronts on breakdown voltage measurement [122]. Some earlier studies [49,50,160,161] concluded that the increase of impulse breakdown voltage as the increase of wavefront can be accounted for corona stabilisation effect. Narbut [161] suggested that corona stabilising effect depends on space charge formation that requires time, and hence it is not so pronounced when wavefront is short. It should be noticed that the previous work [50,160.161] is all V_{50} measurement and it has been concluded that V_{50} characteristic is strongly wavefront dependent, showing a more and more pronounced stabilisation peak as wavefront is increased [143]. Farish and others found that fast-fronted waves give minimum breakdown levels which are much lower than the long-wavefront results[159]. It can be seen from the results obtained in present work, that for SF_6, SF_6/air and SF_6/N_2, the minimum impulse breakdown voltage increases as wavefront increases. The phenomena can not be explained readily by the only effect of corona stabilisation. For minimum impulse breakdown voltage measurement, the increase in minimum impulse breakdown voltage with wavefront is also due to the role of initiatory electrons in breakdown process. In the absence of any other information, this might be taken to indicate the introduction of a corona process during the longer wavefront period, with the increased minimum level demonstrating "partial" stabilisation. However, such a conclusion would be quite inconsistent with the results

obtained [143] that the time lags associated with breakdowns with longer (e.g. 50μs) wavefronts were also short, just as for shorter wavefronts.

It might be argued that the absence of corona stabilisation implies that the rate of rise of the applied voltage is too rapid to allow sufficient time for the development of corona. However, this would not be consistent with the fact that on rising part of the V/p characteristic [52,143], stabilisation can apparently develop rapidly to be active for even the shortest wavefront (1.2μs). In view of this, it would seem reasonable to suggest that corona may not require to spread over the point-electrode surface but may simply involve the development of the first filamentary, reilluminating discharge which itself could inhibit the subsequent development of breakdown. Thus, whether or not a "stabilising corona" occurs for any given set of conditions, may be critically dependent upon the statistics associated with the production of initiating electrons in the critical volume of the gap. How discharges develop will depend on the value of the applied voltage at the instant an initiating electron appears in the critical volume.

The statistics of electron production are obviously highly complex for non-uniform field gaps. The initiating electrons will be produced mainly by detachment from negative ions [121] so their rate of production in the critical volume will itself depend upon the applied waveform. Long wavefronts may well result in sweeping the majority of negative ions out of a gap before the discharge can be developed. Previous chapters and some relevant work [103,104] had shown that the initiatory electrons have great effect on breakdown characteristic, i.e., the minimum impulse

breakdown voltage decreases as the number of initiatory electrons increases beyond a certain limit. It would not be surprising that minimum impulse breakdown voltage increases as the wavefront increases since negative ions would be, more or less in number, swept out of the gap during the longer wavefront period and consequently, the number of initiatory electrons that can be detached from these naturally occurring negative ions is less. Indeed, it had been reported that almost all ions are swept out of the SF_6 gas filled gaps in about 8μs[162]. It [105] has been pointed out that non-uniform-field breakdown involves the development of a series of streamer/leader steps that propagate from the point electrode towards the plane. Theoretically, there is evidence [17,80] that leaders propagate, not in continuous, but in a step-wise fashion, even in very short gaps. The physics governing the production of individual leader steps is not understood but at any given time in the development of a leader, whether a new step is produced or the leader simply dies out, may well depend upon the availability of free electrons in close proximity to the leader tip. Therefore, the probability of a leader, once initiated, propagating from the point to the plane, may also depend upon the negative-ion density and the rate of electron detachment throughout the gap. The increase in minimum impulse breakdown voltage as the wavefront increases may account for the sweep off action.

It can be noticed that in all the gases/gas mixtures tested, the minimum impulse breakdown voltage decreases as negative space charges were injected. This was discussed as the effect of initiatory electrons detached from the negative ions injected. The rate of decreasing in minimum impulse breakdown voltage being the largest when wavefront is 1.2μs and the smallest when wavefront is 19μs. This could

be explained readily considering the role of initiatory electron and the sweeping effect. When wavefront duration is relative short (eg 1.2μs), less negative ions are swept out during the relative shorter time period. So plentiful initiatiory electrons can be detached from negative ions, breakdown is more readily to occur and breakdown levels are lower. As the wavefront increases, more negative ions are to be swept out and the number of initiatory electrons is less. As a consequence, the decreasing effect on minimum impulse breakdown voltages due to negative space charges is not very pronounced for longer wavefronts.

As for positive space charge injection, the minimum impulse breakdown voltage increases a little bit for short wavefront (eg 1.2μs), but for longer wavefronts, the minimum impulse breakdown voltage is not very much affected. As discussed previously, when no space charge is injected (V_c=0kV), the longer the wavefront period, the more naturally occurring negative ions in the gap would be swept out.

It has been known [118,119] that the sweeping effect exists as positive bias voltage is applied (in [119] this kind of positive bias voltages were called sweeping voltage). As can be noticed from the results, for longer wavefronts, the minimum impulse breakdown voltage is almost unaffected by the positive space charges injection. It would be reasonable to suggest that, the sweeping effect due to the positive bias voltage does not have too much further effect because the majority of ions have already been swept out during the longer wavefront period. For shorter wavefront, the injection of positive space charges results in an increase in minimum impulse breakdown voltage. It can be explained as those naturally occurring negative ions

that are not able to be swept out during the shorter wavefront duration, are swept out under the effect of positive bias voltage. Therefore, under the shorter wavefront duration, there is an increase in minimum impulse breakdown voltage.

It was also noticed that for SF_6/freon, minimum impulse breakdown voltage increases as the wavefront increases, but the rate of increasing is very small. For SF_6/freon this phenomenon is believed to be associated with the creation of Cl^- ions from the freon molecule. Recently, it [119] had been suggested that the chlorine molecule is associated with the enhanced dielectric strength of the mixtures, and indeed any other additive which is capable of producing negative ions of chlorine, will be beneficial in that it will mitigate the reduction in performance associated with the almost inevitable presence of water vapour and metallic conducting particles in GIS. These Cl^- ions, preferentially produce very stable negative ions which do not readily detach. As it was discussed earlier, increase in wavefront would result in sweeping out the negative ions in the critical volume. It would not be difficult to understand that the sweeping effect on negative ions is not so pronounced as the rate of detachment of negative ions in SF_6/freon mixtures is lower itself.

6.5 Conclusions

The general conclusions were drawn from the chapter,

1. In SF_6, SF_6/air(50/50) and SF_6/N_2(50/50) mixtures, the minimum impulse breakdown voltage increases as the wavefront increases. This is concluded as the

sweeping off action. In SF_6/R12(95/5) and SF_6/R20(95/5), the phenomenon is not very pronounced. This is related to ion chemistry.

2. Minimum impulse breakdown voltage decreases as the negative ions were injected. The longer the wavefront, the smaller the rate of decreasing in minimum impulse breakdown voltage. The reason is believed to be the sweeping off action being more significant as the wavefront increases.

3. Minimum impulse breakdown voltage is not very much affected by the injection of positive ions, especially under longer wavefronts. It is understood that the naturally occurring negative ions in the gap are swept out effectively under positive dc bias voltage (sweeping voltage) or during the relatively long wavefront period. Consequently, there is not much difference whether positive ions were injected or not.

Chapter 7 General conclusions

The impulse breakdown characteristics of SF_6 and its mixtures in highly non-uniform field gaps were studied throughout the present work. Emphases were placed upon the effect of space charge, artificial irradiation, different gas mixtures, different additive gases and different wavefronts on impulse breakdown characteristics.

Although high voltage equipment is designed to work under uniform field conditions, high divergent fields are actually inevitable. The dielectric characteristics of uniform fields are fully studied and fairly well understood. On the other hand, the dielectric characteristics of gases in non-uniform fields are much more complicated and they are not fully understood. Earlier study [89] had shown that the non-uniform breakdown mechanism is much affected by space charge. The study of space charge effect on impulse breakdown characteristics of SF_6 and its mixtures in highly nonuniform field gaps has become an increasingly important subject. Especially, since SF_6 had been identified by the Intergovernmental Panel on Climate Change [167] as a potent greenhouse gas, there has been a tremendous need to find ideal substitutes for pure SF_6 insulation.

The effect of space charge on impulse breakdown voltage was studied extensively using two kinds of space charge injection methods — corona pin arrangement and direct injection method. The study was carried out using pure SF_6 and its mixtures with air, N_2, R12 or R20 as gaseous dielectrics. It had been found that space charges

injected by either method have nearly the same effect on minimum impulse breakdown voltage and corona activity. The role of negative and positive space charges on breakdown and pre-breakdown processes is somewhat different. When negative space charges are injected, the minimum impulse breakdown voltage decreases while the corona activity increases. The reason is on account of abundance of initiatory electrons resulting from detachment of plentiful negative ions injected. For positive space charges, on the other hand, the minimum impulse breakdown voltage remains almost constant or slightly increases when the positive dc bias/applied voltages are relatively low. This is mainly because of the sweeping effect and it is helpful in obtaining improved voltage recovery by depleting the ion population. Further increase in positive bias/applied voltage results in the reduction in minimum impulse breakdown voltage. The phenomenon was noticed in some earlier studies [102, 117] and the effect of higher concentration of positive ions in reducing the breakdown strength is not understood at present and should be further investigated.

The time lag measurement had shown that space charges, notably, negative space charges increase the mean value of time lag to breakdown. This is understood on the basis that there is an increasing probability that an initiating electron would appear in the critical volume when the voltage has reached the corona onset voltage. A filamentary corona will be established and it is necessary that the voltage be increased to a higher value and the field near the plane electrode be space charge enhanced before breakdown can take place. Thus the time lag to breakdown is relatively longer.

An optical photomultiplier (PM) was used and the PM outputs were measured as the function of the dc bias voltage. It had been found that as the number of negative space charges increases, the output of PM increases. Whilst the PM output almost remain constant under the influence of positive space charges. The measurement is absolutely consistent with the breakdown and time lag measurement. The above conclusions were confirmed by PM measurement.

It had been known that apart from the detachment of negative ions, the direct ionisation of neutral molecules by artificial irradiation or natural irradiation [122] is another possible source of free electrons. The effect of artificial irradiation is thus studied to achieve a better understanding of the initiatory electron effect. The initiatory electrons produced from the direct ionisation of neutral molecules by artificial irradiation (supplied by either a 125W quartz-mercury lamp or a piece of 5mCi capsule ^{137}Cs) and natural irradiation have effect on minimum impulse breakdown voltage and corona activity. It had been found that the direct ionisation of neutral molecules has the kind of effect that is similar to that of detachment of negative ions.

A set of tests were so designed to study the combined effect of space charge and artificial irradiation. In the hope that it could be understood how much the breakdown and prebreakdown processes can be affected by initiatory electrons. It had been found that although initiatory electrons have considerable effect on breakdown and prebreakdown processes, there is a limit beyond which the

breakdown and prebreakdown processes cannot be further affected by increasing initiatory electron population. It was concluded that there is a certain number of initiatory electrons which has to be reached so that the breakdown process can be initiated and further affected. It was also concluded that any extra initiatory electrons exceeding the number of the threshold make very little, if any, contribution to breakdown process.

The effect of initiatory electrons was studied using SF_6/N_2 (50/50) and SF_6/air (50/50) mixtures. It had been shown that initiatory electrons have the same effect on pure SF_6 and its mixtures with air and N_2. The results obtained in SF_6/R12 (95/5) and SF_6/R20 (95/5) had shown that when the tests were carried out in either of these two chlorine-bearing additives, neither space charge nor artificial irradiation has very pronounced effect on breakdown or prebreakdown process. It is believed that these chlorinated freons preferentially produce very stable negative ions (Cl^-) which do not readily detach or ionise and consequently, there would be a definite reduced likelihood of initiatory electrons.

The effect of different wavefront on breakdown characteristics in SF_6 and its mixtures was studied, as it has been known that the rate of production of initiatory electrons is wavefront related. The tests were carried out in SF_6, SF_6/air(50/50), SF_6/N_2(50/50), SF_6/R12(95/5) and SF_6/R20(95/5). It had been found that in SF_6, SF_6/air and SF_6/N_2, the minimum impulse breakdown voltage increases as the wavefront increases. This is concluded as the effect of sweeping off action. It was

also concluded that the sweeping off action being the most significant when wavefront duration is long.

The wavefronts have little effect on minimum impulse breakdown voltage measured in SF_6/R12 and SF_6/R20. The present results add further evidence to the suggestion that the marked improvement in the insulating performance of SF_6 and hence to the tolerance of the gas to metallic particle in GIS when a chlorinated freon is present is related to ion chemistry. It is unlikely, however, due to environmental pressures, that in further GIS installations chlorinated freons would be considered as feasible. Indeed, at the present time, and again for environmental reasons, there is a drive to explore alternative gases to pure SF_6. A better physical understanding of the factors which contribute to "good" insulating gases will assist in making informed choices for the next generation of GIS.

Chapter 8 Recommendations for further studies

As it was summarised in Chapter 1, the breakdown characteristics in nonuniform fields are more complicated than in uniform fields. The reason is probably due to the complex effect of space charge on breakdown process [3]. Nonuniform fields are inevitable in high voltage insulated equipment and there is considerable interest in the breakdown characteristics of nonuniform field gaps in SF_6 and its mixtures. Although much work had been done and it [105] had been pointed out that nonuniform field breakdown involves the development of a series of streamer/leader steps which propagate from the point electrode towards the plane. It [106] had also been realised that the successful development of impulse breakdown relies on there being a supply of electrons in the gap volume such that each streamer step can be initiated. The breakdown mechanism in nonuniform field has not been, up until now, fully understood. The effect of space charge was studied and the influence of initiatory electrons were evaluated. It had been found that initiatory electrons, beyond a certain limit, have considerable effect on prebreakdown and breakdown processes. As a further proposal, the density of space charges is to be measured. Thus it could be determined how the initiatory electrons affect the breakdown and prebreakdown processes, quantitatively.

A series of tests in the present work had shown that different SF_6 mixtures with different buffer gases behave differently under the effect of initiatory electrons. This is believed due to the different ion characteristics, mainly ion mobility. The measurement of ion mobility would certainly help to obtain a better physical understanding of the factors which contribute to "good" SF_6 mixtures. Consequently,

it would be helpful in making informed choices for more benign SF_6 mixtures. One of the practical ways of measuring ion mobility being considered was suggested by Waters and other [166]. The method is based on the concept that the average mobility is a function of discharge current.

The prebreakdown process under the effect of space charge and/or irradiation was observed using photomultiplier in the present work. If an image intensifier with a very high gain and a high speed camera were in use, more information about breakdown and prebreakdown processes could have been obtained.

The sweeping effect was noticed as the positive ions were injected. It is of great interest to note that sweeping effect can increase the minimum impulse breakdown voltage. It is not understood, at present stage, that in what way and to what extent the minimum impulse breakdown voltages are affected by these positive ions. As the sweeping effect might have a potential effect on improving dielectric strength. The effect of positive ions and sweeping effect must be further studied.

List of publications

1. Qiu, X.Q. and Chalmers, I.D., "The effect of initiatory electrons on breakdown characteristics in highly nonuniform gap", *Conference Record of the 1996 IEEE International Symposium on Electrical Insulation*, Montreal, Quebec, Canada, June 16-19, 1996, pp786-788

2. Qiu, X.Q. and Chalmers, I.D., "On the effect of space charges on breakdown strength by using two different injection methods", *Proceedings of Seventh International Conference on Dielectric Materials Measurements & Applications*, Bath, UK, September 23-26, 1996, pp180-183

3. Chalmers, I.D. and Qiu, X.Q., "The effect of injected space charges on the dielectric strength of SF_6 mixtures", Proceedings of the 12th International Conference on Gas Discharges & their applications, Greifswald, Germany, September 8-12, 1997, pp(I-)228-231,

4. Qiu, X.Q. and Chalmers, I.D., "The role of initiatory electrons in highly nonuniform field breakdown", *Conference Record of the 1998 IEEE International Symposium on Electrical Insulation*, Arlington, USA, June 8-11,

5. Chalmers, I.D., Qiu, X.Q. and Coventry, P., "The study of SF_6 mixtures with buffer gases", *Proceedings of the 8th International Symposium on Gaseous Dielectrics*, Virginia, USA, June 2-5, 1998

Acknowledgements

The author wishes to express his sincere gratitude to Professor I.D.Chalmers for the guidance and encouragement throughout the present study.

The author is indebted to his parents for their support, both morally and financially. This will always be remembered with thanks.

The receipt of an Overseas Research Students Award from the Committee of Vice-Chancellors and Principals of the Universities is gratefully acknowledged.

References

[1] Shugg,W.T. *Handbook of electrical and electronic insulating materials*, Second Edition, IEEE Press, NY, 433-452, 1995

[2] Christophorou, L.G. and Dale, S.J. "Dielectric gases", *Encyclopaedia of physical science and technology 4*, 246-262, 1987

[3] Qiu, Y and Kuffel, E., " The breakdown strength of gas mixtures containing a small amount of electronegative gas in non-uniform field gaps", Proceedings GD82, London, 215-218, 1982

[4]Thomson, J.J., *Conduction of electricity through gases*, Cambridge University Press, 2nd. edition, 1906

[5]Townsend, J.S., *Electricity in gases*, Oxford Clarendon Press, 1915

[6]Meek, J.K., "The influence of irradiation on the measurement of impulse voltage with sphere gaps", IEE Journal, Vol.93, pt.II, 97-115, 1946

[7]Hale, D.H., Phys. Rev.,56, 1199, 1948

[8]Schumann, W.O., Arch fur Elecctrotechnik, 12, 593, 1923

[9]Rogowski, W., Archiv. fur Elektrotechnik,20,99, 1928

[10]Raether, H., Zeitschrift fur Physik, 112, 464, 1939

[11]Raether, H., Archiv. fur Elektrotechnik,34, 49, 1940

[12]Meek,J.M., Phys.Rev., 57-72,1940

[13]Davies,A.J., Davies,C.S., and Evans,C.J., "Computer simulation of rapidly developing gaseous discharges", Proc. IEE, Vol.118, 816-823, 1971

[14]Chalmers, I.D., Duffy, H. and Tedford, D.J., Proc. Royal Society A, 329, 171, 1972

[15]Meek, J.M. and Craggs, J.D., *Electrical breakdown of gases*, John Wiley & Sons, 1978

[16]Pederson, A., "Criteria for spark breakdown in sulphur hexafluoride", IEEE Trans., PAS-89, 2043-2048, 1970

[17]Chalmers, I.D., Farish, O., Gibert, A., and Dupuy, J., "Leader development in short point-plane gaps in compressed SF_6", Proc. IEE, 131A, 159-163, 1984

[18]Gallimberti, I., and Wiegert, N., "Streamer and leader formation in SF_6 and SF_6 mixtures under positive impulse conditions", J. Phys. D: Appl. Phys., 19, 2351-2373, 1986

[19]Kurimoto,A., "Schlieren studies of impulse breakdown in air gaps", Proc. IEE. Vol. 125, No. 8, 767-769, 1978

[20]Les Renardieres Group, "Negative discharges in long air-gaps at Les Renardieres: 1978 results", Electra, No.74, 67-74, 1981

[21]Bayle, P., Bayle, M., Dupuy, J. and Gilbert, A., "Heating of neutrals in glow-to-spark transition in air and SF_6", Fourth Int. Sym. on High Voltage Engineering, Paper 31.09, 1983

[22]Bayle, P., "Schlieren study of the transition to spark of a discharge in air and SF_6", J.Phys. D:Appl. Phys., 16, 1493-1506, 1983

[23]Woolsey, G.A., Ijumba, N.M. and Farish, O., "Measurement of neutral densities and temperatures in negative air corona using an optical interferometer and a thermocouple", J. Phys. D: Appl. Phys. 19, 2135-2146, 1986

[24]Kurimoto, A. and Farish, O., "Negative dc corona study in atmospheric air using Schlieren and interferometric techniques" IEE Proc. Vol. 127, No. 2, pt.A, 89-94, 1980

[25]Farish, O., Ibrahim, O.E. and Korasli, C., "Corona stabilisation and breakdown in SF_6 and SF_6/N_2 mixtures", Proc. 5th Int. Conf. on Gas Discharges, IEE Publ. 165, 320-323, 1978

[26]Niemeyer, L. and Pinnekamp, F., J. "Leader discharges in SF_6", J.Phys.D: Appl. Phys. 16, 1031-1046, 1983

[27]Bhalla, M.S. and Craggs, J.D., "Measurements of ionisation and attachment coefficients in SF_6 in uniform fields", Proc. Phys. Soc., Vol. 80, 151-160, 1962

[28]Maller, V.N. and Naidu, M.S., "Sparking potentials and ionisation coefficients in SF_6", Proc. IEE, Vol. 123, 107-108, 1976

[29]Kuffel, E. and Zaengl, W.S., *High voltage engineering fundamentals*, Pergamon Press, 1984

[30]Farish, O. and Ibrahim, O.E., "Effect of electrode surface roughness on breakdown in nitrogen/SF_6 mixtures", Proc. IEE, Vol. 123, 1047-1050, 1976

[31]Pedersen, A and Brengsbo, E., "Estimation of breakdown voltage in compressed SF_6", Int. High Voltage Symp., Zurich, 432-436, 1975

[32]Nitta, T. and Shibuya, Y., "Electrical breakdown of long gaps in sulfur hexafluoride", IEEE Trans. PAS, Vol. 89, 1065-1070, 1971

[33]Malice, HRH., "Streamer breakdown criterion for compressed gases", IEEE Trans. Electrical Insulation, EI-16, 463-467, 1981

[34]Crichton, B.H. and Tedford, D.J., "The application of low-pressure experimental data to the calculation of electrical discharge thresholds in compressed gases", J.Phys.D: Appl. Phys. Vol. 9, 1079-1083, 1976

[35]Somerville, I.C., Tedford, D.J. and Crichton, B.H., "Electrode roughness in SF_6 — a generalised approach", Proc. XIII Int. Conf. on Phenomena in ionised gases, Berlin, 429-430, 1977

[36]Pedersen, A., "The effect of surface roughness on breakdown in SF_6", IEEE Trans., Vol.PAS-94, 1749-1754, 1975

[37]Cookson, A.H., "Electrical breakdown for uniform fields in compressed gases", Proc. IEE, Vol. 117, 269-280, 1970

[38]Nitta, T., Yamada, N. and Fujiwara, Y., "Area effect of electrical breakdown in compressed SF_6", IEEE Trans., PAS-93, 623-629, 1974

[39]Farish,O., "Corona-controlled breakdown in SF_6 and SF_6 mixtures", Proc. XVIth Int. Conf. on Phenomena in Ionized Gases, Dusseldorf, 187-195, 1983

[40]Chalmers, I.D., Farish, O., Gibert, A. and Dupuy, J., "Leader development in short point-plane gaps compressed SF_6", Proc. IEE, Vol. 131A, 159-163, 1984

[41]Pinnaduwage, L.A. and Christophorou, L.G., "A possible new mechanism involved in nonuniform field breakdown in gaseous dielectrics", in Gaseous Dielectrics VII, Plenum Press, NY, 123-130, 1994

[42]Christophorou,L.G., "Electron-excited molecule interactions", Invited Lectures, Proc.XXth Int. Conf. on Ionization Phenomena in Gases, Pisa, 3-13, 1991

[43] Christophorou,L.G., Pinnaduwage, L.A. and Datskos, P.G., *Electron attachment to excited molecules*, Plenum Press, 415-442, 1994

[44]Sangkasaad, S., "Corona inception and breakdown voltages in nonuniform fields in SF_6", Proc. Int. High Voltage Symp., Zurich, 379-384, 1975

[45]Azer, A and Comsa, R.P., "Influence of field nonuniformity on the breakdown characteristics of sulfur hexafluoride", IEEE Trans. Vol. EI-8, 136-142, 1973

[46]Hazel, R. and Kuffel, E., "Static filed anode corona characteristics in sulphur hexafluoride", IEEE Trans. Vol. PAS-95, 178-186, 1976

[47]Liapin, A.G., Popkov, V.I. and Shevtsov, E.M., "Positive DC point-plane dielectric strength of compressed gases", Proc. 4th Int. Conf. Gas Discharge, London, 169-171,1976

[48]Kurimoto, A., Dale, S.J., Aked, A. and Tedford, D.J., "Impulse discharge characteristics in long non-uniform field gaps in low pressure SF_6", Proc. Int. High Voltage Symp., Zurich, 349-354, 1975

[49]Anis, H. and Srivastiva, K.D., "Breakdown of rod-plane gaps in SF_6 under positive switching impulses", IEEE Trans., Vol.PAS-101, 537-546, 1982

[50]Ibrhim, O.E. and Farish, O., "Impulse breakdown and prebreakdown corona processes in SF_6 and SF_6/N_2 mixtures", Proc. 2nd Int. Symp. Gaseous Dielectrics, Pergamon Press, 83-92, 1980

[51]Farish, O., Chalmers, I.D. and Vidaud, P., "SF_6 mixtures with enhanced corona stabilisation", Proc. 7th Int. Conf. Gas Discharges, London, 223-226, 1982

[52]Korasli, C. and Farish , O., "Corona and breakdown in coaxial-electrode geometry in SF_6 and SF_6/N_2 mixtures", Proc. 3rd Int. Symp. Gaseous Dielectrics, Pergamon Press, 77-85, 1982

[53]Zhou,L.M., et al, "Pre-existing ionization effect on positive impulse breakdown of air, air/SF_6 and air/R12", Proc. 7th Asian Conf. on Electrical Discharge, Xi'an, 9-12, 1994

[54]Farish, O., Ibrahim, O.E. and Kurimoto, A., "Pre-breakdown corona processes in SF_6 and SF_6/N_2 mixtures", Proc. 3rd Int. Symp. High Voltage Engineering, Milan, paper 31.15, 1979

[55]Ibrahim, O.E. and Farish, O., "Negative-point breakdown and prebreakdown corona processes in SF_6 and SF_6/N_2 mixtures", Proc. 6th Int. Conf. Gas Discharges, 161-164, 1980

[56]Kurimoto, A., Aked, A. and Tedford, D.J., "Pre-breakdown phenomena in large non-uniform-field gaps in SF_6", Proc. 4th Int. Conf. Gas Discharges, London, 162-165, 1976

[57] Kurimoto, A., Aked, A. and Tedford, D.J., "Prediction of the critical pressure in positive point/plane V_{50}, V_d/pressure characteristics in air and SF_6", Proc. 5th Int. Conf. Gas Discharges, London, 324-327, 1978

[58]Bortnik, I.M. and Vertikov, V.P., "Discharge development of long gap in SF_6 gas", Proc. 3rd Int. Symp. High Voltage Engineering, Milan, paper 32.11, 1979

[59]Takuma, T., Watanabe, T., Kita, K. and Aoshima, Y., "Discharge development of long gap in SF_6 gas", Proc. Int. High Voltage Symp., Munich, 386-390, 1972

[60]Watanabe, T. and Takuma, T., "The breakdown voltage and discharge extension of long gaps in nitrogen-SF_6 and air-SF_6 gas mixtures", J. Appl. Phys., 48(8), 3281-3287, 1977

[61]Pigini, A., Rizzi, G. and Branbilla, R., "Dielectric behaviour of SF_6 in non uniform fields near critical pressure", Proc. 7th Int. Conf. Gas Discharges, 203-206, 1982

[62]Voβ, W., "Discharge development of non-uniform gaps in SF_6-N_2 gas mixtures", Proc. 3rd Int. Symp. High Voltage Engineering, Milan, paper 31.13, 1979

[63]Rodrigo, H. and Chatterton, P.A., "Measurement of impulse positive point predischarge growth in 50% SF_6 50% N_2 gas mixtures", Proc. 7th Int. Conf. Gas Discharges, 207-210, 1982

[64]Kurimoto, A., "Prebreakdown phenomena in long nonuniform field gaps in SF_6/N_2 and SF_6/air mixtures", Proc. 7th Int. Conf. Gas Discharges, 211-214, 1982

[65]Sigmond, R.S., "Simple approximate treatment of unipolar space-charge-dominated corona: The Warburg law and the saturation current", J.Appl. Phys., 53(2), 891-898, 1982

[66]Bortnik, I.M., "Corona discharge characteristics in SF_6", Proc. 13th Int. Conf. Phenomena in Ionised Gases, Berlin, 443-444, 1977

[67]Sigmond, R.S., "A narrow-jet model of dc corona breakdown", Proc. 7th Int. Conf. Gas Discharges, 140-142, 1982

[68]Dupuy, J and Gibert, A., "Comparison of point-to-plane discharge in air and SF_6", J.Phys. D: Appl. Phys. Vol.15, 655-664, 1982

[69] Sigmond, R.S., Hegerberg, R and Holberg, O., Proc. 4th Int. Symp. High Voltage Technology, Athens, paper 31.05, 1983

[70]Thorn EMI Electron Tubes Ltd. "Basic physics and statistics of photomultipliers", 1988

[71]China Lights & Power GIS Course Notes, Part I: Breakdown Mechanisms in SF_6, Centre for Electrical Power Engineering, University of Strathclyde, January 1995

[72]Gallimberti, I., "A computer model for streamer propagation", J.Phys. D: Appl. Phys. Vol. 5, 2179-2189, 1972

[73]Hartman, G. and Gallimberti, I., "The influence of metastable molecules on the streamer progression", J.Phys. D: Appl. Phys. Vol. 8, 670-680, 1975

[74]Ibrhim, O.E., *PhD Thesis*, University of Strathclyde, 1980

[75]Selim, E.O., and Waters, R.T., IEEE Conf. on Electrostatics, 136-141, 1978

[76]Les Renardieres Group, Electra, Vol.53, 31-153, 1977

[77]Waters, R.T., "Breakdown in nonuniform fields", Proc. IEE Vol.128, pt.A, No.4, 319-325, 1981

[78]Lemke, E., Z. elekr. Inf. Energietech., Vol. 3, 186-192, 1973

[79]Pinnekamp, F., Proc. 4th Int. Symp. High Voltage Technology, Athens, paper 31.04, 1983

[80]Pinnekamp, F. and Niemeyer, L., "Qualitative model of breakdown in SF_6 in inhomogeneous gaps", J. Phys. D: Appl. Phys., Vol. 17, 1293-1302, 1983

[81]Niemeyer, L., Proc. 4th Int. Symp. High Voltage Technology, Athens, paper 31.02, 1983

[82]Pinnekamp, F., Proc. 4th Int. Symp. High Voltage Technology, Athens, paper 31.03, 1983

[83]Niemeyer, L . and Pinnekamp, P., "Surface discharge in SF_6", Proc. 3rd Int. Symp. Gaseous Dielectrics, 379-385, 1982

[84]Farish, O., Davidson, R.C. and Tedford, D.J., *Ann. Rep. Conf. Electrical Insulation and Dielectric Phenomena*, 380-389, 1977

[85]Chatterton, P.A., "A model for the breakdown of SF_6 in the presence of positive impulse corona", Proc. 3rd Int. Symp. High Voltage Technology, Milan, paper 31.07, 1979

[86]Malik, N.H., "Corona stabilisation and the critical pressure in SF_6", Proc. 7th Int. Conf. Gas Discharges, 219-222, 1982

[87]Farish, O., Dale, S., and Sletten, A.M., "Impulse breakdown of positive rod-plane gaps in hydrogen and hydrogen-SF_6 mixtures", IEEE Trans. Vol. PAS-95, 1639-1647, 1976

[88]Ryan, H.M., et al, "Factors affecting the insulation strength of SF_6 filled systems", CIGRE, paper 15.02, 1976

[89]Qiu, Y. and Kuffel, E., "The breakdown strengths of gas mixtures containing a small amount of electronegative gas in non-uniform field gaps", Proc. 4th Int. Conf. Gas Discharges, 215-218, 1982

[90]Kuffel, E and Yializis, A., "Impulse breakdown of positive and negative rod-plane gaps in SF_6-N_2 mixtures", IEEE Trans., Vol. PAS-97, 2359-2366, 1978

[91]Goldman, A., Chalmers, I.D. and Doremieux, J.L., "Influence of organic vapor traces on corona corrosion of electrodes in SF_6", Proc. 4th Int. Symp. High Voltage Technology, Athens, paper 32.07, 1983

[92]Cooke, C.M., and Velazquez, R., "The insulation of ultra-HV in coaxial systems using compressed SF_6 Gas", IEEE Trans. on PAS, Vol.96, 1491-1497, 1977

[93]Cooke, C.M., Wootton, R.E. and Cookson, A.H., "Influence of particles on ac and dc electrical performance of gas insulated systems at extra-HV", IEEE Trans. on PAS Vol.96, 768-777, 1977

[94]Christophorou, L.G., et al, "Recent advance in gaseous dielectrics at Oak Ridge National Laboratory", IEEE Trans. on EI, Vol. 19, 550-566, 1984

[95]Dale, S.J. and Hopkins, M.D., "Methods of particle control in SF_6 insulated CGIT systems", IEEE Trans. on PAS, Vol.101, 1654-1663, 1982

[96]Loeb, L.B., *Electrical Coronas*, University of California Press, 1965

[97]Sangkasaad, S., "Dielectric strength of compressed SF_6 in nonuniform fields", ETH Zurich, No.5738, 1976

[98]Comer, J., Schulz, G.J., "Measurement of electron detachment cross sections from O_2^-", J.Phys.B:Atom Molecule Physics, Vol.7:L249-253, 1974

[99]Laue, M. von, Phys. Lpz. 76, 1925, p261

[100]Zuber, K, Ann. Phys. Lpz. 76(1923), p231

[101]Berg, D and Works, C.N., "Effect of space charge on electric breakdown of sulphur hexfluoride in non-uniform fields", AIEE Trans. 77, 820-822, 1958

[102]Qiu, Y., Chalmers, I.D. and Li, H.M., "Effect of injected space charges on the positive impulse breakdown of SF_6 in a point-plane gap", J.Phys.D: Appl. Phys., 25, 326-328, 1992

[103] Qiu, X.Q. and Chalmers, I.D., "The effect of initiatory electrons on breakdown characteristics in highly nonuniform gap", Conf. Record of the 1996 IEEE Inter. Symp. on Electrical Insulation, 787-788, 1996

[104]Qiu, X.Q. and Chalmers, I.D., "On the effect of space charges on breakdown strength by using two different injection methods", 7th Inter. Conf. on Dielectric Materials Measurements & Applications, 180-183, 1996

[105]Chalmers, I.D., Gallimberti, I., Gibert, A. and Farish, O., "The development of electrical leader discharges in a point-plane gap in SF_6", Proc. Royal Society A, 412, 285-308, 1987

[106]Farish, O., Chalmers, I.D., Gibert, A. and Dupuy, J., "The streamer-leader transition in SF_6 and SF_6-Freon mixtures", Proc. 6th Int. Symp. on High Voltage Engineering, Vol.2, paper 32.03, 1989

[107]Boggs, S.A. and Wiegart, N., 1984, "Influence of experimental conditions on dielectric properties of SF_6 insulated systems — theoretical considerations", Gaseous Dielectrics IV, Knoxville, 531-539

[108]Nakanishi, K., "New gaseous insulation", IEEE Trans. on Electrical Insulation, Vol. 21, 933-937, 1986

[109]Nord, G.L., "Effect of ultraviolet on breakdown voltage", AIEE Trans., Vol. 54, 955-958, 1935

[110]Kuffel, E. and Zaengl, W.S. *High Voltage Engineering*, Pergamon Press, 1984

[111]Hiesinger, H., *Discuation on* Fujinami, H. and Kuffel, E's "Breakdown characteristics of non-uniform gaps in SF_6 under fast oscillating impulse voltages", Gaseous Dielectrics, VI, Knoxville, 247-253, 1991

[112]Hibma, T. and Zeller, H.R., "Direct measurement of space-charge injection from a needle electrode into dielectrics", J.Phys., Vol.59, No.5, 1614-1620,1986

[113]Davidson, R. et al, "Corona and breakdown in N_2-SF_6 and N_2-O_2 mixtures in static and flowing gas", Proceedings of 4th Int. Conf. on Gas Discharges and their Applications, 242-245,1976

[114]Selim, E.O. and Waters, R.T., "Electrical characteristics of negative rod/plane in air at atmospheric pressure and below", Proc. 6th Int. Conf. on Gas Discharges and their Applications, 146-149, 1980.

[115]Berg, D. and Works, C.N., "Effect of space charge on electric breakdown of sulfur hexafluoride in nonuniform fields", Trans. AIEE, Vol.77, 820-823, 1958

[116]Siodla, K., et al., "Breakdown of SF_6 in non-uniform field gaps under combined dc, fast oscillating impulse and standard lightning impulse voltages", IEEE Trans., Vol. EI-28, No.2, 253-260, 1993

[117]Qiu, Y., et al, "Space charges effect on impulse breakdown of SF_6, N_2 and SF_6/N_2 in a highly non-uniform field gap", 8th Int. Sym. on High Voltage Engineering, 53-56, 1993

[118]Qiu, Y., "Impulse breakdown characteristics of enclosed sphere gaps", 4th Int. Symp. on High Voltage Engineering, Paper 33.07, 1983

[119]Chalmers, I.D., et al, "Insulation performance of SF_6 mixtures", Gaseous Dielectrics VII, 601-608, 1994

[120]MacGregor, S.J., *Electrical breakdown in SF_6 and SF_6 air mixtures*, Ph.D. thesis, University of Strathclyde, 1986

[121]Somerville, I.C. and Tedford, D.J., "The statistical time-lag to spark breakdown in high pressure SF_6", Gaseous Dielectrics III, 267-273, 1982

[122]Binns, D.F. and Hardy, D.R., "Irradiation of small sphere gaps for voltage measurement", Trans. of AIEE, 155-159, 1962

[123]Guenfoud, O., et al, "Atmospheric ions and positive point corona", Proc. 4th Int. Symp. on High Voltage Engineering, paper 41.03, 1983

[124]Somerville, I.C., et al, "The influence of atmospheric negative ions on the statistical time lag to spark breakdown", Gaseous Dielectrics IV, 137-144, 1984

[125]Boyd, H.A. and Crichton, G.C., "Uniform-field breakdown voltage measurement in sulphur hexafluoride", Proc. IEE, Vol. 119, 275-276, 1972

[126]Christophorou, L.G., "Basic physics of gaseous dielectrics", IEEE Trans. Electrical Insulation, Vol.EI-25(I), 55-74, 1990

[127]*The Effects on Populations of Exposure to Low Levels of Ionizing Radiation,* National Academy Press, Washington, D.C., 44, 1980

[128]Hilal, Y.H. and Christophorou, L.G., "Energy to produce an electron-ion pair in SF_6 and SF_6/N_2 mixtures", J.Phys. Vol. D20, 975-976, 1987

[129]Nakannishi, K., et al., "Penning ionization ternary gas mixtures for diffuse discharges switching applications", J.Phys. Vol. 58, 633-641, 1985

[130]Schmidt, W.F. and Van Brunt, R.J., "Comments on the effect of electron detachment in initiating breakdown in gaseous dielectrics", Gaseous Dielectrics, III, 561-563, 1984

[131]Van Brunt, R.J. and Misakian, M., "Role of photodetachment in initiation of electric discharges in SF_6 and O_2", J.Appl. Phys., Vol.54, 3074-3079, 1983

[132]Wiegart, N., "A model for the production of initial electrons by detachment of SF_6^- ions", IEEE Trans. on Electrical Insulation, Vol.20, 587-594, 1985

[133]Olthoff, J.K., et al., "Collisional electron detachment and decompositions rates of SF_6^-, SF_5^-, and F^- in SF_6: implication for ion transport and electrical discharges", J.Chem. Phys. Vol. 91, 2261-2268, 1989

[134]Wang, Y., et al., "Collisional electron detachment and decomposition cross section for SF_6^-, SF_5^-, and F^- on SF_6 and rare gas targets", J. Chem. Phys. Vol. 91, 2254-2260, 1989

[135]Schweinler, H.C., and Christophorou, L.G., "Calculation of electric field-induced detachment rates of electrons from mononegative ions; relevance to gaseous dielectrics", Gaseous Dielectrics II, 12-24, 1980

[136]Nelson, J.K., "Positive corona processes in electronegative gaseous dielectrics", IEEE Trans., 1985, Vol. EI-20, No.3, 601-607, 1985

[137]Farish, O., et al., "SF_6 mixtures with enhanced corona stabilisation", Proc. 7th Int. Conf. Gas Discharges and their Applications, London, UK, 223-226, 1982

[138]Chalmers, I.D., et al., "Extended corona stabilisation in SF_6/freon mixtures", J.Phys.D: Appl.Phys., Vol.18, No.8, L107-112, 1985

[139]Qiu, Y., et al., "Improved dielectric strength of SF_6 gas with a trichlorotrifluoroethane vapor additive", IEEE Trans. on Electric Insulation, Vol.EI-22, No.6, 763-768, 1987

[140]Qiu, Y., et al., "Measurement of ionisation and attachment coefficients in trichlorotrifluoroethane and SF_6 mixtures", J.Phys. D:Appl. Phys., Vol. 20, No.6, 801-802, 1987

[141]Qiu, Y., et al., "Breakdown of SF_6 and some SF_6 mixtures in a point-plane gap", Proc. 7th Int. Symp. High Voltage Engineering, Dresden, Germany, paper 32.09, Vol.3, 83-86, 1991

[142]Qiu, Y. and Wen, X., "Measurement of ionisation and attachment coefficients in difluorodichloromethane and SF_6 gas mixtures", J.Phys, D:Appl. Phys., Vol. 20, No.9, 1203-1204, 1987

[143]Chalmers, I.D., et al., "The effect of impulse waveshape on point/plane breakdown in SF_6", Gaseous Dielectrics IV, 344-351, 1984

[144]Christophorou, L.G. and van Brunt, R.J., "SF_6/N_2 mixtures—basic and HV insulation properties", IEEE Trans. on Dielectric and Electrical Insulation, Vol.2, No.5, 952-1003, 1995

[145]*Gaseous Dielectrics*, Christophorou, L.G., (Ed.), Volume I (Oak Ridge National Laboratory Report CONF-780301, 1978), Volume II to V (Pergamon Press, NY, 1980, 1982, 1984 and 1987) and Volume VI to VII (Plenum Press, NY, 1990, 1994)

[146]Pedersen, A., "Evaluation of the effect of surface defects on breakdown in strongly electronegative gases or gas mixtures", *Gaseous Dielectrcis II*, Pergamon Press, NY, 201-208, 1980

[147]Prdersen, A., "On the assessment of new gaseous dielectrics for GIS", IEEE Trans. PAS, Vol.104, 2233-2237, 1985

[148]Farish, O., et al, "Effect of electrode surface roughness on breakdown in nitrogen/SF_6 mixtures", Proc. IEE, Vol.123, 1047-1050, 1976

[149]Aschwasnden, Th., "Swarm parameters in SF_6 and SF_6/N_2 mixtures determined from a time resolved discharge study", *Gaseous Dielectrics IV*, Pergamon Press, NY, 24-32, 1984

[150]Cookson, A.H., et al., "Analysis of the HV breakdown results for mixtures of SF_6 with CO_2, N_2 and air", 3rd ISH, Milan, paper 31.10, 1979

[151]Qiu, Y. and Feng, Y.P., "Calculation of dielectric strength of the SF_6/N_2 gas mixture in macroscopically non-uniform fields", Proc. 4th Int. Conf. on Properties and Applications of Dielectric Materials, Vol.1, 87-90, 1994

[152]Qiu, Y. and Feng, Y.P., "Prospects for SF_6/N_2 gas mixtures as a replacement of SF_6 in gas-insulated cables", Proc. of Joint Conf.: 1993 Inter. Workshop on Electrical Insulation and 25th Symp. on Electrical Insulating Materials, Nagoya, 183-186, 1993

[153] Qiu, Y, et al, "Breakdown of SF_6/air mixtures in non-uniform field gaps under lightning impulse voltages", GD-92, Swansea, 398-401, 1992

[154]Wootton, R.E., et al, "Investigation of high voltage particle-initiated breakdown in gas insulated systems", ERPI reports RP7835, 1977

[155]Qiu, Y and Feng, Y.P., "Investigation of SF_6-N_2, SF_6-CO_2 and SF_6-Air as substitutes for SF_6 insulation", Conf. Record of the 1996 IEEE Inter. Symp. on Electrical Insulation, 766-769, 1996

[156]Siddagangappa, M.C., et al, "Studies of ionization and attachment in mixtures of N_2-O_2, N_2-CO_2, N_2-O_2-CO_2, N_2-CCl_2F_2 and N_2-O_2-CCl_2F_2", Proc. 7th Int. Conf. on Gas Discharges and their Applications, London, 350-352, 1982

[157]Cobine, J.D., Chapter IV, "Ionization and deionization" in *Gaseous Conductors: Theory and Engineering Applications*, Dover Publications, Inc. New York, 1958

[158] Feng, Y., et al, "The influence of voltage waveshape on particle-initiated breakdown voltages of gaps in SF_6 and SF_6/air mixtures", Proc. 5th Int. Symp. on High Voltage Engineering , paper 15.02, 1987

[159]Farish, O., et al, "Particle initiated breakdown in a coaxial system in SF_6/air mixtures", Conf. Record of IEEE Int. Symp. on Electrical Insulation, 206-209, 1986

[160]Qiu, Y., et al, "Variation of the impulse breakdown voltage for nonuniform field gaps in air and SF_6 with different wavefronts", Conf. Record of IEEE Int. Symp. on Electrical Insulation, 213-216, 1986

[161]Narbut, O.E., et al., "Factors controlling electrical strength of gaseous insulation", Trans. of AIEE, 545-551, Aug, 1959

[162] Xu, X., et al., "Prediction of breakdown in SF_6 under impulse conditions", IEEE on DEI, Vol. 3, No.6, 836-842, 1996

[163]Christophorou, L.G. and Van Brunt, R.J., "SF_6 insulation: possible greenhouse problems and solutions", CIGRE, WG 15.03.06, IWD4, 1996

[164]Christophorou, L.G., "The use of basic physical data in the design of multicomponet gaseous insulators", Proceedings of the 5th International Conference on Gas Discharges, Liverpool,1-8, 1978

[165]Pace, O.M., et al, "Application of basic gas research to practical systems", Proceedings of the 7th IEEE/PES Transmission and Distribution Conference and Exposition, Atlanta, 168-177, 1979

[166]Waters, R.T., et al, "Positive and negative ion mobilities in corona discharges in SF_6 and mixtures", Proceedings of the 7th Int. Conf. on Gas Discharges and their Applications, 251-254,1982

[167]Intergovernmental Panel on Climate Change (IPCC), "climate Change 1995", J.T.Houghton, L.G.Meira Filho, B.A.Callander, N.Harris, A.Kattenberg and K.Maskell (Eds.), Cambridge University Press, Cambridge, New York, 22, 1996